

UNIVERSIDADE DE LISBOA

FACULDADE DE FARMÁCIA



**DESIGN AND CHARACTERIZATION OF ENZYMATIC
DEGLYCOSYLATION SYSTEMS TO PRODUCE DRUGS
AGAINST ALZHEIMER'S DISEASE**

HELDER JOÃO FERREIRA VILA REAL

**DOUTORAMENTO EM FARMÁCIA
(QUÍMICA FARMACÊUTICA E TERAPÊUTICA)**

2010

UNIVERSIDADE DE LISBOA

FACULDADE DE FARMÁCIA



**DESIGN AND CHARACTERIZATION OF ENZYMATIC
DEGLYCOSYLATION SYSTEMS TO PRODUCE DRUGS
AGAINST ALZHEIMER'S DISEASE**

Tese orientada por:

Professora Doutora Maria Henriques Lourenço Ribeiro

e co-orientada por:

Professor Doutor António Roque Taco Calado

HELDER JOÃO FERREIRA VILA REAL

**Dissertação apresentada à Faculdade de Farmácia da Universidade de Lisboa, com
vista à obtenção do grau de Doutor em Farmácia**

(Química Farmacêutica e Terapêutica)

Lisboa, 2010

Este trabalho foi desenvolvido sob orientação da Professora Doutora Maria Henriques Lourenço Ribeiro e co-orientação do Professor Doutor António Roque Taco Calado, no iMed.UL – Research Institute for Medicines and Pharmaceutical Sciences, Faculdade de Farmácia da Universidade de Lisboa, bem como no “Department of Chemistry, University of Georgia (USA)”.

O trabalho foi financiado pela Fundação para a Ciência e Tecnologia através da bolsa de doutoramento SFRH/BD/30716/2006.

This work was developed under scientific guidance of Prof. Dr. Maria Henriques Lourenço Ribeiro and co-orientation of Prof. Dr. António Roque Taco Calado, at iMed.UL – Research Institute for Medicines and Pharmaceutical Sciences, Faculty of Pharmacy, University of Lisbon, as well as in the Department of Chemistry, University of Georgia (USA).

The work was financially supported by Fundação para a Ciência e Tecnologia, through the doctoral grant SFRH/BD/30716/2006.

*Daniel answered and said,
Blessed be the name of God for ever and ever,
for wisdom and might are his;
and he changeth the times and the seasons,
he removeth kings, and setteth up kings;
he giveth wisdom unto the wise
and knowledge to them that know understanding.*

(Dn. 2:20-21)

To my wife, sister and parents

Acknowledgements

To Prof. Dr. Maria Henriques Lourenço Ribeiro, my scientific supervisor, I would like to express my deep gratitude for all the trust and sympathy shown since the very beginning of my research work at the Physical-Chemical Sciences sub-group. I am also very grateful for her motivation and guidance that helped me moving into new research fields within the biotechnology area, during my PhD course. I am very grateful for her personal stimulus, support and encouragement in order to present the work done through oral and poster communications and also supporting me with transport and accommodation inherent to foreign conferences. I also thank the proactive and fast publishing of the results obtained, as well as the resiliency shown against adversity, during the writing and review of papers, including this thesis work. Finally I would like to emphasize the human qualities of Prof. Dr. Maria, her dedication to her students and her friendship, which were the keystone that helped me in several situations to feel comfortable and confident, in a way to be able to develop this thesis work.

To Prof. Dr. António Roque Taco Calado, my scientific co-supervisor, I firstly would like to thank the prompt and sympathetic way he received me in his research group, and all the trust showed during the first Physical-Chemistry lessons I was asked to give. Physical-chemistry turned to be one of my favorite subjects during my graduation studies and Prof. Dr. Calado has decisively made the difference through his great dedication to students, unfortunately not always recognized, scientific rigor and availability for interesting and productive discussions. As co-supervisor of my PhD thesis, I am grateful for his proactive support concerning critical thinking especially high-pressure issues. I also want to thank for his availability for fast paper and thesis reviewing. At last, I would like to state recognition for his great work as Professor and as a friend with who I can talk about so many interesting aspects of science.

To Prof. Dr. António José Infante Alfaia, I would like to show my gratitude for his friendship and help, concerning numerous tasks including: mathematical models; solving pressure equipment issues; paper writing and reviewing; critical thinking and support in some experimental work, especially during my first steps in the sub-group of Physical-Chemical Sciences.

To Prof. Dr. Manuel António Piteira Segurado, I would like to thank his interest and critical thinking concerning some issues related to high-pressure experiments. I am grateful for his friendship and his outstanding skills as a teacher giving the proper tools to a student as me and letting himself finding the solution by himself.

To Prof. Dr. Robert Stephen Phillips, I would like to acknowledge the way he received me in his biochemical lab during an internship of two months in Georgia, USA.

To Prof. Dr. Maria Emília Rosa, I would like to thank for her kindness, interest and availability concerning Surface Electronic Microscopy methodology.

I would like to thank Prof. Dr. Helder Mota Filipe, Prof. Dr. Bruno Sepodes and Master João Rocha for their interest and availability to test some compounds in animal models. A especial acknowledgement to my friend João Rocha that always showed very interest for this thesis work and accomplished the animal assays in a very carefully and competent way. I want to thank João for his scientific support, perseverance and critical thinking during four years of coffee and coke breaks. I also want to show my recognition for his friendship, support, positive thinking and altruism above all.

To Prof. Dr. Maria do Rosário Bronze, I would like to thank her interest, availability and sympathy for HPLC-MS analysis.

To Prof. Dr. Dora Brites, Prof. Dr. Adelaide Fernandes and to Master Andreia Barateiro, I would like to acknowledge for their interest and availability in *in vitro* and *in vivo* studies, in particular Prof. Dr. Adelaide Fernandes for her sympathy and methodical way of work concerning experiments with mice.

To Prof. Dr. Pedro Góis, I would like to thank the supply of a great amount of ionic liquids as well as his proactive thinking in order to use ionic liquids as template additives of sol-gel.

To the Faculty of Pharmacy, University of Lisbon (FFUL) represented by Prof. Dr. José Cabrita da Silva as Assembly President; Prof. Dr. José Guimarães Morais as Director and President of the Management Council; Prof. Dr. Matilde Castro as President of the Scientific Council and Prof. Dr. Maria Henriques Lourenço Ribeiro as President of the Pedagogic Council and to the CBT group of *iMed.UL* – Institute for Medicines and Pharmaceutical Sciences, University of Lisbon represented by Prof. Dr. Rui Moreira as *iMed.UL* institute leader; and Prof. Dr. Matilde Castro as the CBT group leader; for the reception and institutional support. I would like to thank you all for your dedicated work to these institutions.

A specially thanks to the sympathetic and “sportinguista” Prof. Dr. Rui Moreira and to Prof. Dr. Matilde Castro, who is for me a truly life example for her dedication to the family, friends, colleagues, students, faculty and science... I would like to thank Prof. Dr. Maria de Fátima Alfaiate Simões, with who I gave the first steps into the research field, for her availability, trust, friendship, sympathy and care; and also to Prof. Dr. Helena Cabral Marques and Prof. Dr. Camila Batoréu, for having written me a recommendation letter in order to apply for a PhD grant. I also would like to acknowledge some teachers and researchers of the CBT group including: Prof. Dr. Rita Guedes, Prof. Dr. Lídia Pinheiro, Prof. Dr. Célia Faustino, Prof. Dr. Nuno Oliveira and Master Ana Matos. In particular, I would like to emphasize the friendship, sympathy, support and comradeship of Prof. Dr. Ana Francisca and Dr. Isabel Ribeiro.

I also want to point out the exemplary conduct and friendship of Mrs. Felicidade, Mrs. Alice and Mrs. Prazeres, dedicated employees of FFUL institution.

To Fundação para a Ciência e a Tecnologia (FCT), for financial support. PhD grant: SFRH / BD / 30716 / 2006.

I would like to express my gratitude to my friends and lab mates; especially the above-mentioned João Rocha and Tiago Rodrigues for his tireless support during lunch and indispensable breaks for constructive scientific and non-scientific talks. I also would like to emphasize his friendship and comradeship. I want thank also my lab mates, including: Ana Sofia Fernandes, Joana Russo, João Marques, Inês Eusébio, Luís Ferreira, Maria Inês, Mário Nunes and Susana Vieira; and also my graduation friends: André Silva, Carla Gonçalves, Cláudia Oliveira, David Lopes, Nicole Carocha, Nuno Silva, Raquel Pirraça, Rute Ferreira, Solange Escobar and Telmo Silva, for their friendship and continuous support.

I would like to show my gratitude to my beloved parents and grandmother for their love, effort, encouragement, support, rightness, entrepreneurship, motivation, education and the transmission of proper Christian values. I am also grateful to my older sister for her love, care, support and protection. I want to acknowledge my parents, sister, parents-in-law and sister-in-law for their comprehension whenever the work was heavy and the spare time was reduced and also for their motivation and belief in this work. In

addition, I want to thank my sister-in-law, Cady, for helping me organizing the bibliography references of this thesis.

I would like to thank my beloved wife, Susana, for her love, support to move things forward and patience for some late home arrivals as well as for helping me organizing the bibliography references of this thesis. It really made a difference the way you believed in this project, so not surprisingly it changed into even better, since I met you. At last, more than dedicate this work to you, there is a part of it that really belongs to you 😊!

Finally, I want to praise God for His endless love and fidelity!

International peer-reviewed papers

This PhD thesis is based on the following papers:

Vila-Real, H.; Alfaia, A. J.; Bronze, M. R.; Calado, A. R. T.; Ribeiro, M.H., Biocatalytic production of the flavone glucosides: prunin and isoquercetin; and the aglycones: naringenin and quercetin (Submitted).

Vila-Real, H.; Alfaia, A. J.; Calado, A. R.; Phillips R. S.; Ribeiro, M. H. L., Stability of α -L-rhamnosidase and β -D-glucosidase activities expressed by naringinase, against temperature inactivation under high-pressure (Submitted).

Vila-Real, H.; Alfaia, A. J.; Phillips R. S.; Calado, A. R.; Ribeiro, M. H. L., Pressure-enhanced activity and stability of α -L-rhamnosidase and β -D-glucosidase activities expressed by naringinase. *J Mol Catal B: Enzym* **2010**, 65, 102-109.

Vila-Real, H.; Alfaia, A. J.; Rosa, M. E.; Calado, A. R.; Ribeiro, M. H. L., An innovative sol-gel naringinase bioencapsulation process for glycosides hydrolysis. *Process Biochem* **2010**, 45, 841-850.

Vila-Real, H.; Alfaia, A. J.; Rosa, M. E.; Calado, A. R.; Ribeiro, M. H. L., Improvement of activity and stability of soluble and sol-gel immobilized naringinase in co-solvent systems. *J Mol Catal B: Enzym* **2010**, 65, 91-101.

Vila-Real, H.; Alfaia, A. J.; Rosa, J. N.; Gois, P. M. P.; Rosa, M. E.; Calado, A. R. T.; Ribeiro, M. H., α -Rhamnosidase and β -glucosidase expressed by naringinase immobilized within new ionic liquid sol-gel matrices: activity and stability studies. *J Biotechnol* (doi:10.1016/j.jbiotec.2010.08.005).

Vila-Real, H.; Barateiro, A.; Fernandes, A.; Rocha, J.; Bronze, M. R.; Brites, D.; Ribeiro, M.H.R., *In vitro* anti-inflammatory effect of the flavanones: naringin, prunin and naringenin; distribution studies in mice plasma and brain (In preparation).

Contents

Figures	IX
Tables	XIII
Abbreviations and Symbols	XV
Resumo	XXIII
Abstract	XXVII
CHAPTER 1: Scientific background and objectives	1
1.1 General introduction	3
1.2 Alzheimer's disease	8
1.2.1 AD progression mechanisms	9
1.2.1.1 Formation of amyloid- β peptide plaques	9
1.2.1.2 Formation of neurofibrillary tangles	10
1.2.1.3 Inflammation	11
1.2.2 AD therapy	13
1.2.2.1 Amyloid cascade approaches	13
1.2.2.2 Tau pathology approaches	15
1.2.2.3 Anti-inflammatory approaches	15
1.3 Flavones – potential therapeutic drugs against AD	18
1.3.1 Chemical classification	18
1.3.2 Pharmacological activity	20
1.3.2.1 Naringin	22
1.3.2.2 Prunin	22
1.3.2.3 Naringenin	22
1.3.2.4 Rutin	23
1.3.2.5 Isoquercetin	23
1.3.2.6 Quercetin	23
1.3.3 Antioxidant therapy drawbacks in AD treatment	24
1.3.4 The role of the glycosidic residue	25
1.3.5 Enzymatic deglycosylation of flavone glycosides	26
1.3.5.1 Naringinase	27
1.4 Enzymatic biocatalysis	29
1.4.1 Structure of enzymes	29
1.4.2 Enzymatic kinetics	30
1.4.2.1 Kinetic parameters	32
1.4.3 Thermodynamic parameters	33

1.4.3.1	Temperature dependence at constant pressure	35
1.4.3.2	Pressure dependence at constant temperature	38
1.4.4	Enzymatic stability	42
1.4.4.1	Temperature	42
1.4.4.2	Pressure	43
1.4.4.3	Cosolvents	46
1.4.4.4	pH	47
1.4.4.5	Ionic activity	48
1.4.5	Enzymatic inactivation models	48
1.5	Enzymatic immobilization	50
1.5.1	Methods	51
1.5.1.1	Occlusion method	52
1.5.2	Immobilization supports	53
1.5.3	Immobilization within silica glasses through sol-gel method	54
1.5.3.1	Inorganic sol-gels	56
1.5.3.2	Organically modified silicates	57
1.5.3.3	Organic-inorganic nanocomposite sol-gels	58
1.5.3.4	Templated sol-gels	58
1.7	Objectives	61
1.8	Thesis design	63
CHAPTER 2: Biocatalytic production of the flavone glucosides, prunin and isoquercetin; and the aglycones, naringenin and quercetin		
2.1	Introduction	67
2.2	Material and Methods	69
2.2.1	Chemicals	69
2.2.2	Enzyme solution	69
2.2.3	Analytical methods	69
2.2.4	Activity measurement	70
2.2.5	pH profile	70
2.2.6	Inactivation kinetics	70
2.2.7	Experimental design	71
2.2.8	Statistical analysis	72
2.2.9	Verification experiments	73
2.2.10	Production and purification methods	73

2.3	Results and discussion	74
2.3.1	pH profile	74
2.3.2	Inactivation kinetics	75
2.3.3	RSM	76
2.3.4	Verification of the optimal temperature and pH inactivation conditions	79
2.3.5	Compounds production and identification	80
2.4.	Conclusions	82
 CHAPTER 3: Enzymatic biocatalysis using naringinase under pressure		83
3.1	Introduction	85
3.2	Material and Methods	87
3.2.1	Chemicals	87
3.2.2	Enzyme solution	87
3.2.3	High-pressure equipment	87
3.2.4	Analytical methods	89
3.2.5	Activity measurement	89
3.2.5.1	Inactivation kinetics	89
3.2.5.2	Reaction thermodynamic functions	89
3.2.5.3	Naringin bioconversion: combined effects of pressure and temperature	91
3.2.6	Inactivation conditions	91
3.2.6.1	Atmospheric pressure	91
3.2.6.2	Pressurized conditions	92
3.2.7	Parameters estimation	92
3.2.7.1	Inactivation rate constants	92
3.2.7.2	Reaction thermodynamic parameters	92
3.2.7.3	Enzymatic kinetic parameters	93
3.3	Results and Discussion	94
3.3.1	Inactivation kinetics	94
3.3.1.1	Thermal inactivation of α -L-rhamnosidase and β -D-glucosidase, at atmospheric pressure	94
3.3.1.2	Thermal inactivation of α -L-rhamnosidase and β -D-glucosidase, under pressure	96
3.3.2	Reaction thermodynamic functions	100
3.3.2.1	Pressure dependence	100

3.3.2.2	Temperature dependence	103
3.3.3	Combined effects of pressure and temperature on the kinetic parameters of naringin bioconversion	105
3.4	Conclusions	108
CHAPTER 4: Naringinase immobilization within silica glasses through sol-gel method		
111		
4.1	Introduction	113
4.2	Material and methods	116
4.2.1	Chemicals	116
4.2.2	Enzyme solution	116
4.2.3	Analytical methods	118
4.2.4	Naringin solubility	118
4.2.5	Immobilization protocol	118
4.2.5.1	Sol-gel precursors	119
4.2.5.2	Ionic liquids as additives of sol-gel	119
4.2.6	Matrix properties	120
4.2.7	Scanning Electron Microscopy	121
4.2.8	Activity measurement	121
4.2.8.1	Naringinase immobilized using several sol-gel precursors ..	121
4.2.8.2	Biocatalysis with immobilized naringinase using organic solvents	122
4.2.8.3	Sol-gel immobilization of naringinase using ILs as additives	122
4.2.9	Naringinase biochemical properties	123
4.2.10	Immobilization yield	123
4.2.11	Immobilization efficiency	124
4.2.12	Operational stability	124
4.2.12.1	Naringinase immobilized using several sol-gel precursors ..	125
4.2.12.2	Biocatalysis with immobilized naringinase using organic solvents	125
4.2.12.3	Sol-gel immobilization of naringinase using ILs as additives	126
4.3	Results and discussion	127
4.3.1	Optimization of naringinase immobilization using several sol-gel precursors	127
4.3.1.1	Effect of aging time / sol-gel precursors	128

4.3.1.2	Influence of TMOS/DGS ratio in matrix D	129
4.3.1.3	Effect of pH on gel formation	130
4.3.1.4	Influence of naringinase concentration	131
4.3.1.5	Drying conditions during aging	132
4.3.1.6	Immobilization characterization	133
4.3.1.7	Operational stability	137
4.3.2	Biocatalysis with immobilized naringinase using organic solvents	138
4.3.2.1	Biphasic systems	138
4.3.2.2	Aqueous cosolvent systems	138
4.3.2.3	Cosolvent stability studies	140
4.3.2.4	Kinetic study of naringin bioconversion.....	147
4.3.3	Sol-gel immobilization of naringinase using ILs as additives	149
4.3.3.1	Influence of ILs structure on sol-gel naringinase immobilization efficiency	150
4.3.3.2	Influence of ILs on the matrix structure and properties	155
4.3.3.3	Kinetic study of naringin and prunin bioconversion	159
4.3.3.4	Pressure influence on the stability of immobilized naringinase	161
4.4	Conclusions	163
CHAPTER 5: Study of the flavanones: naringin, prunin and naringenin in cell culture and animal models		165
5.1	Introduction	167
5.2	Material and methods	169
5.2.1	Chemicals	169
5.2.2	Cell cultures	169
5.2.3	Animal	170
5.2.4	Distribution studies	170
5.2.5	Blood sample preparation	170
5.2.6	Brain sample preparation	171
5.2.7	HPLC-MS analysis	171
5.3	Results and discussion	173
5.3.1	<i>In vitro</i> anti-inflammatory effect of naringin and naringenin	173
5.3.2	Preliminary studies concerning the distribution of the flavanones: naringin, prunin and naringenin in plasma and brain of mice after intraperitoneal administration	174
5.4	Conclusions	176

CONTENTS

CHAPTER 6: General discussion	177
CHAPTER 7: General conclusions and future perspectives	183
REFERENCES	187
ANNEX	213

FIGURES

Figure 1.1	Major pathways involved in the molecular activation mechanism of inflammation during aging and age-related diseases.	5
Figure 1.2	Aloysius Alzheimer.	8
Figure 1.3	The amyloid cascade.	9
Figure 1.4	Tau pathology.	10
Figure 1.5	Molecular structures of: phenylalanine amino acid and chromen-4-one.	18
Figure 1.6	Molecular structures of: 2- phenylchromen-4-one, 2,3-dihydro-2-phenylchromen-4-one and 3-hydroxy-2-phenylchromen-4-one.	19
Figure 1.7	Molecular structures of the flavanones: naringin, prunin and naringenin and the flavonols: rutin, isoquercetin and quercetin.	20
Figure 1.8	Radical mechanism of hydroquinone oxidation through a semiquinone radical intermediate to the quinone 1,4-benzoquinone.	21
Figure 1.9	Radical mechanism of a compound derived from the 3-hydroxy-2-phenylchromen-4-one nucleus.	21
Figure 1.10	Scheme of the production of flavonoid glucosides and aglycones starting from its rutosides precursors using an enzymatic approach.	27
Figure 1.11	Tridimensional structures of proteins.	29
Figure 1.12	Elliptic phase protein denaturing diagram.	45
Figure 1.13	Sol preparation: complete hydrolysis of a tetra-alkoxysilane, followed by condensation and polycondensation.	56
Figure 2.1	pH profiles of β -D-glucosidase and α -L-rhamnosidase.	74
Figure 2.2	Thermal inactivation of β -D-glucosidase and α -L-rhamnosidase, under combined temperature and pH conditions.	76
Figure 2.3	Response surface fitted to the experimental data points, corresponding to α -L-rhamnosidase residual activity, as a function of temperature and pH.	79
Figure 2.4	Inactivation kinetics of β -D-glucosidase and α -L-rhamnosidase, at 81.5°C and pH 3.9.	80
Figure 2.5	TLC of naringin, prunin, naringenin, rutin, isoquercetin and quercetin.	80
Figure 3.1	Pressure apparatus.	88

FIGURES

Figure 3.2	Temperature change inside the reaction vessel along time, during depressurization followed by pressurization till the desired pressure.	88
Figure 3.3	Thermal inactivation kinetics of: β -D-glucosidase (a) and α -L-rhamnosidase (b), at 0 MPa.	94
Figure 3.4	Temperature dependence of the inactivation constants of β -D-glucosidase and α -L-rhamnosidase, at 0 MPa.	96
Figure 3.5	Inactivation kinetics of β -D-glucosidase at 75.0 °C (a) and α -L-rhamnosidase at 85.0 °C (b), under several pressure conditions.	97
Figure 3.6	Pressure dependence of the inactivation constant of β -D-glucosidase at 75.0 °C and α -L-rhamnosidase at 85.0 °C.	99
Figure 3.7	Pressure dependence of the equilibrium constant of β -D-glucosidase and α -L-rhamnosidase.	101
Figure 3.8	Pressure dependence of: β -D-glucosidase, α -L-rhamnosidase and naringinase.	103
Figure 3.9	Michaelis-Menten kinetics of naringinase, at different temperatures, at 0 MPa (a) and 150 MPa (b).	105
Figure 3.10	Temperature dependence of the Michaelis-Menten of naringinase, at 0 MPa and 150 MPa.	106
Figure 3.11	Temperature dependence of the catalytic constant (a) and second order constant (b) of naringinase, at 0 MPa and 150 MPa.	107
Figure 4.1	Influence of the aging time on the immobilization reuse efficiency coefficient of the sol-gel matrices, A – F; for five runs (a) and after five runs (b).	129
Figure 4.2	Influence of the TMOS/DGS ratio on the immobilization reuse efficiency coefficient of the sol-gel matrix D, for five runs (a) and after five runs (b).	130
Figure 4.3	Influence of pH on the immobilization efficiency coefficient of the sol-gel matrices A – D.	131
Figure 4.4	Influence of the naringinase concentration on the immobilization efficiency coefficient of the sol-gel matrices A – D.	131
Figure 4.5	a) Influence of the aging system (open-air, half-open and closed) on the naringinase residual activity of the sol-gel matrix B, after 23 successive runs and b) diameter. c) SEM microphotographs of the sol-gel matrices (TMOS + glycerol) obtained under different conditions for encapsulated naringinase.	133
Figure 4.6	Diameter and Volume of matrices: A – D. Photo of matrices: A – D.	134
Figure 4.7	a) Temperature profile of free and immobilized naringinase in sol-gel matrices: A – D. b) pH profile of free naringinase and naringinase immobilized within sol-gel matrices: A – D.	135

Figure 4.8	Yield and efficiency of immobilized naringinase within matrices: A – D.	136
Figure 4.9	a) Residual activity of naringinase after fifty reutilization runs of the sol-gel matrices: A – D. b) SEM micrographs of the sol-gel matrices: A – D with encapsulated naringinase.	137
Figure 4.10	Stability of α -L-rhamnosidase expressed by soluble and immobilized naringinase in cosolvent systems.	143
Figure 4.11	Stability of β -D-glucosidase expressed by soluble and immobilized naringinase in cosolvent systems.	144
Figure 4.12	Michaelis-Menten kinetics of soluble naringinase, in several aqueous cosolvent systems.	148
Figure 4.13	Michaelis-Menten kinetics of naringinase, in aqueous cosolvent system composed of different concentrations of 1,2-dimethoxyethane.	148
Figure 4.14	Influence of ILs on the efficiency of α -L-rhamnosidase (a) and β -D-glucosidase (b) immobilized in TMOS sol-gel matrices with and without glycerol, after 19 consecutive runs.	149
Figure 4.15	Influence of the incorporation of ILs in silica sol and in the enzymatic solution, on the efficiency of α -L-rhamnosidase (a) and β -D-glucosidase (b), after 19 consecutive reutilizations.	150
Figure 4.16	Influence of ILs on the immobilization reuse efficiency of α -L-rhamnosidase encapsulated within sol-gel matrices repeatedly used over 50 runs.	152
Figure 4.17	Influence of ILs on the immobilization reuse efficiency of β -D-glucosidase encapsulated within sol-gel matrices repeatedly used over 50 runs.	153
Figure 4.18	Macroscopic structure of matrices before use: I (TMOS/Glycerol), II (TMOS/Glycerol/[C ₂ OHMIM][PF ₆]) and III (TMOS/Glycerol/[OMIM][Tf ₂ N]); and matrices reused over 50 runs: I ₅₀ (TMOS/Glycerol), II ₅₀ (TMOS/Glycerol/[C ₂ OHMIM][PF ₆]) and III ₅₀ (TMOS/Glycerol/[OMIM][Tf ₂ N]).	156
Figure 4.19	SEM microphotographs of matrices before use: I (TMOS/Glycerol), II (TMOS/Glycerol/[C ₂ OHMIM][PF ₆]) and III (TMOS/Glycerol/[OMIM][Tf ₂ N]); and matrices reused over 50 runs: I ₅₀ (TMOS/Glycerol), II ₅₀ (TMOS/Glycerol/[C ₂ OHMIM][PF ₆]) and III ₅₀ (TMOS/Glycerol/[OMIM][Tf ₂ N]).	157
Figure 4.20	SEM structure detail of the sol-gel matrix III (TMOS/Glycerol/[OMIM][Tf ₂ N]). III _S corresponds to the surface of the lens while III _I is the inner part of the matrix.	157
Figure 4.21	a) Michaelis-Menten kinetics of naringin hydrolysis into prunin by α -L-rhamnosidase b) Michaelis-Menten kinetics of prunin hydrolysis into naringenin by β -D-glucosidase.	160

FIGURES

Figure 4.22	Residual activity of α -L-rhamnosidase (a) and β -D-glucosidase (b), from immobilized naringinase entrapped within a TMOS/Glycerol matrix, under 0 or 150 MPa, at 50.0 °C.	161
Figure 4.23	Residual activity of α -L-rhamnosidase, from immobilized naringinase entrapped within a TMOS/Glycerol/[OMIM][Tf ₂ N] matrix, under 0 or 150 MPa, at 50.0 °C.	162
Figure 5.1	Determination of TNF- α concentration, after an incubation time period of 4 h with: LPS, naringin, indomethacin and naringenin; as well as co-incubation of LPS with naringin, indomethacin and naringenin.	173
Figure 5.2	Determination of TNF- α concentration, after an incubation time period of 8 h with: LPS, naringin, indomethacin and naringenin; as well as co-incubation of LPS with naringin, indomethacin and naringenin.	173
Figure 5.3	Determination of TNF- α concentration, after an incubation time period of 24 h with: LPS, naringin, indomethacin and naringenin; as well as co-incubation of LPS with naringin, indomethacin and naringenin.	174

TABLES

Table 2.1	Coded and decoded levels of the experimental factors used in experimental design.	72
Table 2.2	Optimum pH values of β -D-glucosidase and α -L-rhamnosidase. ...	75
Table 2.3	Thermal inactivation parameters of β -D-glucosidase and α -L-rhamnosidase, under combined temperature and pH conditions.	76
Table 2.4	Effects and respective significance levels of temperature and pH on α -L-rhamnosidase residual activity.	77
Table 2.5	Second-order model equations for the response surfaces fitted to the experimental data points of α -L-rhamnosidase residual activity, as a function of temperature and pH, and respective R^2 and R^2_{adj}	78
Table 2.6	Results of TLC analysis of naringin, prunin, naringenin, rutin, isoquercetin and quercetin.	81
Table 3.1	Correspondence between the temperature overheating and the attained pressure values of 150, 200 and 250 MPa and respective compression rates.	88
Table 3.2	Thermal inactivation parameters of β -D-glucosidase and α -L-rhamnosidase, at 0 MPa.	95
Table 3.3	Thermodynamic parameters of the thermal inactivation of β -D-glucosidase and α -L-rhamnosidase, at 0 MPa.	96
Table 3.4	Inactivation kinetics parameters of β -D-glucosidase at 75.0 °C and α -L-rhamnosidase at 85.0 °C, under several pressure conditions.	97
Table 3.5	Thermodynamic parameters of the inactivation kinetics of β -D-glucosidase at 75.0 °C and α -L-rhamnosidase at 85.0°C, under several pressure conditions.	100
Table 3.6	Estimation of the reaction volumes of β -D-glucosidase and α -L-rhamnosidase.	101
Table 3.7	Estimation of the activation volumes of β -D-glucosidase, α -L-rhamnosidase and naringinase.	103
Table 3.8	Temperature activation parameters of β -D-glucosidase, α -L-rhamnosidase and naringinase, at 0 MPa.	104
Table 4.1	Ionic liquids used in sol-gel bio-immobilization.	117
Table 4.2	Immobilization protocol using several sol-gel precursors.	119
Table 4.3	Immobilization protocol within different sol-gel/ILs matrices.	120
Table 4.4	Characterization of matrix B according to the aging system used. ...	133

TABLES

Table 4.5	Properties of matrices A – D and naringinase efficiency.	134
Table 4.6	Optimum pH values of the sol-gel matrices A – D.	136
Table 4.7	Yield, efficiency and operational stability characterization of sol-gel matrices, A – D.	138
Table 4.8	Naringin solubility in several cosolvents systems, at 25 °C.	139
Table 4.9	Residual activity of β -D-glucosidase and α -L-rhamnosidase expressed by soluble naringinase, in 5 % (v/v) of cosolvent.	140
Table 4.10	Inactivation parameters of α -L-rhamnosidase expressed by soluble and immobilized naringinase within cosolvent systems.	145
Table 4.11	Inactivation parameters of β -D-glucosidase expressed by soluble and immobilized naringinase within cosolvent systems.	146
Table 4.12	Kinetic parameters of soluble naringinase, in 10 % (v/v) aqueous cosolvent systems.	147
Table 4.13	Kinetic parameters of soluble naringinase, in aqueous cosolvent system composed of 1,2-dimethoxyethane.	148
Table 4.14	Influence of ILs on the immobilization reuse efficiency of α -L-rhamnosidase and β -D-glucosidase encapsulated within sol-gel matrices.	154
Table 4.15	Partition coefficients between matrix and 20 Mm acetate buffer at pH 4.0, of the substrates and products used in this study.	158
Table 4.16	Physical properties of TMOS/Glycerol/[OMIM][Tf ₂ N], TMOS/Glycerol/[C ₂ OHMIM][PF ₆] and TMOS/Glycerol matrices.	158
Table 4.17	Kinetic parameters of the hydrolysis of naringin and prunin by α -L-rhamnosidase and β -D-glucosidase using free and immobilized naringinase within sol-gel matrices.	160

ABBREVIATIONS AND SYMBOLS

a	Enzymatic activity
A	Enzymatic specific activity; Empirical fitting parameter
A_0	Specific activity of the initial active enzyme
A_1	Specific activity of the enzyme intermediate
A_2	Specific activity of the final enzyme state
$A\beta$	Amyloid- β peptide
AD	Alzheimer's disease
A_{\max}	Maximum enzyme specific activity
AMs	Adhesion molecules
<i>APOE</i>	Apolipoprotein E gene
APP	Amyloid precursor protein
<i>APP</i>	Amyloid precursor protein gene
APS	3-Aminopropyltrimethoxysilane
A_r	Residual activity
A_{rel}	Relative activity
A_t	Enzyme specific activity after a certain inactivation period
atm	Atmosphere
a_y	Ionic activity
B	Empirical fitting parameter
BACE1	β -site APP cleaving enzyme 1
BBB	Blood-brain barrier
[BF ₄]	Tetrafluoroborate
[BMIM]	1-Butyl-3-methylimidazolium
c	Concentration
C	Empirical fitting parameter
°C	Celsius degrees
c_0	Initial concentration
CCRD	Central composite rotatable design
[Cl]	Chloride
CNS	Central nervous system
CO ₂	Carbon dioxide

ABBREVIATIONS AND SYMBOLS

[C ₂ OHMIM]	1-Ethanol-3-methylimidazolium
COX	Cyclooxygenase
COX-2	Cyclooxygenase-2
C _p	Specific heat capacity
ΔC _p	Specific heat capacity change
<i>CRI</i>	Complement receptor 1 gene
<i>c_x</i>	Concentration of cosolvent
<i>d</i>	Derivative
DAD	Photodiode array detector
DCA	Dicyanoamide
DGS	Diglycerylsilane
<i>d_m</i>	Matrix density
<i>D_m</i>	Matrix diameter
DMEM	Dulbecco's modified Eagle's medium
[DMP]	Dimethylphosphate
DNA	Deoxyribonucleic acid
DNS	3,5-Dinitrosalicylic acid
E	Enzyme
E ⁻	Inactive deprotonated enzyme
<i>E_a</i>	Activation energy
EH	Active enzyme
EH ₂ ⁺	Inactive protonated enzyme
Eq.	Equation
[EMIM]	1-Ethyl-3-methylimidazolium
[E ₂ -MPy]	1-Ethyl-2-methylpyridinium
[E ₃ -MPy]	1-Ethyl-3-methylpyridinium
ES	Enzyme-substrate complex
ESI	Electrospray ion source
E _t	Total enzyme amount
[ESO ₄]	Ethylsulphate
<i>F</i>	Snedecor statistical parameter
<i>F_c</i>	Snedecor statistical critical value
FCS	Fetal calf serum

FEG-SEM	Scanning electron microscopy – field emission gun
F-test	Fisher-Snedecor test
g	Gram
G	Gibbs energy
ΔG	Gibbs energy change
$\Delta^\ddagger G$	Gibbs energy of activation
ΔG°	Standard Gibbs energy
$\Delta^\ddagger G^\circ$	Standard Gibbs energy of activation
G_D	Gibbs energy of the protein denatured state
GFAP	Glial fibrillary acidic protein
GLUT2	Glucose transporter-2
G_N	Gibbs energy of the protein native state
GP_x	Glutathione peroxidase
GSH	Glutathione
GSR	Glutathione reductase
h	Hour
h	Plank constant ($6.6260693 \times 10^{-34}$ J s) (IUPAC, 2006)
H	Enthalpy
ΔH	Enthalpic term; Enthalpy change
$\Delta^\ddagger H$	Activation enthalpy
ΔH°	Standard enthalpy
$\Delta^\ddagger H^\circ$	Standard activation enthalpy
H^+	Proton
hCBG	Cytosolic β -glucosidase
HMG-CoA	3-hydroxy-3-methyl-glutaryl-coenzyme A
HPLC	High performance liquid chromatography
IKK	I kappa B kinase
IL	Interleukin; Ionic liquid
ILs	Ionic Liquids
iNOS	Inducible nitric oxide synthase
i.p.	Intraperitoneal administration
J	Joule
k	Reaction rate constant; inactivation rate constant

ABBREVIATIONS AND SYMBOLS

k^o	Standard reaction rate constant
K	Equilibrium constant
K^\ddagger	Equilibrium constant for the quasi-equilibrium
K	Kelvin
k_1	First inactivation rate constant
K_1	First equilibrium constant
k_2	Second inactivation rate constant
K_2	Second equilibrium constant
K_a	Association constant
k_{atm}	Inactivation rate constant at a atmospheric pressure
k_B	Boltzmann constant ($1.3806505 \times 10^{-23} \text{ J K}^{-1}$) (IUPAC 2006)
k_{cat}	Catalytic constant
$k_{\text{cat}} \cdot K_M^{-1}$	Specificity constant; Apparent second-order rate constant
KJ	Kilojoule
K_M	Michaelis-Menten constant
k_P	Inactivation rate constant at a certain pressure value
L	Litre
μL	Microlitre
LDL	Low-density lipoprotein
ln	Natural logarithm
log	Decimal logarithm
$\log P$	Decimal logarithm of the octanol/water partition coefficient
LPH	Lactase-phlorizin hydrolase
LPS	Bacterial endotoxin lipopolysaccharide
LRP-1	Low-density lipoprotein receptor-related protein 1
m	Meter
M	Molarity
μM	Micromolar concentration
[MeOEtOEtOSO ₃]	2-(2-Methoxyethoxy)ethylsulphate
min	Minute
mL	Millilitre
mM	Millimolar concentration
mm	Millimetre

mmol	Millimole
mol	Mole
μmol	Micromole
MAPKs	Mitogen-activated protein kinases
MPa	Megapascal
MS	Mass spectrometer
MTS	Methyltrimethoxysilane
<i>n</i>	Sample size
N_A	Avogadro constant ($6.0221415 \times 10^{23} \text{ mol}^{-1}$) (IUPAC 2006)
NF-κB	Nuclear factor kappa-light-chain-enhancer of activated B cells
NFTs	Neurofibrillary tangles
4-NGP	<i>p</i> -Nitrophenyl β-D-glucopyranoside
NMDA	N-methyl-D-aspartate
n_m	Size of the matrices sample
4-NRP	<i>p</i> -Nitrophenyl α-L-rhamnopyranoside
NSAIDs	Non-steroidal anti-inflammatory drugs
Ormosils	Organically modified silicates
[OMIM]	1-Octyl-3-methylimidazolium
OX-42	CR3 complement receptor of microglia
<i>p</i>	Significance level
<i>P</i>	Pressure
p.	Page
P	Product
Pa	Pascal
PAI-1	Low-density lipoprotein receptor-related protein 1
PBS	Phosphate buffered saline
PEG	Polyethylene glycol
[PF ₆]	Hexafluorophosphate
pH	$-\log [\text{H}_3\text{O}^+]$
pH _{opt}	Optimum pH value
p <i>K</i> _a	$-\log [K_a]$
$P_{m/s}$	Partition coefficient between matrix and external solvent
<i>PS1</i>	Presenilin 1 gene

ABBREVIATIONS AND SYMBOLS

<i>PS2</i>	Presenilin 2 gene
<i>q</i>	Number of parameters
<i>R</i>	Correlation coefficient; Gas constant (8.314472 J K ⁻¹ mol ⁻¹) (IUPAC 2006)
<i>R</i> ²	Coefficient of determination
<i>R</i> ² _{adj}	Adjusted coefficient of determination
RAGE	Receptor for advanced glycation end products
Rf	Retention factor
RNS	Reactive nitrogen species
ROS	Reactive oxygen species
RS	Reactive species
RSM	Response surface methodology
s	Second
<i>S</i>	Entropy
ΔS	Entropy change
$\Delta^\ddagger S$	Activation entropy
ΔS°	Standard entropy
$\Delta^\ddagger S^\circ$	Standard activation entropy
<i>S</i>	Substrate
SD	Standard deviation
SE	Standard error
SEM	Scanning electron microscopy
SLGT1	Sodium dependent glucose transporter
SOD	Superoxide dismutase
SSE	Sum of square residues
<i>t</i>	Time
<i>T</i>	Temperature; absolute temperature
<i>t</i> _{0.01%}	Time that corresponds to a relative activity of 0.00001
<i>t</i> _{1/2}	Reuse half-life time, Inactivation half-life time
<i>t</i> _{1/2 imm}	Reuse half-life time of immobilized enzyme
<i>t</i> _{1/2 sol}	Reuse half-life time of soluble enzyme
TEOS	Tetraethylortosilicate
TFA	Thermodynamic functions of activation

[TFA]	Trifluoroacetate
[Tf ₂ N]	Bis(trifluoromethylsulfonyl)imide
TfO	Trifluoro methane sulfonate
TGF-β	Transforming growth factor-beta
TLC	Thin layer chromatography
TMOS	Tetramethylortosilicate
TNF-α	Tumour necrosis factor-alpha
TST	Transition state theory
TΔS	Entropic term
UV	Ultra-violet
v	Initial reaction rate
v	Volume
V	Volume
ΔV	Volume change
$\Delta^\ddagger V$	Activation volume
ΔV°	Standard volume
$\Delta^\ddagger V^\circ$	Standard activation volume
V_D	Denatured state volume
VEGF	Vascular endothelial growth factor
v_{free}	Rate of the reaction catalyzed by the free enzyme
v_{imm}	Rate of the reaction catalyzed by the immobilized enzyme
V_{is}	Internal solvent volume
V_{m}	Matrix volume
v_{max}	Maximum initial reaction rate
V_{N}	Native state volume
ΔV_{reac}	Reaction volume
$\Delta V_{\text{reac}}^\circ$	Standard reaction volume
vs.	Versus
V_{s}	Volume occupied by water
V_{t}	Total system volume
w	Mass
w_{E}	Mass of enzyme
w_{Eimm}	Mass of the immobilized enzyme

ABBREVIATIONS AND SYMBOLS

w_{Eimm}	Mass of the total amount of enzyme
w_{m}	Matrix mass
x	Independent variable
y	Immobilization yield
y	Dependent variable
α	Specific activity ratio; Thermal expansion factor
α_1	Specific activity ratio ($A_1 \times A_0^{-1}$)
α_2	Specific activity ratio ($A_2 \times A_0^{-1}$)
β	Compressibility factor
β_0	Empirical coefficient
β_1	Empirical coefficient
β_2	Empirical coefficient
β_{11}	Empirical coefficient
β_{12}	Empirical coefficient
δ	Partial derivative
Δ	Finite change
$\Delta\beta$	Isothermal compressibility
$\Delta\beta^\circ$	Standard isothermal compressibility
$\Delta^\ddagger\beta$	Isothermal compression of activation
$\Delta^\ddagger\beta^\circ$	Standard isothermal compression of activation
η	Efficiency coefficient
$[]$	Concentration

RESUMO

O Século XX trouxe consigo uma profunda alteração demográfica nos países industrializados impulsionada pelo desequilíbrio entre as taxas de fertilidade e mortalidade, levando a um aumento proporcional da população mais idosa que continuará pelo século XXI. O envelhecimento populacional observado condiciona deste modo o direccionar da descoberta de novos fármacos para novos campos de investigação. A demência surge de entre as doenças relacionadas com a idade como uma preocupação de saúde pública à escala mundial. Em particular, alguns estudos apontam para um crescimento galopante da doença de Alzheimer, a forma mais comum de demência irreversível. A doença de Alzheimer é por isso um motivo de crescente preocupação dado que não só é baixa a qualidade de vida do portador e de quem cuida do doente mas também o investimento por parte do sistema de saúde será cada vez mais avultado. Urge assim a necessidade de investigar novas terapêuticas com efeito modificador da doença, uma vez que os medicamentos actualmente existentes no mercado apenas aliviam sintomas.

Neste sentido, esta tese de doutoramento sustenta o desenvolvimento de uma abordagem biotecnológica com vista à produção de flavonas potencialmente activas contra a doença de Alzheimer. Na base deste potencial desempenho terapêutico está a evidência de fenómenos inflamatórios característicos da patologia da doença de Alzheimer, bem como a actividade anti-inflamatória descrita como propriedade farmacológica comum aos compostos pertencentes ao grupo dos flavenóides, como é o caso das flavonas. Os compostos biossintetizados poderão constituir a chave para a resolução de problemas relacionados com a dificuldade em permear a barreira hematoencefálica e deste modo serem direccionados para o cérebro onde poderão actuar contra a doença de Alzheimer numa abordagem anti-inflamatória.

Mais detalhadamente, este trabalho ambiciona a produção respectiva de glucósidos e agliconas, através da desglicosilação enzimática de substratos naturais abundantes como os rutinósidos de flavonas: naringina e rutina. A concepção deste bioprocessos faz uso de ferramentas chave como sejam a pressão e a imobilização enzimática, entre outras condições que incluem: a temperatura, o pH e a utilização de solventes orgânicos e líquidos iónicos. A modulação e optimização destas condições, tem como objectivo maximizar a eficiência desta abordagem biotecnológica que encerra em si própria os seguintes objectivos específicos. (I) Desenvolver um processo biocatalítico, visando a

produção dos glucósidos: prunina e isoquercetina, bem como as agliconas: naringenina e quercetina, partindo dos respectivos rutinósidos de flavonas: naringina e rutina, utilizando a naringinase; (II) Utilizar a pressão como ferramenta que poderá permitir aumentar a eficiência do bioprocesso: quer por aumento da estabilidade do biocatalisador a temperaturas elevadas, preservando o seu estado nativo; quer por aumento da actividade desse mesmo biocatalisador, acelerando o processo em si. (III) Utilizar o processo de imobilização enzimática como meio de facilitar a sua recuperação do meio reaccional, permitindo deste modo a sua reutilização. A imobilização da naringinase em matrizes de sol-gel visa alcançar uma boa performance do biocatalisador, incluindo: rendimento, actividade e estabilidade operacional; um outro objectivo da imobilização da naringinase consiste no aumento da sua estabilidade contra a inactivação provocada por solventes orgânicos. (IV) Por último, mas não menos importante, estudar uma possível utilização vantajosa de glucósidos e agliconas para permear a barreira hemato-encefálica, por oposição aos rutinósidos, com vista a direccionar determinadas flavonas para o cérebro.

Em virtude de um delineamento experimental adequado os objectivos acima descritos puderam ser concretizados. Quanto à concepção do bioprocesso em si mesmo, os objectivos alcançados dividem-se em três tarefas distintas.

- A produção das agliconas: naringenina e quercetina, partindo respectivamente da naringina e rutina, por meio da naringinase. Quanto à produção dos glucósidos: prunina e isoquercetina, partindo dos rutinósidos referidos foi necessário recorrer a um método de desactivação selectiva da β -D-glucosidase expressa pela naringinase, através de condições optimizadas de temperatura (81.5 °C) e pH (3.9). Após esta desactivação selectiva foi possível produzir os glucósidos em causa utilizando a actividade remanescente da α -L-ramnosidase. Todos os produtos foram obtidos com elevada pureza e com um bom rendimento atendendo ao seu valor económico, sobretudo os glucósidos: prunina e isoquercetina. Deste modo foi desenvolvido um método potencialmente bastante competitivo sobretudo para a produção destes glucósidos.

- As condições de pressão estudadas permitiram aumentar a estabilidade de ambas as actividades expressas pela naringinase: β -D-glucosidase e α -L-ramnosidase quando sujeitas a temperaturas elevadas. No caso da α -L-ramnosidase verificou-se um aumento da estabilidade em 32 vezes (250 MPa e 85.0°C) relativamente à pressão atmosférica, enquanto que no caso da β -D-glucosidase se verificou um aumento de 30 vezes (200

MPa e 75.0 °C). Este facto é concordante com um diagrama de fase de desnaturação proteica, com uma forma elíptica. Este efeito protector da pressão é bastante útil, permitindo aumentar a temperatura reaccional o que não só aumenta a velocidade da reacção, mas também a solubilidade dos substratos: naringina e rutina, os quais se tornam mais solúveis em água com o aumento da temperatura. Quanto à influência da pressão sobre a velocidade reaccional, verificou-se que a actividade da α -L-ramnosidase é favorecida pela pressão ($\Delta^\ddagger V = -7.7 \pm 1.5 \text{ mL mol}^{-1}$) contrariamente à actividade da β -D-glucosidase ($\Delta^\ddagger V = 6.5 \pm 1.9 \text{ mL mol}^{-1}$), ambas expressas pela naringinase. De acordo com estes resultados faria supor que as condições de pressão apenas seriam úteis no caso da produção de glucósidos a partir de rutinósidos, por meio da actividade da α -L-ramnosidase. Contudo, o estudo da hidrólise da naringina a naringenina sob condições de pressão demonstrou que também no caso da produção de agliconas partindo de rutinósidos, a pressão é uma ferramenta adequada para acelerar a reacção enzimática ($\Delta^\ddagger V = -20 \pm 5.2 \text{ mL mol}^{-1}$), que neste caso ocorre em dois passos consecutivos. A pressão demonstrou assim ser uma óptima ferramenta para a eficiência global do bioprocessamento em estudo.

- A imobilização da naringinase em matrizes de sol-gel foi conseguida com sucesso, podendo assim ser recuperada do meio reaccional e reutilizada durante um número bastante elevado de ciclos. A imobilização da naringinase em matrizes de sol-gel (TMOS/glicerol) apresentou uma elevada performance (89% de rendimento, 72% de eficiência e 100% de actividade residual ao fim de 50 reutilizações). A naringinase imobilizada nesta matriz demonstrou uma elevada resistência contra a inactivação provocada por um vasto portfólio de cossolventes em estudo (aumento do tempo de meia-vida superior a 3 vezes). A importância destes resultados incide novamente na baixa solubilidade das flavonas utilizadas como substratos, a qual pode ser aumentada através da utilização de cossolventes orgânicos. A adição dos líquidos iónicos [OMIM][Tf₂N] e [C₂OHMIM][PF₆] à matriz de sol-gel permitiu aumentar a eficiência das actividades da α -L-ramnosidase e da β -D-glucosidase, respectivamente.

Finalmente, considerando a potencial aplicação dos compostos biossintetizados na terapêutica da doença de Alzheimer, estudos preliminares suportam a hipótese da utilização do glucósido prunina bem como da aglicona naringenina no sentido de permear a barreira hemato-encefálica, que é uma vantagem importantíssima para assim poder atingir o local de acção dentro do cérebro, quando comparado com o rutinósido

RESUMO

naringina que com base nos resultados disponíveis não parece ser capaz de atravessar a barreira hemato-encefálica.

Palavras-chave: Doença de Alzheimer, flavonas, pressão, imobilização, naringinase.

ABSTRACT

This thesis sustains a biotechnological approach design for the production of potential active flavones against Alzheimer's disease (AD), based on inflammation evidences observed on AD pathology and the common shared anti-inflammatory activity of flavonoids. The produced compounds may be the key to circumvent some issues related to blood-brain barrier (BBB) permeability, targeting AD through an anti-inflammatory approach.

This work aims to produce the respective glucosides and aglycones of the flavone glycosides: naringin and rutin, through enzymatic deglycosylation. The bioprocess design makes use of pressure and biocatalyst immobilization as keystone tools among other conditions, including: temperature, pH and use of organic solvents and ionic liquids. The modulation and optimization of these conditions aims to maximize the efficiency of this biotechnological approach.

In bioprocess design, the achievements are divided into three groups. The first one consisted on the production of glucosides and aglycones of naringin and rutin, respectively, with naringinase and partially inactivated naringinase at optimized conditions of 81.5 °C and pH 3.9. A second one showed how pressure increased α -L-rhamnosidase activity leading to an activation volume of $-7.7 \pm 1.5 \text{ mL mol}^{-1}$. Moreover the stability against heat of α -L-rhamnosidase and β -d-glucosidase expressed by naringinase increased, respectively, 32-fold at 250 MPa and 85.0 °C, and 30-fold at 200 MPa and 75.0 °C, than at 0 MPa. Finally, the third one is related with the high performance shown by naringinase entrapped within silica glasses (TMOS/glycerol) through sol-gel method (89% yield, 72% efficiency and 100% residual activity). Naringinase within this matrix showed a high resistance against cosolvent inactivation (half-life time increase, more than 3 fold). The addition of the ionic liquids [OMIM][Tf₂N] and [C₂OHMIM][PF₆] to the sol-gel matrices increased the efficiency of both α -L-rhamnosidase and β -D-glucosidase activities, respectively.

Considering the potential application of the produced drugs on the therapeutics of AD, preliminary studies support the hypothesis that prunin and naringenin can cross the BBB, which is a striking advantage to target AD comparing to naringin.

Key-words: Alzheimer's disease, flavone, pressure, immobilization, naringinase.

SCIENTIFIC BACKGROUND AND OBJECTIVES

Chapter 1

1.1 General introduction

20th century brought deep demographic changes in industrialized countries due to fertility and mortality rates imbalance, leading to a proportion increase of the older population, which will continue through the 21st century. Not only European but also American population projections show that around 2050-2060 up to 25 – 30% of the population will be aged 65 years or older (Bustacchini *et al.*, 2009). This demographic change is the basis of the increase of age-related diseases incidence and is shifting drug research into new fields. Within the group of age-related diseases are included many diseases such as: atherosclerosis, hypernatremia, metabolic syndrome, cancer, prostate enlargement, osteoporosis, osteoarthritis, insulin resistance, age-related macular degeneration, dementia, cognitive dysfunction, Alzheimer's (AD) and Parkinson's diseases (Baquer *et al.*, 2009; Blagosklonny *et al.*, 2009; Chung *et al.*, 2009). Among these, dementia has become a public health concern worldwide (Fothui *et al.*, 2009); not only due to the patient clinical and functional status, but also due to the low life quality of caregivers, as well as the healthcare costs associated with medical assistance and healthcare interventions (Bustacchini *et al.*, 2009). Eliminating AD won't increase that much the maximum human lifespan, due to the existence of so many other diseases (Blagosklonny *et al.*, 2009), but at least it will eliminate a very heavy disease concerning the patient's family as well as the healthcare system.

According to Shineman *et al.*, 2010 is not yet known whether cognitive aging may be the beginning of a process that sometimes ends in dementia or if other events are needed. Pure dementia cases are only a small percentage that contributes to brain atrophy inside a large quantity of genetic and environmental factors such as: apolipoprotein E genotype, obesity, diabetes, hypertension, head trauma, systemic illnesses and obstructive sleep apnea (Fothui *et al.*, 2009). Simultaneously it is known the role played by oxidative stress through oxidative damage and redox imbalance in the pathogenesis of neurodegenerative diseases (Chung *et al.*, 2009), particularly Alzheimer's disease (Sultana *et al.*, 2006).

The "oxidative stress hypothesis" (Yu and Yang, 1996), an upgrade version of the free radical theory of aging (Harman, 1956), describes the actual knowledge of the aging mechanism, where nucleic acids, proteins and lipids suffer an oxidative damage by uncontrolled production of reactive oxygen species (ROS), reactive nitrogen species (RNS) and also reactive lipid species. In the case of cell membrane fatty acids and

proteins the radical species action leads to permanent function impairment, but in the case of DNA damage they can lead to DNA mutations, which may turn to be the basis of age-related disorders, among others, such as cancer (Khansari *et al.*, 2009). In 1972, Harman found that mitochondria were responsible for the initiation of most of the free radical reactions, due to aerobic respiration. Nowadays, several cellular activities are known to generate radical species (RS), including: lipoxygenase; cyclooxygenase (COX); plasma membrane-associated NADPH oxidase; mitochondrial electron transport system; ubiquinone; NADH dehydrogenase; cytochrome P450; cytochrome b₅; microsomal electron transport; flavoproteins; oxidases in peroxisome and xanthine oxidase cytosol (Bodamyali *et al.*, 2000). Besides the RS produced from cellular metabolism there is also the contribution of environmental factors, including: physical, biological and chemical stressors, where pollution is a major concern contributing to systemic oxidative stress (Gomez-Mejiba *et al.*, 2009). In order to fight against oxidative damage, the human body possesses an antioxidant defence system that includes enzymes, such as: superoxide dismutase (SOD), glutathione peroxidase (GPx), glutathione reductase (GSR) and catalase; endogenous non-enzymatic defences: glutathione (GSH), bilirubin, thiols, albumin, and uric acid; and nutritional factor including vitamins and phenols (Lykkesfeldt *et al.*, 1998; Fusco *et al.*, 2007).

The basis of the oxidative damage, during aging, is this debility of antioxidant defences that triggers a redox imbalance (Chung *et al.*, 2009). Aging is responsible for weaken the antioxidant defence, being characterized by a decrease of GSH and GSR levels, one of the most abundant and effective anti-oxidative reductant (Cho *et al.*, 2003). Specifically concerning brain, the age related neuronal damage is even stressed by other factors, such as: high oxygen consumption rate from aerobic metabolism; abundant lipid content and low antioxidant enzymes content, when compared to other organs (Baquer *et al.*, 2009). Oxidative damage is suggested to mediate mitochondria dysfunction which may play a significant role in aging and age-related neurological diseases, including: Alzheimer's, Parkinson's, Huntington's, amyotrophic lateral sclerosis and Freidreich ataxia. As a result of the interaction of mutant proteins with mitochondrial proteins, the electron transport chain is disrupted and generates ROS that inhibit the ATP mitochondrial production, which is a vital energy source for brain cells; further, the accumulation of mitochondrial DNA may contribute to mitochondria dysfunction during aging (Reddy, 2008).

Figure 1.1 shows how oxidative stress may cause a chronic molecular inflammation which was found to be the major biological mechanism behind aging process and age-related diseases (Chang *et al.*, 2006; Khansari *et al.*, 2009). The generated redox imbalance enhances upstream signalling pathways such as I κ B kinase (IKK) and mitogen-activated protein kinases (MAPKs) that modulate the activity of the nuclear factor kappa-light-chain-enhancer of activated B cells (NF- κ B), a DNA transcription factor (Zandi *et al.*, 1997; Karin, 2006). Consecutively NF- κ B induces the up regulation of pro-inflammatory mediators, like: TNF- α ; interleukins (IL-1 β , IL-2 and IL-6); adhesion molecules (AMs) and enzymes including cyclooxygenase-2 (COX-2) and inducible nitric oxide synthase (iNOS) (Brand *et al.*, 1996; Böhrer *et al.*, 1997). In the case of chronic diseases, the NF- κ B activation instead of being short-lived is not well controlled (Yu and Yang, 2006), causing a worse scenario once some of the pro-inflammatory mediators, as: TNF- α , IL-1, IL-6 and COX-2 are activators of NF- κ B, creating an auto-activation cycle (Handel *et al.*, 1995; Fischer *et al.*, 1996). In addition the consequent tissue damage induced by the inflammatory mediators leads to a vicious cycle through the production of more RS, which increases the redox imbalance (Chung *et al.*, 2009; Khansari *et al.*, 2009). This molecular inflammation mechanism may in last case be a cause or part of disease progression, contributing to the aging process as well as to the chronicity of age-related diseases (Chung *et al.*, 2006).

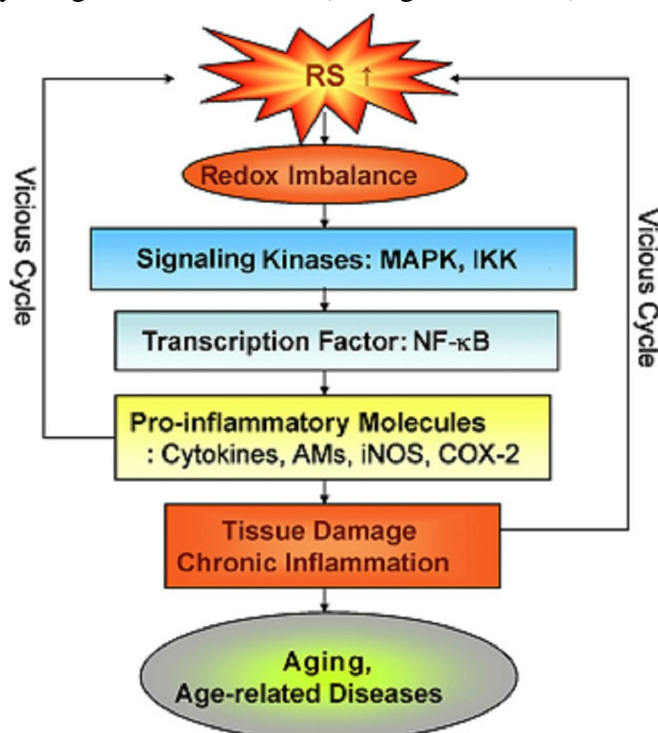


Figure 1.1 Major pathways involved in the molecular activation mechanism of inflammation, during aging and age-related diseases (adapted from Chung *et al.*, 2009).

This relation between free radicals and aging related diseases is the basis of antioxidant therapy to fight against this kind of diseases (Harman, 2003; Khansari *et al.*, 2009). An antioxidant is a substance capable of inhibiting or limiting the oxidation of a certain substrate, while present in a very small concentration. Besides endogenous antioxidants that belong to body antioxidant defence system there are also exogenous antioxidants provided by nutrition. Many of these nutritional oxidants belong to the phenol family (Fusco *et al.*, 2007). Polyphenols are a group of chemical compounds containing multiple phenolic functionalities, usually referred as natural occurrence, although a wide amount of synthetic polyphenols also do exist (Tückmantel *et al.*, 1999). These ubiquitous natural compounds, very common in higher plants, come from the plant's secondary metabolism and play several roles related to the plant's survivability (Joseph *et al.*, 2009). Polyphenolic compounds are divided into main groups that are: flavonoids, phenolic acids, phenolic alcohols, stilbenes and lignans (Yoshihara, 2010). Some polyphenols are specifically found in a particular plant, while others are found in most plants and generally occurring in complex mixtures (D'Archivio *et al.*, 2010). More than 8,000 polyphenols (Guo *et al.*, 2009) have been identified within fruit, vegetables, tea, red wine, coffee, chocolate, olives, herbs, spices, nuts and algae (Crozier *et al.*, 2009).

Epidemiological evidences have shown the benefit of consuming a diet of food containing polyphenols (D'Archivio *et al.*, 2010). The majority of these compounds act by scavenging radical species, neutralizing in a direct way the free radicals; reducing peroxide amount and repairing oxidized membranes; quenching iron that reduces oxygen species production; or through lipid metabolism, where oxygen species are neutralized by short-chain free fatty acids and cholesteryl esters (Handique and Baruah, 2002; Berger, 2005). However, some polyphenols under certain circumstances may behave as pro-oxidants (Tückmantel *et al.*, 1999). The role of polyphenolic compounds ends up being more complex than just antioxidant activity (Masella *et al.*, 2005). They may exert other activities including: inhibition of cancer cell proliferation (Noratto *et al.*, 2009) and cholesterol uptake (Leifert and Abeywardena, 2008); modulation of enzymes such as telomerase (Naasani *et al.*, 2003); anti-inflammatory activity through the inhibition of COX-2 (Hussain *et al.*, 2005), lipoxygenase (Sadik *et al.*, 2003) and also NF- κ B, which is a master regulator of infection and inflammation (Guo *et al.*, 2009); interaction with signal transduction pathways (Kong *et al.*, 2000); prevention of

endothelial dysfunctions (Carluccio *et al.*, 2003); and also interfering with caspase dependent pathways (Way *et al.*, 2005) and cell cycle regulation (Fischer *et al.*, 2000). Following this, acting as free radical scavengers, polyphenols may slow or prevent the progression of age-related diseases, in particular AD. Some evidence facts coming from food diet have already been published, where the consumption of diets rich in antioxidants compounds may provide beneficial effects against aging and preventing or delaying cognitive dysfunction (Letenneur *et al.*, 2007), long-term risk of dementia, Alzheimer's disease (Joseph *et al.*, 2009; Devore *et al.*, 2010) and others neurodegenerative diseases (Joseph *et al.*, 2009).

1.2 Alzheimer's disease

Aloysius Alzheimer (Figure 1.2), born on the 14th of July of 1864, in Marktbreit, Baviera was a famous German neurologist known to be the first author who distinguished the neurodegenerative disease as a distinct pathologic entity, actually called Alzheimer's disease. AD is an age-related disease and the most common form of irreversible dementia (Citron, 2010). It is generally characterized by a slow but inflexible progression of dementia, associated with cognitive and memory decline, speech loss and personality changes. The memory loss is characteristic of



Figure 1.2 Aloysius Alzheimer

AD, firstly a gradual loss of short-period memory occurs, which ultimately is extended to the more consolidated memory (Nowak, 2004). As a consequence, AD places a high burden not only on patients but also on caregivers. In line with the population aging within industrial countries, studies show how in the United States aging will lead to a three times increase of AD patients in 2050 comparing to the year 2000, reaching around 13.2 millions of people (Herbert *et al.*, 2003). Consequently the annual costs of AD are growing up each year, making the healthcare system investments to grow up in a scaring way (Citron, 2010). All together, both the devastating socioeconomic impact of AD as well as the incidence increase makes AD a disease of major concern.

Epidemiological studies show evidences of AD as a disease of multifactor causes, including: biological, genetic, environmental, behavioral factors and also as a secondary consequence of certain health conditions (Citron, 2010). Advanced age is the biological and primary risk factor for late-onset AD (Yoshitake *et al.*, 1995). Concerning genetic factors, some mutations have been identified in the following genes: amyloid precursor protein (*APP*), presenilin 1 (*PS1*) and presenilin 2 (*PS2*), which are related with early-onset AD; on the other hand the presence of the $\epsilon 4$ allele of the apolipoprotein E (*APOE*) is a major risk factor for late-onset AD (Cruts and vanBroeckhoven, 1998). Regarding environmental factors, higher education is considered to be a beneficial factor against AD. Cigarette smoking is a behavioral risk factor, while physical exercise (Yoshitake *et al.*, 1995) and mental activity seem to be beneficial factors (Citron, 2010). Finally, certain health conditions are associated with increased risk of AD, including:

head injury, high blood pressure, obesity, diabetes and metabolic syndrome (Citron, 2010).

1.2.1 AD progression mechanisms

Considering the histopathological post-mortem observation of human brains of AD patient's, two kinds of hallmark lesions can be observed, consisting on both senile plaques and neurofibrillary tangles (NFTs) in the brain memory and cognition regions (Alzheimer *et al.*, 1995). These senile plaques consist on deposits of extracellular amyloid- β peptide ($A\beta$) (Mark *et al.*, 1995), while NFTs are formed by the accumulation of abnormal filaments of tau protein (McGeer *et al.*, 2007). Not less important is the evidence of inflammatory processes and immune response (McGeer *et al.*, 2007). The aim of studying the mechanisms underlying this histopathological scenario is to find potential targets to block or delay the progression of AD.

1.2.1.1 Formation of amyloid- β peptide plaques

The mechanism underlying the formation of $A\beta$ peptide plaques is called the amyloid cascade (Figure 1.3), which starts with the sequential cleavage of the amyloid precursor protein (APP), a transmembrane protein, by β -secretase (also known as β -site APP cleaving enzyme 1; BACE1) and γ -secretase. From the proteolytic fragmentation of APP, several isoforms of $A\beta$ peptide are released, among which $A\beta_{42}$, a very low soluble isoform 42 amino acid long. The aggregation of $A\beta_{42}$ peptide leads to the formation of toxic oligomers that deposit in amyloid plaques. Ultimately, the formation of oligomers is responsible for the induction of synaptotoxic effects, while the amyloid plaques cause an inflammatory response (Walsh and Selkoe, 2007).

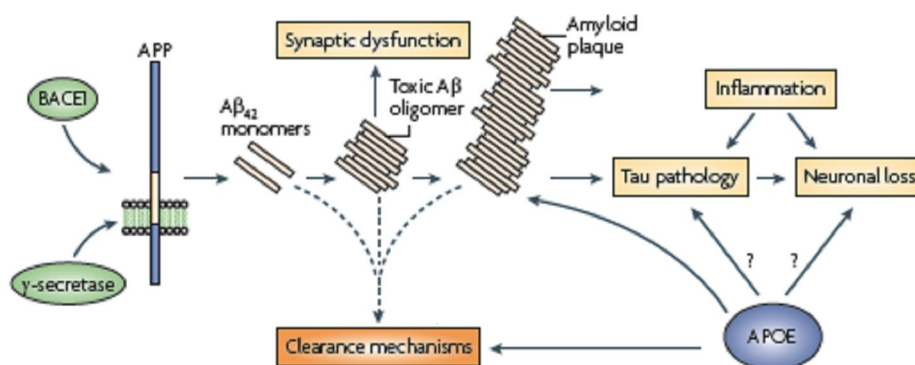


Figure 1.3 The amyloid cascade (adapted from Citron, 2010).

The amyloid cascade hypothesis is thought to play an essential role in AD pathogenesis, being strongly supported by pathological and genetic evidences. The presence of amyloid burden in peripheral amyloidoses is strong pathological evidence; also, both the acute synaptic toxicity effects caused by A β oligomers and the pro-inflammatory effects of amyloid plaque contribute even more for neuronal toxicity. In the case of genetic evidences, *APOE4* allele is a risk factor not only in AD but also in a number of neurological disorders, which suggests a direct effect on neurodegeneration; also APOE seems to interfere directly with the amyloid cascade that affects the A β peptide deposition and clearance (Bu, 2009). Another important fact, concerning genetic evidences is that all the mutations behind the familial early onset AD lead to an increase of A β_{42} peptide production or at least an increase of A β_{42} /A β_{40} ratio, where A β_{40} is an isoform less prone to aggregate and finally also these mutations enhance the amyloidogenic APP processing (Walsh and Selkoe, 2007).

1.2.1.2 Formation of neurofibrillary tangles

NFTs are formed by the accumulation of abnormal filaments of tau. Tau is a soluble microtubule-binding protein, which supports axonal transport and cytoskeleton growth, by stabilizing microtubules and promoting tubulin assembly into microtubules. Figure 1.4 shows how the hyperphosphorylation of tau proteins in AD, causes the detachment of tau proteins from the microtubule. The soluble tau proteins may then aggregate into soluble tau aggregates and insoluble paired helical filaments that ultimately end in the formation of NFTs. This microtubule destabilization caused by direct toxic effects of both soluble hyperphosphorylated tau and fibrillar tau leads to axonal transport impairment causing a progressive loss of neurons (Goedert, 2006).

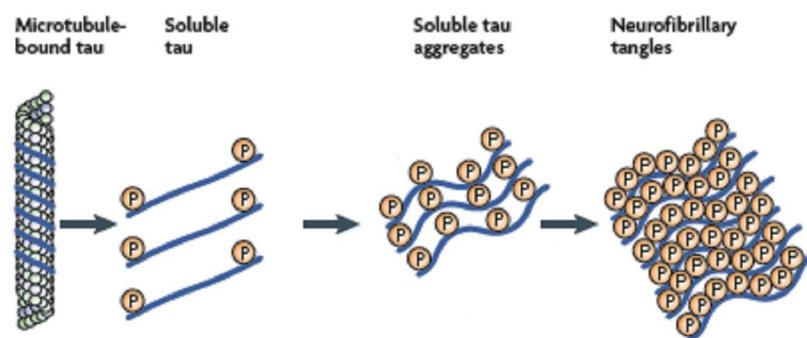


Figure 1.4 Tau pathology (adapted from Citron, 2010).

Tau pathology may be regarded as consequence rather than a cause of AD due to the fact that tau and tangle pathology also occur in other neurological disorders, besides AD and also the possibility of being triggered through an upstream mechanism by amyloid cascade in AD (Figure 1.3) (Citron, 2010). However, this is not clear, because correlations between cognitive dysfunction and tangle load in AD do exist (Thal *et al.*, 2000). Also tau mutations were found to cause some forms of frontotemporal dementia, showing how tau pathology alone causes cell loss and dementia (Hutton *et al.*, 1998).

1.2.1.3 Inflammation

Inflammation has been shown to be related and significantly contribute to the development of dementia that might be relevant for the development of neurodegenerative diseases (Chung *et al.*, 2009). Concerning AD, it was suggested that inflammatory processes may modulate it contributing to its pathogenesis (Peila and Launer, 2006). Moreover an increase concentration of inflammatory markers do occur in AD patients including: members of the complement, prostaglandins, cytokines (IL-1 β , IL-6, TNF- α , TGF- β), acute-phase reactive proteins, coagulation factors, reactive astrocytes and activated microglia cells (Wyss-Coray and Mucke, 2002; Citron, 2010). Also, the levels of nitric oxide synthase enzymes were shown to be increased in the frontal, neurons, astroglial cells and blood vessels of post-mortem AD brains (Lüth *et al.*, 2002).

Considering the role of oxidative stress on the inflammatory response, several studies were accomplished in order to best understand the inflammatory mechanism underlying AD. Evidences show that oxidative damage may be implicated in mechanisms of neuronal cell injury (Kolosova *et al.*, 2006), in particular in AD pathogenesis (Nunomura *et al.*, 2006). Oxidative stress is thought to influence AD pathogenesis on three different levels, by acting on proteins, nucleic acids and lipids. Concerning protein damage, an increase nitrative stress was proved to occur in human AD brains, leading to increased levels of protein oxidation and nitration (Hensley *et al.*, 1998). Taking into account both nuclear and mitochondrial DNA, several oxidized bases and increased levels of 8-hydroxy-2-deoxyguanosine do occur in human AD cerebral cortex and cerebellum. Finally, increased lipid peroxidation was detected in AD brains, as well as increased modification of phosphatidylserine, a key lipid for membrane integrity

(Bader-Lange *et al.*, 2008). Noteworthy is the fact that oxidative stress is a common mechanism behind major etiologic known factors of AD:

- a) Old age is related with debility of the body antioxidant defence system, which also seems to occur in both early and late-onset of AD. The decrease of key antioxidant enzyme activities expression such as: SOD, catalase, GPx and GSR is reported to trigger the redox imbalance (Sinclair *et al.*, 1998; Galbusera *et al.*, 2004). In addition, the Inflammatory Hypothesis of Dementia corroborates the idea that brain aging is caused by inflammatory processes (McGeer and McGeer, 1995).
- b) Concerning genetic risk factors, both the presence of *APOE4* allele, as well as mutations on *APP*, *PS1* and *PS2* genes are related to oxidative stress mechanism. Interestingly is even a report of a recent study which shows a genetic association between inflammation and AD, where the complement receptor 1 gene (*CR1*) that enables the innate immune humoral response was identified as another risk factor of AD (Lambert *et al.*, 2009).
- c) Finally, also behavioral factors such as cigarette smoking and certain health conditions including diabetes and brain injury are associated with oxidative stress (Nunomura *et al.*, 2006).

Inflammation is undoubtedly the less known mechanism underlying AD. In addition oxidative stress seems to be correlated with major etiological known factors. It is plausible to draw a hypothesis where certain risk factors may give rise to oxidative stress that consequently leads to inflammation and tissue damage, causing AD. Inflammation is regarded not only as a consequence of oxidative stress but is also correlated with it in a cyclical way. Unfortunately, the complexity of studying this mechanism is very high and inflammation may ultimately be just a response to a damage, caused by something else (Kamat *et al.*, 2008). For instance, some *in vivo* models of AD amyloidosis show antioxidant defence impairment, increased protein oxidation and lipid peroxidation (Pratico *et al.*, 2001; Schuessel *et al.*, 2005); also some studies show that that A β and APP may cause oxidative stress (Mark *et al.*, 1995; Meda *et al.*, 1995), and even that the interaction between A β with the receptor for advanced glycation end products (RAGE) seem to activate NF- κ B, which may be responsible for the inflammatory response (Deane *et al.*, 2004). These facts support the potential role of oxidative stress and inflammation on the toxicity mediated by the amyloid mechanism of AD. At the same time they also give rise to the doubt of whether oxidative stress and

inflammation are a cause or a consequence of AD. Despite inflammation might only be a consequence of AD, the fact that it may generate a vicious cycle that produces RS (Figure 1.1) turns inflammation into a relevant target for AD targeting in order to avoid increased tissue damage.

1.2.2 AD Therapy

Targeting AD is an audacious task, not only due to the mechanistic complexity of the disease but also due to the heterogeneity of the etiologic factors. Actual drugs mainly act to improve cognitive function, such as acetylcholinesterase inhibitors: galantamine, tacrine, donepezil and rivastigmine, used in mild to moderate AD (Scarpini *et al.*, 2003); and *N*-methyl-D-aspartate (NMDA) receptor antagonist, memantine, used in mild to severe AD (Sonkusare *et al.*, 2005). In the case of other symptoms, including: mood disorder, agitation and psychosis is usually required medication, even though, there isn't a specific indicated drug (Citron, 2010). It's now more than ever urgent to find new therapeutic approaches capable of modifying the progression of the disease. The population is getting old in a fast way and the actual market drugs are ineffective to target AD progression mechanism. The purpose of developing disease modifying drugs relays on the blockage or delay of the disease progression, rather than on a fast symptomatic improvement. Concerning AD progression mechanisms, several approaches are being studied to target AD.

1.2.2.1 Amyloid cascade approaches

The amyloid cascade targeting approaches aim to avoid the formation of A β peptide plaques, based on the mechanism of the formation of the toxic A β oligomers and plaques. Several therapeutic strategies are being researched, including: modulation of A β production, inhibition of A β aggregation, enhancement of A β degradation, A β immunotherapy and APOE-related treatment (Citron, 2010).

A β production can be modulated through the inhibition of γ -secretase, inhibition of β -secretase or stimulating α -secretase, which is an enzyme that competes with β -secretase for APP substrate and cleaves the A β peptide in two. Inhibiting γ -secretase was found to reduce A β peptide in mice (Dovey *et al.*, 2001), however these inhibitors have shown to cause intestinal metaplasia in adult animals, due to the inhibition of Notch 1 cleavage (Milano *et al.*, 2004). New inhibitors seem now to have overcome this issue, and

semagacestat from Lilly has entered Phase III studies (Fleisher, 2008). The inhibition of β -secretase, a transmembrane aspartic protease, has been quite challenging because it may cause a possible blockage of remyelination after injury (Citron, 2010), also the hydrophilic properties of aspartic protease inhibitors make it hard to penetrate the blood-brain barrier (BBB) (Durham *et al.*, 2006). Finally, stimulating α -secretase has the limitation of the entrance of much more APP to the α -secretase than the β -secretase pathway. No α -secretase agonists are reported to be in clinical trials (Citron, 2010).

The inhibition of A β aggregation is based on the development of brain penetrable small-molecules capable of interfering with A β -A β peptide interactions (Citron, 2010). A cyclohexanol isomer is in phase II trials (McLaurin *et al.*, 2006).

Considering now the enhancement of A β clearance, key enzymes were found to be involved in A β degradation, such as: neprilysin, insulin-degrading enzyme and plasmin (Eckman and Eckman, 2005). Once plasmin cleaves A β , one potential therapeutic approach consists on the inhibition of plasminogen activator inhibitor (PAI-1), due to the fact that this molecule inhibits plasminogen activator that is required to generate plasmin from plasminogen. Still within the A β clearance approach, two potential other targets are the inhibition of RAGE, which mediates A β influx into the brain, and the activation of the low-density lipoprotein receptor-related protein 1 (LRP-1), which mediates the efflux of A β from the brain through the BBB. Phase II trials are being undertaken for a RAGE inhibitor (Citron, 2010).

A β immunotherapy is nowadays a very promising area for AD targeting. Actually, there are three antibodies against A β in Phase III trials: intravenous immunoglobulin G, from Baxter, (Tsakanikas *et al.*, 2008); bapineuzumab, from Elan and Wyeth, (Salloway *et al.*, 2009); solanezumab, from Eli Lilly (Siemers *et al.*, 2008). Despite the success of immunotherapy, some bothering issues related to efficacy and safety shall be regarded attentively. A major concern issue is the side effect of intracerebral hemorrhage observed in a few plaque-binding antibodies (Citron, 2010). Also a phase I trial, consisting on an active immunization against A β peptide, where two patients showed extensive post-mortem evidence of A β removal had still progressed to end-stage AD (Holmes *et al.*, 2008). This evidence may be critical for the success of amyloid therapeutics as an approach for AD targeting.

In what concerns to the APOE related treatment it is still to answer the question of whether the presence of allele ϵ 4 is a risk factor due to increased toxic properties

relative to the allele $\epsilon 3$, or if it has lost the beneficial function of allele $\epsilon 3$ against $A\beta$ deposition as Fagan *et al.*, 2002 supports.

1.2.2.2 Tau pathology approaches

The two main treatment strategies concerning tau pathology consist on the inhibition of tau aggregation and blockade of tau hyperphosphorylation (Schneider *et al.*, 2008).

Inhibiting tau aggregation, not only avoids the formation of toxic neurofibrillary tangles but also the detrimental activity of tau aggregates (Bulic *et al.*, 2009). This approach is however quite challenging. Not only the potential inhibitor must specifically disrupt protein-protein interactions of tau aggregates, it also has to be able to cross the BBB (Bulic *et al.*, 2009). Only methylthioninium chloride is being studied in Phase II trials, after being reported to dissolve tau filaments and to prevent tau aggregation in cell models. Preliminary data show evidence, that methylthioninium chloride is capable of arresting the disease progression (Wischik *et al.*, 2008).

Blocking tau hyperphosphorylation can turn to be an even higher challenge. Not only it's not yet known how critical hyperphosphorylation is to tau pathology, a potential pathogenic kinase wasn't yet consensually identified. As both these facts weren't enough, there is even a last big issue, consisting on the development of a safety small molecule kinase inhibitor suitable for chronic administration. Safety issues and side effects related to chronic inhibition are of major concern, as all marketed kinase inhibitor drugs in USA and Europe are used for cancer therapy (Citron, 2010).

1.2.2.3 Anti-inflammatory approaches

Although some mechanistic uncertainty flies above the inflammation role in AD, some evidences place inflammation as a promissory potential for AD disease. For instance the use of anti-inflammatory drugs in *in vivo* studies showed suppression of amyloid plaque pathology and $A\beta$ levels, reducing concomitantly pro-inflammatory mediators, reactive astrocytes and microglia activation (Lim *et al.*, 2000; Townsend and Pratico, 2005). Epidemiological studies with chronic intake of non-steroidal anti-inflammatory drugs (NSAIDs) showed more than 50% of risk decrease for AD development (McGeer *et al.*, 1996). More interesting was the fact that certain NSAIDs showed to modulate γ -secretase in such a way that $A\beta_{42}$ is reduced and a smaller $A\beta_{42}$ isoform, less prone to aggregate, is increased (Jarrett *et al.*, 1993). In this case, Notch cleavage was not

blocked, in opposition to what characterizes some γ -secretase inhibitors (Weggen *et al.*, 2001). Other studies proved that the reduction of $A\beta_{42}$ wasn't mediated by COX inhibition, or other common targets of NSAIDs, a direct interaction occurred between NSAIDs and γ -secretase or its substrate instead (Leuchtenberger *et al.*, 2006; Kukar *et al.*, 2008).

Inflammation response, while a consequence of oxidative stress, turns antioxidant therapy into a powerful tool to prevent not only oxidative stress but also the consecutive inflammation response in an upward perspective. Antioxidant strategies may be divided into three categories, including: free radical scavengers; preventive antioxidants, which include metal chelators, antioxidant enzymes such as GPx and SOD; and *de novo* and repair enzymes such as lipases, proteases and DNA repair enzymes (Nunomura *et al.*, 2006). A group of nonspecific antioxidants also do exist, including: melatonin (Feng *et al.*, 2006), omega-3 polyunsaturated fatty acid (Nunomura *et al.*, 2006), curcumin (Yang *et al.*, 2005), ubiquinone (Beal *et al.*, 2004) and α -lipoic acid (Quinn *et al.*, 2007).

Some epidemiologic reports have shown that the consumption of high amounts of fruits and vegetables, as well as vitamin supplements, lowers AD rates (Fusco *et al.*, 2007). S-adenosyl methionine is an antioxidant compound found in apple, which was reported to be beneficial to improve neuropathological features of AD in mice models (Chan and Shea *et al.*, 2006). Other dietary compounds also showed interesting anti-AD activities, including: caffeine (Arendash *et al.*, 2006), epigallocatechin-gallate esters from green tea (Rezai-Zadeh *et al.*, 2005) and red wine (Wang *et al.*, 2006a). The curry spice, curcumin, was found to facilitate disaggregation and reduction of $A\beta$ in AD associated neuropathology (Yang *et al.*, 2005). Among the antioxidant compounds most studied in order to target AD is Vitamin E. Vitamin E has proved to decrease lipid peroxidation susceptibility by 60% in AD patients (Veinbergs *et al.*, 2000). Clinical studies, concerning cognitive disorders and AD were developed. While some clinical trials show positive effects against cognitive disorders such as: Honolulu-Asia Aging study (3,385 men) (Masaki *et al.*, 2000); Chicago Health and Aging Project (815 subjects) and Nurses' Health Study (14,986 women) (Grodstein *et al.*, 2003); other studies showed negative results that include: Honolulu-Asia Aging study (2459 men) (Peyser *et al.*, 1995; Luchsinger *et al.*, 2003; Laurin *et al.*, 2004), Washington Heights Study (980 subjects) and Cache Country Study (4740 subjects) (Zandi *et al.*, 2004). So, although

vitamin E has been pointed out to be beneficial against AD, taking into account the clinical trials results, its activity against AD is not conclusive. In order to fully understand the potential benefits of vitamin E other clinical trials are underway, either alone or in combination with several compounds including: memantine, selenium, α -lipoic acid, vitamin C, coenzyme Q, curcumin, melatonin and lutein (Kamat *et al.*, 2008). Clioquinol is a metal chelator, included in the preventive antioxidants category, which is in Phase II trials for AD (Lannfelt *et al.*, 2008).

Much like the difficulty found to describe the inflammation mechanism underlying AD it is also hard to identify the exact mechanism of action of antioxidants against AD. Some agents exert other activities beyond antioxidant functions (Karmat *et al.*, 2008). Curcumin for instance, besides its antioxidant activity, has anti-inflammatory effects inhibiting both cyclooxygenase and lipoxygenase (Rao, 2007), and also inhibits amyloid aggregation (Yang *et al.*, 2005)

1.3 Flavones – potential therapeutic drugs against AD

The treatment of AD using flavones, focus on targeting the inflammation process that is behind the disease progression. This anti-inflammatory therapeutic approach is based on their action to prevent oxidative stress and consequent inflammation, acting as antioxidants through free radical scavenging.

Flavonoids belong to the wide group of polyphenolic compounds and consist on one of the largest groups within the known natural products, both in quantity and quality (Havsteen, 2002). Flavones are a very large sub-group within the flavonoids to whom much attention has been dropped, in order to find compounds of potential pharmacological use. As part of flavonoids group, flavones share with them common biosynthetic routes, presence in certain plant organs as well as pharmacological activities, based on similar mechanisms of action.

1.3.1 Chemical classification

The biosynthetic process starts by removing the amino group of phenylalanine, leading to phenylpyruvate. The thiamine pyrophosphate, from the pyruvate dehydrogenase complex, operates the oxidative decarboxylation of two molecules of phenylpyruvic acid, producing two active aldehydes molecules, which together with a C₁-fragment (-CHO) in an oxidative step drives to the nucleus of phenyl- γ -pyrone, a synonym of chromen-4-one (Figure 1.5) (Havsteen, 2002). Individual flavonoids are then produced through multiple hydroxylation in different positions, oxidation/reduction steps and derivatization of the hydroxyl groups with methyl groups (Gauthier *et al.*, 1998), carbohydrates (Matern *et al.*, 1981) and isoprenoids. Theoretically, considering a possible combination of all these sources of variability, more than $2 \cdot 10^6$ different flavonoid compounds can occur (Havsteen *et al.*, 2002).

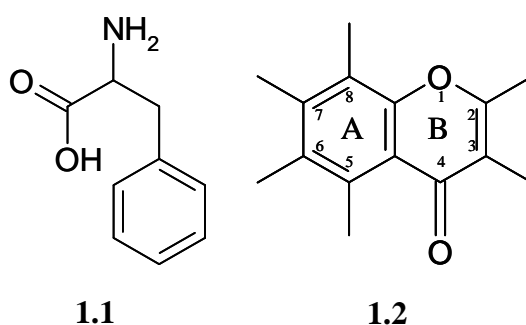


Figure 1.5 Molecular structures of: phenylalanine amino acid (**1.1**) and chromen-4-one (**1.2**).

Flavones are derived from the skeleton structure of 2-phenylchromen-4-one (Figure 1.6), a derivative of the basic nucleus, chromen-4-one (Figure 1.5). Many compounds belong to the group of flavones that includes the flavonols: rutin, isoquercetin and quercetin as well as the flavanones: naringin, prunin, and naringenin, which are object of study within this thesis (Figure 1.7). Concerning these flavones, naringin and rutin are two rutinosides that are derived from the disaccharide rutinose (rhamnose + glucose) and the respectively aglycones naringenin and quercetin. Prunin and isoquercetin are glucosides from both naringenin and quercetin, respectively. In addition, although both flavanones and flavonols share the same basic nucleus of flavones, flavanones are derived from the 2,3-dihydro-2-phenylchromen-4-one nucleus (Figure 1.6), while flavonols are derived from the 3-hydroxy-2-phenylchromen-4-one nucleus (Figure 1.6).

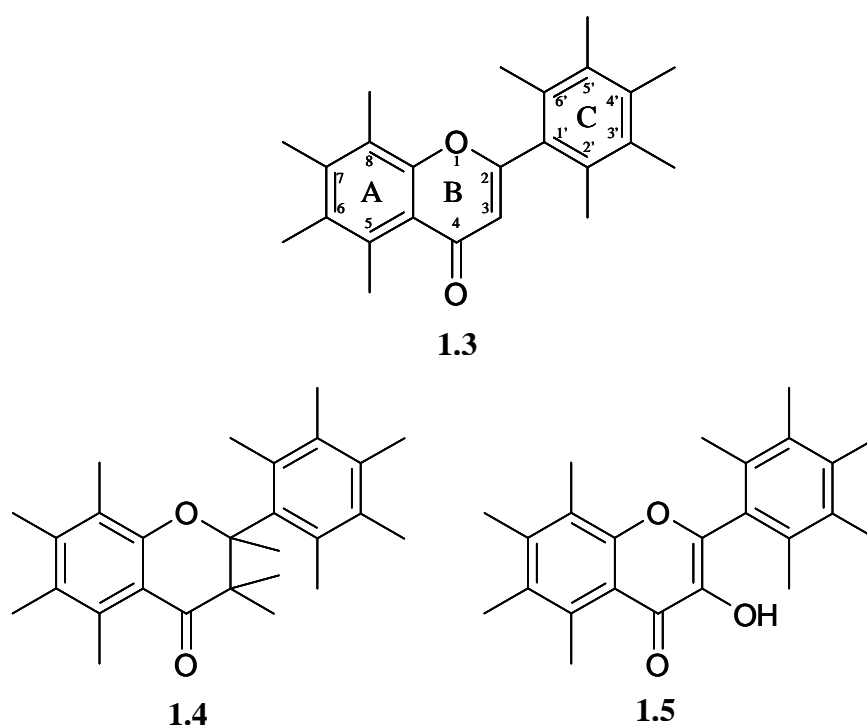


Figure 1.6 Molecular structures of 2- phenylchromen-4-one (1.3), 2,3-dihydro-2-phenylchromen-4-one (1.4) and 3-hydroxy-2-phenylchromen-4-one (1.5).

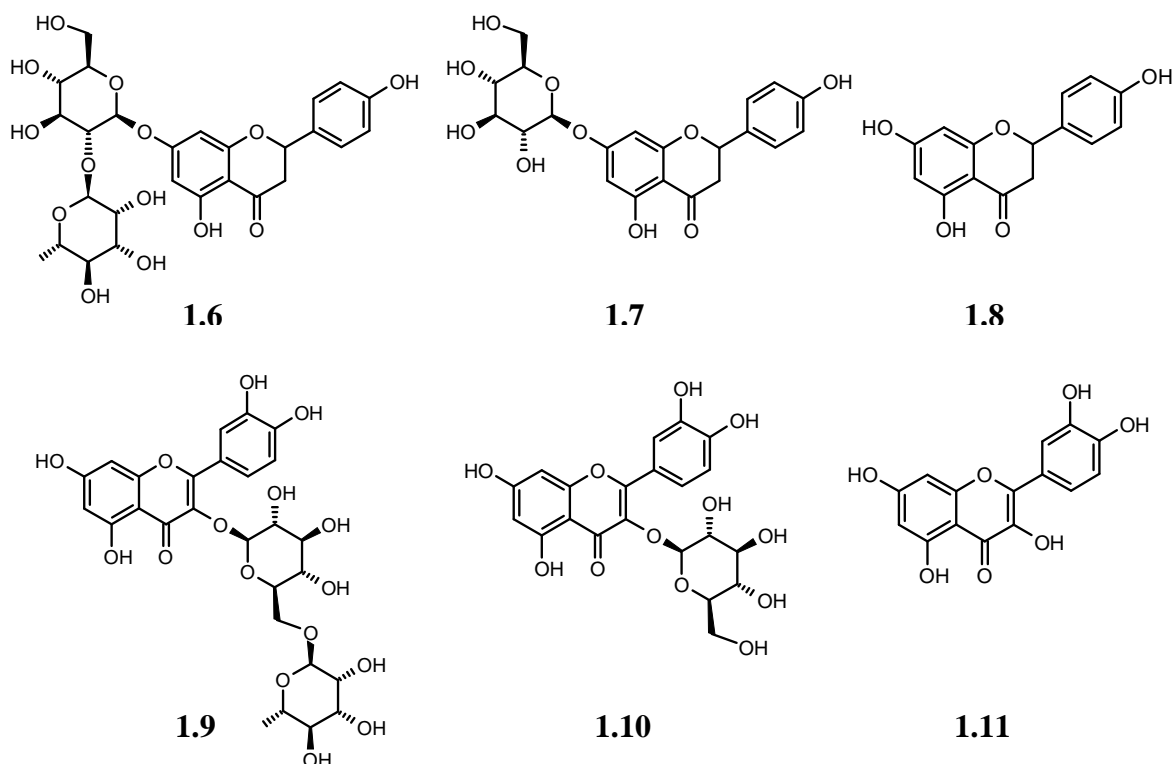


Figure 1.7. Molecular structures of the flavanones: naringin (**1.6**), prunin (**1.7**) and naringenin (**1.8**) and the flavonols: rutin (**1.9**), isoquercetin (**1.10**) and quercetin (**1.11**).

1.3.2 Pharmacological activity

A vast number of pharmacological activities are shared by flavonoids. Free-radical scavenging, antioxidant and anti-inflammatory activities are the most common, but plenty other activities are described, including: anti-tumour, atherosclerosis preventive activity, through the protection of human low-density lipoprotein (LDL) against oxidation ; hypocholesterolemic activity, through the inhibition of 3-hydroxy-3-methylglutaryl-coenzyme A reductase (HMG-CoA reductase); antithrombotic activity, by preventing platelet aggregation; anti-allergic activity; inhibition or killing of many bacterial strains; inhibition of viral enzymes; destruction of some pathogenic protozoans and even stimulation of some hormones and neurotransmitters (Havsteen, 2002).

Antioxidant properties rely on the tendency of flavonoids to oxidize from phenols to quinones (Havsteen, 2002). Although intimately connected, free-radical scavenging and antioxidant properties are distinct, once the first depends on the presence of an unpaired electron and the last one depends on the oxidation-reduction potential (Marinov and Evtodienko, 1994). Oxidation is however, the basis of the mechanism underlying free-radical scavenging property. Figure 1.8 shows the general mechanism of flavonoids

oxidation, consisting on a first irreversible oxidation step of flavonoids into a hydroquinone. The hydroquinone formed is further oxidised into a quinone, producing a semiquinone radical intermediate, through a reversible reaction. Ultimately, the quinone polymerises into an insoluble substance, which is eliminated afterwards. Figure 1.9 exemplifies a more complex free-radical mechanism of a compound derived from the 3-hydroxy-2-phenylchromen-4-one nucleus, from which the flavonols rutin, isoquercetin and quercetin are also derived (Havsteen, 2002).

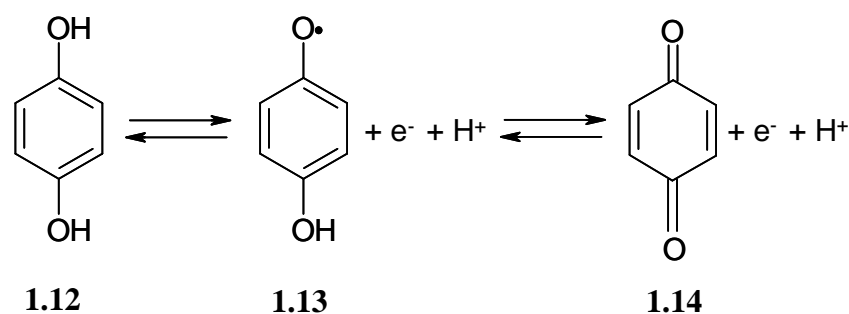


Figure 1.8 Radical mechanism of hydroquinone (1.12) oxidation through a semiquinone radical intermediate (1.13) to the quinone, 1,4-benzoquinone (1.14) (adapted from Havsteen, 2002).

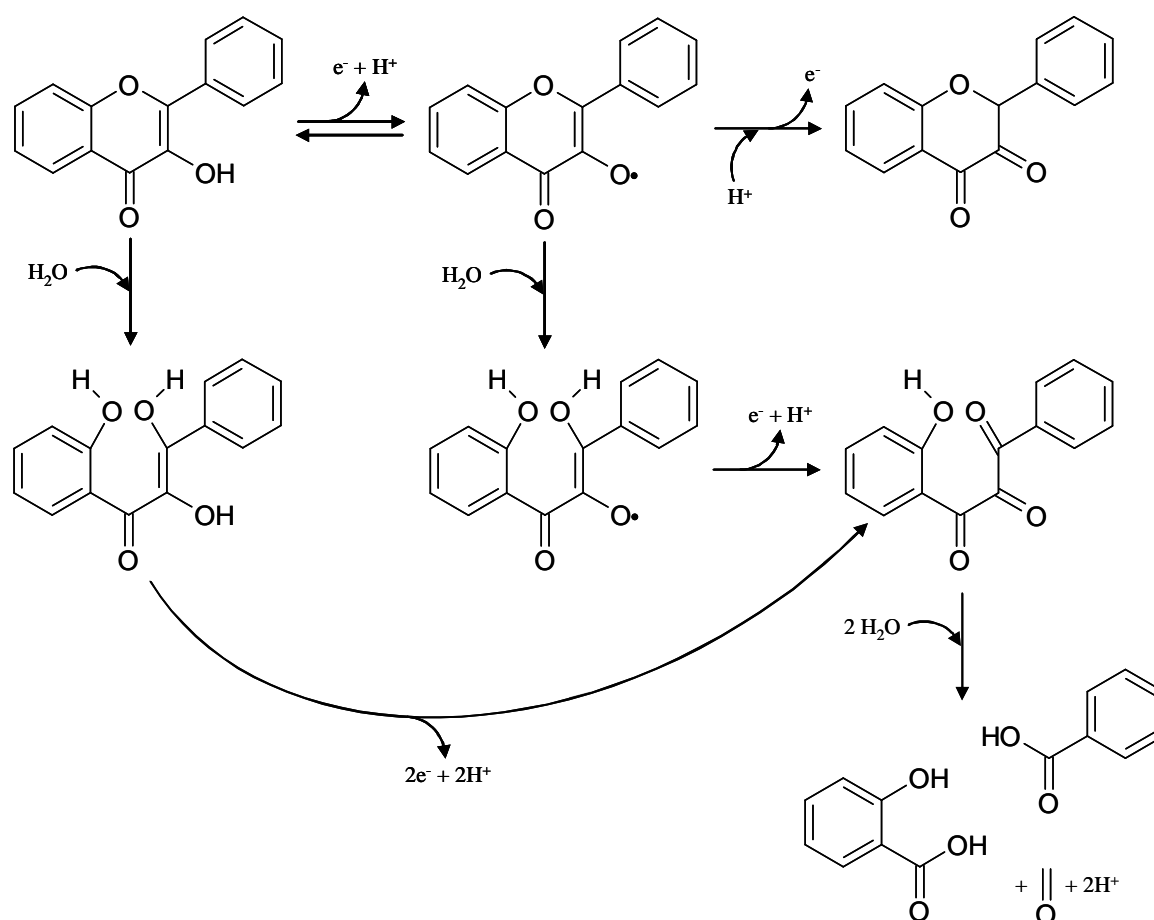


Figure 1.9 Radical mechanism of a compound derived from the 3-hydroxy-2-phenylchromen-4-one nucleus (adapted from Havsteen, 2002).

Several other pharmacological activities may be found in the literature, for the studying compounds (Figure 1.7).

1.3.2.1 Naringin

Naringin is reported to possess *in vitro* free-radical scavenging activity (Rajadurai *et al.*, 2007) and *in vivo* antioxidant (Jeon *et al.*, 2001; Rajadurai *et al.*, 2007) and anti-inflammatory activity (Amaro *et al.*, 2009). Naringin also shows atherosclerosis preventive activity (Lee *et al.*, 2008; Lee *et al.*, 2009), both by hypocholesterolemic (Jung *et al.*, 2003; Kim *et al.*, 2006) and antihyperlipidemic activities (Jung *et al.*, 2006; Kim *et al.*, 2006; Morikawa *et al.*, 2008). Concerning cancer therapy, naringin can potentially be used as antineoplastic agent (Ofer *et al.*, 2005; Schindler *et al.*, 2006; Ali *et al.*, 2009; Miller *et al.*, 2008) as well as chemotherapy adjuvant (Jagetia *et al.*, 2003; Cariño-Cortés *et al.*, 2010). Diabetes is also a potential field of application, due to its hypoglycaemic activity, by increasing hepatic glycolysis and glycogen concentration and/or by lowering hepatic gluconeogenesis (Jung *et al.*, 2004; Jung *et al.*, 2006; Punithavathi *et al.*, 2008). Other potential target diseases are: osteoporosis (Wong *et al.*, 2006; Wu *et al.*, 2008; Pang *et al.*, 2010), cerebral ischemia (Gaur *et al.*, 2009), septic shock (Kanno *et al.*, 2006) and even anxiety (Fernández *et al.*, 2006).

1.3.2.2 Prunin

Concerning prunin, studies report hypocholesterolemic activity and hypoglycaemic activity (Choi *et al.*, 1991a, b), antiviral activity (Kaul *et al.*, 1985), antithrombotic activity (Itoh *et al.*, 2009), activity as chemotherapy adjuvant (Han *et al.*, 2008).

1.3.2.3 Naringenin

Naringenin exhibits a higher antioxidant capacity and both hydroxyl and superoxide radical scavenger efficiency, than naringin (Cavia-Saiz *et al.*, 2010). Besides anti-inflammatory activity (Ribeiro *et al.*, 2008b; Amaro *et al.*, 2009; Vafeiadou *et al.*, 2009), it also has immunomodulatory activity acting against asthma. The hypocholesterolemic activity shown *in vivo* (Jeon *et al.*, 2007) is helpful against atherosclerosis disease, while hypoglycaemic activity (Andrade and Burgess, 2007) may be useful for diabetes. Concerning cancer, naringenin can be used in adjuvant chemotherapy (Fang *et al.*, 2010), or as potential antineoplastic agent in oral

carcinogenesis (Miller *et al.*, 2008), in endogenous hormone 17 β -estradiol-dependent cancers (Bulzomi *et al.*, 2010) and malignant melanoma (Lentini *et al.*, 2007). Osteoporosis (La *et al.*, 2009) and hepatitis C infection (Nahmias *et al.*, 2008) are other potential target diseases.

1.3.2.4 Rutin

Rutin exhibits free-radical scavenging (Sun *et al.*, 2007) and antioxidant activities (Matsunami *et al.*, 2006) as well as antineoplastic activity, where it may lead to the inhibition of breast cancer tumour proliferation through the inhibition of vascular endothelial growth factor (VEGF) (Schindler *et al.*, 2006).

1.3.2.5 Isoquercetin

Isoquercetin shows free-radical scavenging activity (Matsunami *et al.*, 2006), higher antioxidant activity than rutin (Sun *et al.*, 2007; Soundararajan *et al.*, 2008) and *in vivo* anti-inflammatory activity (Rogerio *et al.*, 2007). It may be highly useful in the treatment of asthma (Fernandez *et al.*, 2005; Rogerio *et al.*, 2007), diabetes (Paulo *et al.*, 2008) and obesity through the inhibition of the glucose transport across intestinal cells, via glucose transporter-2 (GLUT2), while rutin does not (Kwon *et al.*, 2007).

1.3.2.6 Quercetin

Quercetin shows free-radical scavenging activity, however may show a deleterious pro-oxidant instead of antioxidant activity in high concentrations (Johnson and Loo, 2000). As isoquercetin, it exhibits potential activity against obesity through the inhibition of glucose and fructose transport by GLUT2 (Kwon *et al.*, 2007). Concerning this property it is running a phase II clinical trial, started at July 2003, for the therapeutic use of quercetin with the following title: “Investigating the Use of Quercetin on Glucose Absorption in Obesity, and Obesity With Type 2 Diabetes” (<http://clinicaltrials.gov/ct2/show/NCT00065676>, 09/12/2010). Quercetin is also active against cancer, as a tyrosine kinase inhibitor (Ferry *et al.*, 1996), asthma and hypertension (Emura *et al.*, 2007).

Free-radical scavenging is a common property within these flavones, which makes them potential useful against AD, by stopping the mechanism of redox imbalance, oxidative

stress and chronic inflammation. Naringin and naringenin are also reported to inhibit NF- κ B which is responsible for triggering pro-inflammatory molecules (Kanno *et al.*, 2006; Shi *et al.*, 2009). Naringenin is seen as a potential chemopreventive agent against AD, by reducing the micromolecular A β -induced oxidative cell stress (Heo *et al.*, 2004). *In vitro* studies showed that quercetin inhibits A β aggregation and destabilizes pre-formed A β fibrils (Ono *et al.*, 2003), showing also protective effects of neuronal cells from oxidative stress-induced by A β peptide (Ansari *et al.*, 2009) and even more interestingly, inhibiting β -secretase (Shimmyo *et al.*, 2008). Finally, Tedeschi *et al.* (2010) found a possible molecular basis to explain the neuroprotective effect of flavonoids, including: rutin, quercetin, naringin and naringenin, consisting on a flavonoid-dependent rigidifying effect on the cellular membrane that hinders the permeabilization of A β into the bilayer, protecting the cell death induced by aggregated A β .

The apparent low toxicity of flavonoids turns them very promising for radical scavenging in biological systems, being also included in the normal human nutrition. Quercetin, for instance, had however been pointed out as being genotoxic. Several *in vitro* studies, including bacterial test systems and also eukaryotic cells support this idea, but conversely, studies examining genotoxic endpoints in mice and rats showed consistently that quercetin does not exert mutagenic or genotoxic properties *in vivo* (Utesh *et al.*, 2008).

1.3.3 Antioxidant therapy drawbacks in AD treatment

Some drawbacks concerning antioxidant therapy to treat AD have occurred. Several antioxidants including vitamin C and E, only offer symptomatic treatment without changing the neurodegenerative and pathological course of the disease (Kamat *et al.*, 2008). In order to find explanations to these drawbacks, several hypothesis come out, including: possible insufficient exposure time; eventual need of combined effects between antioxidants in order to achieve the desired effect; difficult translation of animal results to humans; the relationship between pro-oxidant and oxidant factor; clinical trial addressed at a very late disease state; therapeutic window issues and even inappropriate animal model, which is not homologous to human AD (Fusco *et al.*, 2007; Kamat *et al.*, 2008). Moreover drug pharmacokinetics must have played a decisive role. This lack of antioxidant therapy efficacy against AD may be related with the

distribution into the brain through the BBB or even earlier, during absorption. Concerning vitamin E, it was found to have a low brain bioavailability (Sung *et al.*, 2003). In the case of curcumin for instance, even 3 – 8 g/day was not enough to achieve therapeutic circulating levels in humans (Hsu and Cheng, 2007). According to these statements one major issue concerning the use of flavones to target AD must be the drug passage across the BBB, which also occurs in the cases of β -secretase inhibitors and tau aggregation inhibitors.

Not only AD, but targeting any disease within the central nervous system (CNS) is challenging due to the BBB, which is formed by a layer of endothelial cells connected with tight junctions, expressing several efflux transporters and drug-metabolizing enzymes (Pardridge, 1997; Tamai and Tsuji, 2000). Both brain tissue binding and permeability of BBB play an important role on the disposition of drugs to target CNS (Summerfield *et al.*, 2007). The influence of brain tissue binding is higher in the case of lipophilic drugs, where it may act as sink to help maintaining the diffusion gradient across the BBB (Summerfield *et al.*, 2007). On the other hand, drug permeation across BBB is dependent not only on the physicochemical properties of the molecule, but also on the potential to interact with transport systems at the BBB (Summerfield *et al.*, 2007). Concerning these physicochemical properties, it has been suggested that 300 to 400 Da is the ideal molecular mass for passage through BBB (Fischer *et al.*, 1998); with a low polar surface area (Clark, 1999) and low hydrogen-bonding ability (Young *et al.*, 1988). The interaction with transport systems at the BBB may turn to be decisive not only for the entrance into the CNS, through receptors recognition, but also for its exit through BBB efflux pumps (Summerfield *et al.*, 2006).

1.3.4 The role of the glycosidic residue

Flavonoids, depending on their content of glycosides, isoprenoids and aliphatic ethers, can acquire almost any polarity (Havsteen, 2002). Particularly, the glycosidic residue of certain compounds influences not only its pharmacokinetics but also its pharmacodynamics (Kren and Martinkova, 2001). From a pharmacokinetic point of view, the glycosidic residue may play very distinct roles, allowing or restricting the passage through the cell membrane. The glycosidic residue is responsible for turning the compound more hydrophilic, which reduces the solubility within the cell membrane and consequently makes it harder to get into the cell. On other side, a possible recognition of

the glycosidic residue by a certain cell membrane receptor, such as the glucose transporter, may turn it easier to get into the cell. Concerning pharmacodynamics, the biological activity of compound with or without the glycosidic residue can differ substantially, depending on the global molecular structure (Kren and Martinkova, 2001). These facts are undoubtedly interesting in order to find a molecule with the proper polarity to target CNS or eventually being recognized by certain receptors of the BBB, also taking into account the activity against AD.

In line with the above statements and comparing the respective rutinoides, glucosides and aglycones (Figure 1.7) may perform better than rutinoides in order to cross the BBB. Flavone aglycones are more hydrophobic than the respective rutinoides, which makes them more suitable for passive diffusion across the BBB, due to their lower polar surface area (Clark, 1999). For instance, Youdim *et al.* (2004) showed that the aglycone, quercetin can pass through the BBB. On the other hand, flavone glucosides have an exposed glucose moiety, while rutinoides have a rhamnose. The glucose moiety of glucosides may be recognized by specific receptors, including glucose receptors and being transported into the brain (Summerfield *et al.*, 2006). Some studies show that the sodium dependent glucose transporter (SLGT1) may actively transport the glucoside isoquercetin (Hollman *et al.*, 1999; Walgren *et al.*, 2000; Wolfram *et al.*, 2002; Walle and Walle, 2003). SLGT1 is not only present in the BBB, but also in intestine, kidney and endothelium.

1.3.5 Enzymatic deglycosylation of flavone glycosides

Although all compounds shown on Figure 1.7 occur in nature, the glucosides: prunin and isoquercetin and the aglycones: naringenin and quercetin are scarcer than the rutinoides: naringin and rutin. Naringin occurs abundantly in the internal epidermis of citrus fruits, mostly in orange and grapefruit and is responsible for a bitter flavour (Caccamese *et al.*, 2003). Rutin also occurs in citrus fruits (Wood, 2005) and some plants such as: *Fagopyrum esculentum* Moench (Kreft *et al.*, 1999), *Asparagus officinalis* L. (Wang *et al.*, 2003) and *Dimorphandra mollis* Benth (Féres *et al.*, 2006). The scarcity of prunin, isoquercetin, naringenin and quercetin makes them very expensive to isolate, especially in the case of the glucosides prunin and isoquercetin. Additionally, flavonoid family compounds are very difficult to separate due to its structural resemblance and easy decomposition (Havsteen, 2002). As consequence, the

market price of isoquercetin is very much higher than rutin, the rutinose that may generate isoquercetin through the hydrolysis of a rhamnose molecule. The same happens also in the case of prunin when comparing with naringin.

The enzymatic deglycosylation of both naringin and rutin comes out as a suitable process in order to produce the respective glucosides and aglycones (Figure 1.10), due to the specificity and mild conditions of enzymatic reactions, avoiding additional purification steps and preserving unstable products. Hydrolases are the enzymes that catalyze hydrolytic reactions, namely the hydrolysis of a glycosidic bond (Metzler, 2001; Buckow, 2006).

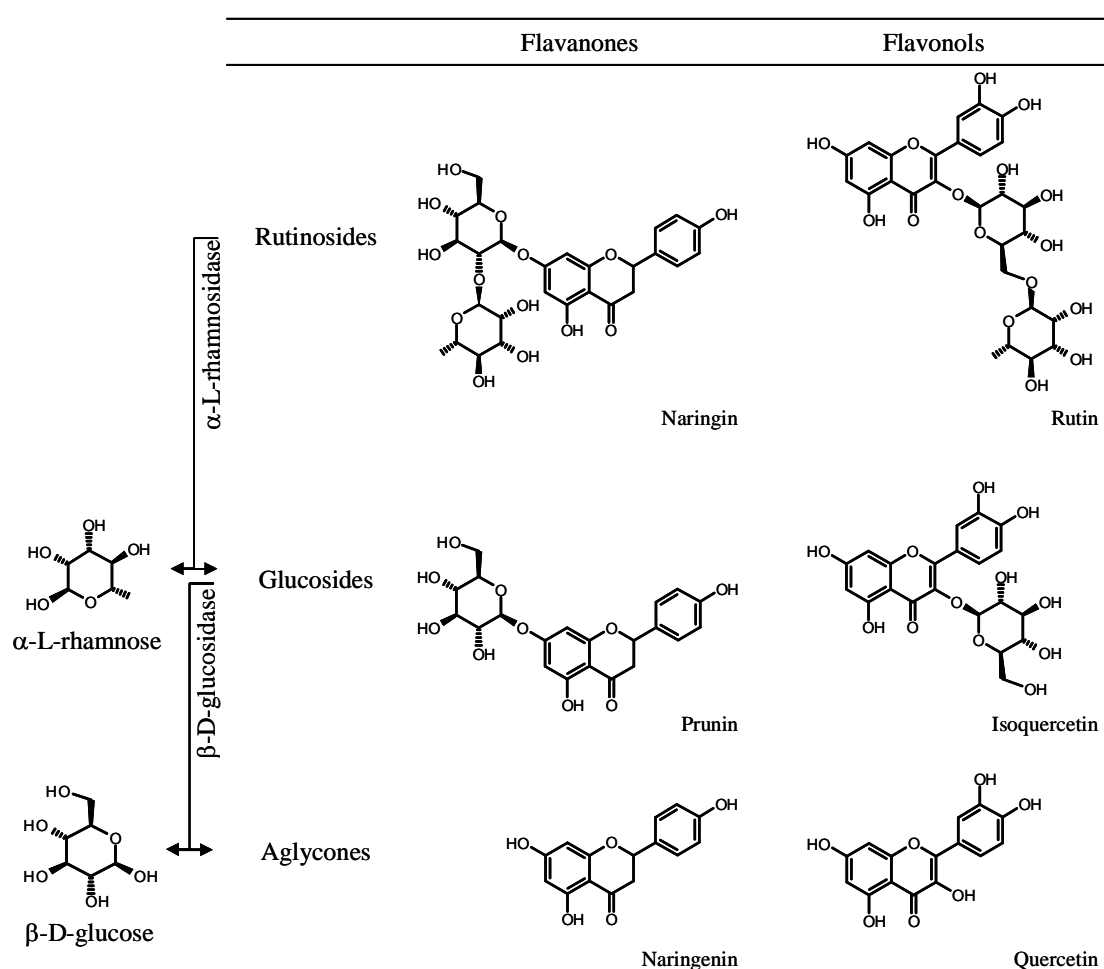


Figure 1.10 Scheme of the production of flavonoid glucosides and aglycones starting from its rutinoides precursors using an enzymatic approach (α -L-rhamnosidase and β -D-glucosidase).

1.3.5.1 Naringinase

Naringinase is a hydrolase consisting of a multi-enzyme complex obtained from *Penicillium sp.* or *Aspergillus sp.* (Yalim *et al.*, 2004), which provides both α -L-rhamnosidase (EC 3.2.1.40) and β -D-glucosidase (EC 3.2.1.21) activities. In this work,

it is used a naringinase from *Penicillium decumbens*. Mamma *et al.*, 2005 purified the naringinase from *Penicillium decumbens* and identified a α -L-rhamnosidase with a molecular mass of 58 kDa and a β -D-glucosidase assembled in a tetramer with monomers of 120 kDa. Naringinase is a very attractive hydrolase in the commercial point of view and possesses several applications within the pharmaceutical and food industry (Puri and Banarjee, 2000). Among these applications, naringinase can be used to hydrolyze both naringin and rutin into prunin and isoquercetin, respectively, with α -L-rhamnosidase activity and consecutively to the aglycones, naringenin and quercetin, respectively, by means of β -D-glucosidase activity (Figure 1.10). A rhamnose is released in the first step and a glucose molecule in the second one.

1.4 Enzymatic biocatalysis

Enzymes are catalysts used to accelerate chemical reactions, which in other way would occur in a very slow way. They cause the decrease of the activation energy, which favors the reaction occurrence; and are not destroyed by the reaction and don't shift the chemical equilibrium either. Their specificity for a certain type of reactions and substrates makes them unique when comparing with a chemical catalyst. In addition, their lability against temperature, pH and other denaturing agents is related with their own nature while proteins (Metzler, 2001).

1.4.1 Structure of enzymes

The functional properties of enzymes are determined by their tridimensional structure. Their structure folds spontaneously from a unique amino acid sequence, a polypeptide chain, under physiological conditions. Usually there is only one conformation where the enzyme remains active, which is called the native conformation. Enzymes possess a primary, secondary, tertiary and also a quaternary structure in the case of the association of two or more polypeptide chains (Figure 1.11) (Lehninger *et al.*, 2005).

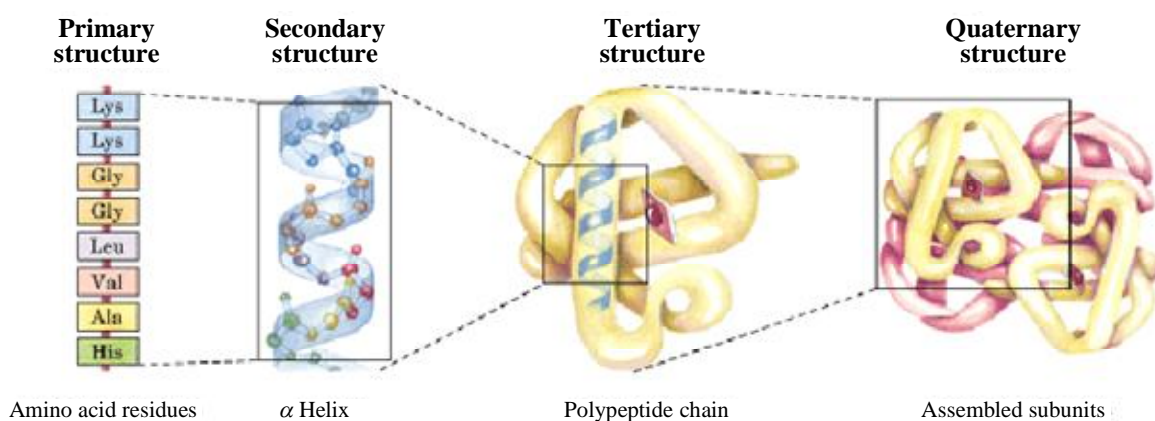


Figure 1.11 Tridimensional structures of proteins (adapted from Lehninger *et al.*, 2005).

The primary structure consists on aminoacids linked through peptide bonds. The aminoacids sequence on the primary structure is responsible for the chemical and biological properties of the enzyme, defining the next levels of structural organization. The secondary structure defines the spatial arrangement of the polypeptide chain. It is established through hydrogen bridges between the carbonyl and the amine group of another amino acid. Hydrogen bridges are an intermediate type of interactions, between

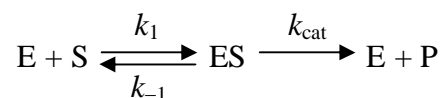
covalent bond and electrostatic bonds. This kind of interaction plays a decisive role in order support the secondary structure (Lehninger *et al.*, 2005; Scharnagl *et al.*, 2005).

The tertiary structure is the product of structural arrangements of the polypeptide chain at the secondary structure and the interactions between the lateral chains of geometrically and spatial closed amino acids. The structure and stability of the tertiary structure of the enzymes is dependent on several interactions, including disulfide bridges, electrostatic interactions, *van der Walls* forces, hydrogen bridges and hydrophobic interactions. Disulfide bridges are established between cysteine amino acids, and as covalent bonds are extremely important to support the tertiary structure. Electrostatic interactions are settled by close charges present in the lateral chain of certain amino acids, but their contribution to the enzyme structure is low. In the case of *Van der Walls* forces, an electrostatic type of interaction established between non-charged polar groups, despite the low energy of these interactions, their importance for the enzyme structure is high due to the high number of these interactions. Hydrophobic interactions are established between close hydrophobic residues and play an important role whenever the enzyme is solubilized in a polar solvent. The hydrophobic groups have tendency to hide inside the enzyme, interacting with each other and repelling the solvent (Metzler, 2001; Lehninger *et al.*, 2005).

Finally, the quaternary structure consists on the spatial arrangement of two or more subunits of the enzyme. This structure is only present in multimeric enzymes, which consist of two or more associated polypeptide chains (Scharnagl *et al.*, 2005).

1.3.2 Enzymatic kinetics

The reaction rates of enzymatic catalyzed reactions are, generally, proportional to the first potential of the enzyme concentration, while the dependence with the substrate concentration is not that linear. A reversible complex formation between enzyme and substrate has been shown to be the first step in enzymatic catalysis. This enzyme-substrate complex (ES) can either lead to the formation of products and free enzyme or break up into substrate and free enzyme again. In order to describe this system Michaelis and Menten (1913) proposed the following scheme:



where E is the free enzyme, S is the substrate and k_1 , k_{-1} and k_{cat} are rate constants. The following approximations are also considered (Metzler, 2001):

- a) the reversible reaction for the formation of the enzyme-substrate complex starting from free enzyme and product can be omitted during the study of the initial rate period, when the product concentration is low;
- b) the combination of free enzyme and substrate leads instantaneously to the enzyme-substrate complex. This step is fast and reversible;
- c) the substrate concentration is in large excess comparing with enzyme concentration, where for a certain short time during rate measurement the concentration of the enzyme-substrate complex is constant (steady-state approximation);
- d) the conversion of the enzyme-substrate complex into product and free enzyme is slow and doesn't change the equilibrium between enzyme plus substrate and the enzyme-substrate complex ($k_{\text{cat}} \ll k_{-1}$).

Michaelis and Menten (1913), proposed the following equation (Equation 1.1):

$$v = \frac{v_{\text{max}} [S]}{[S] + K_M} \quad (1.1)$$

where v is the initial reaction rate, v_{max} is the maximum initial reaction rate and K_M is the Michaelis-Menten constant. This model can be reduced to a first order equation relative to the substrate concentration, whenever the substrate concentration is much smaller than the Michaelis-Menten constant ($[S] \ll K_M$), (Equation 1.2):

$$v = \frac{v_{\text{max}}}{K_M} [S] \quad (1.2)$$

On the other hand, when the substrate concentration is much higher than the Michaelis-Menten constant ($[S] \gg K_M$), this model is reduced to a zero order equation relative to the substrate concentration (Equation 1.3). Under these conditions all the enzyme is saturated and converted into enzyme-substrate complex. v_{max} is a numerical constant that represents the maximum velocity obtained when E is completely converted to ES (Michaelis and Menten, 1931).

$$v = v_{\text{max}} \quad (1.3)$$

1.4.2.1 Kinetic parameters

The Michaelis-Menten kinetics is also referred as a hyperbolic kinetics because a plot of v against $[S]$ has the shape of a rectangular hyperbola through the origin, having two asymptotes ($v = v_{\max}$ and $[S] = -K_M$). According to this model the initial reaction rate tends asymptotically to the maximum reaction rate. In these conditions neither the K_M nor the v_{\max} can be determined reliably. In order to determine these kinetic parameters is useful to linearize the Michaelis-Menten equation using the Lineweaver-Burk representation (double reciprocal plot) (Equation 1.4), which is obtained from the direct inversion of the Michaelis-Menten equation terms. Through the representation of $1/v$ against $1/[S]$ it is obtained a straight line with a slope corresponding to $K_M \cdot v_{\max}^{-1}$ and an ordinate origin equal to v_{\max}^{-1} . Following this, the experimental kinetic parameters can be determined through linear regression fit of the obtained experimental data (Lineweaver and Burk, 1934).

$$\frac{1}{v} = \frac{1}{v_{\max}} + \frac{K_M}{v_{\max} [S]} \quad (1.4)$$

Despite the generalized use of the double reciprocal plot, their estimates are both biased and imprecise (Ritchie and Prvan, 1996). This method gives excessive emphasis on enzyme rates at low substrate concentration, where also the relative errors of the experimental data are higher. In this thesis, to avoid these limitations, the kinetic parameters were determined by non-linear least-squares regression, using the Michaelis-Menten equation. The parameters obtained by the double reciprocal plot were used only as initial values of the non-linear regression parameters.

Michaelis-Menten constant

In many cases k_{cat} is much smaller than k_{-1} , so in these cases the Michaelis-Menten constant equals the dissociation constant for the breakdown of the enzyme-substrate complex into free enzyme and substrate. Thus, Michaelis-Menten expresses an inverse relationship to the strength of substrate binding to the enzyme. It is a characteristic of each enzyme-substrate system at a certain temperature and pH and measures the affinity of the enzyme in relation to the substrate. A small Michaelis-Menten constant indicates high affinity for the substrate and in this case the maximum initial reaction rate will be approached more quickly. In addition, Michaelis-Menten constant represents the

substrate concentration at which the reaction rate reaches half of its maximum value (Metzler, 2001).

Catalytic constant

The catalytic constant (k_{cat}) is a kinetic constant of first order for the conversion of the enzyme-substrate complex into product plus free enzyme. This constant is related with the reaction properties of the enzyme-substrate, enzyme-intermedium compound and enzyme-product complexes and can be determined according to Equation 1.5:

$$k_{\text{cat}} = \frac{v_{\text{max}}}{[E_t]} \quad (1.5)$$

where E_t is the total enzyme amount (Equation 1.6):

$$E_t = E + ES \quad (1.6)$$

Specificity constant

The enzyme specificity is observed not only in binding but also in the rate that converts the enzyme-substrate complex into products, following this, the $k_{\text{cat}} \cdot K_M^{-1}$ ratio shows up as a specificity constant besides being an apparent kinetic constant of second order. This ratio expresses the specificity for substrates that are in competition for the enzyme active site (Metzler, 2001).

1.4.3 Thermodynamic parameters

The transition state theory (TST) was developed through Pelzer and Wigner (1932), Eyring (1935), Wynne-Jones and Eyring (1935), and Evans and Polanyi (1935, 1937) work. This theory allows the description of a chemical reaction concerning its physical behavior, correlating both kinetic and thermodynamic parameters. It was primarily used as a qualitative basis to achieve mechanistic information on chemical reactions (Truhlar *et al.*, 1996). Accurate experimental data on rate constants can be used to successfully calculate thermodynamic functions of activation (TFA) and show some insights on catalysis, at a macroscopic level. TST supports its mathematical formulation on the following assumptions (Ritchie, 1990):

- a) Within each reactional mechanism step of a certain chemical reaction, the transition of reactants into products, or reverse, follows an intermediate state, called the transition state.
- b) The Quasi-Equilibrium assumption states the existence of quasi-equilibrium between the reactants and the activated complexes, which precedes the thermodynamic equilibrium between reactants and products, according to the following scheme:



where K^\ddagger is the equilibrium constant of the quasi-equilibrium between reactants and the activated complex.

- c) The kinetic theory calculates the conversion rate of activated complexes into products, which is directly proportional to the concentration of the configurations present within the transition state multiplied by the frequency ($k_B T/h$); where k_B is the Boltzmann constant, h is the Planck constant and T is the absolute temperature.

Assuming the existence of the quasi-equilibrium, which is governed by an equilibrium constant it's possible to define thermodynamic functions in a similar way to the functions determined from usual equilibrium constants. Following this and according to the formulated assumptions, it is possible to establish the fundamental equation of TST (Equation 1.7):

$$k^\circ = \frac{k_B T}{h} e^{-\frac{\Delta^\ddagger G^\circ}{RT}} \quad (1.7)$$

where the standard reaction rate constant (k°) is related to the change of the standard Gibbs free energy of activation ($\Delta^\ddagger G^\circ$); R is the gas constant.

By other way, through Equation 1.8:

$$\Delta^\ddagger G^\circ = \Delta^\ddagger H^\circ - T\Delta^\ddagger S^\circ \quad (1.8)$$

where $\Delta^\ddagger H^\circ$ and $\Delta^\ddagger S^\circ$ represent, respectively, the change of the standard activation enthalpy and the change of the standard activation entropy, between the initial and the transition states, Equation 1.7 can adopt another look, leading to Equation 1.9:

$$\ln k^\circ = \ln \frac{k_B T}{h} + \frac{\Delta^\ddagger S^\circ}{R} - \frac{\Delta^\ddagger H^\circ}{R} T^{-1} \quad (1.9)$$

Considering both Equations 1.7 and 1.9, it is possible to determine TFA, through the derivatization of k° in respect to independent variables. TFA reflect physical interactions and represent the properties differences between the initial state and the structure of the transition state. Following this, they have been quite useful to analyse the structure and mechanism of reactional systems.

1.4.3.1 Temperature dependence at constant pressure

The effect of temperature gives information concerning energy aspects of the reactional process. The thermodynamic activation functions at constant pressure are obtained from their isobaric variation with temperature:

Standard Gibbs energy of activation

The reason why enzymes accelerate reactions is because they reduce the standard Gibbs energy of activation, when compared with non-catalyzed reactions, by stabilizing the transition state. The standard Gibbs energy of activation (Equation 1.10) is a function of rigorous determination that gives similar information to the reaction rate coefficient. Due to the enthalpy-entropy compensation, this parameter is low sensitive to changes between initial and transition states (Segurado, 1989; Pinheiro, 1999). For instance an effect that lowers enthalpy, due to a higher linkage degree between two molecules also lowers entropy, due to movement freedom restriction of those two molecules (Boots and Bokx, 1989). Nevertheless, a decrease of the standard Gibbs energy of activation of a certain reaction caused by the presence of an enzyme may be driven by a decrease of the standard activation enthalpy and/or by an increase of the standard activation entropy (Cabral, 2003).

$$\Delta^\ddagger G^\circ = RT \left(\ln \frac{k_B T}{h} - \ln k \right) \quad (1.10)$$

Standard activation enthalpy

The standard activation enthalpy (Equation 1.11) is a function that gives information concerning the intrinsic energy associated with linkages formation and rupture within the transition state, as well as the intrinsic energy associated with solvation of both initial and transition states (Segurado, 1989). The enzyme shall provide a structure with ideally positioned groups in order to interact with substrate in the activated complex.

$$\Delta^\ddagger H^\circ = \left(\frac{\partial \frac{\Delta^\ddagger G^\circ}{T}}{\partial \frac{1}{T}} \right)_P = -R \left(\frac{\partial \ln \frac{k}{T}}{\partial \frac{1}{T}} \right)_P = RT^2 \left(\frac{\partial \ln \frac{k}{T}}{\partial T} \right)_P \quad (1.11)$$

Standard activation entropy

The standard activation entropy (Equation 1.12) is a function that gives information concerning the molecular structure of reactional species, activation complex and mechanism. It includes contributions inherent to the freedom of translation, vibration and rotation movements; entropic electrostatic factors, linked to the electrostriction effect; and changes related to solvation entropy, between the initial and the transition states. Negative values of $\Delta^\ddagger S^\circ$ mean a more organized transition state than the initial state (Segurado, 1989; Pinheiro, 1999). In the case of enzymatic catalyzed reactions the substrate binds to the enzyme to form the activated complex and is maintained in a favorable geometry for the reaction to proceed. On the other side, in the case of non-catalyzed reactions the substrate needs to find an eventual other substrate in order to form the activated complex, which involves a high entropy loss. This proximity effect caused by the enzyme turns activation entropy more favorable (Cabral, 2003).

$$\Delta^\ddagger S^\circ = - \left(\frac{\partial \Delta^\ddagger G^\circ}{\partial T} \right)_P = R \ln \left(\frac{h}{k_B} \right) + R \left[\frac{\partial \left(T \ln \frac{k}{T} \right)}{\partial T} \right]_P \quad (1.12)$$

TFA at constant pressure can be determined after choosing the mathematical model that best fits to the experimental data of k against T . Several mathematical models have been proposed to describe the dependency of k with temperature, but only the two simpler models were studied:

Arrhenius model

It is a well known experimental fact that k is temperature dependent, and the empirical Arrhenius equation still constitutes the main mathematical relation used to describe it. This equation, a first order polynomial describing $\ln k$ as function of T^{-1} , can be written as Equation 1.13:

$$\ln k = A + \frac{B}{T} \quad (1.13)$$

where A and B are empirical parameters related to TFA and temperature independent. With respect to Arrhenius model (Arrhenius, 1887), and considering both Equation 1.13 and TST, $\Delta^\ddagger H^\circ$ and $\Delta^\ddagger S^\circ$ are determined, respectively, from the experimental kinetic data using Equations 1.14 and 1.15:

$$\Delta^\ddagger H^\circ = -R(B + T) \quad (1.14)$$

$$\Delta^\ddagger S^\circ = R \left(\ln \frac{h}{k_B} + A - 1 - \ln T \right) \quad (1.15)$$

Standard Gibbs energy of activation can be calculated directly from the k value through Equation 1.16.

$$\Delta^\ddagger G^\circ = RT \left(\ln \frac{k_B T}{h} - \ln k \right) \quad (1.16)$$

Wold and Ahlberg model

In case of enzymatic biocatalysis, often is found that the former relation frequently does not fit satisfactorily to experimental data, probably because proteins are not rigid structures. A second order polynomial relation known as the Wold and Ahlberg equation (Equation 1.17) can be considered to determine TFA values; in this equation besides A and B , C is also an empirical parameter (Wold and Ahlberg, 1970).

$$\ln k = A + \frac{B}{T} + \frac{C}{T^2} \quad (1.17)$$

With respect to Wold and Ahlberg model (Wold and Ahlberg, 1970), and considering both Equation 1.17 and TST, $\Delta^\ddagger H^\circ$ and $\Delta^\ddagger S^\circ$ are determined, respectively, from the experimental kinetic data using Equations 1.18 and 1.19:

$$\Delta^\ddagger H^\circ = -R \left(B + \frac{2C}{T} + T \right) \quad (1.18)$$

$$\Delta^\ddagger S^\circ = R \left(\ln \frac{h}{k_B} + A - 1 - \frac{C}{T^2} - \ln T \right) \quad (1.19)$$

Standard Gibbs energy of activation can be calculated from Equation 1.16.

1.4.3.2 Pressure dependence at constant temperature

The effect of pressure gives information concerning volumetric aspects of the reactional process. The thermodynamic activation functions at constant temperature are obtained from their isothermal variation with pressure:

Standard Gibbs energy of activation

The standard Gibbs free energy of activation at constant temperature is determined in a direct way from the reaction rate values, from the experimental kinetic assays under pressure, according to Equation 1.10. Its meaning has already been discussed on 1.4.3.1.

Standard activation volume

The standard activation volume ($\Delta^\ddagger V^\circ$) (Equation 1.20) is a function that measures the volume change between the activation complex and reactants (Van Eldik *et al.*, 1989). It is a very important function in order to study the structure and properties of the transition state as well as the reaction mechanisms. $\Delta^\ddagger V^\circ$ shows a very discriminative character concerning the solvent involvement, even though is sensible to a less number of factors, when compared with $\Delta^\ddagger S^\circ$. Pressure accelerates processes where the initial state occupies a larger volume than the transition state. The rate constant increases with pressure as long as the activation volume change is negative.

$$\Delta^\ddagger V^\circ = \left(\frac{\partial \Delta^\ddagger G^\circ}{\partial P} \right)_T = -RT \left(\frac{\partial \ln k}{\partial P} \right)_T \quad (1.20)$$

Activation volume has been interpreted in a molecular way according to intrinsic and solvent contributions (Mozhaev *et al.*, 1996). The intrinsic contributions depend on the molecular packing density and to the breaking or formation of covalent bonds. The volume change corresponding to covalent bond formation is around -10 mL mol^{-1} , while in the case of angles bond variation and packing density is practically null (Mozhaev *et al.*, 1996). Following this, except in the cases of breaking or formation of covalent bonds, the solvent contribution is of most importance concerning volume change. The solvent contribution comes from weak interactions hydration, including: electrostatic interactions, hydrogen bonds and hydrophobic interactions. Concerning electrostatic interactions, the formation of ionic charges is associated with a volume decrease due to electrostriction effect, consisting on the compression of the dipoles

generated by water molecules surrounding the ion electric field. The hydrogen bonds are stabilized with pressure due to the lowering of the inter-atomic distance, although the volume change associated with hydrogen bridges is small. On other side the formation of hydrophobic interactions are associated with a volume increase, which turns its formation disfavoured with pressure (Mozhaev *et al.*, 1996; Balny, 2004).

Standard isothermal compression of activation

The standard isothermal compression of activation (Equation 1.21) is an activation function that represents the dependence of the activation volume in respect to pressure (Viana and Reis, 1996). It measures the compressibility change between the activation complex and the reactants. Its magnitude depends on the physical and chemical properties of the solvent, particularly its action on the activation process (Segurado, 1989).

$$\Delta^\ddagger \beta^\circ = - \left(\frac{\partial \Delta^\ddagger V^\circ}{\partial P} \right)_T = -RT \left(\frac{\partial^2 \ln k}{\partial P^2} \right)_T \quad (1.21)$$

TFA at constant temperature can be determined after choosing the mathematical model that best fits to the experimental data k vs. P . Several mathematical models have been proposed to describe the dependency of k with P . As in the case of TFA at constant pressure, where the experimental data have an average accuracy, only the more simplistic models were studied.

Burris and Laidler model

The Burris and Laidler mathematical model (Equation 1.22) (Burris and Laidler, 1955) is the more simple dependence between $\ln k$ vs. P :

$$\ln k = A + BP \quad (1.22)$$

where A and B are empirical parameters independent from pressure. This equation supports an independence of the activation volume in respect to pressure, leading to a null isothermal compression of activation. The change of the standard activation volume is determined through Equation 1.23.

$$\Delta^\ddagger V^\circ = -RTB \quad (1.23)$$

Golinkin, Laidlaw and Hyne model

The Golinkin, Laidlaw and Hyne mathematical model (Equation 1.24) (Golinkin *et al.*, 1966) describes a second order polynomial dependence between $\ln k$ vs. P :

$$\ln k = A + BP + CP^2 \quad (1.24)$$

where besides A and B , C is an empirical parameter independent from pressure. $\Delta^\ddagger V^\circ$ can be calculated from the fitting of Equation 1.24 to experimental data and is given by Equation 1.25. In addition, this model implies a constant value for the standard isothermal compression of activation change, which is given by Equation 1.26.

$$\Delta^\ddagger V^\circ = -RT(B + 2CP) \quad (1.25)$$

$$\Delta^\ddagger \beta^\circ = 2RTC \quad (1.26)$$

Generalized polynomial equations model

The generalized polynomial equations model, suggested by Walling and Tanner (1963), make use of a potencies series in respect to pressure (Equation 1.27), to describe the dependence between $\ln k$ vs. P :

$$\ln k = A_0 + A_1P + A_2P^2 + A_3P^3 + \dots + A_nP^n \quad (1.27)$$

where $A_0, A_1, A_2, A_3 \dots A_n$ are empirical parameters independent from pressure. The essential empirical behaviour of this model, as well as Burris and Laidler model and Golinkin, Laidlaw and Hyne model, which are particular cases of this general polynomial equation doesn't allow finding relevant conclusions. On other side, these models have a vast applicability once they don't impose a certain reactional model (Segurado, 1989). $\Delta^\ddagger V^\circ$ can be calculated from Equation 1.28 and $\Delta^\ddagger \beta^\circ$ is given by Equation 1.29:

$$\Delta^\ddagger V^\circ = -RT(A_1 + 2A_2P + 3A_3P^2 + \dots + nA_nP^{n-1}) \quad (1.28)$$

$$\Delta^\ddagger \beta^\circ = RT[2A_2 + 6A_3P + \dots + n(n-1)A_nP^{n-2}] \quad (1.29)$$

Baliga and Whalley model

Baliga and Whalley model is represented by Equation 1.30 (Baliga and Whalley, 1970):

$$\ln k = \frac{A + BP}{1 + CP} \quad (1.30)$$

According to this model, $\Delta^\ddagger V^\circ$ can be calculated from Equation 1.31 and $\Delta^\ddagger \beta^\circ$ is given by Equation 1.32

$$\Delta^\ddagger V^\circ = -RT \frac{(B - AC)}{(1 + CP)^2} \quad (1.31)$$

$$\Delta^\ddagger \beta^\circ = -2RTC \frac{(B - AC)}{(1 + CP)^3} \quad (1.32)$$

Despite not being an activation function, the standard reaction volume is a very useful thermodynamic parameter, which is determined through an isothermal variation with pressure:

Standard reaction volume

The standard reaction volume ($\Delta V^\circ_{\text{reac}}$) (Equation 1.33) is an important thermodynamic function to be determined whenever the effect of pressure is studied, giving information about volumetric changes between the reactants and products. Pressure favours processes where products occupy a smaller volume than reactants according to *Le Chatelier* principle. The reaction equilibrium constant (K) increases with pressure as long as the reactional volume change is negative (Van Eldik *et al.*, 1989).

$$\Delta V^\circ_{\text{reac}} = \left(\frac{\partial \Delta G^\circ}{\partial P} \right)_T = -RT \left(\frac{\partial \ln K}{\partial P} \right)_T \quad (1.33)$$

The interpretation of the molecular events underlying the standard reaction volume is analogous to the standard volume of activation. In the case of the activation volume it measures the volumetric changes between the transition state and the reactants, while in the case of the reaction volume what is measured is the volumetric change between products and reactants (Van Eldik *et al.*, 1989).

The determination of the standard reaction volume can also be done using analogous models used for the determination of the standard volume of activation. In the case of the activation volume, its determination is based on a dependence of the reaction rate constant with pressure, while in the case of the reaction volume it is determined through an equilibrium constant dependence with pressure. From $\ln K$ dependence with pressure is estimated the reaction volume. Following this, in order to determine the reaction volume the reaction rate, k , shall be substituted by the equilibrium constant, K in the models describing the dependency of k with P (Calado, 1986; Van Eldik *et al.*, 1989).

1.4.4 Enzymatic stability

The enzyme stability is crucial for an entire biotechnological process, once the enzyme activity is dependent on the integrity of its native state, in order to maximize the process productivity. While protein, the enzyme stability can be defined through a simplistic approach of a 2-state model: native and denatured state (Cooper, 1999). The native state comprises all states where enzyme remains active, while the states where the enzyme completely loses its activity are included in the denatured state. Considering the folding-denaturing transition as phase transition (Hawley, 1971), a Gibbs energy change (ΔG) can be established between the denatured (G_D) and the native state (G_N), according to Equation 1.34:

$$\Delta G = G_D - G_N \quad (1.34)$$

The magnitude of the Gibbs energy change measures how easily an enzyme may suffer denaturation (Scharnagl *et al.*, 2005). A large Gibbs energy change is consistent with a very stable enzyme, which is dependent on the enthalpic/entropic compensation ruled by Equation 1.35, where ΔH is the enthalpy change and ΔS is the entropy change (Scharnagl *et al.*, 2005).

$$\Delta G = \Delta H - T\Delta S \quad (1.35)$$

Several variables influence the enzyme stability and ΔG assumes a multidimensional function of all these parameters (Equation 1.36), including: temperature (T), pressure (P), cosolvent type and concentration (c_x), pH, ionic activity (a_y), etc (Jurado *et al.*, 2004):

$$\Delta G = \Delta G^\circ + f(T, P, c_x, \text{pH}, a_y, \dots) \quad (1.36)$$

1.4.4.1 Temperature

The influence of temperature on the reaction rate of enzyme catalysed reactions is similar to chemical reactions, but the proteic nature of enzymes may turn it a bit more complex. Bellow optimal temperature, the enzymatic reaction rate increases with temperature, but above the optimal temperature value the inactivation caused by heat leads to a reaction rate decrease. On the basis of inactivation is the structural change of protein that occurs under these conditions. As temperature is raised the enthalpy change between the native and the denatured state starts to increase as well as the entropy

change, due to the destruction of the ordered water structures around the protein. Above the temperature value where entropy compensates enthalpy the denatured state is favored, corresponding to a negative Gibbs energy change (Cabral *et al.*, 2003; Scharnagl *et al.*, 2005). During the temperature-induced denaturing transition the protein native structure is destroyed into a random-coil structure, where the hydrophobic aminoacids initially impelled into the inside of the protein through hydrophobic interaction are exposed to the outside, contacting with water (Scharnagl *et al.*, 2005).

1.4.4.2 Pressure

The protein stability against pressure can be divided into a high and a low pressure range values, considering two distinct transitions between the native and the denatured states. No matter the pressure magnitude, hydrostatic pressure induces protein denaturation following the principle of *Le Chatelier*, favoring the smaller volume state. Concerning a high pressure range, above some threshold pressure value, which depends on the enzyme in study, the volume change (ΔV) between the native (V_N) and the denatured state (V_D) is negative, as rule (Equation 1.37):

$$\Delta V = V_D - V_N \quad (1.37)$$

Underlying this fact is the presence of voids, eventually in the protein pockets, that are squeezed. Therefore, the denatured state is favored under high pressure range once pressure favours the state that occupies a smaller volume. Denaturation occurs after crossing a certain pressure value where ΔG is null.

The low pressure range, it is limited not only to low pressure but also to high temperature, once it would be necessary negative pressures to study the denaturation at a large temperature range. Within these two boundaries (low-pressure/high-temperature) the pressure decrease may lead to denaturation. In this case the volume change is positive, by contrast with the high pressure range. During pressure decrease the denatured state is favoured once it occupies a larger volume than the native state, leading to a positive volume change (Scharnagl *et al.*, 2005).

The effect of pressure on the biocatalyst structure is a major issue in pressure biocatalysis. The primary structure established through peptide bonds is not affected by pressure, while in the case of the hydrogen bridges of the secondary structure a pressure

magnitude ranging from 300 to 700 MPa is needed to disturb them. The destruction of the secondary structure leads to the enzyme denaturation and consequent loss of catalytic activity (Mozhaev *et al.*, 1996; Buckow, 2006). In order to influence the tertiary structure is needed a pressure magnitude around 200 MPa, which is similar to the pressure magnitude needed to dissociate a quaternary structure, which is around 150 MPa (Mozhaev *et al.*, 1996; Buckow, 2006). It is on the tertiary and quaternary structure level that pressure may exert influence on the protein conformation. The presence of small cavities within the proteins allows the adoption of different conformations that are dependent on weak interactions between polypeptide chains (Mozhaev *et al.*, 1996; Lullien-Pellerin and Balny, 2002; Balny, 2004; Buckow, 2006).

Enzymatic stability against temperature under pressure

As a phase transition, the folding-denaturing of proteins under both pressure and temperature conditions draws an elliptical line in a P - T plane (Figure 1.12) (Hawley, 1971), where ΔG is null, delimiting a closed range, where the protein adopts a stable native state ($\Delta G > 0$). Crossing the boundary of that region, the native conformation loses its stability and the protein unfolds. As this transition is characterized by a latent heat of first order, the phase boundary slope can be determined according to the Clausius-Clapeyron equation (Equation 1.38) (Hawley, 1971; Heremans and Smeller, 1998; Smeller, 2002; Scharnagl *et al.*, 2005; Wiedersich *et al.*, 2008):

$$\left(\frac{\partial P}{\partial T}\right)_{\Delta G} = \frac{\Delta S}{\Delta V} \quad (1.38)$$

The boundaries of the stability phase diagram can be determined from a solution of Clausius-Clapeyron equation, assuming that the specific heat capacity (C_p), the compressibility factor (β) and the thermal expansion factor (α) are independent on both pressure and temperature. The integration of Clausius-Clapeyron equation leads to Equation 1.39 (Hawley, 1971; Smeller, 2002):

$$\Delta G(P,T) = \frac{\Delta\beta}{2}(P-P_0)^2 - \frac{\Delta C_p}{2T_0}(T-T_0)^2 + \Delta\alpha(P-P_0)(T-T_0) + \Delta V_0(P-P_0) - \Delta S_0(T-T_0) + \Delta G_0 = 0 \quad (1.39)$$

Equation 1.39 is a second order curve in the P - T plane, being a general mathematical equation for a conic section that can adopt an elliptic, hyperbolic or parabolic shape

(Wiedersich *et al.*, 2008). T_0 and P_0 are arbitrarily chosen reference values for pressure and temperature, known as standard conditions. It was found that in the case of proteins this equation adopts an elliptic shape due to a mathematical constraint (Inequation 1.40) (Smeller, 2002), which happens to be satisfied by the different signs of ΔC_P and $\Delta\beta$ in first studies by Hawley (1971), involving chymotrypsinogen and ribonuclease.

$$\Delta\alpha^2 > \frac{\Delta C_P \Delta\beta}{T_0} \quad (1.40)$$

It shall be stressed that the phase transition approach has its limits, concerning not only the approximations made but also differences between proteins, which strongly disperses it (Scharnagl *et al.*, 2005). Nevertheless, this approach seems to describe well many proteins fold-denaturing thermodynamics (Scharnagl *et al.*, 2005). The elliptic phase protein denaturing diagram (Figure 1.12) is the base of a potential use of pressure to avoid biocatalyst inactivation caused by heat. Considering the grey region that bounds the native state, a temperature increment from (a) to (b) (Figure 1.12) leads to the protein unfolding. If, coupled to temperature increment pressure is raised, from (a) to (c), the enzyme native state is preserved. This stated antagonistic effect between pressure and temperature is the basis of pressure stabilization of the enzyme native state at high temperatures (Balny, 2004; Scharnagl *et al.*, 2005).

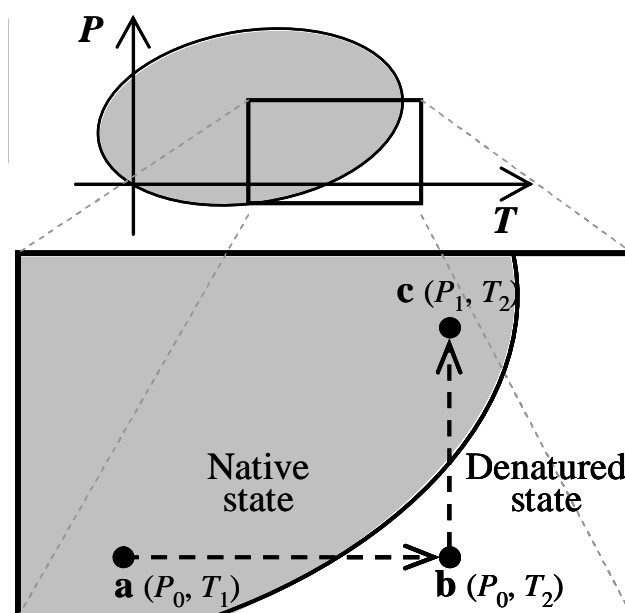


Figure 1.12 Elliptic phase protein denaturing diagram.

Scharnagl *et al.* (2005) proposed a hypothesis to explain this effect, based on the behaviour of protein stability under pressure. The use of pressure as a tool to avoid the biocatalyst heat denaturation is based on the fact that at a high pressure range the induced denatured state has a different structure than at a low pressure range. At a high pressure range the denatured state is still a kind of globular state where protein shrinks due to the squeezing of voids, so that $V_D < V_N$. On the other hand at a low pressure range and at sufficiently high temperature the volume change is positive $V_D > V_N$. At these conditions unfolding to a random-coil structure is still possible, which occupies a larger volume than the native state, due to the exposure of hydrophobic aminoacids to the solvent. As pressure favours the state that occupies a smaller volume, native state is favoured in detriment of denatured state, at high temperature within a low pressure range.

The protecting effect of pressure against heat inactivation has its own boundaries and two distinct modes of action may occur according to the pressure magnitude. These two modes of action are separated by a critical pressure value, which is specific for each enzyme, where the volume change associated with denaturation is null. Above this critical pressure value, the volume change associated with denaturation happens to be negative; meaning that in this case pressure will favour the denatured state which is the smallest volume state. On the opposite, below this critical pressure value the volume change associated with denaturation is positive, so in this case pressure favours the native state of the enzyme. Following this, pressure magnitude is critical for the stabilization of the enzyme native state under high temperature. Of course that a critical temperature value also do exist, which bounds the maximum temperature where pressure is still able to antagonize the denaturing effect of heat. It is below this critical temperature and pressure values that pressure can turn to be a very helpful favouring the native state, which corresponds in this case to the smaller volume state (Scharnagl *et al.*, 2005).

1.4.4.3 Cosolvents

Water is the solvent where enzymes exist and work in a natural way. By this way the dynamic of the water molecules present within the protein hydration shell are directly associated with the enzyme stability. Then, any cosolvent that interferes with this hydration shell leads to enzyme inactivation. The possible mechanisms underlying the

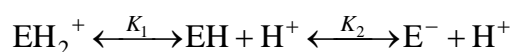
enzyme denaturation caused by organic cosolvents can be divided into: direct contact between the cosolvent molecules and enzyme; indirect interaction, which is caused by a disturbance of the water molecules dynamic that constitute the hydration shell of enzymes; or through the combination of both mechanisms (Scharnagl *et al.*, 2005).

Cosolvents can be classified into: compatible if they don't disturb the protein functionality; non-compatible if they induce protein structure disruption; and compensatory cosolvents, which stabilize the folded structure against external stresses (Scharnagl *et al.*, 2005). The stability of the enzyme native state depends greatly on the hydrophobic effect, which comes from the tetrahedral structure that characterizes the water molecules. Any solvent that is not compatible with the tetrahedral arrangement of water molecules ends up weakening the hydrophobic effect, leading to enzymatic denaturation. The denaturation caused by the presence of cosolvents is similar to heat denaturation, where hydrophobic amino acids are exposed to the involving water (Scharnagl *et al.*, 2005).

1.4.4.4 pH

The pH value influences the ionization of the aminoacids that constitute the enzyme, according to their specific pKa values. The aminoacids charges determine the three-dimensional enzyme structure. Also when the substrate has electrical charges, the approximation to the enzyme active centre depends on the charge of the residues involved in the bonding process. Therefore, an optimal pH value at which the enzyme activity is maximal can be fixed using an adequate buffer system (Cabral *et al.*, 2003; Jurado *et al.*, 2004; Scharnagl *et al.*, 2005).

The influence of pH on enzymatic activity can be analysed according to a kinetic model in which the enzyme is subjected to successive deprotonation according to the following equilibrium:



where EH_2^+ is the inactive protonated enzyme; EH is the active enzyme; E^- is the inactive deprotonated enzyme; K_1 is the first equilibrium constant and K_2 is the second equilibrium constant (Jurado *et al.*, 2004) that can be expressed, respectively, according to Equations 1.41 and 1.42:

$$K_1 = \frac{[EH] \times [H^+]}{[EH_2^+]} \quad (1.41)$$

$$K_2 = \frac{[E^-] \times [H^+]}{[EH]} \quad (1.42)$$

Making an overall balance (Equation 1.43), the influence of pH on the enzymatic specific activity (A) can be described by Equation 1.44, where A_{\max} is the maximum enzyme specific activity.

$$[E_t] = [EH_2^+] + [EH] + [E^-] \quad (1.43)$$

$$A = \frac{A_{\max}}{1 + 10^{pK_1 - pH} + 10^{pH - pK_2}} \quad (1.44)$$

Optimum pH values (pH_{opt}) can be determined from Equation 1.45:

$$pH_{\text{opt}} = \frac{pK_1 + pK_2}{2} \quad (1.45)$$

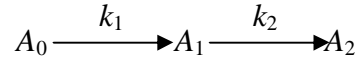
The deduction of Equations 1.44 and 1.45 can be found in annex 1.

1.4.4.5 Ionic activity

The presence of certain ions may influence the enzyme native state. In some cases, the enzyme inactivation occurs mostly when the ions diameter is small, penetrating the enzyme native structure and inducing conformational changes; others can increase the resistance against heat inactivation due to the reduction of polypeptide chain flexibility (Scharnagl *et al.*, 2005).

1.4.5 Enzymatic inactivation models

The study of the influence of the above-mentioned conditions over the stability of enzymes requires the use of mathematical models. Henley and Sadana (1985), proposed a series-type enzyme inactivation sequence involving a first-order inactivation sequence and an active intermediate according to the following scheme:



where k_1 and k_2 are the first and second inactivation rate constants, respectively. A_0 , A_1 and A_2 are specific activities of the initial active enzyme, enzyme intermediate and final enzyme state, respectively. This model is described by Equation 1.46. α_1 and α_2 are the specific activities ratio $A_1.A_0^{-1}$ and $A_2.A_0^{-1}$, respectively and A_r is the enzyme residual activity (Henley and Sadana, 1985).

$$A_r = \alpha_2 + \left[1 + \frac{\alpha_1 k_1}{k_2 - k_1} - \frac{\alpha_2 k_2}{k_2 - k_1} \right] e^{-k_1 t} - \left[\frac{\alpha_1 k_1}{k_2 - k_1} - \frac{\alpha_2 k_1}{k_2 - k_1} \right] e^{-k_2 t} \quad (1.46)$$

In cases of biphasic inactivation Equation 1.46 leads to Equation 1.47, where the final state is totally inactivated ($\alpha_2 = 0$) (Henley and Sadana, 1985).

$$A_r = \left[1 + \frac{\alpha_1 k_1}{k_2 - k_1} \right] e^{-k_1 t} - \left[\frac{\alpha_1 k_1}{k_2 - k_1} \right] e^{-k_2 t} \quad (1.47)$$

This model also includes the cases described by a single-step first-order inactivation process, according to Equation 1.48, where both α_1 and α_2 are equal to zero (Henley and Sadana, 1985).

$$A_r = e^{-k_1 t} \quad (1.48)$$

In addition, the inactivation kinetics half-life time ($t_{1/2}$), i.e., the time needed to reduce its original activity to 50 %, in the case of a first order kinetic can determined according to Equation 1.49:

$$t_{1/2} = \frac{\ln 2}{k} \quad (1.49)$$

1.5 Enzymatic immobilization

The immobilization of enzymes is a very common technique used in biotechnology, consisting on confining the enzyme within a restricted area and retaining simultaneously the enzymatic catalytic activity (Cabral *et al.*, 2003). The success of this methodology depends on the compensation of a large range of advantages over eventual limitations that shall be minimized.

The general advantages of enzymatic immobilization include: the retention of the enzyme inside a reactor; achieving high concentration of enzyme; modulation of the enzyme micro-environment and easy separation of product and enzyme, which facilitates downstream processing. More specifically, the retention of the enzyme inside a reactor allows not only repeated but also continuous utilization. A high concentration of enzyme is important whenever a fast bioconversion is needed due to unstable substrates. In the case of modulation of the enzyme microenvironment, several advantages may arise, including: increased catalytic activity, modulation of enzymatic specificity; tuning the partition characteristics of the matrix and increasing the enzyme stability against temperature, pH and organic solvents (Tischer and Kasche, 1999; Cabral *et al.*, 2003).

The enzymatic immobilization process has however some limitations mainly regarding the loss of catalytic activity and the empiricism of the process, which requires a case by case process optimization. The activity loss may occur during the immobilization or bioconversion step or eventually being a direct cause of the immobilization matrix. Before choosing a certain immobilization procedure it is important to study the adequacy between the studying enzyme and certain immobilization conditions such as pH, ionic strength and temperature conditions as well as the presence of toxic agents required for the immobilization step. Concerning the micro-environment it is important to avoid the exclusion of macromolecules as well as restriction transfer effects and stereochemical restriction to the enzyme active centre. Local pH variations are also an important issue to avoid the enzyme activity loss caused by the immobilization matrix. Finally, the enzymatic activity can be lost during the bioconversion process, due to several main issues including: enzyme loss; chemical or physical susceptibility of the immobilization matrix; pore diameter heterogeneity; accumulation of inhibitors inside the matrix and matrix retention of small solid particles in suspension (Tischer and Kasche, 1999; Cabral *et al.*, 2003).

In order to obtain useful bioimmobilizates, some requirements must be fulfilled, such as: high biocatalyst activity, long-term stability, good accessibility to substrates, resistance to leaching, resistance against denaturation and avoiding biocatalyst loss during immobilization. An eventual decrease on the rate and extension of the reaction must be overcome by the repeated use of the immobilized enzyme (Tischer and Kasche, 1999; Jin and Brennan, 2002).

1.5.1 Methods

The immobilization methods can be classified according to the combination of the nature of the support and the kind of interaction that is responsible for immobilization. The immobilization methods can be divided into binding methods and physical retention methods (Cabral *et al.*, 2003). The selection of an adequate method relies on the advantages and disadvantages that are inherent to each method (Tischer and Kasche, 1999).

The binding methods include: immobilization by reticulation and immobilization by carrier binding method. In the case of immobilization by reticulation, bifunctional reagents are used in order to do the cross-link of enzymes through covalent bonds. The carrier binding method includes: immobilization by covalent binding, ionic binding, physical adsorption and chelation. The strength of the interaction established between the enzyme and the support is a very important issue in the case of binding methods. The strength of the interaction increases from adsorption binding methods, passing by ionic methods till covalent binding methods. Weak interactions may lead to the enzyme release from the support under certain reactional conditions, including; pH, temperature, ionic strength and dielectric constant. On the other hand a strong interaction such as covalent binding may involve a complex immobilization method and catalytic activity loss (Cabral *et al.*, 2003).

The physical retention methods are divided into: immobilization by occlusion, immobilization using membranes and microencapsulation. The immobilization by occlusion consists on entrapping the enzyme inside a gel. This immobilization method is described in more detail in 1.5.1.1. The immobilization using membranes consist on arresting the enzyme using a selective porous membrane. The advantages of using this method consist on neither changing the enzyme structure nor its microenvironment, but some other issues rise, including: adsorption of enzyme, products or substrates; enzyme

loss through pores and low biotransformation rate due to high mass transfer resistance effects caused by the membrane. The microencapsulation method includes both microcapsules and inverted micelles. Microencapsulation consists on immobilizing the enzyme inside a semi permeable membrane. Microcapsules lead to lower mass transfer effects than gels produced by occlusion method, but on the other hand the aggressive conditions of the formation of membranes may lead to catalytic activity loss. Inverted micelles are aggregates in which the polar groups are concentrated in the interior and the apolar groups constitute the external layer extend outward into the solvent. They have been used in the bioconversion of substrates with low water solubility, using organic solvents, but one major disadvantage is the recovery of the enzyme and products, after the bioconversion process (Cabral *et al.*, 2003).

1.5.1.1 Occlusion method

The immobilization by occlusion consists on entrapping the enzyme inside a gel, which is insoluble in water. There are two main methods concerning the occlusion methodology that includes reticulation of a polymeric solution and reticulation of monomers. The reticulation of polymeric solutions may occur through ionic binding, precipitation and polymerization, while the reticulation of monomers needs an inductor agent of the formation of crossed-bridges (Cabral *et al.*, 2003).

In the case of simple inclusion no additional link steps are required, which is advantageous once the enzyme activity is preserved without the need to derivatize it, nor establishing contact forces between the enzyme and other surfaces (Tischer and Kasche, 1999). Also the occlusion method helps preserving the catalytic activity against external agents, as in the case of the presence of organic cosolvents. The occlusion of an enzyme within a porous matrix may allow the exclusion of aggressive or inhibitory compounds by modulating the support hydrophobicity and porosity, which also allows the optimization of the partition characteristics and mass transfer effects. In order to minimize the diffusional restriction of mass transfer, the support particle size shall be as small as possible (Cabral *et al.*, 2003).

Some drawbacks may arise from immobilization by inclusion caused by mass transfer limitations or eventually limited access to the active centre of the enzymatic biocatalyst caused by steric hindrance (Tischer and Kasche, 1999). Internal mass-transfer effects may occur due to partition effects and porous diffusion, while external mass transfer

effects depend on the thickness of the diffusion layer outside the carrier (Mateo *et al.*, 2007). Also, during the immobilization process an eventual exposure of the enzyme to temperature changes, pH, or chemical aggressive agents may lead to some inactivation (Cabral *et al.*, 2003).

1.5.2 Immobilization support

The choice of the immobilization support is crucial for the success of the global immobilization process. In fact it must be chosen in accordance to the enzyme, immobilization method, process conditions and characteristics of the support. Supports can be divided into organic and inorganic, concerning a chemical based classification; or eventually into porous and non-porous supports, concerning their morphology. On the selection of a certain support, some aspects related to their characteristics must be considered including: the presence of functional reactive groups; the definition of the hydrophobic/hydrophilic character; the chemical, mechanical and biological resistance; the geometry; the cost/availability ratio and its porosity (Cabral *et al.*, 2003).

Concerning the presence of functional groups, organic supports are compatible with reticulation techniques and are more biocompatible than inorganic supports; in addition there is a large range of techniques for surface activation for organic supports when compared with inorganic supports. The definition of the hydrophobic/hydrophilic character is mainly accomplished in the case of synthetic organic supports. The chemical, mechanical and biological resistance is particular high, in the case of inorganic supports. Inorganic supports have increased stability against pH, ionic strength, organic solvents, temperature and hydrostatic or hydrodynamic extreme conditions. The support geometry is better defined in the case of synthetic rather than natural supports, but in terms of the cost/availability ratio the synthetic supports are less suitable than the natural occurring supports (Cabral *et al.*, 2003).

Organic polymers can be used for carrier binding immobilization and by occlusion methods. It's easy to add functional reactive groups at the surface of organic polymers for the enzyme binding, although its mechanical and chemical resistance is low. Synthetic polymers have the advantage of reduced microbial growth over natural polymers; they also have a low variation of porosity degree and high chemical composition range by combining different monomers. Inorganic supports have the advantage of being chemically inert and have a good mechanical and thermal stability.

Unfortunately, inorganic compounds have some limitations concerning the presence of functional groups for the enzyme covalent binding; also there are few techniques to do the activation of the support (Cabral *et al.*, 2003).

Finally, porosity enables the protection of the enzyme against an adverse macro-environment; a high surface area/mass ratio allows a high load of enzyme. On the other side, porosity leads to significant diffusional restrictions and the compatibility with macromolecular substrates is reduced. Small pores avoid the loss of enzyme, but lead to diffusional restrictions for product and substrate, which may reduce the global process productivity. Large pores lead to low diffusional restriction effects, but the enzyme may easily get out of the matrix. The ideal pore size results from a process optimization; in addition matrices with controlled pore size are more expensive (Cabral *et al.*, 2003; Ribeiro, 1994).

1.5.3 Immobilization within silica glasses through sol-gel method

Silica has been regarded as a very interesting material to be used as a carrier immobilization material due to several characteristics such as: mechanical strength, chemical stability, shape flexibility, non-toxicity and biological inertia. Another advantage is the capability of not swelling in aqueous or organic solvents which prevents leaching of entrapped biomolecules, such as: proteins, nucleic acids, organelles and cells (Livage *et al.*, 2001). Despite all these advantages a major limitation to the bio-encapsulation within inorganic materials, such as glasses or ceramics, relied on their synthetic procedure that traditionally involved high temperature processes. A method that could combine tough materials, with fragile biomolecules, retaining much of its physicochemical characteristics was found, the so called sol-gel process (Avnir, 1995). First reports on encapsulation of enzymes using silica glasses were published by Dickey (1955) and Johnson *et al.* (1971), although only in the 90s a real development has started (Braun *et al.*, 1990).

The application of sol-gel for the entrapment of biomolecules started to be generalized and nowadays a wide variety of biological species have been entrapped including: enzymes, antibodies, regulatory proteins, membrane-bound proteins, nucleic acids and even whole cells (Livage *et al.*, 2001; Jin and Brennan, 2002). The bioactivity coupled with the intrinsic characteristics of silica turned these new hybrid materials very attractive for several applications, including: biosynthesis, medicine, environmental

technology, sensors and photonics (Livage *et al.*, 2001). Biosynthesis is a wide field for sol-gel glasses applications such as biocatalyst bioencapsulation.

Sol-gel method is an inclusion immobilization method, consisting on the formation of mineral phases starting from soluble precursors, which suffer an inorganic polymerization reaction. The so called hybrid materials rise from the incorporation of biomolecules within the inorganic hosts, only possible due to the soft reaction conditions that take place at room temperature, in water or organic solvents and in a wide range of pH and ionic strength conditions (Coradin *et al.*, 2006). The sol-gel bio-immobilizates are generally prepared following three main steps: sol preparation, gel formation and aging. The sol preparation includes hydrolysis of a specific precursor followed by condensation and polycondensation, as outlined on Figure 1.13, which illustrates a complete hydrolysis of a tetra-alkoxysilane. After the production of a silica colloid the gel is obtained through pH change (Jin and Brennan, 2002), by the addition of a buffer solution containing the biomolecule. The aging step is a drying process, where the solvent is removed coupled with continuous condensation reactions leading to the xerogel (Coradin *et al.*, 2006; Jin and Brennan, 2002). While the initial gels are soft and have high water content and large pores (up to 200 nm diameter), the aged gels, called xerogels have a pore diameter ranging from 2–20 nm due to an overall matrix shrinkage during interstitial water loss (Jin and Brennan, 2002). Xerogels suffer additional cross-linking and densification during aging comparing to hydrogels, which makes them more mechanical and chemical resistant than hydrogels (Gil, 2001). On the other hand, the smaller pore size observed in xerogels can be a disadvantage when compared to hydrogels due to possible diffusional limitations, also enzymes such as can denature with complete dehydration that occurs in xerogels by contrast with hydrogels (Gil, 2001).

The major advantages of sol-gel derived silicate materials for enzymes immobilization are: the optical transparency, which allows absorbance or fluorescence signal reading; the variety of possible chemical modifications through addition of organically modified silanes (Ormosils), polymers and several kind of fillers; tuneable pore size and distribution, which allows small substrate molecules to diffuse into the matrix, avoiding the leaching of the enzyme (Jin and Brennan, 2002). However, some limitations shall be regarded: materials can crack; enzymes can denature during immobilization due to alcohol release, pH conditions or ionic strength; the pore size can be too small and turn difficult the diffusion of small substrate molecules into the matrix or eventually be too

large to prevent enzyme leaching; enzyme-silica and substrate-silica interactions may lead to enzyme denaturation or difficult substrate approaching to the gel.

Taking into account the potential of sol-gel derived silicate materials, several sol-gel precursors and additives are in continuous research in order to fight against the above limitations (Jin and Brennan, 2002). According to the precursors and additives employed in the formation of the material several gels can be prepared, including: inorganic sol-gels, Ormosils, organic-inorganic nanocomposite sol-gels and templated sol-gels.

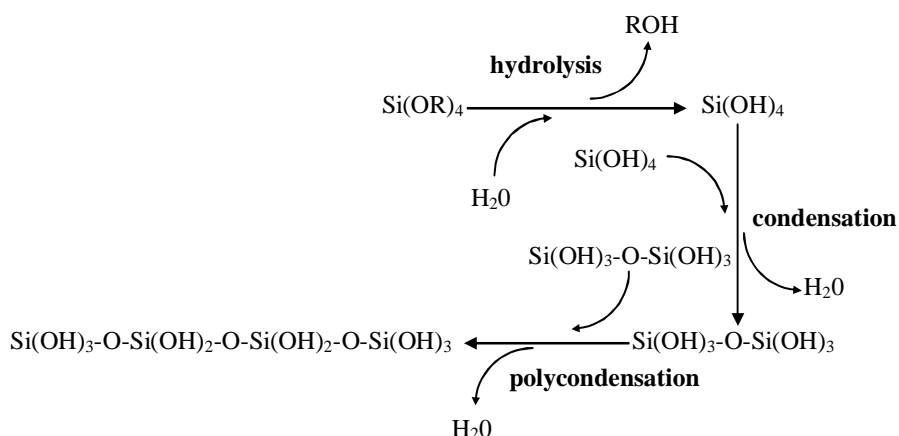


Figure 1.13 Sol preparation: complete hydrolysis of a tetra-alkoxysilane, followed by condensation and polycondensation.

1.5.3.1 Inorganic sol-gels

Inorganic sol-gels are generally derived from alkoxide-based sol-gel processes, mostly using tetramethylortosilicate (TMOS) or tetraethylortosilicate (TEOS); other inorganic sol-gels can also be made from sodium silicate and silica mixed with metal oxides, including: aluminium, titanium, zirconium, vanadium, and molybdenum (Gil, 2001). The use of sodium silicates is even older than alkoxides (Iler, 1979), but some disinterest has risen due to the reactivity of silicates, which is harder to control than alkoxides (Jolivet, 2000). The use of metal oxides is limited due to their brittleness and limited porosity (Gil, 2001).

The sol-gel process studied on this thesis is an alkoxide-based sol-gel process, using TMOS as precursor. Silicone alkoxides are very convenient for bio-encapsulation for several reasons, including: the ability to control the pore size through changing the hydrolysis pH, where acidic conditions lead to dense microporous (pore size < 2 nm) network and alkaline conditions to mesoporous gels (2 nm < pore size < 50 nm)

(Coradin *et al.*, 2006); ready synthesis; physicochemical robustness and optical transparency (Gill, 2001). On the other hand, some disadvantages may occur, including: high shrinkage degree that leads small pore diameters (2–10 nm), causing diffusional limitations; enzyme inactivation due to alcohol release, during alkoxide hydrolysis; lack of modifiable chemical functionality; electrostatic interactions between silica and substrate or with the entrapped enzyme, due to the high proportion of deprotonated silanol groups (Jin and Brennan, 2002).

Some of the above disadvantages can however be overcome. The small pore diameters of the xerogels can be circumvented by the use of hydrogel, and eventually control the aging conditions in order to find a matrix with intermediate pore size diameter between hydrogel and xerogel. The potential inactivation of the enzyme due to methanol release, during TMOS hydrolysis can be avoided by the use of a glycerated silane precursor (Gill and Ballesteros, 1998). Finally, the lack of modifiable chemical functionality and the electrostatic interactions of inorganic silica can be modified by the addition of ormosils, which can also be used to tune the pore size diameter (Coradin *et al.*, 2006). All these strategies, to avoid alkoxide disadvantages were studied on 4.3.1.

1.5.3.2 Organically modified silicates (Ormosils)

Ormosils are produced starting from precursor silanes with organic groups attached by hydrolytically stable Si-C bonds, constituting alkyl-alkoxysilanes, allowing the formation of poly-(organosiloxanes) with an inorganic siloxane backbone and free organic moieties. The organic group can vary from a simple alkyl linear chain to complex chains with multiple functionalities, a major advantage comparing to silicone alkoxides once hydrophilic, hydrophobic, ionic, and H-bonding properties can be tuned; they also display good porosities (Keeling-Tucker and Brennan, 2001). These properties can be useful to change the partition coefficient of a substrate in order to increase its affinity for the matrix or eventually increasing the stability of the immobilized enzyme (Jin and Brennan, 2002). On the other hand these materials have limited transparency and are more fragile than inorganic matrices, once the alkyl group reduces the cross-linking (Gill, 2001); also only a limited percentage of the precursor can be added before reaching a solubility limit (Pierre, 2004). Two kinds of alkyl-alkoxysilanes were used towards naringinase immobilization (4.3.1). The purpose of using 3-aminopropyltrimethoxysilane (APS) was to change the ionic environment to increase

wettability leading to an extended gel biocompatibility (Gill and Ballesteros, 1998; Venton *et al.*, 1984). Methyltrimethoxysilane (MTS) was used to increase the hydrophobic gel properties, which could be interesting to increase the affinity of the gel matrices for the flavanone substrates (Gill and Ballesteros, 2000). In addition, both these alky-alkoxysilanes aimed to tune the pore size diameter of the hydrogel.

1.5.3.3 Organic-inorganic nanocomposite sol-gels

Organic-inorganic nanocomposite sol-gels consist on a combination of an inorganic or organic silicate precursor with several kinds of additives including hydrophobic and hydrophilic polymers, silicones, surfactants, sugars, dyes, redox species and even fillers that improve mechanical properties, such as graphite, cellulose, fumed silica or clays (Gill, 2001; Jin and Brennan, 2002). Polymers such as: poly(ethylene glycol), poly(vinylimidazole) or poly(ethyleneimine) can not only reduce adsorption of proteins and analytes onto the silica increasing the overall activity (Heller and Heller, 1998; Keeling-Tucker *et al.*, 2000; Keeling-Tucker and Brennan, 2001), but also reduce the material shrinkage by sterically preventing the pore collapse (Wambolt and Saavedra, 1996; Baker *et al.*, 1998). Many other polymers can also be used, such as alginate, carrageenan, gelatin, agar, poly(vinyl alcohol), poly(vinylpyrrolidone), poly(glyceryl methacrylate), poly(hydroxyethyl acrylate), poly(acrylamide) and polyurethane (Gil, 2001).

The advantage of these sol-gels comparing to inorganic gels and ormosils rely on a wide rigidity spectrum and hydrophilic/hydrophobic properties, tuneable pore sizes, large and ordered pores, improved mechanical stability and better biocompatibility (Gill, 2001; Jin and Brennan, 2002).

1.5.3.4 Templated sol-gels

Within the group of templated sol-gels are all the sol-gel matrices produced with structure-directing and pore-forming agents. These agents include polyols such as glycerol, hydroxyacids, PEG, surfactants and ionic liquids (ILs). These compounds may modify the sol-gel structure through the formation of several systems including: microemulsions and macroemulsions, vesicular or liquid-crystalline phases, foams or H-bonded aggregates (Gil, 2001). Beck and Vartuli (1996) at Mobil Research and Development Corporation, during their research on mesoporous materials, mixed silicon

alkoxides with surfactants, demonstrating that molecular systems can be used as structuring agents, or templates, to control the structure and morphology of inorganic phases.

Comparing templated sol-gels with organic-inorganic nanocomposite sol-gels some similarities do exist, such as the reduction of the gel shrinkage by sterically preventing pore collapse as well as the availability of biocompatible templating agents; in opposition, templates are removed after aging. Meso to macroporous materials are produced, making templating agents a great promise to produce highly ordered and porous biodoped sol-gels (Gill and Ballesteros, 1998; Wei *et al.*, 2000).

Glycerol was a templating agent used along the immobilization studies (chapter 4), acting simultaneously in the reduction of the material shrinkage and preventing the pore collapse and also as drying-control additive, during its slow release from the gel (Gill and Ballesteros, 2000).

Ionic liquids were also studied (4.3.3) as templates for nanostructured gels. Ionic liquids are compounds, comprised entirely of ions: cations and anions that have a melting point below 100 °C. They are versatile compounds due to the possibility to tune the desired property such as polarity, conductivity, thermal and chemical stability, density, viscosity, melting point, and their solvent capacity just by combining different anions and cations. Indeed, depending on the anion and alkyl group of the cation, ILs can solubilize carbonyl compounds, alcohols, alkyl halides, supercritical CO₂, and also transition metal complexes. In addition to this, they can have low miscibility with dialkyl ethers, alkanes, water and may be insoluble in supercritical CO₂. ILs have been recognized as “greener” solvents compared with classic organic solvents mainly due to their negligible vapor pressure, high thermal and chemical stability and possibility of reutilization (Welton, 1999; Wasserscheid and Keim, 2000; Dupont *et al.*, 2002; Martins *et al.*, 2008).

Regarding the properties of ILs there are some important features which should be mentioned. In terms of solubility, ILs containing the alcohol group in the side chain are generally miscible with water whereas more hydrophobic side chains on the cationic unit tend to reduce this miscibility. Regarding the anion effect, more hydrophobic groups such as PF₆⁻ or the bis-triflimide increase the immiscibility with water and the IL viscosity while the BF₄⁻ anion improves the solubility in water affording less viscous ILs. Halides, dicyanoamide (DCA), trifluoroacetate (TFA), trifluoro methane sulfonate (TfO) are more polar anions which result in ILs with an increased affinity towards water

(Welton, 1999; Wasserscheid and Keim, 2000; Dupont *et al.*, 2002; Greaves and Drummond, 2008).

These vast tunable properties of ILs makes them a potential alternative reaction media for biocatalysis, increasing reactivity, selectivity and stability of enzymes (Park and Kazlauskas, 2003), but also as sol-gel additives, acting as templating agents enhancing the immobilized biocatalysts activity and stability (Liu *et al.*, 2005a, b; Lee *et al.*, 2007a, b).

1.6 Objectives

The work that sustains this thesis emerged within the multidisciplinary field of pharmaceutical sciences, where the convergence of distinct knowledge areas may give rise to innovation. This thesis focuses on a biotechnological approach to produce potential active drugs against AD. On the basis of this approach is the optimization of the enzymatic deglycosylation conditions of natural flavone glycosides, including naringin and rutin. The bioprocess optimization is carried out in order to maximize the efficiency of this bioprocessing approach, making use of pressure and biocatalyst immobilization as cornerstone tools among other conditions including: temperature, pH and use of organic solvents. The purpose of this thesis comprises the following specific goals:

- a) Development of a biocatalytic process to produce the flavone glucosides: prunin and isoquercetin; and the aglycones: naringenin and quercetin; starting from the natural glycosylated flavones: naringin and rutin, using naringinase as biocatalyst. Inherent to this goal is the study of a selective inactivation of β -D-glucosidase from naringinase, remaining the α -L-rhamnosidase activity, which is needed to obtain the flavone glucosides: prunin and isoquercetin.
- b) Use of pressure as a tool to increase the overall bioprocess efficiency, through modeling the stability and activity of the biocatalyst. The increased stabilization of the biocatalyst against temperature as well as the acceleration of the biocatalytic reaction is the two main goals, concerning pressure application. In one hand the use of pressure aims to increase the stability of both α -L-rhamnosidase and β -D-glucosidase from naringinase, under high temperature conditions. These high temperature conditions not only increase the reaction rate but are also simultaneous desirable for an increased solubility of the natural flavone substrates. On other hand, pressure aims to increase the reaction rate constants and maintaining simultaneously high equilibrium constants.
- c) Use of naringinase immobilization in order to its easy separation from the reaction media and re-use. Naringinase immobilization within sol-gel matrices through sol-gel method aims to achieve a good performance of the bio-immobilizate including

immobilization yield, activity and operational stability. Moreover, ionic liquids may be useful to improve the activity of immobilized naringinase. A secondary goal of naringinase immobilization is to increase its stability against organic solvents, which can be used to solubilize the flavone substrates.

- d) Study the anti-inflammatory activity of naringin and naringenin on a CNS cell model and show the advantage of using aglycones and glucosides to cross the BBB, instead of rutinosides, in order to treat AD.

1.8 Thesis design

The work that sustains this thesis is structured into seven chapters, where chapter 1 and 7, respectively, consist on the introduction and conclusion of this thesis, while the main work is briefly approached on the remaining chapters.

- a) Chapter 2 describes the production of the flavone glucosides: prunin and isoquercetin; and the aglycones: naringenin and quercetin; starting from the glycosylated flavones: naringin and rutin, with naringinase. Also within chapter 2 the Response Surface Methodology (RSM) is used to determine the optimized combination of pH and temperature conditions to selective inactivate β -D-glucosidase from naringinase, remaining a high residual activity of α -L-rhamnosidase.
- b) Chapter 3 focus on to the use of naringinase under pressure. Pressure is used to increase the stability of both α -L-rhamnosidase and β -D-glucosidase activities, expressed by naringinase, against inactivation caused by heat. In addition pressure is used to enhance its activity.
- c) Chapter 4 is related to the use of sol-gel method to entrap naringinase within silica glasses. On this chapter is described an optimization of naringinase bioencapsulation and an improved stability of immobilized naringinase in cosolvent systems. Moreover, this chapter focus on the use of ionic liquids to improve the activity of immobilized naringinase.
- d) On Chapter 5, naringin and naringenin were studied in an anti-inflammatory cell culture model. Moreover, an animal model was used to investigate the potential of naringin, prunin and naringenin to cross the BBB and reach brain.
- e) Finally, Chapter 6 consists on a general discussion about this thesis.

**BIOCATALYTIC PRODUCTION OF THE FLAVONE
GLUCOSIDES, PRUNIN AND ISOQUERCETIN, AND THE
AGLYCONES, NARINGENIN AND QUERCETIN**

Chapter 2

2.1 Introduction

The development of a biocatalytic process to obtain the flavone aglycones: naringenin and quercetin, starting respectively from the natural flavone rutosides naringin and rutin is quite straightforward. More difficult to obtain are the very expensive flavone glucosides: prunin and isoquercetin, starting respectively from naringin and rutin. Behind this issue is the fact that naringinase from *Penicillium decumbens* provides simultaneously both α -L-rhamnosidase and β -D-glucosidase activities, turning it difficult to obtain the intermediate glucosides products, which are immediately hydrolyzed by β -D-glucosidase into the respective aglycones (Figure 1.10).

In order to circumvent this issue some authors propose chromatographic separation methods to purify α -L-rhamnosidase from naringinase (Mamma *et al.*, 2005), while others suggest the use of selective inhibitors of β -D-glucosidase (Chang and Muir, 2003). In this work, to circumvent this problem and also the use of expensive processes, another approach is suggested, consisting on the study of the susceptibility of both α -L-rhamnosidase and β -D-glucosidase of naringinase against several pH-temperature conditions in order to selectively inactivate β -D-glucosidase.

Statistical design of experiments is a useful tool to provide experimental schemes where the parameters under study are combined at different levels to determine the influence of a particular factor on the response. Moreover, by choosing a particular experimental design, individual effects can be determined as well as interactions between factors. Response surface methodology (RSM) is an efficient statistical technique for the modeling and optimization of multiple variables in order to predict the best performance conditions considering a minimum number of experiments (Giovanni, 1983). It consists on a group of mathematical and statistical procedures that can be used to study relationships between one or more responses and a number of independent variables. RSM defines the effect of the independent variables, alone or in combination, on the process. In addition, to analyze the effects of independent variables, this experimental methodology generates a mathematical model that accurately describes the overall process. This method finds its major application when the effect of one variable is affected by the setting of another one. Such interactions between variables are difficult to detect by a traditional experimental setup where one variable is changed at a time. These experiments are set up so that the coefficients of the mathematical model (usually

a polynomial equation) representing the variations of the experimental response of interest may be evaluated with the best possible precision. In addition, RSM has the advantage of being less expensive and time-consuming than the classical methods. RSM is a non-conventional approach that has been successfully used for the optimization of enzymatic reactions conditions (Ribeiro et al., 2003; Marques et al., 2007; Amaro et al., 2009) and medium composition (Ribeiro et al., 2006; Vásquez et al., 2006).

In this work, a central composite rotatable design (CCRD) and RSM were used to evaluate the combined effects of temperature and pH in order to selectively inactivate β -D-glucosidase expressed by naringinase and produce the glucosides: prunin and isoquercetin, starting respectively from naringin and rutin.

2.2 Material and Methods

2.2.1 Chemicals

p-Nitrophenyl α -L-rhamnopyranoside (4-NRP), *p*-Nitrophenyl β -D-glucopyranoside (4-NGP), naringin, naringenin and rutin were from Sigma-Aldrich. All other chemicals were of analytical grade and obtained from various sources.

2.2.2 Enzyme solution

Naringinase (CAS n°. 9068-31-9, cat. n°. 1385) from *Penicillium decumbens* was obtained from Sigma-Aldrich and stored at -20°C . The lyophilized naringinase powder was dissolved in an appropriate buffer solution 24 hours before experiments and kept at 4°C .

2.2.3 Analytical methods

The concentration of *p*-nitrophenol produced after the hydrolysis of 4-NRP and 4-NGP was evaluated using the *Zenith 3100* spectrofluorimeter, at $\lambda = 340$ nm, using a 96 flat well plate. A calibration curve was built for each compound.

The flavone rutosides, glucosides and aglycones were eluted running a thin layer chromatography (TLC) on a RP-18 silica-gel plate with methanol, water and acetic acid (50:44:6, v/v/v) (Gocan and Cimpan, 2004). The spot visualization was done under UV light at 254 nm, followed by spraying with a freshly prepared solution of acetic acid, sulphuric acid concentrated and *p*-anisaldehyde (100:2:1, v/v/v) and by heating at 150°C for 5 min (Pekin et al., 2005).

The HPLC-DAD-ESI-MS/MS experiments used to identify the produced compounds (prunin, naringenin, isoquercetin, quercetin) were performed with a liquid chromatograph (Alliance, Waters 2695 Separation Module) system with a photodiode array detector (DAD, Waters 2996) set at 280 nm (for monitoring) in tandem with a mass spectrometer (Micromass Quattro Micro API) with a Triple Quadrupole (TQ) and an electrospray ion source (ESI) operating in negative mode. Chromatographic conditions were as follow: column C18 (Synergi, Phenomenex) $100\text{ mm} \times 2.0\text{ mm}$, $2.5\text{ }\mu\text{m}$; eluent (A) water-formic acid (99.5:0.5, v/v), (B) acetonitrile (LC-MS grade, Merck). The linear gradient was at initial time 95 % eluent A, at 30 min 60 % eluent A,

at 45 min 10 % eluent A. The flow rate was 0.25 mL/min and the column temperature 35 °C. Mass range was measured from 100-1000 amu. The ESI source conditions were adjusted as follows: source capillary operating at 2.5 kV and the extraction cone at 30 V: the source temperature was 150 °C and the desolvation temperature was 350 °C.

2.2.4 Activity measurement

4-NRP and 4-NGP were used as specific substrates of α -L-rhamnosidase and β -D-glucosidase activities, in order to discriminate the enzymatic activities, expressed by naringinase (Mamma *et al.*, 2005). Therefore, both enzymatic activities were followed and easily measured without the need of a previous subunit protein separation and purifying procedures. In both reactions 1 mol of substrate led to 1 mol of product.

The activities of α -L-rhamnosidase and β -D-glucosidase were evaluated using 0.20 mM of substrate in 20 mM citrate buffer at pH 3.4. A naringinase concentration of 50 mg L⁻¹ was used in these experiments. The enzymatic hydrolysis was followed spectrophotometrically. The absorbance was measured every 1 min during 30 min, 30.0 °C. The enzyme specific activity of α -L-rhamnosidase and β -D-glucosidase expressed by naringinase was calculated by linear regression on the first data-points during the initial 30 min reaction time.

2.2.5 pH profile

The pH profiles of the enzymatic activity were obtained through non-linear regression by minimising the residual sum of squares between the experimental data points of the specific activity vs. pH and those estimated by the model (Equation 1.44), using Solver add-in from Microsoft Excel 2003 for Windows XP and considering the following options: Newton method; 100 iterations, precision of 10⁻⁶, 5 % of tolerance and 10⁻⁴ convergence. The experimental optimum pH values were used as initial parameters of the non-linear regression and no constraints were used. Optimum pH values were then determined using Equation 1.45.

2.2.6 Inactivation kinetics

A temperature range of 75 – 85 °C and a pH range of 3.2 – 6.0 were used in order to study β -D-glucosidase and α -L-rhamnosidase inactivation kinetics. Naringinase thermal

inactivation was carried out in Eppendorf tubes (1.5 mL), at isothermal conditions (± 0.1 °C) using a thermostatic water bath (Julabo Hc/F18). The inactivation period ranged from 2.5 to 160 min according to the temperature used. After removing the enzyme samples from the water bath they were cooled on ice for 5 min to stop the thermal inactivation. Enzyme activity was measured, in triplicate, immediately as well as one day after thermal inactivation, without occurring reactivation. A_0 is the specific activity of the control, *i.e.* the enzyme sample without being submitted to inactivation. To describe the inactivation kinetics the residual activity (A_r) was defined as the ratio between the specific activity after each inactivation period (A_t) and the specific activity of the control.

First-order inactivation rate constants and α parameters were determined by non-linear regression, minimizing the residual sum of squares between the experimental data points of the residual activity *vs.* inactivation time and those estimated by the models described on 1.4.5. The Solver add-in from Microsoft Excel 2003 for Windows XP was used with the following options: Newton method; 100 iterations, precision of 10^{-6} , 5 % tolerance and convergence of 1×10^{-4} . The first-order inactivation rate constant obtained from linear regression of $\ln A_r$ *vs.* t was used as the initial value of the k_1 parameter for the non-linear regression. The non-linear regression parameters were restricted to positive numbers. In addition α_1 was restricted to values lower than 1.

$t_{0.01\%}$ was the time needed to achieve a specific activity of β -D-glucosidase which is 0.01% of the specific activity of α -L-rhamnosidase. At this time ($t_{0.01\%}$) the β -D-glucosidase was considered completely inactivated. These t values were determined through extrapolation of the kinetic inactivation profiles obtained under different conditions of pH and temperature. The residual activity of α -L-rhamnosidase at this period values (t) was determined for each specific condition of pH and temperature.

2.2.7 Experimental design

The optimized temperature and pH inactivation conditions of β -D-glucosidase from naringinase were established through the Response Surface Methodology (RSM). Using this methodology two variables were tested simultaneously with a minimum number of trials, according to adequate experimental designs, which enables to find interactions between variables (Montgomery and Myers, 2002). The experimental design

methodology makes use of statistical tools for selecting a minimum set of experiments adequately distributed in the experimental region (experimental matrix).

In this study, β -D-glucosidase inactivation was carried out following a central composite rotatable design (CCRD). A total of 11 experiments were carried out in the CCRD: four factorial points (coded levels as (+1) and (-1)); four star points (coded as $(+\sqrt{2})$ and $(-\sqrt{2})$) and three centre points (coded as 0) (Table 2.1). The choice of experimental domains resulted from preliminary studies. The response variable was the α -L-rhamnosidase residual activity, after β -D-glucosidase inactivation. The studying factors were pH and temperature. The experiments were performed in random order and in triplicate at all design points.

Table 2.1 Coded and decoded levels of the experimental factors used in experimental design.

CCRD	pH	Temperature (°C)
$-\sqrt{2}$	3.2	75.0
-1	3.6	76.5
0	4.6	80.0
+1	5.6	83.5
$+\sqrt{2}$	6.0	85.0

2.2.8 Statistical analysis

Making use of CCRD, 5 levels for each factor were used which enabled to fit second-order polynomials to the experimental data points. The results of each CCRD were analyzed using the software "StatisticaTM", version 6, from Statsoft, USA. Both linear and quadratic effects of the two variables under study, as well as their interactions, on the α -L-rhamnosidase residual activity were calculated. Their significance was evaluated by analysis of variance.

Experimental data were fitted to a second-order polynomial model and the regression coefficients obtained. The generalized second-order polynomial model used in the response surface analysis was as follows (Equation 2.1):

$$y = \beta_0 + \beta_1 x_1 + \beta_2 x_2 + \beta_{11} x_1^2 + \beta_{22} x_2^2 + \beta_{12} x_1 x_2 \quad (2.1)$$

where β_0 , β_1 , β_2 , β_{11} , β_{22} , and β_{12} are the regression coefficients for intercept, linear, quadratic and interaction terms, respectively, and x_1 , and x_2 are the independent

variables, temperature (1) and pH (2). The fit of the models was evaluated by the determination coefficients (R^2) and adjusted R^2 (R^2_{adj}).

2.2.9 Verification experiments

After finding the optimal conditions for the selective inactivation of β -D-glucosidase activity expressed by naringinase, verification experiments were carried out. The experimental and predicted values determined by RSM were compared in order to validate the model.

2.2.10 Production and purification methods

Prunin was obtained through the hydrolysis of a 10 mM naringin solution, using 50 mg L⁻¹ of naringinase, with its β -D-glucosidase selectively inactivated, in 20 mM citrate buffer, pH 3.4, 60.0 °C for 6 hours. Prunin precipitated after 12 hours at 4 °C and was recovered through vacuum filtration. Afterwards it was dissolved in hot water and was filtered. Prunin was obtained through recrystallization from water.

Naringenin was obtained through the hydrolysis of a 10 mM naringin solution, using 50 mg L⁻¹ of naringinase in 20 mM acetate buffer, pH 4.0, 60.0 °C for 6 hours. Naringenin precipitated after 12 hours at 4 °C and was recovered through vacuum filtration. Afterwards it was dissolved in hot ethanol and was filtered. Naringenin was obtained through recrystallization from ethanol and water.

Isoquercetin was obtained through the hydrolysis of a 5 mM rutin solution, using 50 mg L⁻¹ of naringinase, with its β -D-glucosidase selectively inactivated, in 20 mM citrate buffer, pH 3.4, 60.0 °C for 6 hours. Isoquercetin precipitated after 12 hours at 4 °C and was recovered through vacuum filtration. Afterwards it was dissolved in hot ethanol and was filtered. Isoquercetin was obtained through recrystallization from ethanol and water.

Quercetin was obtained through the hydrolysis of a 5 mM rutin solution, using 50 mg L⁻¹ of naringinase in 20 mM acetate buffer, pH 4.0, 60.0 °C for 6 hours. Quercetin precipitated after 12 hours at 4 °C and was recovered through vacuum filtration. Afterwards it was dissolved in hot ethanol and was filtered. Quercetin was obtained through recrystallization from ethanol and water.

2.3 Results and discussion

2.3.1 pH profile

The pH profile of both α -L-rhamnosidase and β -D-glucosidase activities, expressed by naringinase was studied, between 2.5 and 5.8 in citrate buffer, hydrolysing the specific substrates, 4-NRP and 4-NGP, respectively. The pH profile was studied. Figure 2.1 shows the distinct activity pH profiles of α -L-rhamnosidase and β -D-glucosidase expressed by naringinase. From these studies and adjusting the model of Equation 1.44, the optimum pH was found to be 3.4 and 4.1, with maximum specific activities of 0.181 and 0.060 $\mu\text{mol mg}^{-1} \text{min}^{-1}$, respectively, for α -L-rhamnosidase and β -D-glucosidase (Table 2.2). Jurado et al. (2004) adjusted a similar model to the experimental data of β -galactosidase activity vs. pH.

In previous work, the specific activity of β -D-glucosidase in 20 mM acetate buffer (pH 4.0) was found to be 0.086 $\mu\text{mol min}^{-1} \text{mg}^{-1}$, while in this work using 20 mM citrate a specific activity decrease of 30 % occurs. Also, Norouzian et al. (2000) observed a naringinase activity inhibition with 20 mM citric acid buffer. In line with these results, citrate buffer was used in further studies instead of acetate, concerning the selective β -D-glucosidase inactivation of naringinase.

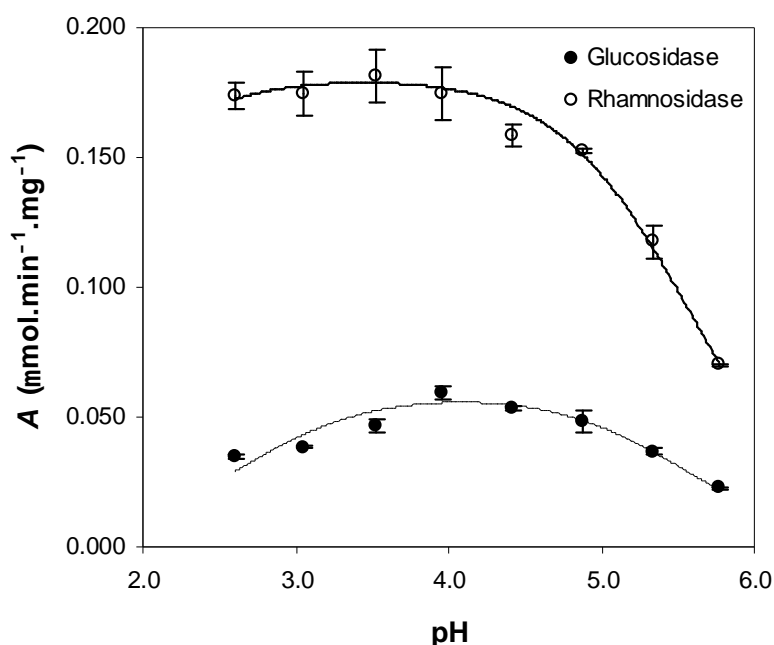


Figure 2.1 pH profiles of β -D-glucosidase and α -L-rhamnosidase (mean value \pm SE).

Table 2.2. Optimum pH values of β -D-glucosidase and α -L-rhamnosidase.

Activity	pH _{opt}	Non-linear parameters	R ²
β -D-glucosidase	4.1	$A_{\max} = 0.060$, $pK_1 = 2.6$, $pK_2 = 5.5$	0.892
α -L-rhamnosidase	3.4	$A_{\max} = 0.181$, $pK_1 = 1.3$, $pK_2 = 5.6$	0.984

2.3.2 Inactivation kinetics

Naringinase was inactivated using combined temperature and pH conditions, respectively between 75.0 – 85.0 °C and 3.2 – 6.0. The influence of temperature and pH on the stability of β -D-glucosidase and α -L-rhamnosidase were evaluated on a minimum set of optimal selected experiments.

The inactivation behaviour of β -D-glucosidase and α -L-rhamnosidase expressed by naringinase was distinct from each other under the same temperature and pH conditions (Figure 2.2). Table 2.3 shows the inactivation parameters determined at different temperature and pH conditions for both β -D-glucosidase and α -L-rhamnosidase. In some cases β -D-glucosidase showed a first inactivation step that was followed by a second one with the existence of an enzymatic intermediate with a lower specific activity than the initial enzyme native state ($\alpha_1 < 1$) (Table 2.3); and a final state where the enzyme is completely inactivated ($\alpha_2 = 0$) (Henley and Sadana, 1985). On the other hand, α -L-rhamnosidase inactivation as well as the inactivation of β -D-glucosidase, under the temperature conditions higher than 80.0 °C, occurred according to the classical first-order inactivation model (Figure 2.2) (Equation 1.48).

Tsen et al., (1989) and Ellenrieder and Daz (1996) reported naringinase (from *Penicillium decumbens*) inactivation profiles at pH 3.5–3.7. α -Rhamnosidase from *Aspergillus terreus* (Gallego et al. 2001) and *Aspergillus nidulans* (Manzanares et al. 2000) when incubated at pH values lower than 4.0 rapidly lost activity, whereas *Aspergillus aculeatus* (Mutter et al. 1994) showed to be insensitive to pH in a 3 – 8 range. Comparing our results with available stability data of purified fungal α -rhamnosidases referred by different authors (Manzanares et al. 2000; Manzanares et al. 2001; Gallego et al. 2001; Soria and Ellenrieder, 2002), it can be pointed out that our developed method, which avoids α -L-rhamnosidase purification, through the inactivation of β -D-glucosidase, is an effective and cheap method.

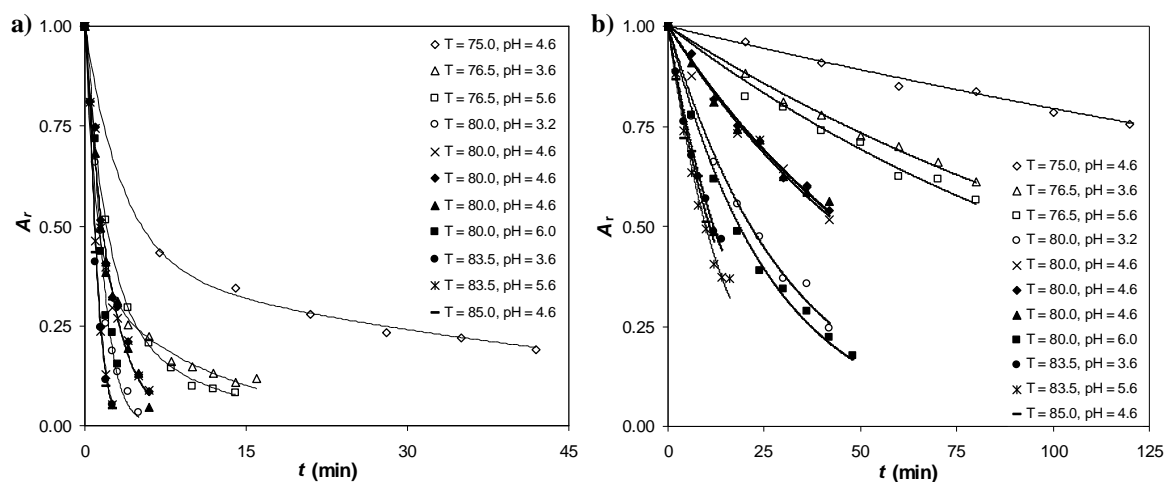


Figure 2.2 Thermal inactivation of β -D-glucosidase (a) and α -L-rhamnosidase (b), under combined temperature and pH conditions.

Table 2.3 Thermal inactivation parameters of β -D-glucosidase and α -L-rhamnosidase, under combined temperature and pH conditions.

T ($^{\circ}\text{C}$)	pH	β -D-glucosidase				α -L-rhamnosidase		A_r (α -L-rhamnosidase)
		α_1	k_1 (h^{-1})	k_2	R^2	k_1 (h^{-1})	R^2	
75.0	4.6	0.376	0.283	0.017	0.999	0.0023	0.990	0.33
76.5	3.6	0.327	0.990	0.084	0.997	0.0062	0.994	0.57
76.5	5.6	0.226	0.486	0.093	0.999	0.0073	0.980	0.56
80.0	3.2	-	0.579	-	0.971	0.0323	0.989	0.73
80.0	4.6	-	0.428	-	0.980	0.0154	0.979	0.74
80.0	4.6	-	0.434	-	0.990	0.0149	0.991	0.75
80.0	4.6	-	0.431	-	0.992	0.0149	0.996	0.75
80.0	6.0	-	0.547	-	0.953	0.0375	0.995	0.71
83.5	3.6	-	0.869	-	0.987	0.0589	0.989	0.71
83.5	5.6	-	0.838	-	0.953	0.0711	0.991	0.65
85.0	4.6	-	0.868	-	0.997	0.0646	0.979	0.68

2.3.3 RSM

In this study a central composite design and response surface methodology (RSM) were applied in order to find the best pH-temperature conditions to selectively inactivate β -D-glucosidase expression from naringinase, retaining the highest α -L-rhamnosidase activity. The experiments were carried out according to a full factorial design 2^2 and a CCRD, as a function of both temperature and pH. The residual activity values of α -L-

rhamnosidase determined after β -D-glucosidase inactivation were used to calculate the significant effects, either linear or quadratic.

Experimental data showed that α -L-rhamnosidase residual activity after β -D-glucosidase inactivation was affected by pH and temperature individually and interactively. On Table 2.4 are presented the effects and respective significance levels (p) of the temperature, pH and interaction between both on the α -L-rhamnosidase residual activity. Therefore, negative effects of the factors temperature, pH or from their interaction indicate that the response decreased with the increase in these factors. Linear and quadratic terms of temperature were high significant ($p < 0.001$); also the linear and quadratic terms of pH were significant ($p < 0.05$) for α -L-rhamnosidase residual activity. A negative interaction between the variables tested ($T \times \text{pH}$) on α -L-rhamnosidase residual activity, indicated that higher activities are obtained at higher temperatures and lower pH values within the experimental domain.

Table 2.4 Effects and respective significance levels (p) of temperature (T) and pH on α -L-rhamnosidase residual activity (A_r).

Variable	A_r (α -L-rhamnosidase)
T (linear term)	18.1467***
T (quadratic term)	- 23.8667***
pH (linear term)	- 2.5064*
pH (quadratic term)	- 2.4592*
$T \times \text{pH}$	- 2.3500

* $p < 0.05$, *** $p < 0.001$

A least squares technique was used to fit quadratic polynomial model and obtain multiple regression coefficients for α -L-rhamnosidase residual activity that is summarized on Table 2.5. Examination of these coefficients using the t-test indicated that, both linear and quadratic terms of temperature effects on α -L-rhamnosidase residual activity were highly significant, $p < 0.001$ (Table 2.5). The linear and quadratic terms of pH were significant on α -L-rhamnosidase residual activity ($p < 0.05$) (Table 2.5).

Therefore a curved surface was fitted to the experimental data (Figure 2.3). Partial differentiation of these polynomial equations was used to find the optimum points, i.e. the stationary points. The least-square estimates of the coefficients of the model were calculated from the values of the response for each experiment in the chosen experimental matrix. The relationship between independent and dependent variables in

the three-dimensional representation is a convex surface (Figure 2.3). The obtained response surface (Figure 2.3) was described by second-order polynomial equations to the experimental data points, as a function of temperature and pH (Table 2.5).

The high values of R^2 and R^2_{adj} of the model (Table 2.5) showed a close agreement between the experimental results and the theoretical values predicted by the model (Vuataz, 1986). The adjusted coefficient of determination for α -L-rhamnosidase residual activity ($R^2_{\text{adj}} = 0.872$) implied that 87.2 % of the variations could be explained by the fitted model.

The ANOVA for the two response variables (temperature and pH) indicated that the model developed for α -L-rhamnosidase residual activity was adequate with the linear and the quadratic term with high statistical significance ($p < 0.05$) (data not showed).

The regression models allowed the prediction of the effects of the two parameters, temperature and pH on α -L-rhamnosidase residual activity and concomitant β -D-glucosidase inactivation. These optimal conditions found were at 81.5 °C and pH of 3.9, remaining a α -L-rhamnosidase residual activity of 0.77. Once tested, the model may be used to predict the value of the response(s) under any conditions within the experimental region.

Table 2.5 Second-order model equations for the response surfaces fitted to the experimental data points of α -L-rhamnosidase residual activity (A_r), as a function of temperature (T) and pH, and respective R^2 and R^2_{adj} .

Coefficient	A_r (α -L-rhamnosidase)	p
β_0	- 63.6717	0.0004
Linear		
β_1	1.5645	0.0004
β_2	0.3661	0.0322
Quadratic		
β_{11}	- 0.0095	0.0004
β_{22}	- 0.0123	0.0355
Cross product		
β_{12}	- 0.0033	0.0530
R^2	0.936	-
R^2_{adj}	0.872	-

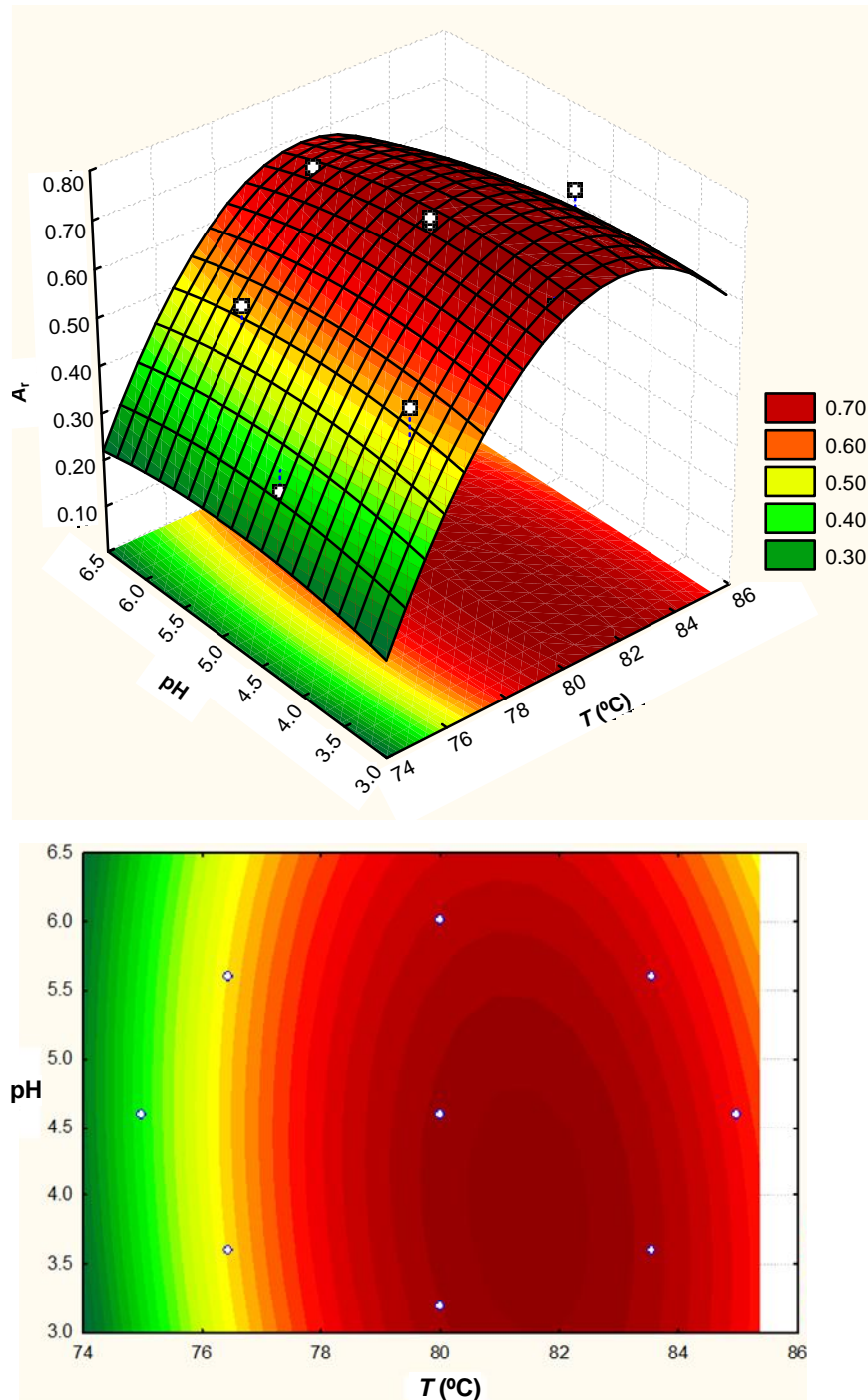


Figure 2.3 Response surface fitted to the experimental data points, corresponding to α -L-rhamnosidase residual activity, as a function of temperature (T) and pH.

2.3.4 Verification of the optimal temperature and pH inactivation conditions

The optimal conditions of temperature and pH found, using RSM, were tested in order to support the predicted results. Figure 2.4 shows the inactivation profiles of both β -D-glucosidase and α -L-rhamnosidase under 81.5 °C and pH 3.9. Moreover, the verification experiments proved that the predicted values for α -L-rhamnosidase residual

activity (0.77) for the model was satisfactorily achieved within more than 95 % confidence interval. The time needed for β -D-glucosidase activity reach 0.01% of α -L-rhamnosidase activity was determined through extrapolation of β -D-glucosidase inactivation and corresponded to 16 minutes. At this time the α -L-rhamnosidase residual activity found was 0.78 which is quite similar to value predicted with RSM (0.77).

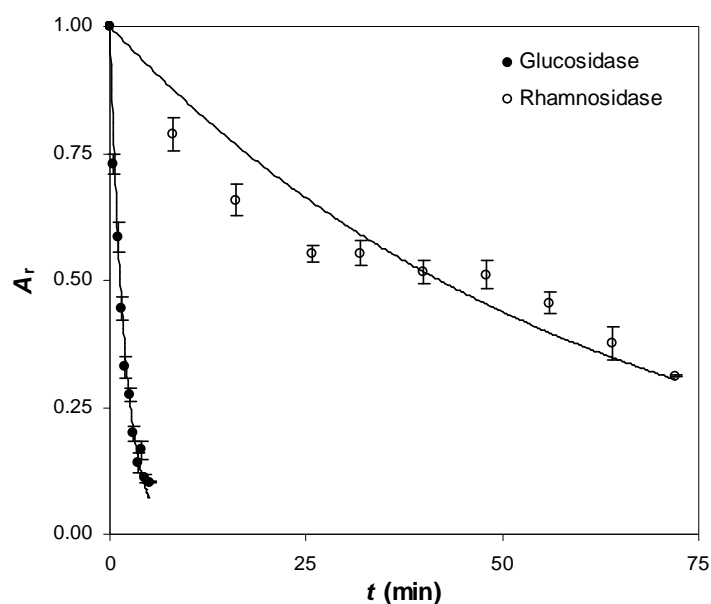


Figure 2.4 Inactivation kinetics of β -D-glucosidase and α -L-rhamnosidase, at 81.5°C and pH 3.9.

2.3.5 Compounds production and identification

Once β -D-glucosidase of naringinase was selectively inactivated, the α -L-rhamnosidase activity was used for the production of flavone glucosides starting from rutosides (Table 2.6 and Figure 2.5). Adequate purification procedures were used and compounds identification was carried out through HPLC-MS/MS analysis. Compounds purity was higher than 95%.



Figure 2.5 TLC of naringin (a), prunin (b), naringenin (c), rutin (d), isoquercetin (e) and quercetin (f).

Table 2.6 Results of TLC analysis of naringin (a), prunin (b), naringenin (c), rutin (d), isoquercetin (e) and quercetin (f).

Compounds	Rf	Visible light	UV light (254 nm)	Acid revelation + heating (150 °C)
Naringin	0.62	invisible	visible	orange
Prunin	0.58	invisible	visible	orange
Naringenin	0.30	invisible	visible	orange
Rutin	0.55	yellow	visible	yellow
Isoquercetin	0.53	yellow	visible	yellow
Quercetin	0.30	yellow	visible	yellow

Naringin enzymatic hydrolysis led to prunin, while isoquercetin was obtained from rutin (Figure 1.10). A production yield of 30% and 61% was obtained, respectively, for both prunin and isoquercetin. The aglycones were also produced from rutinoides using native naringinase, expressing both α -L-rhamnosidase and β -D-glucosidase (Figure 1.10). Naringenin was obtained with a production yield of 49% from naringin, while quercetin was obtained from rutin (Figure 1.10) in a yield of 86%. The sequential removal of the sugar moiety from the rutinoides into the glucoside and finally into the aglycone decreased the molecule polarity, as shown in Figure 2.5. These outcomes showed the high potential of the developed method on the production of the flavone glucosides and aglycones, as well.

2.4. Conclusions

In the current study it was found the best combinations of temperature and pH to selectively inactivate β -D-glucosidase from naringinase. This achievement comprises simultaneously a high remaining α -L-rhamnosidase activity. This α -L-rhamnosidase residual activity, expressed by naringinase, was affected by pH and temperature individually and interactively. The residual activity could be described by a response surface that enabled the fit of second-order polynomial equation. A closed agreement between the experimental α -L-rhamnosidase residual activity (0.78) and the predicted value by the model (0.77) reflects the good fitness of RSM as a tool to accomplish this study. The optimum temperature and pH conditions to selectively inactivate β -D-glucosidase, remaining the highest α -L-rhamnosidase residual activity occur at 81.5°C, pH 3.9 for 16 minutes.

Starting from the natural occurring flavone substrates, naringin and rutin, the flavone glucosides, prunin and isoquercetin, were produced with a production yield of respectively 30% and 61%, while the flavone aglycones, naringenin and quercetin were obtained with a final yield of 49% and 86% respectively.

Naringinase with β -D-glucosidase activity selectively inactivated allowed the production of two very expensive flavone glucosides, prunin and isoquercetin, in an easy and cheap bioprocess starting from naringin and rutin, respectively. This method could also be generalized for obtaining others also expensive flavone glucosides starting from their rutosides.

**ENZYMATIC BIOCATALYSIS USING NARINGINASE UNDER
PRESSURE**

Chapter 3

3.1 Introduction

Pressure is a very promising tool concerning enzymatic biocatalysis. Its influence on enzyme stability is directly dependent on the enzyme tridimensional structure that can be modulated according to the pressure magnitude. On the other hand, it may influence the enzyme activity by changing the reaction limiting step. These two approaches may be used to increase the productivity of a biocatalytic process. Accordingly, the biocatalytic study of naringinase under pressure focuses on two main issues: stability and activity. Therefore the stability of both α -L-rhamnosidase and β -D-glucosidase activities expressed by naringinase was evaluated against temperature inactivation under pressure, as well as the influence of pressure on the activity of these both enzymatic activities.

On the basis of the stability studies against temperature is the importance of this parameter to modulate the reaction rate as well as the solubility of certain substrates such as naringin and rutin (Pulley, 1936; Zi *et al.*, 2007). The low water solubility of these substrates is a limitation to attain higher hydrolysis reaction rates with naringinase in aqueous media, as higher substrate concentrations are required to achieve better reaction rates. Temperature raise favours substrates solubility as well as the reaction rate but only till optimum temperature is reached, excessive high temperature may be deleterious to naringinase native state, which is crucial for its activity.

Pressure can be used in a way to hinder naringinase denaturation under high temperature conditions, as stated on 1.4.4.2. This protecting effect of pressure against heat inactivation is bounded by a critical pressure value, where the volume change associated with denaturation is null and above which turns to be negative (Weemaes *et al.*, 1998; Scharnagl *et al.*, 2005; Buckow *et al.*, 2007). Even though this study focuses on high temperature values, the protective effect of pressure is also bounded by a critical temperature value bellow which this effect exists and can be studied. Both these critical pressure and temperature values are dependent on each specific studied protein, comprising an interesting biotechnological field in order to increase the efficiency of biocatalytic processes.

Beyond the influence of temperature and pressure on the enzyme structure, the enzymatic reaction rate and chemical equilibrium dependence on these two variables is a matter of major biotechnological interest. As stated on 1.4.3, the functional dependence of enzymes activity on the binomial temperature and pressure can be used

to modulate it, in order to attain improved results (Pedro *et al.*, 2007; Hay *et al.*, 2007; Eisenmenger and Reyes-De-Corcuera, 2009). Beyond temperature, pressure has been used to accelerate biocatalytic reactions and even to shift chemical equilibriums according to TST and the *Le Chatelier's principle*, respectively. The determination of the thermodynamic parameters: ΔV_{reac} , $\Delta^\ddagger V$, $\Delta^\ddagger H$, $\Delta^\ddagger S$ and $\Delta^\ddagger G$ are of major importance in order to understand the enzymatic reaction dependence on both pressure and temperature.

This work aims to study a potential increased stability of both α -L-rhamnosidase and β -D-glucosidase from naringinase, under pressure, against high temperature conditions, concerning the stated behaviour of proteins against pressure and temperature (Figure 1.12). Also, optimum pressure conditions under high temperature ought to be found, under which the pressure protecting effect is maximum. Focusing on enzyme activity, the aim is to study the effect of both pressure and temperature over the reaction rate constants of both α -L-rhamnosidase and β -D-glucosidase expressed by naringinase. Also the influence of pressure on the equilibrium constant of both α -L-rhamnosidase and β -D-glucosidase will be studied. Finally, another aim of this study consists on studying the hydrolysis of the flavone rutinoside naringin into naringenin by naringinase.

3.2 Material and Methods

3.2.1 Chemicals

Naringin, 4-NRP and 4-NGP were from Sigma-Aldrich; 3,5-dinitrosalicylic acid (DNS) and glucose were from Merck; all other chemicals were of analytical grade and obtained from various sources.

3.2.2 Enzyme solution

Naringinase (CAS n°. 9068-31-9, cat. n°. 1385) from *Penicillium decumbens* was obtained from Sigma-Aldrich and stored at -20°C . The lyophilized naringinase powder was dissolved in 20.0 mM acetate buffer pH 4.0, at 200 g.L^{-1} concentration. The enzyme stock solution was kept at 4°C for a month, during the experimental period.

3.2.3 High-pressure equipment

Experiments under pressure were carried out in a stainless-steel vessel immersed in a thermostatic water bath (Julabo Hc / F18) according to the sketch in Figure 3.1 assuming isobaric and isothermal conditions (Vila-Real *et al.*, 2007).

A particular concern when working with pressure equipments was the temperature increase whenever pressure was build-up due to adiabatic heat. According to Albuquerque (1979), the temperature increase is dependent on the compression rate but is independent of the temperature value. This overheating may reach 15°C at 250 MPa when the compression rate is 50 MPa min^{-1} (Albuquerque, 1979). After reaching the desired pressure, a maximum temperature was reached followed by a temperature decrease till the working temperature. In order to avoid the possible overheating during pressure build-up due to adiabatic heat, a simple method was developed that consisted on the compensation of the heat of compression with the heat loss during decompression. Previously, the reaction vessel was pressurized at the working pressure waiting till thermal equilibrium was attained. The assay starts with the vessel decompression, following opening and closing to insert the samples and finally a compression of the same magnitude. The temperature inside the reaction vessel was determined by measuring the conductance of a 0.01 mM potassium chloride aqueous solution and fitting a linear dependence between conductivity and temperature. The thermostat was regulated for 30.0°C . The compression rate was standardized in a way

to minimize the overheating (Table 3.1). Figure 3.2 shows the temperature variation inside the reaction vessel along time. The overheating was maximal after 10 minutes and didn't exceed 2.0 °C even at the higher pressure (Table 3.1). Only pressure values of 150, 200 and 250 MPa were studied since at lower pressure the overheating is low.

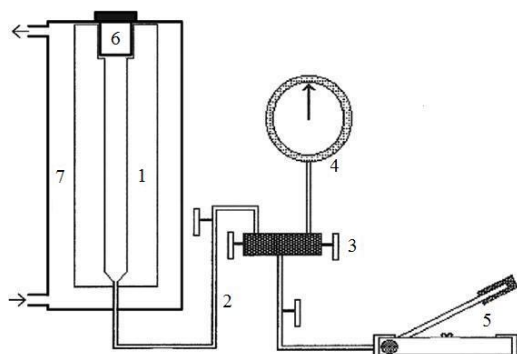


Figure 3.1 Pressure apparatus. Vessel (1); steel pipe (2); valve (3); pressure gauge (4); manual pump (5); vessel cap (6); thermostatic bath (7).

Table 3.1 Correspondence between the temperature overheating and the attained pressure values of 150, 200 and 250 MPa and respective compression rates.

Pressure values (MPa)	Pressure range (MPa)	Compression rate (MPa min ⁻¹)	ΔT (°C)
150	0 – 125	125	0.9 ± 0.0
	125 – 140	15	
	140 – 150	3	
200	0 – 150	150	1.5 ± 0.1
	150 – 190	40	
	190 – 200	3	
250	0 – 150	150	1.7 ± 0.1
	150 – 200	50	
	200 – 250	13	

Mean value ± SE, *n* = 3.

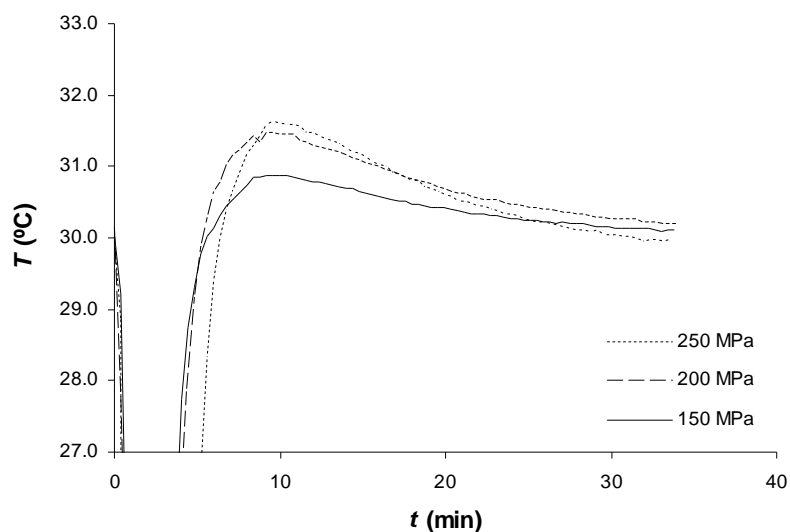


Figure 3.2 Temperature change inside the reaction vessel along time, during depressurization followed by pressurization till the desired pressure (150, 200 and 250 MPa) (thermostatic bath set at 30.0 °C).

3.2.4 Analytical methods

The concentration of the reducing sugars was determined using the DNS assay (Miller, 1959). In this work the DNS macroassay was modified into a microassay procedure using a microtiter plate, having the advantages of higher repeatability, speed, large sample analysis number and sample volume reduction. The microassay developed consisted on the addition of DNS reagent (85 μL) to an equal sample volume in a 96 well microtiter plate. The microplate is heated for 5 minutes at 100 $^{\circ}\text{C}$ and then cooled in a water bath at room temperature. Absorbance is read at 575 nm (*Hitachi 2000, UV-visible* spectrophotometer). The concentration of the reducing sugars was determined against a glucose calibration curve.

The concentration of *p*-nitrophenol released after the hydrolysis of 4-NRP and 4-NGP was evaluated spectrophotometrically (*Hitachi 2000, UV-visible* spectrophotometer coupled to a *Julado F25* thermostat) at 340 nm, using a calibration curve of each compound.

3.2.5 Activity measurement

3.2.5.1 Inactivation kinetics

0.20 mM of 4-NRP and 4-NGP, in 20 mM acetate buffer at pH 4.0, were respectively used as substrates to determine α -L-rhamnosidase and β -D-glucosidase activities, expressed by naringinase. The naringinase concentration used in the assays was 100 mg L^{-1} . There was a linear correlation between enzyme concentration and enzyme activity, from 0 to 300 mg L^{-1} naringinase concentration. The enzyme residual activity was measured spectrophotometrically, throughout the addition of equal volumes of enzyme and substrate solutions. Absorption was measured every 30 s, during 10 min, at 30.0 $^{\circ}\text{C}$, at atmospheric pressure. The enzyme activity was determined by linear regression on the first data-points during the initial reaction time.

3.2.5.2 Reaction thermodynamic functions

0.20 mM of 4-NRP and 4-NGP, in 20 mM acetate buffer at pH 4.0, were respectively used as substrates to determine α -L-rhamnosidase and β -D-glucosidase activities, expressed by naringinase.

In the studies of temperature dependence assays the naringinase concentration used was 100 mg L^{-1} . The enzyme activity was measured spectrophotometrically, throughout the addition of equal volumes of enzyme and substrate solutions. Absorption was measured every 30 s, during 10 min, at atmospheric pressure, within a temperature range of $20.0 - 45.0 \text{ }^\circ\text{C}$. The enzyme activity was determined by linear regression on the first data-points during the initial reaction time.

In the case of the determination of the activation volume within pressure dependence assays, a naringinase concentration of 5 mg L^{-1} was used to study the α -L-rhamnosidase activity and 10 mg L^{-1} was used to study the β -D-glucosidase activity. The absorption was measured every 15 min, during 90 min, at $40.0 \text{ }^\circ\text{C}$, at atmospheric pressure after removing the samples from the high-pressure equipment, within a pressure range of $0 - 200 \text{ MPa}$. Each data point required a new experiment due to the depressurization needed at the end of the incubation period. The enzyme activity was determined by linear regression on the first data-points during the initial reaction time.

Naringin bioconversion studies were performed in 20 mM acetate buffer at $\text{pH } 4.0$, with naringinase. Naringin was hydrolyzed into prunin and rhamnose followed by the hydrolysis of prunin into naringin and glucose.

In the studies of temperature dependence it was used 0.2 mM of naringin and a naringinase concentration of 50 mg L^{-1} . Initial reaction rate was evaluated within a 2 hours period, using a continuous sampling method every 10 minutes, along the catalytic reaction. The reaction occurred at atmospheric pressure in a thermostatic water bath (*Julabo HC/F18*) within a temperature range of $25.0 - 45.0 \text{ }^\circ\text{C}$. The reaction was stopped by cooling the samples on ice. The reducing sugars content was measured spectrophotometrically, using DNS assay. The enzyme activity was determined by linear regression on the first data-points during the initial reaction time.

In the case of the determination of the activation volume within pressure dependence assays, it was used a pressure equipment coupled to a UV-visible spectrophotometer (these experiments were carried out in the lab of Prof. Dr. Phillips). It was used a 0.1 mM of naringin and a naringinase concentration of 50 mg L^{-1} . The absorption was measured every 10 s, during 60 min, at $40.0 \text{ }^\circ\text{C}$, within a pressure range of $0 - 250 \text{ MPa}$. The naringenin absorbance was measured spectrophotometrically at 309 nm . The

enzyme activity was determined by linear regression on the first data-points during the initial reaction time.

3.2.5.3 Naringin bioconversion: combined effects of pressure and temperature

Naringin bioconversion studies were carried out in standard solutions of naringin in 20 mM acetate buffer at pH 4.0 and at atmospheric pressure (0 MPa), as well as, under the pressure of 150 MPa. During this bioconversion, naringin is hydrolyzed into prunin and rhamnose followed by the hydrolysis of prunin into naringin and glucose.

At atmospheric, pressure kinetic measurements ranged from 25.0 to 80.0 °C. In the high pressure catalytic reaction studies, each data point required a new experiment due to the depressurization needed at the end of the incubation period. The reaction was immediately stopped, lowering the temperature of solutions below 0 °C and the samples were frozen (−20 °C) until the enzymatic activity assays were carried out. The naringinase concentrations ranged from 5 – 75 mg mL^{−1}, according to the experimental temperature, in order to obtain a straight linear progression during the first 80 minutes, using a continuous sampling method every 10 minutes, along the catalytic reaction. The reducing sugars content was measured spectrophotometrically, using DNS assay. The enzyme activity was determined by linear regression on the first data-points during the initial reaction time.

3.2.6 Inactivation conditions

3.2.6.1 Atmospheric pressure

The thermal inactivation kinetics of α -L-rhamnosidase and β -D-glucosidase was studied at 55 – 85 °C. The thermal inactivation at atmospheric pressure occurred at isothermal conditions (± 0.1 °C) using a thermostatic water bath (*Julabo Hc/F18*). The enzyme solution was kept in Eppendorf tubes (1.5 mL) during the thermal inactivation. After removing the enzyme samples from the water bath they were cooled on ice for 5 min to stop the thermal inactivation. The inactivation time ranged from 180 to 6 min according to the temperature used. Enzyme activity was measured, in triplicate, immediately after inactivation, as well as one day after. A_0 is the specific activity of a control non-heated enzyme sample.

3.2.6.2 Pressurized conditions

The study of naringinase inactivation under pressure was performed at 0 – 250 MPa, at a certain temperature value. Only one temperature condition was studied for each activity of α -L-rhamnosidase (85.0 °C) and β -D-glucosidase (75.0 °C). The temperature conditions chosen were the highest temperature to cause a fast enzymatic inactivation, so eventual protecting effects of pressure from inactivation could be easily measured. The enzyme solution was kept in closed Eppendorf tubes (1.5 mL) during inactivation under pressure. After removing the enzyme samples from the water bath they were cooled on ice for 5 min to stop the thermal inactivation. The inactivation time ranged from 180 to 90 min according to the pressure used. A_0 was the specific activity of a control non-pressurized and non-heated enzyme sample.

3.2.7 Parameters estimation

3.2.7.1 Inactivation rate constants

First-order inactivation rate constants (k_1 and k_2) as well as the α_1 parameter could be determined by non-linear regression by minimizing the residual sum of squares of the experimental data points for the residual activity vs. treatment time and those estimated by the model, using Solver add-in from Microsoft Excel 2003 for Windows XP, considering the following options: Newton method; 100 iterations, precision of 10^{-6} , 5 % of tolerance and 10^{-4} convergence. The first-order inactivation rate constant obtained from linear regression of $\ln A_r$ vs. t was used as the initial value for the non-linear regression k_1 parameter. The non-linear regression parameters were restricted to positive numbers.

In the case of the kinetics obeying to Equation 1.47, $t_{1/2}$ was determined through either interpolation or extrapolation. Concerning the first-order inactivation kinetics, $t_{1/2}$ was calculated using Equation 1.49.

3.2.7.2 Reaction thermodynamic parameters

The reaction thermodynamic parameters could be determined after fitting an adequate model described on 1.4.3 to experimental data of equilibrium constants and reaction rate constants, through linear regression. In the case of Baliga and Whalley model (Equation 1.30) the fit to experimental data was carried out using a non-linear curve-fit program in

Excel for Windows, version 8.0 SR2, by minimizing the residual sum of squares between the experimental data points and the estimated values by the model.

3.2.7.3 Enzymatic kinetic parameters

The fit of the Michaelis-Menten model (Equation 1.1) to experimental data was carried out using a non-linear curve-fit program in Excel for Windows, version 8.0 SR2, by minimizing the residual sum of squares between the experimental data points and the estimated values by the model. The kinetic parameters estimated by linear regression using the Lineweaver-Burk equation (Equation 1.4), which results from the linearization of the Michaelis-Menten equation, were used as initial values of the non-linear regression parameters. The non-linear regression parameters were constricted to positive numbers. The catalytic constant was determined according to Equation 1.5.

3.3 Results and Discussion

3.3.1 Inactivation kinetics

3.3.1.1 Thermal inactivation of α -L-rhamnosidase and β -D-glucosidase, at atmospheric pressure

The effect of temperature on the stability of α -L-rhamnosidase and β -D-glucosidase, expressed by naringinase was studied between 55 – 75 °C, and 70 – 85 °C, respectively (Figure 3.3). Enzyme activity was measured, immediately after, as well as one day after, without occurring reactivation.

In the case of β -D-glucosidase, biphasic inactivation kinetics (Equation 1.47) was observed (Figure 3.3a). This inactivation kinetics, considering a first inactivation step followed by a second one, were in agreement with the existence of an enzymatic intermediate with a lower specific activity than the initial enzyme native state, and a final state where the enzyme was completely inactivated (Henley and Sadana, 1985). The inactivation of α -L-rhamnosidase occurred according to the classical first-order inactivation model (Equation 1.48) (Figure 3.3b).

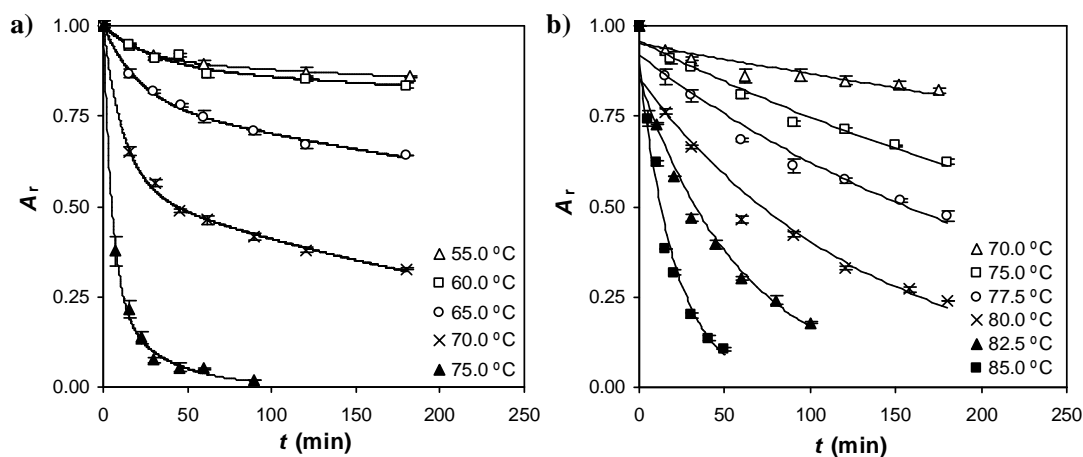


Figure 3.3 Thermal inactivation kinetics of β -D-glucosidase (a) and α -L-rhamnosidase (b), at 0 MPa (mean value \pm SE).

Table 3.2 shows the two inactivation constants calculated for β -D-glucosidase, as well as the α_1 parameter determined for each working temperature. In case of α -L-rhamnosidase a single inactivation constant was determined for all temperature conditions studied (Table 3.2). The half-life parameter of α -L-rhamnosidase (Table 3.2) seemed to be more resistant against inactivation caused by heat than β -D-glucosidase. In fact, at 75.0 °C, β -D-glucosidase exhibited a half-life of 5 min, while the α -L-

rhamnosidase half-life (279 min) was more than 50 fold higher. Almost complete inactivation of β -D-glucosidase and α -L-rhamnosidase occurred at 75.0 °C and 85.0 °C, respectively, within a 1 hour period.

Table 3.2 Thermal inactivation parameters of β -D-glucosidase and α -L-rhamnosidase, at 0 MPa.

T (°C)	α_1	$k_1 \cdot 10^3$ (min ⁻¹)	$k_2 \cdot 10^3$ (min ⁻¹)	$t_{1/2}$ (min)	R^2
β -D-glucosidase					
55.0	0.88 ± 0.04	46 ± 40	0.13 ± 0.22	2211 ± 2500	0.999
60.0	0.87 ± 0.03	34 ± 11	0.26 ± 0.22	3065 ± 1641	0.965
65.0	0.77 ± 0.04	53 ± 22	1.20 ± 0.33	388 ± 56	0.995
70.0	0.54 ± 0.02	84 ± 13	3.08 ± 0.27	42 ± 1	0.998
75.0	0.17 ± 0.06	184 ± 57	27.5 ± 4.6	5.2 ± 1.3	0.999
α -L-rhamnosidase					
70.0	-	0.9 ± 0.1	-	761 ± 89	0.829
75.0	-	2.5 ± 0.1	-	279 ± 14	0.972
77.5	-	3.9 ± 0.2	-	179 ± 11	0.966
80.0	-	7.5 ± 0.1	-	92 ± 1	0.966
82.5	-	16.3 ± 0.6	-	42 ± 2	0.978
85.0	-	46.2 ± 1.0	-	15 ± 0	0.977

Mean value \pm SD, $n = 3$.

The Arrhenius model (Equation 1.13) fitted the experimental data, and the inactivation constants of β -D-glucosidase and α -L-rhamnosidase clearly showed a linear temperature dependence (Figure 3.4), allowing the accurate calculation of thermodynamic parameters. Therefore, the activation enthalpy, entropy and Gibbs energy were determined and are presented in Table 3.3. The positive activation enthalpy is in agreement with bond disruption occurring during denaturation. In the case of β -D-glucosidase where a biphasic inactivation kinetics was observed (Figure 3.3a), the activation enthalpy almost triplicates from inactivation step 1 (104 kJ mol^{-1}) to step 2 (285 kJ mol^{-1}). In fact the activation enthalpy of the first inactivation step was lower than the second, which was consistent with a first small bond disruption where the intermediate enzyme still had some activity followed by a second inactivation step with higher bond disruption.

Both enzymes showed positive activation entropy (Table 3.3), which was consistent with the melting away of the ordered solvent structures. Denaturation occurred when entropy compensated enthalpy turning negative the Gibbs free energy of activation (Table 3.3). The denatured state caused by high temperature led to a random coil-like structure with exposure of hydrophobic groups of amino acids to the aqueous solution.

This process was driven by solvent and enzyme entropy increase mainly due to the greater freedom of the side chains of the amino acids as well as the enzyme backbone (Scharnagl *et al.*, 2005).

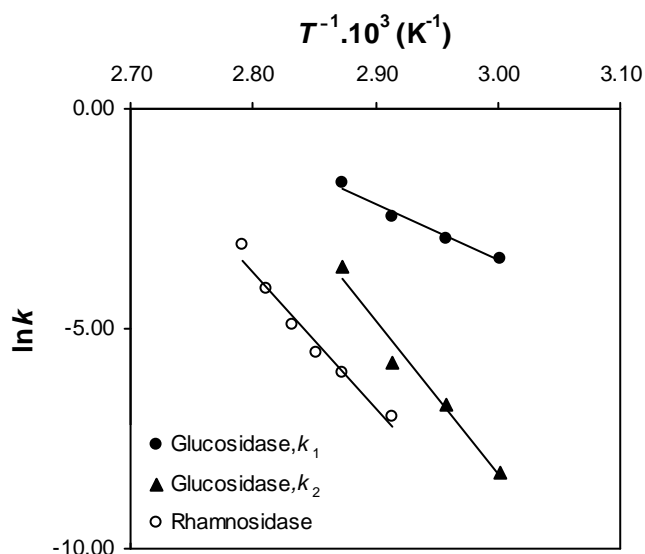


Figure 3.4 Temperature dependence of the inactivation constants of β -D-glucosidase and α -L-rhamnosidase, at 0 MPa.

Table 3.3 Thermodynamic parameters of the thermal inactivation of β -D-glucosidase and α -L-rhamnosidase, at 0 MPa.

	$\Delta^\ddagger H$ (KJ mol ⁻¹)	$\Delta^\ddagger S$ (J mol ⁻¹ K ⁻¹)	$\Delta^\ddagger G$ (KJ mol ⁻¹)	R^2
β -D-glucosidase				
(1 st inactivation)	104 ± 12	37 ± 35	- 12.3 (60 °C) - 12.5 (65 °C) - 12.7 (70 °C) - 12.8 (75 °C)	0.98
(2 nd inactivation)	285 ± 34	539 ± 99	- 179 (60 °C) - 182 (65 °C) - 185 (70 °C) - 188 (75 °C)	0.97
α -L-rhamnosidase	256 ± 24	441 ± 67	- 153 (75 °C) - 154 (77.5 °C) - 155 (80 °C) - 157 (82.5 °C) - 158 (85 °C)	0.97

Mean value ± SD, $n = 3$.

3.3.1.2 Thermal inactivation of α -L-rhamnosidase and β -D-glucosidase, under pressure

The study of the inactivation of β -D-glucosidase and α -L-rhamnosidase under pressure (0 – 250 MPa) was carried out respectively at the temperature conditions of 75.0 and 85.0 °C (Figure 3.5).

Similar to thermal inactivation kinetics, β -D-glucosidase showed a biphasic inactivation kinetics under pressure (Figure 3.5a) and two inactivation constants (k_1 and k_2) were determined as well as the α_1 parameter. On the other hand α -L-rhamnosidase showed first-order inactivation kinetics (Figure 3.5b) with an inactivation constant reported on Table 3.4.

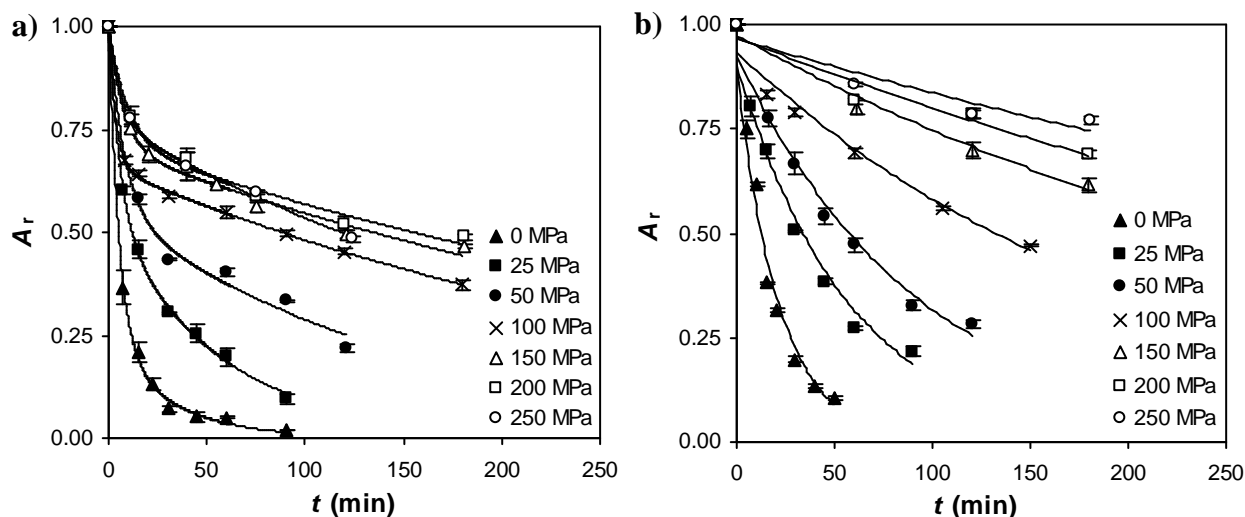


Figure 3.5 Inactivation kinetics of β -D-glucosidase at 75.0 °C (a) and α -L-rhamnosidase at 85.0 °C (b), under several pressure conditions (mean value \pm SE).

Table 3.4 Inactivation kinetics parameters of β -D-glucosidase at 75.0 °C and α -L-rhamnosidase at 85.0 °C, under several pressure conditions.

P (MPa)	α_1	$k_1 \cdot 10^3$ (min ⁻¹)	$k_2 \cdot 10^3$ (min ⁻¹)	$t_{1/2}$ (min)	R^2
β -D-glucosidase					
0	0.17 ± 0.06	190 ± 62	27.9 ± 4.8	5 ± 1	0.99
25	0.48 ± 0.03	166 ± 21	17.8 ± 2.8	12 ± 1	0.99
50	0.53 ± 0.00	126 ± 16	6.6 ± 0.4	23 ± 2	0.99
100	0.65 ± 0.01	293 ± 250	3.2 ± 0.3	88 ± 8	0.99
150	0.70 ± 0.05	147 ± 30	2.6 ± 0.4	133 ± 6	0.99
200	0.70 ± 0.06	136 ± 100	2.3 ± 0.4	154 ± 16	0.99
250	0.76 ± 0.08	482 ± 544	3.6 ± 0.8	118 ± 4	0.99
α -L-rhamnosidase					
0	-	46.3 ± 1.2	-	15 ± 0	0.97
25	-	17.5 ± 0.7	-	40 ± 2	0.96
50	-	10.7 ± 0.5	-	65 ± 3	0.98
100	-	4.7 ± 0.0	-	147 ± 3	0.97
150	-	2.7 ± 0.3	-	263 ± 27	0.98
200	-	1.9 ± 0.1	-	362 ± 15	0.93
250	-	1.4 ± 0.1	-	487 ± 57	0.88

Mean value \pm SD, $n = 3$.

In the case of β -D-glucosidase, as pressure was increased from 0 to 200 MPa the second inactivation constant decreased, while for the first inactivation constant no tendency could be established. This first inactivation rate exhibited a large error reflected on the

large standard errors (Table 3.4). Nevertheless, as expected, the half-life time of β -D-glucosidase increased with pressure from 5 minutes at atmospheric pressure up to a maximum of 154 minutes at 200 MPa (Table 3.4). At 75°C and under a pressure condition of 200 MPa, β -D-glucosidase was 30 fold more resistant against inactivation than at atmospheric pressure. Indeed, the biphasic kinetics observed in Figure 3.5a shows that the first inactivation constant was higher than the second inactivation constant, which means that β -D-glucosidase initially was inactivated more rapidly before reaching the time value of the half-life and afterwards more slowly (Table 3.4), which also occurs in thermal inactivation, at atmospheric pressure.

In the case of α -L-rhamnosidase, the inactivation constant also decreased with pressure, which is in agreement with an increase of its half-life from 15 minutes at atmospheric pressure up to a maximum of 487 minutes at 250 MPa (Table 3.4). In fact, this observed maximum value may be even greater under higher pressure conditions, which could not be tested due to experimental device limitations. α -L-rhamnosidase was 32-fold more resistant against inactivation at 250 MPa and 85 °C than at atmospheric pressure.

Figure 3.6 highlights the inactivation constant dependence with pressure, showing how both the second inactivation constant of β -D-glucosidase and the inactivation constant of α -L-rhamnosidase decreased with pressure. These data are well fitted to the Golinkin Laidlaw and Hyne equation (Equation 1.24), allowing the activation volume determination at atmospheric pressure (Table 3.5). A compressibility coefficient of activation ($\Delta^\ddagger\beta$) was also determined according to Equation 1.26 (Table 3.5), originated by an activation volume change with pressure. The large and positive activation volume obtained (Table 3.5) is consistent with a high volume increase between the reactant state and the transition state. As pressure favors the smaller volume, which is the volume of reactants, pressure led to the stabilization of the native state of both subunits of naringinase. In addition, for each naringinase subunit, this stabilization under pressure was also dependent on the pressure magnitude (Table 3.5). The positive value of the compressibility coefficient of activation is in agreement with a minor effect of pressure over the activation volume until a minimum was reached, corresponding to a null activation volume. The β -D-glucosidase minimum observed in Figure 3.6 corresponded to an optimum pressure value of 173 ± 9 MPa which is the zero of the first derivative of Equation 1.24. In the case of α -L-rhamnosidase, a minimum may be achieved at higher pressures (Figure 3.6), which we were not able to test due to experimental device limitations.

These results corroborate the antagonism between pressure and temperature at high temperature conditions, concerning the stability of proteins. It is also interesting to notice that a temperature increase can be done without compromising an enzyme inactivation increase by means of pressure, when comparing to atmospheric pressure conditions. This comparison can be done through the half-lives of both thermal inactivation at atmospheric pressure and under pressure conditions (Table 3.2 and 3.4). The highest β -D-glucosidase half-life time under pressure is 154 minutes (for 2nd inactivation), at 200 MPa and 75.0 °C (Table 3.4), which is between the inactivation half-lives at 65.0 °C (388 minutes) and 70.0 °C (44 minutes), at atmospheric pressure (Table 3.2). These data support that β -D-glucosidase, under 200 MPa at 75.0°C, showed the same inactivation half-life of a reaction carried between 65.0°C and 70.0°C temperature conditions, at atmospheric pressure; which corresponds to a 5 to 10°C temperature magnitude increment. In an analogous way, α -L-rhamnosidase, which showed an half-life time of 487 minutes, at 250 MPa and 85.0 °C (Table 3.4), had an inactivation half-time which was comprised between the half-lives time of 70.0 °C (761 minutes) and 75.0 °C (279 minutes), of a reaction carried at atmospheric pressure (Table 3.2); which corresponds to a 10 to 15°C temperature magnitude increment. Altogether these data suggest that pressure may allow a reaction temperature increment ranging from 5 to 15°C, according to certain reaction conditions as well as to the naringinase activities, without compromising an enzyme inactivation increase.

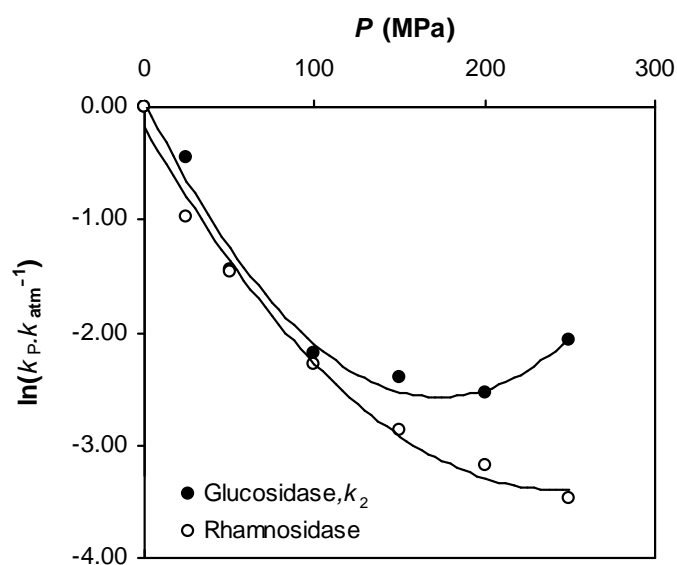


Figure 3.6 Pressure dependence of the inactivation constant of β -D-glucosidase (k_2) at 75.0 °C and α -L-rhamnosidase at 85.0 °C.

Table 3.5 Thermodynamic parameters of the inactivation kinetics of β -D-glucosidase at 75.0 °C and α -L-rhamnosidase at 85.0°C (0 – 250 MPa).

	$\Delta^\ddagger V$ (mL mol ⁻¹)	$\Delta^\ddagger \beta$ (mL mol ⁻¹ MPa ⁻¹)	R^2
β -D-glucosidase	87 ± 8	0.50 ± 0.06	0.98
α -L-rhamnosidase	79 ± 7	0.32 ± 0.06	0.99

Mean value ± SD, $n = 3$.

3.3.2 Reaction thermodynamic functions

3.3.2.1 Pressure dependence

The effect of pressure, from atmospheric pressure (0 MPa) to 200 MPa, at 40 °C, was assessed for both β -D-glucosidase and α -L-rhamnosidase activities expressed by naringinase. These experiments allowed the determination of equilibrium constants and reaction volumes as well reaction rate constants and the activation volumes for both enzymatic reactions as shown below. In addition the activation volume associated with the bioconversion of naringin by naringinase was also determined.

Reaction volume

On Figure 3.7 is shown the pressure dependence of the equilibrium constants of the specific substrates 4-NRP and 4-NGP hydrolyzed by α -L-rhamnosidase and β -D-glucosidase. Lower equilibrium constants of both substrates were obtained as pressure increased.

Pressure effects on equilibrium constants were quantified fitting the experimental data to first, second and third order polynomial equations, respectively described by the models of Burris and Laidler (Equation 1.22) (Burris and Laidler, 1955), Golinkin, Laidlaw and Hyne (Equation 1.24) (Golinkin *et al.*, 1966) and Walling and Tanner (Equation 1.27) (Walling and Tanner, 1963); and also by Baliga and Whalley model (Equation 1.30) (Baliga and Whalley, 1970). The F-test (Fisher-Snedecor test) (Table 3.6) was used to choose the model that fitted better to the experimental results. Baliga and Whalley model was the best to describe the equilibrium constants dependence with pressure, allowing the calculation of reaction volumes (Table 3.6). Positive reaction volumes of 64 and 93 mL mol⁻¹ were obtained, respectively for 4-NGP and 4-NRP, hydrolysis by α -L-rhamnosidase and β -D-glucosidase.

The decrease in hydrolysis equilibrium constants for both 4-NGP and 4-NRP with pressure (Figure 3.7) was in agreement with the positive reaction volumes. These results

indicate that the volume of the system increased when the reaction proceeds from substrate (S) to the products (P). Therefore, as pressure gets higher the equilibrium is directed back to the substrates that occupy together a smaller volume.

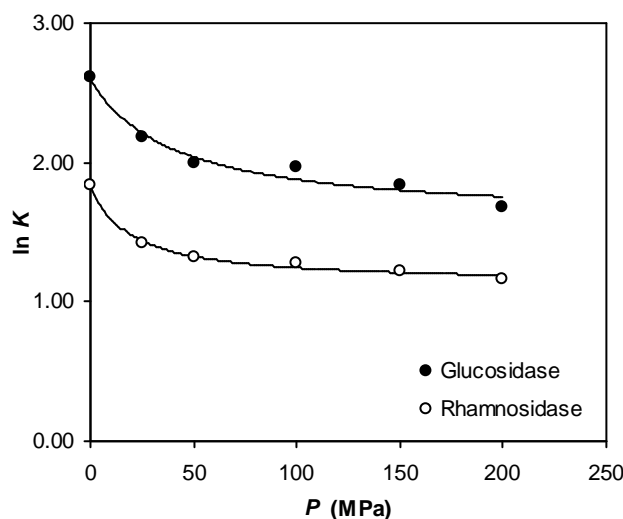


Figure 3.7 Pressure dependence of the equilibrium constant of β -D-glucosidase and α -L-rhamnosidase.

Table 3.6 Estimation of the reaction volumes of β -D-glucosidase and α -L-rhamnosidase.

Models	β -D-glucosidase			α -L-rhamnosidase		
	F-test		ΔV_{reac} (mL mol ⁻¹)	F-test		ΔV_{reac} (mL mol ⁻¹)
	F	F_c		F	F_c	
Golinkin, Laidlaw and Hyne	2.1	10.1	-	3.5	10.1	-
Walling and Tanner	8.9	19	-	8.0	19	-
Whalley and Baliga	14.3	10.1	64 ± 28	113.0	10.1	93 ± 3

Mean value ± SD, $n = 3$.

$F = ((SSE_1 - SSE_2)/(q_2 - q_1)) / (SSE_2 / (n - q_2))$, 95%

$F_c = (p_2 - p_1, n - p_2)$

Activation volume

Experimental values for relative activity of the naringinase enzymatic complex were acquired in the pressure range of 0 – 250 MPa at 40 °C (Figure 3.8), considering the hydrolysis of 4-NGP, 4-NRP and naringin. This flavone rutinoside has both glucose and rhamnose residues that can be hydrolysed by naringinase (Vila-Real *et al.*, 2007), while 4-NRP and 4-NGP possess respectively a rhamnose and a glucose which makes them specific for both α -L-rhamnosidase and β -D-glucosidase, respectively.

The β -D-glucosidase activity of naringinase decreased with pressures greatly at 50 MPa, and at 200 MPa almost reached 50 % inactivation (Figure 3.8).

Both 4-NRP and naringin hydrolysis rates increased with pressure from 0 to 150 MPa. A higher hydrolysis rate occurred on the pressure ranged of 100 – 150 MPa, followed by a decrease of the α -L-rhamnosidase and the naringinase activity for the naringin bioconversion (Figure 3.8).

Naringin hydrolysis by naringinase firstly and faster withdraws the rhamnose residue of naringin, as favored by pressure increase, and later and slower the glucose residue, as β -D-glucosidase expression is deactivated by pressure (Figure 3.8).

Pressure effects on rate constants were quantified according to the best fit of experimental data to first and second order polynomials relating $\ln k$ to P or to P^2 , respectively described by the models of Burris and Laidler (Equation 1.22) (Burris and Laidler, 1955) and Golinkin, Laidlaw and Hyne (Equation 1.24) (Golinkin *et al.*, 1966). These models were used to fit naringinase activity pressure dependence for the substrates: 4-NGP, and 4-NRP and naringin (Table 3.7).

Pressure affected negatively the reaction rate constant for 4-NGP hydrolysis. The experimental results for 4-NGP hydrolysis at different pressure were best fitted to the model of Burris and Laidler with a determination coefficient of 0.969. From the slope of $\ln k$ versus P an activation volume of $6.5 \pm 1.9 \text{ mL mol}^{-1}$ was obtained. This positive activation volume means that 4-NGP hydrolysis rate was not favoured by pressure.

Regarding the 4-NRP and naringin hydrolysis data were best fitted with Golinkin, Laidlaw and Hyne model, with a correlation coefficient of 0.99 and 0.97, respectively. The $\Delta^\ddagger V$ values for 4-NRP and naringin hydrolysis, calculated using Equation 1.25 are respectively -7.7 ± 1.5 and $-20.0 \pm 5.2 \text{ mL mol}^{-1}$. These values are related with an increase of the reaction rate constants at low pressure values, below 100 MPa.

In previous work the effect of pressure on naringinase activity was tested in different systems (Marques *et al.*, 2007; Pedro *et al.*, 2007; Vila-Real *et al.*, 2007; Ribeiro *et al.*, 2010). In fact a positive effect of pressure on reaction rates and a $\Delta^\ddagger V$ of $-15.0 \pm 1.8 \text{ mL mol}^{-1}$ were found using soluble naringinase for the hydrolysis of naringin (Vila-Real *et al.*, 2007). Moreover a negative $\Delta^\ddagger V$ ($-9 \pm 2.8 \text{ mL mol}^{-1}$) was obtained with naringinase immobilized within calcium alginate beads (Pedro *et al.*, 2007).

Solvent contributions may be on the molecular basis of these moderated negative activation volumes by the formation of hydrogen bonds in the transition state (Tanaka *et*

al., 1994), which are stabilized by pressure due to the lowering of the inter-atomic distance (Mozhaev *et al.*, 1996).

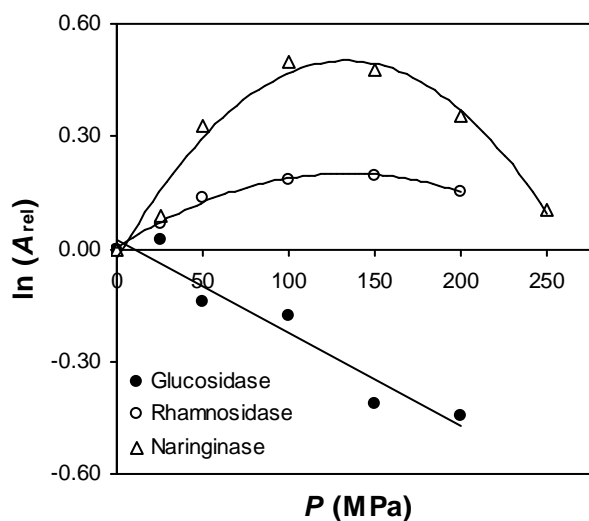


Figure 3.8 Pressure dependence of: β -D-glucosidase, α -L-rhamnosidase and naringinase.

Table 3.7 Estimation of the activation volumes, for the hydrolysis of 4-NGP, -NRP and naringin.

Substrate	4-NGP	4-NRP	Naringin
Fitting model	Burris and Laidler	Golinkin, Laidlaw and Hyne	Golinkin, Laidlaw and Hyne
R^2	0.94	0.99	0.97
F-test			
F	0.1	116.9	114.8
F_c	10.1	10.1	10.1
$\Delta^\ddagger V$ (mL mol ⁻¹)	6.5 ± 1.9	-7.7 ± 1.5	-20.0 ± 5.2
$\Delta^\ddagger \beta$ (mL mol ⁻¹ MPa ⁻¹)	-	-0.06 ± 0.01	-0.15 ± 0.01

Mean value ± SD, $n = 3$.
95%.

3.3.2.2 Temperature dependence

Both α -L-rhamnosidase and β -D-glucosidase activities increased with temperature. Clearly, the representation of the \ln of naringinase specific activity, for the hydrolysis of 4-NRP, 4-NGP and naringin against the absolute temperatures, resulted in a straight line. Indeed, Arrhenius equation (Equation 1.13) fits well to experimental data (Table 3.8). Thermodynamic activation parameters, $\Delta^\ddagger H$, $\Delta^\ddagger S$ and $\Delta^\ddagger G$ were evaluated according to Equations: 1.14, 1.15 and 1.16.

Both hydrolysis of 4-NGP and 4-NRP by naringinase were found to be endothermic and endergonic reactions (Table 3.8). At constant temperature higher rates results in lower

standard Gibbs energy of activation. According to the results depicted in Table 3.7, the hydrolysis of both 4-NGP and 4-NRP occurs faster than the hydrolysis of naringin. This was an expected result as the conversion of naringin to final products takes at least two reaction steps, first into prunin and rhamnose and later into naringenin and glucose. Moreover, the binding energy associated with the specific substrate-enzyme interaction is usually a significant factor in lowering the Gibbs energy change required for reaction, being the large bonding energies of substrates due mostly to the complementary shape of the active site of the enzyme. Same trend occurs in activation enthalpy; in fact it is two and a half times higher in naringin bioconversion. For a bimolecular reaction transition state is formed when the two molecules old bonds are weakened and new bonds begin to form. So, positive and relatively high values for $\Delta^\ddagger H$ occur when covalent bonds are break.

In both 4-NGP and 4-NRP hydrolysis reactions the formation of activated complex occurred with a higher degree of order, as inferred by the negative entropy of activation values (Lonhienne *et al.*, 2000). In fact, activation entropy $\Delta^\ddagger S$ will tend to compensate $\Delta^\ddagger H$. So, the values found for $\Delta^\ddagger H$ on 4-NGP and 4-NRP hydrolysis was accompanied with a large decline in entropy from reactants to the transition state, resulting into very negative values, $-133 \text{ kJ mol}^{-1} \text{ K}^{-1}$ and $-128 \text{ kJ mol}^{-1} \text{ K}^{-1}$, respectively.

The effects of pressure and temperature on the equilibrium or kinetics are antagonistic in molecular terms. As follows from the principle of microscopic ordering, an increase in pressure at constant temperature leads to an ordering of molecules or a decrease in the entropy of the system (Balny, 2004).

Table 3.8 Temperature activation parameters for the hydrolysis of 4-NGP and 4-NRP, at 0 MPa.

Activity	4-NGP	4-NRP	Naringin
R^2	0.97	0.98	0.99
$\Delta^\ddagger H$ (kJ mol ⁻¹)	39.8 ± 9.8	39.6 ± 8.2	105.2 ± 3.8
$\Delta^\ddagger S$ (kJ mol ⁻¹ K ⁻¹)	-133 ± 32	-128 ± 27	46.0 ± 12.5
$\Delta^\ddagger G_{20^\circ\text{C}}$ (kJ mol ⁻¹)	39.0	37.7	
$\Delta^\ddagger G_{25^\circ\text{C}}$ (kJ mol ⁻¹)	39.7	38.3	91.5
$\Delta^\ddagger G_{30^\circ\text{C}}$ (kJ mol ⁻¹)	40.3	39.0	91.1
$\Delta^\ddagger G_{35^\circ\text{C}}$ (kJ mol ⁻¹)	41.0	39.6	90.9
$\Delta^\ddagger G_{40^\circ\text{C}}$ (kJ mol ⁻¹)	41.6	40.3	90.9
$\Delta^\ddagger G_{45^\circ\text{C}}$ (kJ mol ⁻¹)	42.3	40.9	91.6

Mean value ± SD, $n = 3$.

3.3.3 Combined effects of pressure and temperature on the kinetic parameters of naringin bioconversion

Naringin hydrolysis by naringinase was performed under atmospheric pressure as well as under pressure conditions of 150 MPa within a temperature range from 25 to 80 °C (Figure 3.9). The range of naringin concentrations increased with temperature, due to its increased solubility with temperature. In fact due to naringin solubility limits at lower temperatures (25 – 35 °C) only a range of 0.2 to 1 mM concentrations could be used; for temperatures higher than 55 °C, solubility of naringin increased, so a range of 0.2 to 7 mM naringin concentrations were then used (Figure 3.9). The temperature dependence of K_M , k_{cat} and $k_{cat} \cdot K_M^{-1}$ was studied (Figure 3.10 and 3.11).

The naringinase specific activity increased with temperature till 60 °C and 70 °C, respectively, at atmospheric and 150 MPa pressure conditions (Figure 3.9). At atmospheric pressure the rate of naringin hydrolysis decreased for higher temperatures than 70°C.

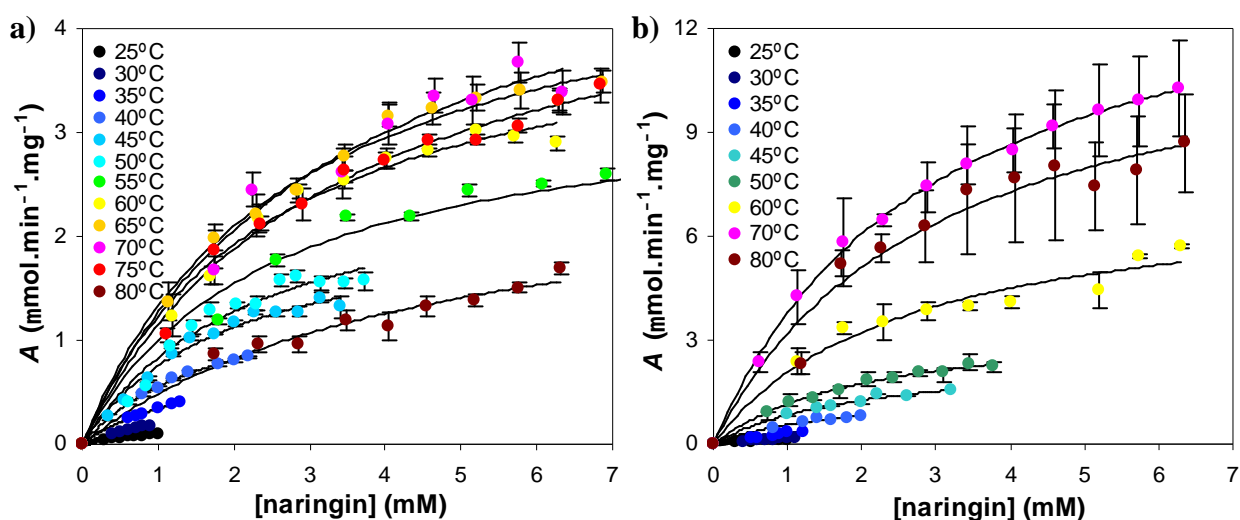


Figure 3.9 Michaelis-Menten kinetics of naringinase, at different temperatures, at 0 MPa (a) and 150 MPa (b) (mean value \pm SE).

A slight increase in K_M was observed with temperatures from 20 to 60 °C, while for higher temperatures (70 and 80 °C) it almost duplicated, from 2 mM to 4 mM, at atmospheric pressure. Under high pressure conditions of 150 MPa, Michaelis-Menten constant remained constant at temperatures from 20 to 50 °C, while for temperatures of 60 to 80 °C a slight increase was observed, from 2 to 2.5 mM (Figure 3.10).

In naringin hydrolysis with naringinase, from *Penicillium* sp., a K_M of 2 mM was described for immobilized naringinase by covalent binding to wood material (Puri *et al.*,

2005), while Puri *et al.* (1996) cited a value of 10 mM for the K_M of naringinase (from *Penicillium* sp.) immobilized in calcium alginate beads under pressure. Pedro *et al.* (2007) obtained a K_M of 0.303 mM and v_{max} of 0.0418 mM min⁻¹ with naringinase immobilized within calcium alginate beads, at atmospheric pressure.

An important consequence of pressure application is that the reaction hydrolysis acceleration due to temperature increase is more significant under higher pressure conditions. The catalytic constant, as well as, the apparent second-order rate constant showed an increase till the temperature of 70 °C was reached, where the enzyme activity was highest, decreasing afterwards. Around this temperature both the catalytic constant and apparent second-order rate constant showed higher values, respectively 15 μmol min⁻¹ mg⁻¹ and 5 L min⁻¹ g⁻¹ under high pressure than at atmospheric pressure, respectively 5 μmol min⁻¹ mg⁻¹ and 1.5 L min⁻¹ g⁻¹ (Figure 3.11). The k_{cat} and $k_{cat} \cdot K_M^{-1}$ for the naringinase-catalyzed hydrolysis of naringin is not only temperature dependent but pressure as well. Under high pressure, at 70 °C k_{cat} and $k_{cat} \cdot K_M^{-1}$ are 3-fold higher than at atmospheric pressure (Figure 3.11) and is even higher at 80 °C, more than 4-fold (Figure 3.11a). When these values are compared at 30 °C a 15-fold increase was observed at 70 °C under 150 MPa. Similar results were obtained with α-chymotrypsin at 50 °C and 360 MPa, with an activity more than 30-fold higher than the activity determined at atmospheric pressure and 20 °C (Mozhaev *et al.*, 1996). These authors assumed that activation volumes values increase with temperature. This stated pressure dependence is also in agreement with a pressure stabilization of protein, underlying a protecting pressure effect on naringinase native state against inactivation caused by heat.

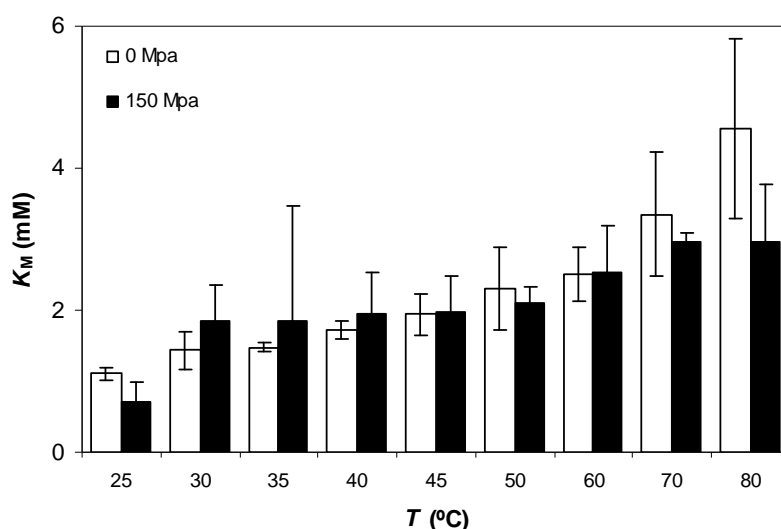


Figure 3.10 Temperature dependence of the Michaelis-Menten of naringinase for naringin bioconversion, at 0 MPa and 150 MPa (mean value \pm SE).

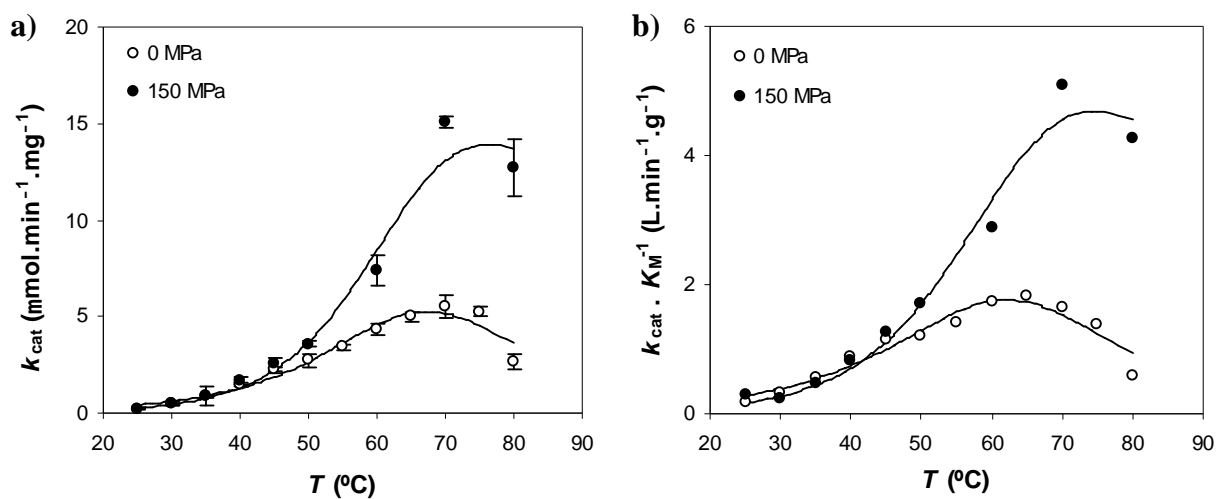


Figure 3.11 Temperature dependence of the catalytic constant (k_{cat}) (a) and second order constant ($k_{\text{cat}} \cdot K_M^{-1}$) (b) of naringinase for naringin bioconversion, at 0 MPa and 150 MPa (mean value \pm SE).

3.4 Conclusions

This study shows how pressure can be turned into a powerful tool in biosynthesis, through the reduction of enzymatic inactivation caused by heat. It is shown how pressure can protect both α -L-rhamnosidase ($\Delta^\ddagger V = 79 \pm 7 \text{ mL mol}^{-1}$, at 85.0 °C) and β -D-glucosidase ($\Delta^\ddagger V = 87 \pm 8 \text{ mL mol}^{-1}$, at 75.0 °C) activities from inactivation at high temperature conditions. In fact an antagonistic behavior between pressure and temperature, concerning the stability of proteins was observed. β -D-glucosidase was 30-fold more resistant against inactivation at 200 MPa than at atmospheric pressure, while α -L-rhamnosidase was 32-fold more resistant against inactivation at 250 MPa than at atmospheric pressure. The best pressure condition to reduce β -D-glucosidase inactivation at 75.0 °C was 173 MPa; while in the case of α -L-rhamnosidase inactivation at 85.0 °C, the optimal pressure condition was above the maximal experimental pressure conditions ($> 250 \text{ MPa}$). From another point of view, pressure allowed a reaction temperature increment ranging from 5 to 15°C, according to the naringinase activity, β -D-glucosidase and α -L-rhamnosidase respectively, without comprising an increase on the enzyme inactivation rate.

Pressure effects on equilibrium constants were quantified according to the fit of experimental data to Baliga and Whalley model. Positive reaction volumes of 64.3 mL mol⁻¹ and 93.1 mL mol⁻¹ were respectively obtained for the hydrolysis of 4-NGP and 4-NRP. The decrease in the hydrolysis equilibrium constants for both 4-NGP and 4-NRP with pressure was in agreement with the positive reaction volumes, which is a consequence of the breaking of the covalent bond between the sugar and *p*-nitrophenol.

Pressure effects on rate constants were quantified according to the best fit of experimental data to the Burriss and Laidler model as well as the Golinkin, Laidlaw and Hyne model. The $\Delta^\ddagger V$ values for 4-NRP and naringin hydrolysis calculated using the Golinkin, Laidlaw and Hyne model were respectively -7.7 ± 1.5 and $-20.0 \pm 5.2 \text{ mL mol}^{-1}$, which is in agreement with a reaction rate increase with pressure. Moreover a positive $\Delta^\ddagger V$ value for the hydrolysis of 4-NGP ($6.5 \pm 1.9 \text{ mL mol}^{-1}$) is in agreement with a reaction rate decrease with pressure.

The catalytic constant as well as the apparent second-order rate for the hydrolysis of naringin catalyzed by naringinase is not only temperature dependent but pressure as well. Under 150 MPa, at 70 °C the apparent second-order rate is 3-fold higher than

atmospheric pressure and is even higher at 80 °C, 4-fold. This stated pressure dependence is in agreement with pressure stabilization of the enzyme native state, at high temperatures. In conclusion the effect of amplification of pressure effects on reaction rates by temperature could have a pragmatic use for accelerating enzymatic reactions.

**NARINGINASE IMMOBILIZATION WITHIN SILICA GLASSES
THROUGH SOL-GEL METHOD**

Chapter 4

4.1 Introduction

In this work naringinase was subjected to immobilization concerning the general advantages of the biocatalyst immobilization technique described on 1.5. Studies regarding immobilization of naringinase and its reusability have been reported. Covalent binding has been used on glutaraldehyde-coated *Bombyx mori* silk fibers (Ellenrieder and Daz, 1996 and 1998), hen egg white (Puri *et al.*, 2001), woodchips (Puri *et al.*, 2005); non-covalent binding was tested on DEAE-Sephadex (Ono *et al.*, 1977), on Celite (Şekeroğlu *et al.*, 2006) and on XAD⁻, an non-ionic microstructured polymer, (Amaro *et al.*, 2009) through adsorption; the entrapment method was developed using hollow fibres of cellulose triacetate (Tsen and Yu, 1991), Ca-alginate (Puri *et al.*, 1996; Pedro *et al.*, 2007; Ferreira, 2008) K-carrageenan (Ribeiro and Ribeiro, 2008a) and also polyvinyl alcohol (Nunes *et al.*, 2010). The low operational stability and low activity are important problems to overcome concerning naringinase immobilization.

Naringinase is immobilized, in this work, through an occlusion method within silica glasses through sol-gel method. This work is divided into three distinct parts. A first one consisting on the optimization of immobilized naringinase using several sol-gel precursors and also glycerol as additive. Afterwards the best naringinase immobilize was used in biocatalytic cosolvent systems and ultimately this best immobilize was changed through the addition of several ionic liquids (ILs).

As an inclusion method, sol-gel glasses share the advantages related to this method as well as the inherent advantages of this kind of immobilization material (*cf.* 1.5). The high quantity of different sol-gel precursors and the many tuneable parameters underlying sol-gel chemistry turns it into a very challenging method. The pore size tuning is a major issue in order to circumvent a disadvantage of the occlusion method, which is related to the internal mass transfer effects.

The main purpose of studying the use of organic solvents is to circumvent the low water solubility of the flavone rutinosides substrates caused by the hydrophobic nature of the phenolic moiety. Naringin and prunin were studied in this work. Beyond temperature, another approach to increase substrate solubility is medium engineering involving the substitution of aqueous reaction media by non-conventional media. Enzymes usually require aqueous environments in which some organic substrates are poorly soluble and in some cases even unstable. A straightforward solution to this problem is the

application of biphasic or cosolvent systems (Filho *et al.*, 2003). In biphasic systems, the enzyme is dissolved in the aqueous phase, while the hydrophobic substrate is present in a high concentration in the organic phase. The occurrence of a liquid–liquid interface and presence of residual amounts of organic solvent in water can lead to deactivation of the biocatalyst. Different approaches to guide the choice of the proper solvent have been proposed, such as that reported by Laane *et al.* (1987) who suggested the use of the polarity of solvents, expressed by the $\log P$ value as the main criterion for optimizing organic solvents in multi liquid-phase biocatalysis. Cosolvent systems come from the addition to the aqueous media of water-miscible solvents such as: acetone, ethanol, acetonitrile or dioxane, used to increase the solubility of apolar reactants. Usually, the addition of small amounts of a water-miscible solvent has little effect on the enzyme activity and stability, in some cases the addition of low concentrations of these solvents may even result in an enhanced enzyme activity and stability. However, an increase in the concentration of most water-miscible solvents may have an inhibitory effect on the biocatalyst (Vermue and Tramper, 1995). This effect is a consequence of disturbing the enzyme native state, where non-compatible solvents lead to its denaturation (Scharnagl *et al.*, 2005). The occlusion immobilization method within sol-gel may contribute in some extent for the preservation of the biocatalyst native structure by excluding aggressive compounds from the porous matrix due to its partition characteristics and also a possible enzyme unfolding physical restriction.

Focusing on ILs as sol-gel additives, the slow diffusion rate of substrate in silica matrices can lower the activity of the immobilized enzymes (Lee *et al.*, 2007a, b). To overcome this drawback some additives can be used, such as sugars that act as stabilizers (Brennan *et al.*, 2003), polymers that reduce the extent of shrinking during the making and drying of the matrix (Wu and Choi, 2004), and other compounds, such as amino acids, polyols, surfactants or cyclodextrins (Reetz *et al.*, 2003). The use of ILs is another approach recently being developed (Sheldon *et al.*, 2002); as templates to make mesoporous silica or as stabilizers to protect some enzymes, e.g. lipases, from the inactivation during sol-gel immobilization process (Lee *et al.*, 2007a, b). ILs are very promising compounds within the sol-gel chemistry beyond biocatalysis. Despite their reported potential as alternative reaction media for biocatalysis through the increase of reactivity, selectivity and stability of enzymes (Park and Kazlauskas, 2003), their application also as sol-gel additives, acting as templating agents, may lead to the enhancement of immobilized biocatalysts activity and stability (Liu *et al.*, 2005a, b; Lee

et al., 2007a, b). On the basis of this application are their versatile tunable properties including: polarity, chemical stability, viscosity and solvent capacity; just by combining different anions and cations. In this work, ILs are used as templates additives of sol-gel glasses in order to improve the activity of immobilized naringinase, towards glycosides hydrolysis. The versatile tuneable properties of ILs turn them into challenging compounds to circumvent a major disadvantage of the inclusion method related to the internal mass transfer effects. Beyond pore size tuning, ILs may also be used for the modulation of the partition characteristics of the sol-gel glasses.

The main goal of this work is the immobilization of naringinase within an inorganic silicate material through sol-gel immobilization method. Intrinsically related with this goal is the development of a biocatalyst immobilizate with high activity, good accessibility to substrate, high resistance against leaching and long-term stability in order to use in glycosides hydrolysis. Other goal consists on the use of sol-gel immobilization to increase naringinase stability against organic cosolvents that may be used to overcome the low solubility of flavone rutinosides in aqueous system and also studying naringin hydrolysis by naringinase in aqueous cosolvent systems. Finally, concerning the use of ILs, this work aims to study several ILs as sol-gel glasses additives, concerning their content and structure in order to increase the activity and stability of α -L-rhamnosidase and β -D-glucosidase from naringinase. Secondly, the study of naringin and prunin hydrolysis by immobilized naringinase within several sol-gel/IL matrices aims to optimize the flavone glycosides hydrolysis.

4.2 Material and methods

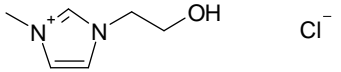
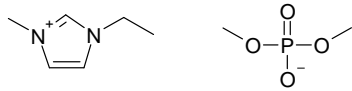
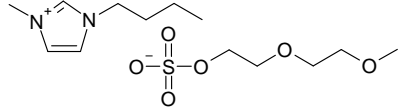
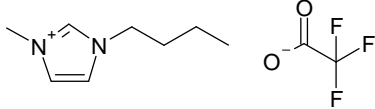
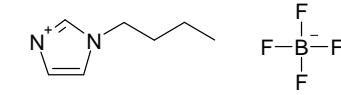
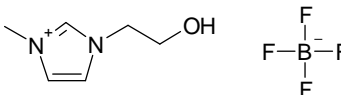
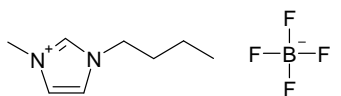
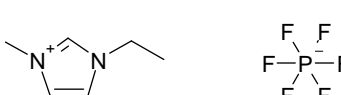
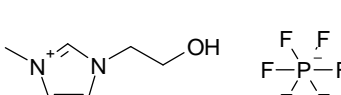
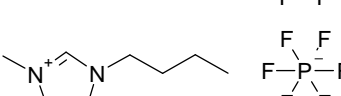
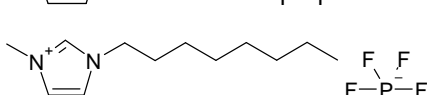
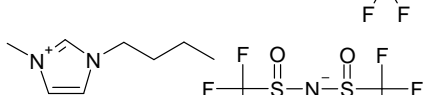
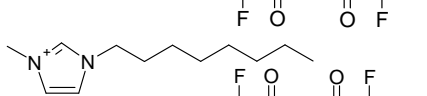
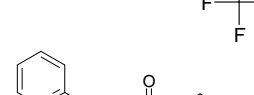
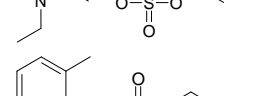
4.2.1 Chemicals

Naringin, naringenin, 3-aminopropyltrimethoxysilane (APS), methyltrimethoxysilane (MTS), 4-NRP, 4-NGP, 1-ethyl-3-methylimidazolium dimethylphosphate (Table 4.1) and rhamnose were from Sigma-Aldrich; tetramethoxysilane (TMOS), 1-butyl-3-methylimidazolium 2-(2-methoxyethoxy)ethylsulphate, and 1-butyl-3-methylimidazolium hexafluorophosphate (Table 4.1) were from Fluka; 1-ethanol-3-methylimidazolium chloride, 1-butyl-3-methylimidazolium trifluoroacetate, 1-butylimidazolium tetrafluoroborate, 1-ethanol-3-methylimidazolium tetrafluoroborate, 1-butyl-3-methylimidazolium tetrafluoroborate, 1-ethyl-3-methylimidazolium hexafluorophosphate, 1-ethanol-3-methylimidazolium hexafluorophosphate, 1-octyl-3-methylimidazolium hexafluorophosphate, 1-butyl-3-methylimidazolium bis(trifluoromethylsulfonyl)imide, 1-octyl-3-methylimidazolium bis(trifluoromethylsulfonyl)imide, 1-ethyl-2-methylpyridinium ethylsulphate and 1-ethyl-3-methylpyridinium ethylsulphate (Table 4.1) were from Solchemar; glycerol, 3,5-dinitrosalicylic acid (DNS) and glucose were from Merck while the protein assay dye reagent concentrate (cat. n° 500-0006) was from Bio-Rad. Diglycerylsilane (DGS) was synthesized by us according to (Brook *et al.*, 2004b). Prunin was biosynthesized according to the method described on Chapter 2. Prunin purity was evaluated using HPLC-MS. All other chemicals were analytical grade and obtained from various sources.

4.2.2 Enzyme solution

Naringinase (CAS n°. 9068-31-9, cat. n°. 1385) from *Penicillium decumbens* was obtained from Sigma-Aldrich and stored at $-20\text{ }^{\circ}\text{C}$. The lyophilized naringinase powder was dissolved in the appropriate buffer solution 24 hours before experiments and kept at $4\text{ }^{\circ}\text{C}$. For the production of prunin starting from naringin the β -D-glucosidase expression of naringinase was inactivated as described on Chapter 2.

Table 4.1 Ionic liquids (structure, name and abbreviation) used in sol-gel bio-immobilization.

Structure	Name	Abbreviation
	1-ethanol-3-methylimidazolium chloride	[C ₂ OHMIM] [Cl]
	1-ethyl-3-methylimidazolium dimethylphosphate	[EMIM] [DMP]
	1-butyl-3-methylimidazolium 2-(2-methoxyethoxy)ethylsulphate	[BMIM] [MeOEtOEtOSO ₃]
	1-butyl-3-methylimidazolium trifluoroacetate	[BMIM] [TFA]
	1-butylimidazolium tetrafluoroborate	[BIM] [BF ₄]
	1-ethanol-3-methylimidazolium tetrafluoroborate	[C ₂ OHMIM] [BF ₄]
	1-butyl-3-methylimidazolium tetrafluoroborate	[BMIM] [BF ₄]
	1-ethyl-3-methylimidazolium hexafluorophosphate	[EMIM] [PF ₆]
	1-ethanol-3-methylimidazolium hexafluorophosphate	[C ₂ OHMIM] [PF ₆]
	1-butyl-3-methylimidazolium hexafluorophosphate	[BMIM] [PF ₆]
	1-octyl-3-methylimidazolium hexafluorophosphate	[OMIM] [PF ₆]
	1-butyl-3-methylimidazolium bis(trifluoromethylsulfonyl)imide	[BMIM] [Tf ₂ N]
	1-octyl-3-methylimidazolium bis(trifluoromethylsulfonyl)imide	[OMIM] [Tf ₂ N]
	1-ethyl-2-methylpyridinium ethylsulphate	[E ₂ -MPy] [ESO ₄]
	1-ethyl-3-methylpyridinium ethylsulphate	[E ₃ -MPy] [ESO ₄]

4.2.3 Analytical methods

The reducing sugars concentration was determined using the DNS microassay on 3.2.3 (Miller, 1959), absorbance is read at $\lambda=575$ nm (*Hitachi 2000, UV-visible spectrophotometer*), against a glucose or rhamnose calibration curve, according to the sugar released during each specific hydrolytic reaction. In the case of the studies focusing on the immobilization of naringinase using ILs as additives, the reducing sugars concentration was determined using the DNS microassay, measuring the absorbance at 595 nm (*Zenith 3100 spectrofluorimeter*).

The concentration of *p*-nitrophenol released after hydrolysis of 4-NRP and 4-NGP was evaluated spectrophotometrically at 340 nm (*Zenith 3100 spectrofluorimeter*), using a calibration curve of each compound.

The protein content was determined using Bradford assay according to the Bio-Rad protein microassay procedure using a naringinase calibration curve, at 595 nm (*Zenith 3100 spectrofluorimeter*) (Bradford, 1976).

In order to calculate the partition coefficient, the concentration of the flavanones, naringin, prunin, naringenin, was determined by measuring the absorbance at 280 nm using a calibration curve of each flavanone; while the compounds 4-NRP, 4-NGP and 4-nitrophenol were determined at 340 nm (*Hitachi 2000, UV-visible spectrophotometer*).

4.2.4 Naringin solubility

Due to the low solubility of naringin in water several solvents were tested in order to increase substrate solubility. The solvents were chosen according to their dielectric constant. The naringin solubility was assessed through the complete dissolution of 10 μmol of naringin in 50, 100, 200, 400 and 800 μL of pure solvent at 25°C. Within cosolvent systems, the following solvents were tested: propylene carbonate; dimethyl sulfoxide; *N,N*-dimethylmethanamide; *N,N*-dimethylacetamide; methanol; acetonitrile; ethanol; acetone; 1-propanol; 2-propanol; 1-butanol; 2-butanol; 3-methyl-1-butanol; 2-butoxyethanol; tetrahydrofuran; 1,2-dimethoxyethane; 2-methyl-2-butanol; 1,4-dioxane.

4.2.5 Immobilization protocol

Naringinase was immobilized within monolithic and lens-shaped hydrogels. The immobilization protocol is divided into two distinct protocols. A first protocol focuses

mainly on the use of several sol-gel precursors, while the second one consists on the use of ionic liquids as additives of sol-gel.

4.2.5.1 Sol-gel precursors

Immobilization matrices using several sol-gel precursors were made according to the immobilization procedures listed in Table 4.2. The silica sol of matrices A, B, D, E and F was prepared in Eppendorf tubes (1.5 mL). The hydrogel matrices were prepared in a 96 round well plate by mixing the sol (25 μL) with the enzyme solution (25 μL) (Musa *et al.*, 2007). In the case of matrix C the sol was prepared inside the 96 well plate.

Three aging and drying conditions were tested including open air, closed (with parafilm) and half-open (closed with parafilm with a 1 mm hole) at room temperature (Table 4.2).

Table 4.2 Immobilization protocol using several sol-gel precursors.

Matrix	Sol preparation	Gel formation	Aging
A	1) water (70 μL), H^+ (15 μL of 40 mM HCl) 2) TMOS (300 μL) 3) Sonication, 0°C, 1 min	[naringinase] = 0.250 $\text{g}\cdot\text{L}^{-1}$, 20 mM acetate buffer, pH 6	Closed system 4 hours
B	1) water (70 μL), H^+ (15 μL of 40 mM HCl) 2) glycerol (96 mg) 3) TMOS (300 μL) 4) Sonication, 0°C, 20 min	[naringinase] = 0.250 $\text{g}\cdot\text{L}^{-1}$, 20 mM acetate buffer, pH 6	Open air 14 hours
C	1) DGS (55 mg) 2) [naringinase] = 0.250 $\text{g}\cdot\text{mL}^{-1}$, 20 mM acetate buffer, pH 6 3) Sonication, 0°C, 5 min		Open air 14 hours
D	1) water (86 μL), H^+ (48 μL of 40 mM HCl) 2) DGS (55 mg) 3) Sonication, 0°C, 10 min 4) TMOS (280 μL) 5) Sonication, 0°C, 5 min	[naringinase] = 0.250 $\text{g}\cdot\text{L}^{-1}$, 20 mM acetate buffer, pH 6	Open air 4 hours
E	1) water (70 μL), H^+ (15 μL of 40 mM HCl) 2) TMOS (300 μL) 3) Sonication, 0°C, 1 min	[naringinase] = 0.250 $\text{g}\cdot\text{L}^{-1}$, 20 mM acetate buffer, pH 6, 0.8% MTS	Closed system 4 hours
F	1) water (70 μL), H^+ (15 μL of 40 mM HCl) 2) TMOS (300 μL) 3) Sonication, 0°C, 1 min	[naringinase] = 0.250 $\text{g}\cdot\text{L}^{-1}$, 20 mM acetate buffer, pH 6, 0.8% APS	Closed system 4 hours

4.2.5.2 Ionic liquids as additives of sol-gel

Three immobilization methods were established to produce lens shape sol-gel/ILs matrices, where naringinase was encapsulated. Matrices were made according to the immobilization procedures listed in Table 4.3. The silica sol was prepared in an

Eppendorf tube (1.5 mL) and the hydrogel was prepared in a 96 well plate by mixing the sol (25 μL) with the enzyme solution (25 μL). The sol-gel was mixed in a vortex and left in an opened 96 well plate, at room temperature in open air for 14 hours.

Table 4.3 Immobilization protocol within different sol-gel/ILs matrices.

Method	Sol preparation	Gel formation
1	1) IL (30 mg) 2) water (70 μL), H^+ (15 μL of 40 mM HCl) 3) glycerol (96 mg) 4) TMOS (300 μL) 5) Sonication, 0°C, 20 min	[Naringinase] = 0.250 $\text{g}\cdot\text{L}^{-1}$, acetate buffer 20 mM, pH 6.0 (25 μL)
2	1) IL (30 mg) 2) water (70 μL), H^+ (15 μL of 80 mM HCl) 3) glycerol (96 mg) 4) TMOS (300 μL) 5) Sonication, 0°C, 20 min	[Naringinase] = 0.250 $\text{g}\cdot\text{L}^{-1}$, 20 mM acetate buffer, pH 6.0 (25 μL)
3	1) IL (30 mg) 2) water (70 μL), H^+ (15 μL of 80 mM HCl) 3) glycerol (96 mg) 4) TMOS (300 μL) 5) Sonication, 0°C, 20 min	[Naringinase] = 0.500 $\text{g}\cdot\text{L}^{-1}$, 20 mM acetate buffer, pH 6.0 (12.5 μL) + IL solution of 12% w/w, 20 mM acetate buffer, pH 6.0 (12.5 μL)

4.2.6 Matrix properties

The sol-gel matrix adopts the shape of the bottom of the each round well from the 96 well plates during gel formation period leading to a lens shape. The lens diameter (D_m) was determined with a micrometer. The matrix volume (V_m) was determined by Equation 4.1:

$$V_m = \frac{(V_t - V_{es})}{n_m} \quad (4.1)$$

where V_t is the total volume of the system (matrices + external solvent), V_{es} is the external solvent volume and n_m is the size of the matrices sample; experiments were carried out in a volumetric flask containing 8 matrices by adding water to a total volume of 1 mL. The matrix density (d_m) is the ratio between matrix mass (w_m) and matrix volume. The internal solvent volume (V_{is}) was determined through air drying of 8 matrices to a constant weight. The weight decrease of each matrix, after evaporation, corresponded to the internal solvent.

The partition coefficient ($P_{m/s}$) of substrates and products was the ratio of the compound concentration between matrices and external solvent and was estimated according to Equation 4.2 (Fukui *et al.*, 1987).

$$P_{m/s} = \left(\frac{c_0 - c}{c} \right) \left(\frac{V_{es}}{V_t - V_{es}} \right) \quad (4.2)$$

c_0 and c are the initial and final concentration of certain compound. It was calculated the $P_{m/s}$ of the following compounds: naringin, prunin, naringenin, 4-NRP, 4-NGP and 4-nitrophenol in 40 mM acetate buffer at pH 4.0. In the case of naringenin due to its low water solubility a 10% hydroethanol solution was used. The experiments were carried out in 96 well plates. A 0.5 mM solution (50 μ L) of each compound, under study, was added to each well with one matrix. After 30 minutes samples were taken and the compound concentration was measured.

4.2.7 Scanning electron microscopy (SEM)

The structure of the matrices was observed using scanning electron microscopy - field emission gun (FEG-SEM). Surfaces of the samples were examined using SEM with a JEOL JSM-7001F FEG-SEM operating at 5.0 kV. The surfaces were previously sputter-coated with a gold layer 20 nm thick to avoid charging effects during observation.

4.2.8 Activity measurement

4.2.8.1 Naringinase immobilized using several so-gel precursors

During the optimization of naringinase immobilization using several sol-gel precursors, the naringinase activity was measured using a 3.91 mM naringin solution (1.00 mL) as substrate in 20 mM acetate buffer at pH 4.0. For the free enzyme assay, a 250 mg L⁻¹ enzyme solution (150 μ L) in 20 mM acetate buffer pH 4.0 was added to the naringin solution; in the immobilized enzyme assay, six matrices were added. The amount of either free or immobilized enzyme corresponded to an enzyme content of 37.5 μ g in the reaction mixture. The reaction took place in a 24 well plate that was placed inside an agitated thermostatic bath at 45.0 °C and 200 rpm for 60 min. The enzyme specific activity was measured using the DNS assay by determining the concentration of the reducing sugars in the collected aliquots during the first 60 min of the reaction. After collecting samples the reaction was immediately stopped, lowering the temperature of

solutions below 0 °C. The activity of naringinase for the bioconversion of naringin was calculated by linear regression of the first data-points. The hydrolysis of naringin into naringenin liberates one molecule of rhamnose followed by one of glucose (both reducing sugars).

4.2.8.2 Biocatalysis with immobilized naringinase using organic solvents

The activities of α -L-rhamnosidase and β -D-glucosidase expressed by naringinase enzyme complex were respectively evaluated using 0.20 mM of 4-NRP and 4-NGP, in 20 mM acetate buffer at pH 4.0. A naringinase concentration of 31.3 mg L⁻¹ was used in these experiments. In the immobilized enzyme assay, only one matrix was used per each well of a 96 flat well plate (200 μ L). The amount of either free or immobilized enzyme, in the reaction mixture, was 6.25 μ g. The enzymatic reaction was followed spectrophotometrically (*Zenith 3100* spectrofluorimeter). Absorbance was measured every 1 min, during 30 min at 30.0 °C. The enzyme activities of α -L-rhamnosidase and β -D-glucosidase expressed by naringinase were calculated by linear regression on the first data-points during the initial 30 min reaction time.

In the case of bioconversion studies within cosolvent systems, naringin bioconversion studies were carried out in standard solutions of naringin in 20 mM acetate buffer at pH 4.0, at 45 °C, using 250 mg L⁻¹ of free naringinase. The naringin concentration varied from 0.30 to 3.0 mM in the aqueous system and to 30 mM in the aqueous cosolvent systems. The activity of naringinase for the bioconversion of naringin was calculated by first order polynomial regression data fit of the initial data, collected every 1 min during 10 min.

4.2.8.3 Sol-gel immobilization of enzyme using ILs as additives

In the studies concerning the use of ILs as additives the activities of α -L-rhamnosidase and β -D-glucosidase expressed by naringinase for the respective hydrolysis of 4-NRP and 4-NGP, were determined as described on the previous point (4.2.8.2).

In the case of bioconversion studies using ILs as additives of sol-gel, the studies were carried out using the substrates naringin and prunin. In these experiments naringin was hydrolyzed only into prunin, because β -D-glucosidase was inactivated according to the conditions described on Chapter 2. The naringin hydrolysis was carried out in standard solutions in 20 mM citrate buffer at pH 3.3 and prunin hydrolysis in 20 mM acetate

buffer at pH 4.0. The naringin concentration varied from 1.5 to 12.0 mM while prunin varied from 0.8 to 6.4 mM. In both cases the hydrolytic reaction took place in a 96 well plate (200 μL), at 50.0 $^{\circ}\text{C}$. A naringinase concentration of 31.3 mg L^{-1} was used in free enzyme studies. An enzyme amount of 6.25 μg in the reaction mixture was used in both free and immobilized system. The activity of $\alpha\text{-L-rhamnosidase}$ and $\beta\text{-D-glucosidase}$ for the respective hydrolysis of naringin and prunin was calculated by first order polynomial regression data fit of the initial data, collected every 10 min during 90 min. The Michaelis-Menten model (Equation 1.1) was used to fit the experimental data, concerning the bioconversion of naringin and prunin. The fit was carried out through non-linear regression by minimising the residual sum of squares between the experimental data points of the initial rate *vs.* substrate concentration and those estimated by the model, using Solver add-in from Microsoft Excel 2003 for Windows XP, considering the following options: Newton method; 100 iterations, precision of 10^{-6} , 5% of tolerance and 1×10^{-4} convergence. The kinetic parameters estimated by Lineweaver-Burk linear regression (Equation 1.4) were used as initial values of this non-linear curve-fit program. The non-linear regression parameters were constricted to positive numbers. Following this methodology, the catalytic constants, k_{cat} , were determined according to Equation 1.5.

4.2.9 Naringinase biochemical properties

The influence of pH on the naringinase specific activity can be described by Equation 1.44. The naringinase activity pH profiles were obtained through non-linear regression by minimizing the residual sum of squares between the experimental data points of the naringinase specific activity *vs.* pH and those estimated by the model. The Solver add-in from Microsoft Excel 2003 for Windows XP was used with the following options: Newton method; 100 iterations, precision of 10^{-6} , 5% of tolerance and 10^{-4} of convergence. The optimum experimental pH values were used as initial parameters of the non-linear regression and no constraints were used. Optimum pH values were then determined from Equation 1.45.

4.2.10 Immobilization yield

The immobilization yield, y was determined following Equation 4.3 where w_{Eimm} and w_{Et} are the amount of enzyme entrapped within sol-gel and the total initial amount of enzyme, respectively.

$$y = \frac{w_{\text{Eimm}}}{w_{\text{Et}}} \times 100 \quad (4.3)$$

w_{Et} corresponds to the total amount of enzyme (25 μL of a 250 mg L^{-1} naringinase solution, 6.25 μg) that was placed inside each well of the microplate to produce each biocatalyst. w_{Eimm} represents the difference between the total amount of enzyme and the enzyme present in the buffer (2x25 μL of a 20 mM acetate buffer at pH 4.0) that was used to wash each matrix. The 100% yield is defined as if the total amount of naringinase is immobilized (no naringinase recovered in the washing buffer). The concentration of protein in the enzyme solution was determined before and after immobilization in the supernatant and the effluent of the washing steps. The amount of protein in solution was evaluated by the Bradford method. Naringinase activity in the washing buffer was assessed by adding naringin to the buffer to a final concentration of 3.91 mM.

4.2.11 Immobilization efficiency

The efficiency coefficient (η) was determined according to Equation 4.4 where v_{imm} and v_{free} refer to the rates of the reaction catalyzed by the immobilized and free enzyme, respectively (Tischer and Kasche, 1999):

$$\eta = \frac{v_{\text{imm}}}{v_{\text{free}}} \quad (4.4)$$

4.2.12 Operational stability

To test the stability of immobilized naringinase within the studying conditions, three different operational stability protocols were established: a first one covering the optimization of the immobilization of naringinase using several sol-gel precursors, a second one focused on the biocatalysis with immobilized naringinase using organic solvents and a third and last one concerning the use of ILs as additives of sol-gel used to immobilized naringinase.

4.2.12.1 Naringinase immobilized using several sol-gel precursors

To test the stability of the encapsulated naringinase, the sol-gel matrices were used several times for the hydrolytic reaction, which was conducted in 20 mM acetate buffer at pH 4.0. After each run of 1 hour, the matrices were separated and washed with acetate buffer pH 4.0. The reaction medium was then replaced with fresh medium. The activity of the freshly prepared matrices in the first run was defined as 100% (A_0).

The enzyme inactivation kinetics of naringinase during successive reuses was described by both biphasic inactivation (Equation 1.47) and single-step first-order inactivation (Equation 1.48). First-order inactivation rate constants (k_1 and k_2) and the α_1 parameter were then determined by non-linear regression, minimizing the residual sum of squares between the experimental data points of the residual activity vs. runs and those estimated by the model. The Solver add-in from Microsoft Excel 2003 for Windows XP was used with the following options: Newton method; 100 iterations, precision of 10^{-6} , 5 % tolerance and 1×10^{-4} of convergence. The first-order inactivation rate constant obtained from linear regression of $\ln A_r$ vs. t was used as the initial value for the non-linear regression k_1 parameter. The non-linear regression parameters were restricted to positive numbers.

The reuse half-life ($t_{1/2}$) of the biocatalyst was determined according to the models fitted to the inactivation profiles. When the model used was Equation 1.48, the reuse half-life was determined using Equation 1.49. In other cases the reuse half-life was determined by interpolation or extrapolation.

4.2.12.2 Biocatalysis with immobilized naringinase using organic solvents

The activity and stability of α -L-rhamnosidase and β -D-glucosidase expressed by soluble and sol-gel immobilized naringinase were evaluated, in several aqueous cosolvent systems using several solvent concentrations.

Firstly, a primary solvent screening according to the effect over α -L-rhamnosidase and β -D-glucosidase expressed by free naringinase was carried out. An inactivation protocol was established in order to study the selective stability of α -L-rhamnosidase and β -D-glucosidase expressed by naringinase enzyme complex. Enzyme inactivation assays were followed in 20 mM acetate buffer at pH 4.0, using 0, 2.5, 5 and 10 % (v/v) of cosolvent, at 65 °C and 80 °C, respectively for β -D-glucosidase and α -L-rhamnosidase of soluble naringinase. In this first case an enzyme concentration of 625 mg L⁻¹ were

used in 20 mM acetate buffer at pH 4.0, with 5 % (v/v) of cosolvent, during 30 minutes at 65 °C and 80 °C, respectively, and aliquots were collected during 4 hours. The activity of non deactivated soluble naringinase (A_0) was used as the reference (100% activity).

In the second case, the immobilized naringinase was used for periods of 30 minutes under the above mentioned inactivation conditions during a total of six hours. After each inactivation period the matrices were washed and its activity was measured. The enzyme activity (A_0) of freshly prepared matrices before the first inactivation run was defined as 100 %.

The enzyme inactivation kinetics of both α -L-rhamnosidase and β -D-glucosidase, during successive reuses was described by both biphasic inactivation (Equation 1.47) and single-step first-order inactivation (Equation 1.48). The inactivation rate constants (k_1 and k_2) and the α_1 parameter, according to the model adjusted, were determined through non-linear regression by minimising the residual sum of squares between the experimental data points of the residual activity vs. runs and those estimated by the model, using Solver add-in from Microsoft Excel 2003 for Windows XP, considering the following options: Newton method; 100 iterations, precision of 10^{-6} , 5 % of tolerance and 1×10^{-4} convergence. The first-order inactivation rate constant obtained from linear regression of $\ln(A_r)$ vs. t was used as initial values of the non-linear regression k_1 parameter. The non-linear regression parameters were constricted to positive numbers.

The reuse half-life time of the biocatalyst was determined according to the models fitted to the inactivation profiles. When the model used was Equation 1.48, the reuse half-life is determined by Equation 1.49. In other cases the reuse half-life was determined by interpolation or extrapolation.

4.2.12.3 Immobilization of naringinase using ILs as additives

To test the stability of the encapsulated naringinase, the sol-gel/ILs matrices were used fifty times for the hydrolytic reaction, in 20 mM acetate buffer at pH 4.0. After each run of 20 minutes the matrices were separated and washed with 20 mM acetate buffer at pH 4.0. The reaction medium was then replaced by fresh medium. The activity and stability of α -L-rhamnosidase and β -D-glucosidase expressed by soluble and sol-gel immobilized naringinase were evaluated on the hydrolysis of 4-NRP and 4-NGP.

4.2 Results and discussion

The results of this study about the immobilization of naringinase within silica glasses through sol-gel method are divided into three main parts: a first one covering the optimization of the immobilization of naringinase using several sol-gel precursors, a second one focused on the biocatalysis with immobilized naringinase using organic solvents and a third and last one concerning the use of ILs as additives of sol-gel used to immobilize naringinase.

4.3.1 Optimization of naringinase immobilization using several sol-gel precursors

Initial immobilization studies were related to sol preparation and gel formation.

In the sol preparation both the basic and acidic hydrolysis of TMOS were tested using HCl and NaOH, respectively. TMOS acid catalysis performed better than basic catalysis for immobilization of naringinase. In the later case, naringinase was easily leached from the matrices. Basic catalysis increased the pore diameter via fast condensation, which occurred simultaneously with hydrolysis.

The sonication time period, which is the period needed to form one layer of sol was optimized, once the sonication period influences the pore size, with longer periods making smaller pores (Roux *et al.*, 1997).

The monolith size and buffer/sol ratio were also studied. Initially the matrices were prepared with a conical shape. These particles had volumes around 0.10, 0.50 or 2.00 mL. When they were used in naringin bioconversion, we observed an increase in naringinase activity with decreasing diameter. In order to increase naringinase activity, the monoliths were produced inside 96 round well plates, making lens-shaped monoliths with an average volume of 0.05 mL. In this situation a higher naringinase activity was recorded, which is consistent with a reduction of mass-transfer impedance due to the higher surface-area/volume ratio, as observed by Tischer and Kashe (1999). In order to avoid enzyme inactivation by methanol release, various buffer/sol ratios were assayed, namely 6:1, 3:1, 2:1 and 1:1. However, the higher ratio matrices were fragile and the enzyme was readily released.

After these initial studies, an optimization process was performed by varying the following parameters: aging time, sol-gel precursor, buffer solution pH, enzyme concentration and drying conditions during aging. In addition, the performance of the

bio-immobilizates was evaluated according to the immobilization yield, efficiency and operational stability.

4.3.1.1 Effect of aging time and sol-gel precursors

The hydrogel aging and drying led to gel densification with increased strength but low pore size due to gel shrinking, which was probably responsible for mass transfer impedance (Gill and Ballesteros, 2000). During aging the wet silica shrinks up to 85%, resulting in a decrease of pore size from 200 nm to 2 – 20 nm depending on the extent of drying (Jin and Brennan, 2002). The pore size must be sufficiently large to allow molecules and ions to diffuse into the matrix and small enough to prevent entrapped biomolecules from leaching (Tischer and Kasche, 1999; Jin and Brennan, 2002; Pollard and Woodley, 2007). Therefore aging is critical to control enzyme loss and substrate entrance. A 24 h aging period was initially used, but it was excessive leading to the gel shrink and cracking. The minimum time needed for the gel formation for all matrices was the time of four hours. Following this, two aging times were studied: 4 h and 14 h. The TMOS used in matrix A was modified to be a more biocompatible by transesterification with glycerol in matrix B and by using DGS in matrix C (Brook *et al.*, 2004b) (Figure 4.1). The use of poly(glyceroxysilane) precursors may prevent pore collapse due to its low water content, and the slow release of glycerol during aging acting as a drying-control additive (Gill and Ballesteros, 2000). Using diglycerylsilane as the sol-gel precursor prevented methanol production during the hydrolysis step that may be toxic for naringinase. In this work, the buffer/DGS ratio was minimized leading to harder matrices when compared to Brook *et al.* (2004b) work. In matrix D, both DGS and TMOS were used (Figure 4.1).

Alkyl-alkoxysilanes, as methyltrimethoxysilane (MTS) and 3-aminopropyltrimethoxysilan (APS), were used in matrices E and F (Figure 4.1), respectively, to modulate the ionic environment, surface tension and diameter of the pore, focusing on decreasing mass-transfer rates (Gill and Ballesteros, 2000). The influence of aging time and sol-gel precursor on the immobilization efficiency was studied for five consecutive reutilizations (Figure 4.1). To compare the different sol-gel matrices and find the best ones to be used in further optimization studies, we considered the immobilization efficiency of naringinase during the fifth run (Figure 4.1). The best efficiency was achieved with naringinase immobilized within matrix D (TMOS/DGS)

aged for 4 h. A significant statistical difference ($p < 0.05$) between other matrices was observed, exception to matrix A (TMOS) aged for 4 h, B (TMOS /glycerol) aged for 14 h and C (DGS) aged for 14 h. After five consecutive runs matrices B, C and F aged for longer periods (14 h) had higher efficiency than those with shorter aging times (4 h). These results indicate that the enzyme retention in these matrices was increased with aging and may be due to a decrease of pore size. In the case of matrix F, the enzyme may have formed a peptide bond via the amino group on APS and a carboxylate moiety on naringinase. This may have also reduced enzyme activity.

On the other hand, matrices A and D showed higher efficiency with less aging. In this case, 14 h was probably too long and caused excessive pore shrinkage compromising mass transfer. This was consistent with the lower efficiency obtained in the first run of A and D aged for 14 hours compared to 4 h (Figure 4.1).

In conclusion, the best matrices were A (aged for 4 h), B (aged for 14 h), C (aged for 14 h) and D (aged for 4 h).

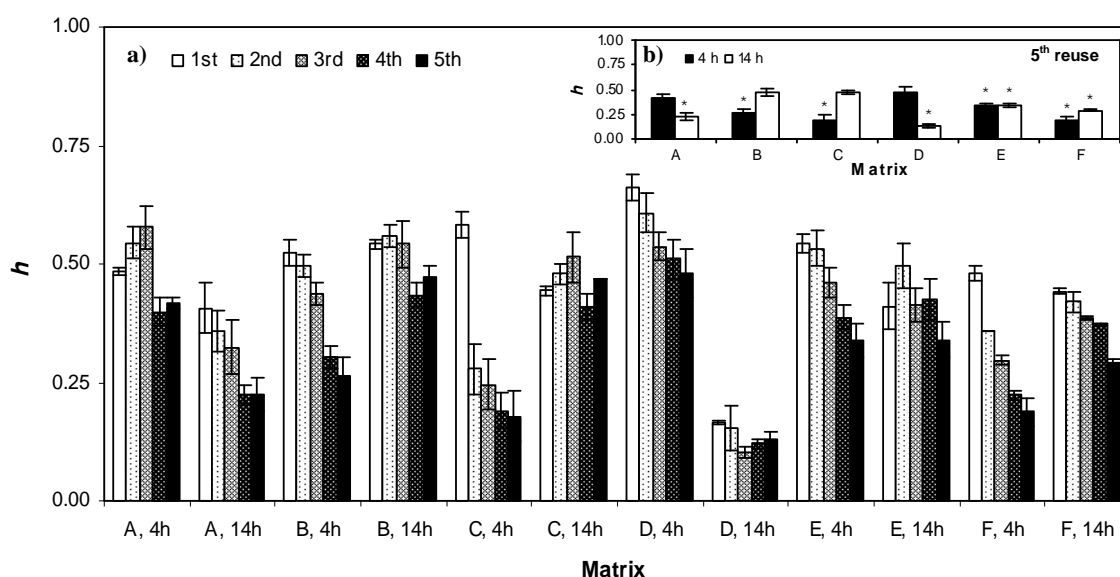


Figure 4.1 Influence of the aging time on the immobilization reuse efficiency coefficient of the sol-gel matrices, A – F; for five runs (a) (mean value \pm SD, $n = 3$) and after five runs (b) (mean value \pm SD, $n = 3$, * $p < 0.05$ vs. matrix D-4h, independent two-tailed Student T-test).

4.3.1.2 Influence of TMOS/DGS ratio in matrix D

Once matrix C (made from DGS) became too fragile, it was combined with TMOS to improve its strength. Matrix D was produced from different ratios of DGS and TMOS. Preliminary studies showed different reuse efficiencies among these matrices. The influence of the TMOS/DGS ratio on the reuse efficiency was studied (Figure 4.2). The

TMOS/DGS ratio significantly influenced the naringinase efficiency after the fifth use. The optimum ratio of 5:1 (w/w) caused the highest efficiency after the fifth run (Figure 4.2). In further studies this ratio was used to maximize the efficiency of matrix D.

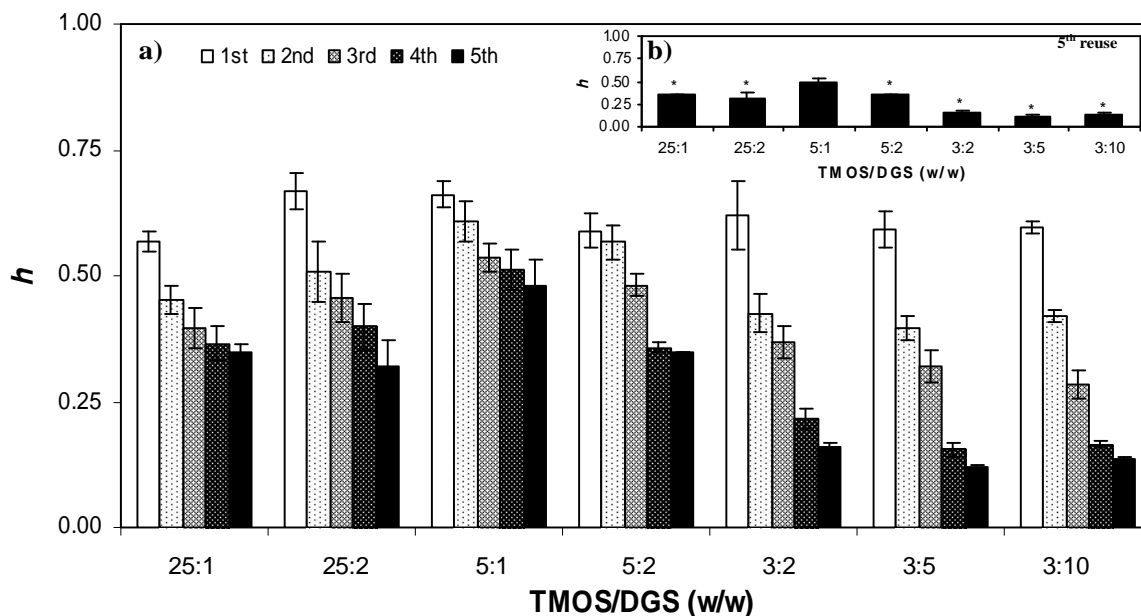


Figure 4.2 Influence of the TMOS/DGS ratio on the immobilization reuse efficiency coefficient of the sol-gel matrix D; for five runs (a) (mean value \pm SD) and after five runs (b) (mean value \pm SD, $n = 3$, * $p < 0.05$ vs. 5:1 (w/w), independent two-tailed Student T-test).

4.3.1.3 Effect of pH on gel formation

Gel formation occurs due to a pH change after the addition of a buffer solution to the sol. This buffer solution must have a pH high enough to ensure gel formation but low enough to preserve naringinase activity. Some low pH values were initially tested but a consistent gel was only obtained when pH was higher than pH 4.0 using TMOS as the only precursor. In bioconversion trials, free naringinase showed activity at pH below 6.0, so a range of 4.0 – 6.0 was chosen to study the effect of pH. In addition, other authors had described a higher gel formation rate between pH 4.0 and 6.0 (Brook *et al.*, 2004b).

In Figure 4.3 the influence of pH on naringinase immobilization efficiency is shown. Choosing the pH 6.0 value as a reference for gel formation of each matrix, significant statistical differences ($p < 0.05$) were observed between gels formed at pH 6.0 and other pH values. The highest efficiency was achieved at pH 6.0.

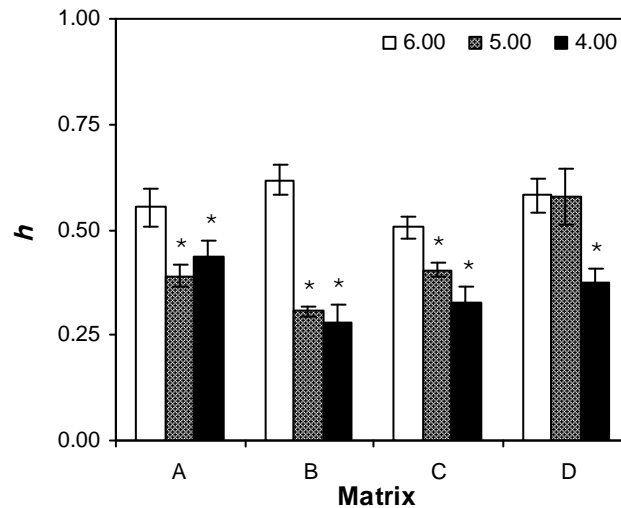


Figure 4.3 Influence of pH on the immobilization efficiency coefficient of the sol-gel matrices A – D (mean value \pm SD, $n = 3$, * $p < 0.05$ vs. pH 6.0, independent two-tailed Student T-test).

4.3.1.4 Influence of naringinase concentration

Immobilization efficiency decreased with increasing naringinase concentration (Figure 4.4). Internal mass-transfer limitations may have occurred at high naringinase concentrations, since the specific activity remained constant within the naringinase concentration range used.

The high efficiency observed with lower naringinase concentrations and the statistical analysis in Figure 4.4 led us to choose 0.25 g L^{-1} of naringinase for subsequent studies.

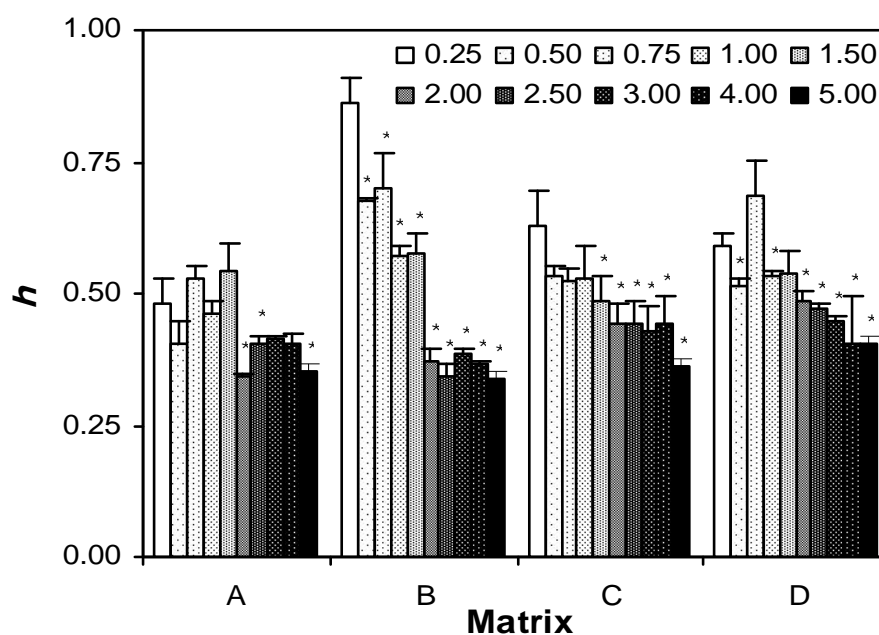


Figure 4.4 Influence of the naringinase concentration on the immobilization efficiency coefficient of the sol-gel matrices A – D (mean value \pm SD, $n = 3$, * $p < 0.05$ vs. $[E] = 0.25 \text{ g L}^{-1}$, independent two-tailed Student T-test).

4.3.1.5 Drying conditions during aging

The drying conditions during aging influence solvent loss and may influence the biocatalyst activity. Matrix B showed the highest efficiency (Figure 4.4) and was chosen for a further study. In this system three aging/drying conditions were tested, namely: open air, closed and half-open. The effect of drying conditions on matrix B reuse efficiency is shown on Figure 4.5a. After the second reutilization no protein was detected in the liquid phase. The activity data and inactivation models fitted to the data points are presented in Figure 4.5a. The inactivation profile of naringinase in the sol-gel open air and the half-open system could be well described by a first-order inactivation model. A considerably higher operational stability with a half-life of 6.5 h was observed for naringinase in the half-open system. This value was more than two folds the value obtained for naringinase in the closed system, which has an exponential decay with a first-order inactivation constant of 0.19 h^{-1} (Table 4.4).

The higher naringinase operational stability occurred in the open system, which showed the best result. During the 23 consecutive runs, no loss of activity was observed, theoretically resulting in an infinite half-life. The matrices produced in the three different systems had different diameters ($p < 0.05$, One Way ANOVA) (Figure 4.5b). For matrix B, faster drying conditions caused a reduction in the diameter of the monoliths (Table 4.4). Comparison of the diameter of the B matrices with their half-lives (Table 4.4) indicates that half-life decreases with a monolith diameter increase. To better understand this process the structure of the matrices was analyzed using SEM. SEM micrographs of TMOS plus glycerol gels made with different drying conditions showed similar porosity around 20-30 nm (Figure 4.5c).

The hydrogel aging process was an efficient method for increasing operational stability. After hydrolysis the TMOS solution still contains some methanol that may be detrimental to the enzyme activity. The slower the evaporation rate, the longer the exposure of the enzyme to the methanol, which would promote protein denaturation and may explain the lower half-lives obtained for the matrices that were aged in half-open and closed containers.

Subsequently, matrices were aged in open containers except for matrix A, which cracked under these conditions.

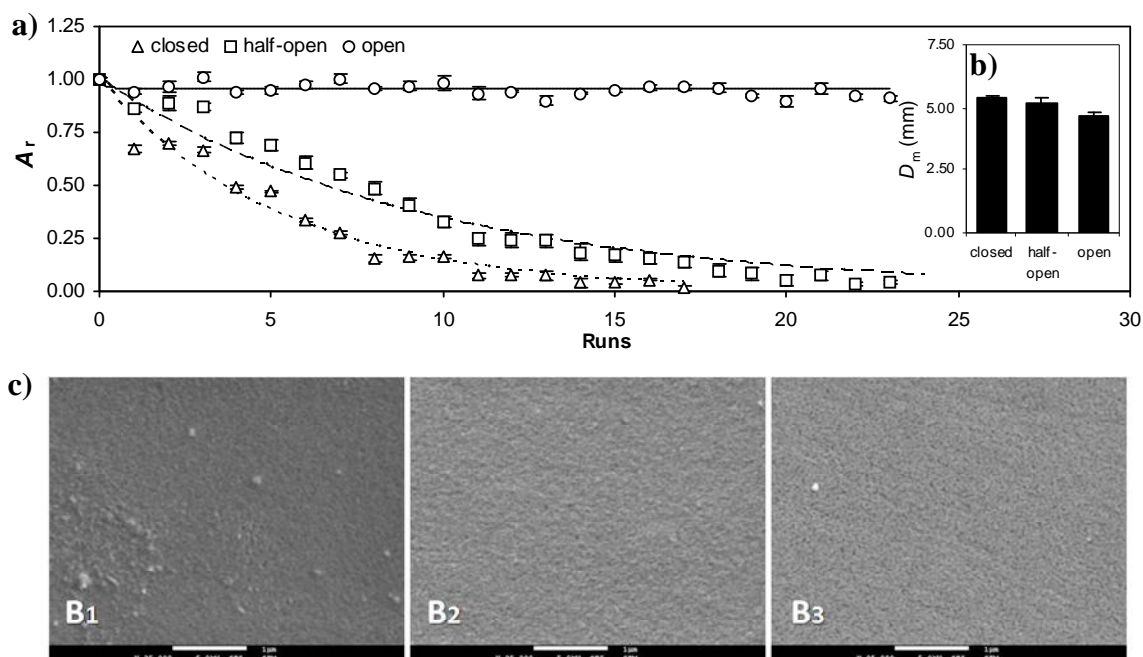


Figure 4.5 a) Influence of the aging system (open-air, half-open and closed) on the naringinase residual activity of the sol-gel matrix B, after 23 successive runs (mean value \pm SD, $n = 3$) and **b)** diameter (mean value \pm SD, $n = 3$). **c)** SEM microphotographs of the sol-gel matrices (TMOS/glycerol) obtained under different conditions [closed (B₁), half-open (B₂) and open-air (B₃)] for encapsulated naringinase. The bar represents 1 μ m.

Table 4.4 Characterization of matrix B according to the aging system used.

Aging system	Immobilization efficiency	D_m (mm)	$t_{1/2}$ (h)	kinetic parameters	R^2
Closed	0.67 ± 0.01	5.44 ± 0.02	3.64 ± 0.11	$k_1 = 0.19 \text{ h}^{-1}$	0.97
Half-opened	0.72 ± 0.01	5.19 ± 0.07	6.40 ± 0.20	$k_1 = 0.11 \text{ h}^{-1}$	0.99
Opened	0.72 ± 0.01	4.71 ± 0.06	∞	-	-

Mean value \pm SD, $n = 3$.

4.3.1.6 Immobilization characterization

Matrix properties

All four matrices (A – D) showed mechanical resistance in buffer solution and did not compact during the reutilization assays. According to Figure 4.6a and Table 4.5, a small decrease in monolith diameter caused a large decrease in volume. Matrix B had the smallest diameter and the highest density and surface area/volume ratio, followed by matrix D (Table 4.5). Figure 4.6b demonstrates the lens-shape of the four matrices studied.

The partition coefficient of the flavanones, naringin and naringenin were determined according to Equation 4.2 (Table 4.5). The partition coefficient of naringin increased with the efficiency coefficient. Theoretically, matrix A was the less hydrophilic which was made from TMOS, comparing to matrix B (TMOS/glycerol) and matrix D (TMOS/DGS). According to Brook *et al.* (2004a), glycerol in matrix B would have been washed from the gel, while in matrix D, some diglycerylsilane would have remained inside the monolith making it more hydrophilic. These gel characteristics may have influenced the partition coefficient of naringin affecting consecutively the efficiency of each matrix, leading to the conclusion that a more hydrophilic matrix would be more efficient on decreasing internal mass-transfer effects (Tischer and Kasche, 2009).

Table 4.5 Properties of matrices A – D and naringinase efficiency.

Matrix	D_m (mm)	V_m (μL)	d_m ($\text{g}\cdot\text{mL}^{-1}$)	$P_{m/s}$ naringin	$P_{m/s}$ naringenin	η
A	5.77 ± 0.02	46.0	0.67	0.65 ± 0.06	0.77 ± 0.14	0.66 ± 0.04
B	4.71 ± 0.02	23.3	0.89	0.68 ± 0.15	0.65 ± 0.08	0.72 ± 0.01
C	6.02 ± 0.08	60.4	-	-	-	1.07 ± 0.02
D	5.51 ± 0.06	31.1	0.86	0.97 ± 0.10	0.80 ± 0.04	0.76 ± 0.01

Mean value \pm standard deviation, $n = 3$.

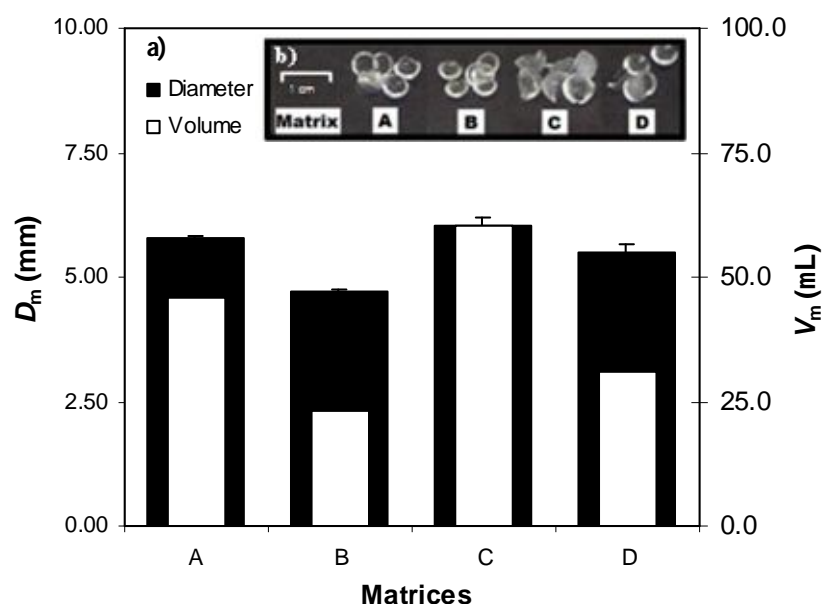


Figure 4.6. a) Diameter and volume of matrices: A – D (mean value \pm SD, $n = 3$). b) Photo of matrices: A – D.

Effects of temperature and pH on naringinase activity

The naringinase temperature profile was studied between 40.0 and 80.0 °C and the optimum activity was recorded around 70 °C (Figure 4.7a) for free naringinase as well as for immobilized naringinase within the four matrices. According to this, these sol-gel monoliths do not seem to protect naringinase against heat-inactivation, which is similar to the results obtained by Bernardino *et al.* (2009) with penicillin acilase immobilized onto sol-gel microcapsules; in opposition to dry-aged sol-gels where the optimum temperature is shifted towards higher temperatures (Jin and Brennan, 2002). In this last case, the enzyme native state is favoured in dry-aged gels due to gel restriction, increasing its thermal stability (Jin and Brennan, 2002).

The optimum temperature around 70 °C for the hydrolysis of naringin into naringenin by naringinase in sol-gel matrices increases the potential for immobilized naringinase to be used on an industrial scale where higher temperatures are used to reduce the viscosity of the bioreaction medium and also improving naringin solubility.

The pH profile was studied between 3.5 and 6.0 (Figure 4.7b) and the optimum pH was found to be 4.3 (Table 4.6) for free naringinase.

The student T-test showed that there was no statistical difference between the optimum pH values for free naringinase and naringinase immobilized in the four matrices A – D (Table 4.6). This may have been due to the small matrix size or the high buffer capacity (Tischer and Kasche, 1999). A maximum naringinase specific activity of 0.86 $\mu\text{mol min}^{-1} \text{mg}^{-1}$ was obtained for naringinase immobilized within matrices A and D, with similar pK_1 and pK_2 at an optimum pH of 4.3 ± 0.1 (Table 4.6).

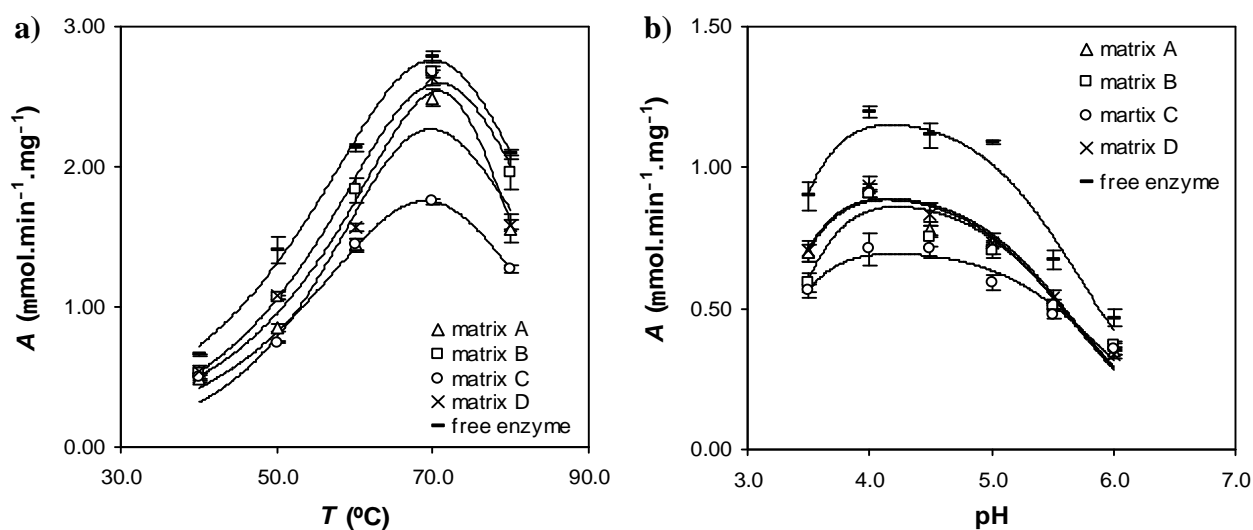


Figure 4.7 a) Temperature profile of free and immobilized naringinase in sol-gel matrices: A – D (mean value \pm SD, $n = 3$). **b)** pH profile of free naringinase and naringinase immobilized within sol-gel matrices: A – D (mean value \pm SD, $n = 3$).

Table 4.6 Optimum pH values of the sol-gel matrices A – D.

	pH _{opt}	Non-linear parameters	R ²
Matrix			
A	4.4 ± 0.1	A _{max} = 0.82, pK ₁ = 3.1, pK ₂ = 5.7	0.84
B	4.4 ± 0.2	A _{max} = 0.68, pK ₁ = 2.8, pK ₂ = 5.9	0.91
C	4.3 ± 0.1	A _{max} = 0.85, pK ₁ = 2.9, pK ₂ = 5.7	0.91
D	4.3 ± 0.1	A _{max} = 0.86, pK ₁ = 2.9, pK ₂ = 5.7	0.95
Free enzyme	4.3 ± 0.1	A _{max} = 1.11, pK ₁ = 2.9, pK ₂ = 5.7	0.93

Mean value ± SD; n = 3; * p < 0.05 vs. free enzyme; independent two-tailed Student T-test

Immobilization yield and efficiency

During the immobilization procedure a very low naringinase loss occurred in all the four matrices tested, leading to an immobilization yield higher than 82% for all of them (Figure 4.8), calculated according to Equation 4.1. The best immobilization yield was 92% in the case of matrix D, although there was no statistical difference between each matrix ($p > 0.05$, One Way ANOVA).

The naringinase immobilization efficiency coefficients of the four matrices A – D were high (> 0.70), which is consistent with reduced mass transfer effects (Figure 4.8). A significant statistical difference existed between the efficiency coefficients of these matrices. Matrix C showed a very high efficiency compared to the other three matrices, possibly because naringinase native state is better preserved in matrix C, which was produced without alcohol formation during gel formation.

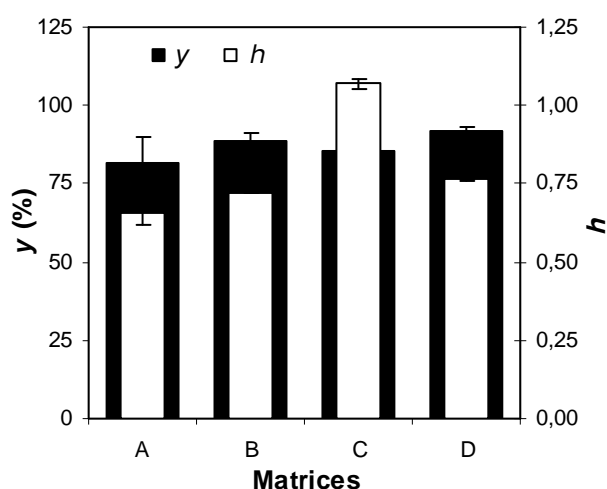


Figure 4.8 Yield and efficiency of immobilized naringinase within matrices: A – D (mean value ± SD, n = 3).

4.3.1.7 Operational stability

All matrices tested (A – D) were able to retain naringinase activity over repeated uses (Figure 4.9a). The structure of these matrices was observed using SEM. Figure 4.9b shows SEM micrographs of matrices A (TMOS), B (TMOS/glycerol), C (DGS) and D (TMOS/DGS). Matrices A and C showed a coarser structure with a porosity around 100 nm, while the structure of matrices B and D was finer showing a porosity of 20-30 nm.

The inactivation model of Henley and Sadana (1985) (Equation 1.47) fits well to the experimental data in the case of matrices A, C and D (Figure 4.9a, Table 4.7). Among these matrices, D was by far the best matrix, showing a reduced loss of activity with a half-life time of 115 h (Table 4.7).

Matrix B had no detectable loss of activity after 50 successive reutilizations, theoretically showing an infinite half-life time (Table 4.7). In fact, matrix B seemed to protect naringinase from heat inactivation to some extent, since the thermal inactivation of free naringinase under these reaction conditions had a half-life of 169 h. This operational stability study showed outstanding behaviours of matrices D and especially B, with very long half-life times, high efficiency (72% and 76%, respectively) and high immobilization yields around 90% (Table 4.7).

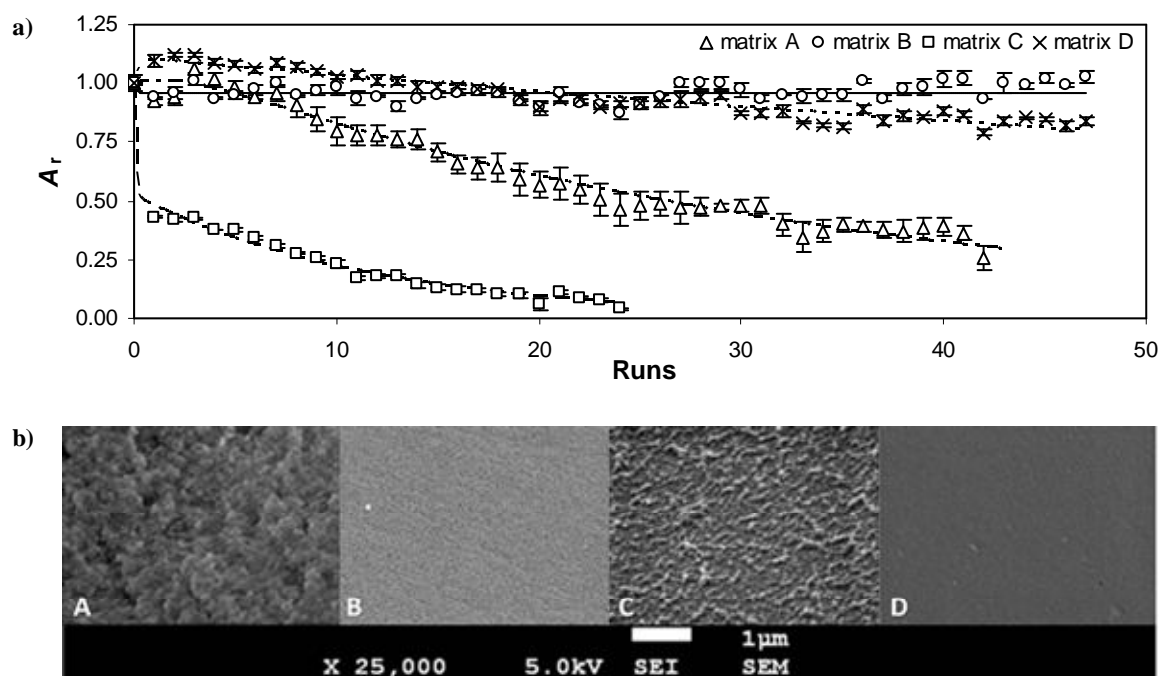


Figure 4.9 a) Residual activity of naringinase after several reutilization runs of the sol-gel matrices: A – D (mean value \pm SD, $n = 3$). b) SEM micrographs of the sol-gel matrices: A – D with encapsulated naringinase. The bar represents 1 μm .

Table 4.7 Yield, efficiency and operational stability characterization of sol-gel matrices, A–D.

Matrix	y (%)	η	$t_{1/2}$ (h)	kinetic parameters	R^2
A	82 ± 8	0.66 ± 0.04	26.4 ± 7.1	$\alpha_1 = 1.81, k_1 = 0.0314 \text{ h}^{-1}, k_2 = 0.46 \text{ h}^{-1}$	0.97
B	89 ± 2	0.72 ± 0.01	∞	-	-
C	85 ± 6	1.07 ± 0.02	0.62 ± 0.12	$\alpha_1 = 0.52, k_1 = 14.0 \text{ h}^{-1}, k_2 = 0.085 \text{ h}^{-1}$	0.99
D	92 ± 2	0.76 ± 0.01	115 ± 9	$\alpha_1 = 60, k_1 = 0.0069 \text{ h}^{-1}, k_2 = 3.88 \text{ h}^{-1}$	0.91

Mean value \pm SD, $n = 3$.

4.3.2 Biocatalysis with immobilized naringinase using organic solvents

In order to overcome the low solubility of naringin in aqueous media (0.50 g L^{-1} at 20°C ; Pulley, 1936) which limits the productivity and yield of the enzymatic bioconversion, several approaches based on biphasic and cosolvent systems were studied.

4.3.2.1 Biphasic systems

Towards the use of liquid–liquid biphasic conditions for naringin biocatalysis, a selection of different solvents was carried out according to their $\log P$ values and functionality. The following solvents were tested with the purpose to increase naringin solubility: octane and n-hexane were representative of unbranched alkanes; cyclohexane of cyclic alkanes; 1-octanol, 2-octanol and 1-hexanol of alcohols; toluene and anisole of aromatic compounds; ethylic ether of ethers; ethyl acetate of esters; carbon tetrachloride and chloroform of halogenated solvents. Unsatisfactory results were afforded due to the low solubility of naringin in these non-polar solvents, despite its low solubility in water. The biphasic design system was excluded from the bioprocessing of naringin.

4.3.2.2 Aqueous cosolvent systems

Another approach to enhance naringin concentration is the use of water cosolvent systems, which were tested according to solvents relative permittivity. The main goal consists on maximizing naringin dissolution in the aqueous system, keeping naringinase with a high retention activity and stability.

Table 4.8 presents several organic solvents tested, the respective dielectric constant and naringin solubility. Naringin showed a low solubility ($< 12.5 \text{ mM}$) in the following

organic solvents: acetonitrile, 3-methyl-1-butanol and 2-methyl-2-butanol. Propylene carbonate, 1 and 2-propanol, 1 and 2-butanol slightly improved naringin dissolution. Acetone; dimethyl sulfoxide; *N,N*-dimethylmethanamide; *N,N*-dimethylacetamide; methanol; ethanol; tetrahydrofuran; 1,2-dimethoxyethane and 1,4-dioxane showed to be the best organic solvents, allowing a naringin dissolution higher than 100 mM.

Afterwards, the effect of these solvents (5 %) was tested over the activity of α -L-rhamnosidase and β -D-glucosidase, through the hydrolysis of specific substrates: 4-NRP and 4-NGP respectively.

Table 4.8 Naringin solubility in several organic solvents, at 25 °C.

Solvent	Dielectric constant	[Naringin] (mM)
water	80.10	< 12.5
Propylene carbonate	65.00	[12.5 – 25[
Dimethyl sulfoxide	47.20	[100 – 200[
<i>N,N</i> -dimethylmethanamide	40.10	> 200
<i>N,N</i> -Dimethylacetamide	38.80	> 200
Methanol	36.60	> 200
Acetonitrile	36.60	< 12.5
Ethanol	25.30	[100 – 200[
Acetone	21.01	> 200
1-propanol	20.80	[25 – 50[
2-propanol	20.18	[25 – 50[
1-butanol	17.84	[12.5 – 25[
2-butanol	17.26	[12.5 – 25[
3-methyl-1-butanol	15.63	< 12.5
2-Butoxyethanol	9.57	[50 – 100[
Tetrahydrofuran	7.60	> 200
1,2-Dimethoxyethane	7.40	> 200
2-Methyl-2-butanol	5.97	< 12.5
1,4-Dioxane	2.22	[100 – 200[

As it is shown on Table 4.9, β -D-glucosidase shows a high (> 50 %) residual activity in the presence of 1,4-dioxane, 1,2 dimethoxyethane, tetrahydrofuran, acetone, ethanol, methanol and acetonitrile, while α -L-rhamnosidase shows high activities (> 50 %) with almost all the solvent tested, except to 1-butanol, 3-methyl-1-butanol and 2-butoxyethanol.

According to this preliminary studies, considering the naringin solubility together with the residual activity of α -L-rhamnosidase and β -D-glucosidase, eight solvents (dimethyl sulfoxide; *N,N*-dimethylmethanamide; methanol; ethanol; acetone; tetrahydrofuran; 1,2-

dimethoxyethane and 1,4-dioxane) were chosen to be used in further stability and activity studies.

Table 4.9 Residual activity of β -D-glucosidase and α -L-rhamnosidase expressed by soluble naringinase.

Cosolvent	Residual Activity	
	β -D-glucosidase	α -L-rhamnosidase
Propylene carbonate	0.34 \pm 0.04	0.57 \pm 0.03
Dimethyl sulfoxide	0.85 \pm 0.06	1.01 \pm 0.01
<i>N,N</i> -dimethylmethanamide	0.52 \pm 0.04	0.78 \pm 0.05
<i>N,N</i> -Dimethylacetamide	0.54 \pm 0.01	0.80 \pm 0.04
Methanol	0.80 \pm 0.06	0.92 \pm 0.07
Acetonitrile	0.73 \pm 0.04	0.90 \pm 0.01
Ethanol	0.73 \pm 0.01	0.83 \pm 0.04
Acetone	0.64 \pm 0.01	0.81 \pm 0.02
1-propanol	0.50 \pm 0.02	0.52 \pm 0.06
2-propanol	0.72 \pm 0.03	0.83 \pm 0.08
1-buthanol	0.10 \pm 0.01	0.40 \pm 0.04
2-buthanol	0.48 \pm 0.02	0.77 \pm 0.04
3-methyl-1-buthanol	0.41 \pm 0.01	0.08 \pm 0.03
2-Butoxyethanol	0.26 \pm 0.02	0.26 \pm 0.02
Tetrahydrofuran	0.70 \pm 0.02	0.65 \pm 0.02
1,2-Dimethoxyethane	0.80 \pm 0.04	0.81 \pm 0.06
2-Methyl-2-butanol	0.46 \pm 0.04	0.93 \pm 0.06
1,4-Dioxane	0.58 \pm 0.01	0.83 \pm 0.06

Mean value \pm SE, $n = 3$.

4.3.2.3 Cosolvent stability studies

In this work, stability studies with α -L-rhamnosidase and β -D-glucosidase expressed by soluble and immobilized naringinase were performed in aqueous cosolvent systems, at 0, 2.5, 5 and 10 % (v/v), of dimethyl sulfoxide, acetone, *N,N*-dimethylacetamide, methanol, 1,2-dimethoxyethane, ethanol, tetrahydrofuran, 1,4-dioxane. Naringinase was immobilized within sol-gel matrices of TMOS and glycerol (Matrix B). In these aqueous cosolvent systems, the use of naringinase immobilized onto sol-gel matrices allowed higher residual activities of α -L-rhamnosidase and β -D-glucosidase with respect to the corresponding soluble enzyme. At the lowest cosolvent concentration, the immobilized biocatalyst was always more stable than the soluble one (Figure 4.10 and 4.11). In the case of β -D-glucosidase a residual activity greater than 100 % was attained with all cosolvents, even at higher concentrations (10 %), with the exception to dimethyl sulfoxide (Figure 4.11). A 1.5 increase in β -D-glucosidase residual activity was observed with the cosolvent 1,2-dimethoxyethane.

These results showed a protective effect of sol-gel matrices within cosolvents systems, in the three concentrations tested, being this effect more pronounced for β -D-

glucosidase (Figure 4.11) than for α -L-rhamnosidase (Figure 4.10), when comparing with soluble enzyme. There was a good fit between experimental inactivation kinetics of α -L-rhamnosidase and β -D-glucosidase of soluble naringinase and a simple exponential decay model was adjusted, allowing the calculation of k_1 and the half-life time, except in the case of soluble β -D-glucosidase without cosolvent, where a biphasic system was fitted (Tables 4.10 and 4.11). In all the cosolvent systems tested an increase in the inactivation parameters k_1 with a correspondent decrease of half-life times were observed for soluble naringinase (Table 4.10 and 4.11). An activity increase was seen whenever the sol-gel immobilized naringinase was reused for the first time. This fact may be explained by some glycerol release from the sol-gel matrix (a precursor used during the immobilization procedure). This glycerol release may lead to a better substrate access to the immobilized enzyme, increasing enzyme activity after the first run. The inactivation of α -L-rhamnosidase and β -D-glucosidase from the immobilized naringinase was well described by a biphasic inactivation (Equation 2.7). The parameters k_1 , k_2 , α_1 and the half-life time of the biocatalysts were calculated (Table 4.10 and 4.11). Improved enzyme stability is associated to a decrease in the inactivation parameters k_1 or k_2 with a corresponding increase in half-life time or an increase in enzyme residual activity, α_1 .

The results reported on Table 4.10 and 4.11 support an improved stabilization of naringinase for the hydrolysis of 4-NRP and 4-NGP, for all cosolvent systems tested; which are easily supported by the increased half-life times of sol-gel immobilized naringinase (Table 4.10 and 4.11), when compared with soluble naringinase. The stabilization of α -L-rhamnosidase activity by sol-gel immobilized can be highlighted in the case use of tetrahydrofuran using concentrations of 2.5, 5.0 and 10.0 %, which originated an increase of 7, 13 and 21-fold, on the half-life time, respectively, with respect to the corresponding soluble enzyme (Table 4.10). This is an example of the high protective effect of the sol-gel (Matrix B) to the enzyme naringinase over different cosolvent concentrations. In the case of β -D-glucosidase activity, expressed by sol-gel immobilized naringinase, almost a 60-fold increase in the half-life time was observed, respectively from 0.33 (soluble enzyme) to 19.2 hours, concerning as well a tetrahydrofuran cosolvent system (10%) (Table 4.11). For all the aqueous cosolvents systems an half-life time increase greater than 3 fold with immobilized enzyme was observed, comparing to soluble enzyme (Table 4.10 and 4.11). At the higher cosolvent

concentration used (10 %) the sol-gel protective effect was much more pronounced, as shown by increased half-life times, e.g. 11-fold with ethanol, 13-fold with 1,4 dioxane, 14-fold with 1,2 dimethoxyethane, 18-fold with acetone, 24-fold with *N,N*-dimethylacetamide and the best one 59-fold with tetrahydrofuran, in the case of the hydrolysis of 4-NGP, by β -D-glucosidase.

The immobilization of naringinase through sol-gel technique improved both α -L-rhamnosidase and β -D-glucosidase resistance against inactivation in the presence of organic cosolvents. Enhanced biocatalyst stabilization, in all solvent range tested, was achieved through immobilization. The different stability behaviours in certain solvent conditions, using soluble and immobilized enzyme, may arise from distinct mechanisms of inactivation. The role of glycerol as compensatory cosolvent must not be forgotten, which stabilizes the folded form against denaturation under external stress (Scharnagl *et al.*, 2005). In this case, of naringinase immobilization onto sol-gel (TMOS/glycerol), glycerol may prevent unfolding at high concentrations of organic cosolvents.

According with these findings, Brena *et al.*, 2003 also reports an enzymatic stabilization through immobilization. Brena showed a half-life time increase from 8 to 100 h after immobilization of *E. coli* β -galactosidase onto glutaraldehyde-agarose, in 18 % (v/v) dioxane, also in 36 (%) dimethylformamide, a half-life time increase from 0.3 to 1 h was reported (Brena *et al.*, 2003). Some authors stabilized α -glucosidase by immobilization onto macroporous poly(GMA-co-EGDMA) (Radivoje *et al.*, 2006). The immobilized enzyme had 4 and 10-fold higher half-life times than the soluble one in dimethyl sulfoxide and methanol, respectively (Radivoje *et al.*, 2006). In other work, water miscible cosolvents, like dimethyl sulfoxide, were used to increase substrate solubility (Roccatano *et al.*, 2006); however, the catalytic activity of P450 was significantly lower. The effect of methanol, ethanol, dimethyl sulfoxide, and acetonitrile on the catalytic activities of nine human cDNA-expressed cytochrome P-450s in aqueous cosolvent systems was also tested (Busby *et al.*, 1999).

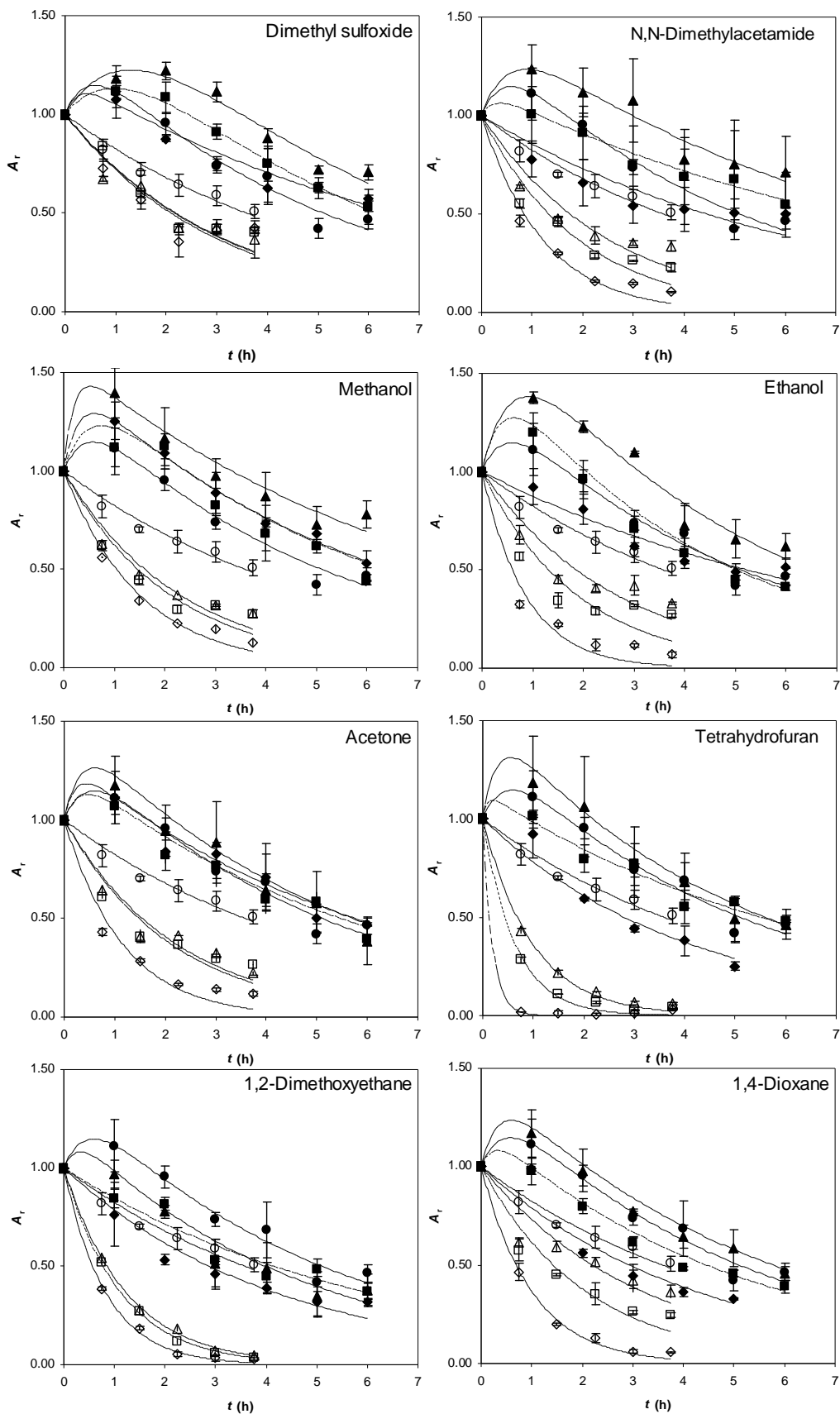


Figure 4.10 Stability of α -L-rhamnosidase expressed by soluble and immobilized naringinase in cosolvent systems. 0%, 2.5%, 5% and 10% (v/v) are cosolvent percentages used with soluble (\circ , \triangle , \square , \diamond) and immobilized (\bullet , \blacktriangle , \blacksquare , \blacklozenge) naringinase, respectively.

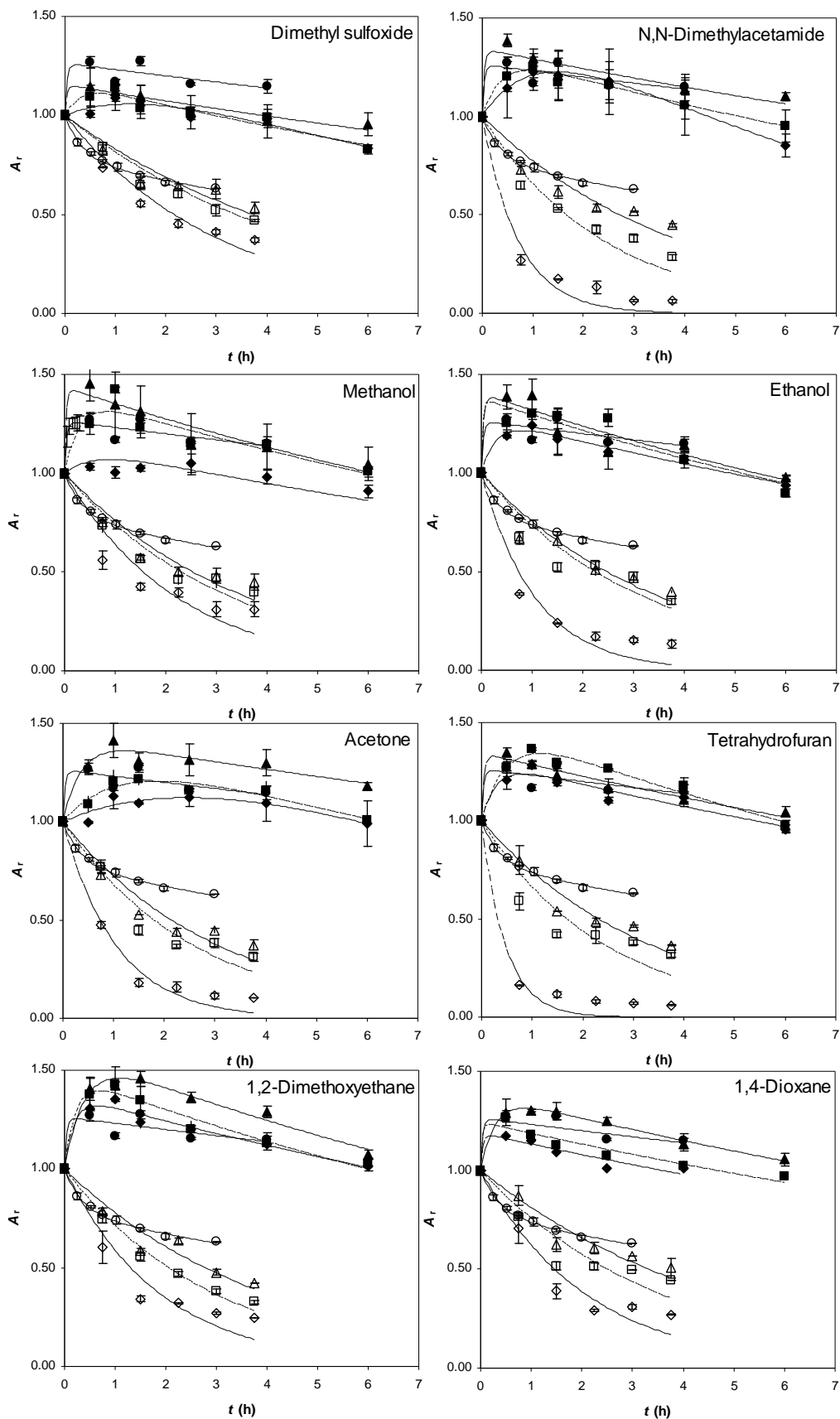


Figure 4.11 Stability of β -D-glucosidase expressed by soluble and immobilized naringinase in cosolvent systems. 0%, 2.5%, 5% and 10% (v/v) are cosolvent percentages used with soluble (\circ , \triangle , \square , \diamond) and immobilized (\bullet , \blacktriangle , \blacksquare , \blacklozenge) naringinase, respectively.

Table 4.10 Inactivation parameters of α -L-rhamnosidase expressed by soluble and immobilized

		α -L-rhamnosidase										
Cosolvent [% (V/V)]	(Expressed by soluble naringinase)					(Expressed by sol-gel immobilized naringinase)					R^2	$f_{1/2, \text{imm.}}, f_{1/2, \text{sol}}^{-1}$
	k_1 (h ⁻¹)	$t_{1/2, \text{sol}}$ (h)	R^2	a_1	k_1 (h ⁻¹)	k_2 (h ⁻¹)	$t_{1/2, \text{imm}}$ (h)	R^2				
Dimethyl sulfoxide												
0	0.19 ± 0.01	3.63 ± 0.31	0.96	1.29 ± 0.02	2.18 ± 0.29	0.21 ± 0.05	5.22 ± 0.57	0.96	1			
2.5	0.32 ± 0.02	2.20 ± 0.16	0.91	1.58 ± 0.01	0.72 ± 0.13	0.20 ± 0.01	7.30 ± 0.26	0.95	3			
5	0.32 ± 0.0	2.30 ± 0.05	0.94	1.39 ± 0.21	0.82 ± 0.26	0.12 ± 0.05	6.67 ± 0.99	0.99	3			
10	0.33 ± 0.02	2.10 ± 0.12	0.87	1.17 ± 0.05	0.21 ± 0.09	0.13 ± 0.01	6.33 ± 0.12	0.94	3			
N,N-Dimethylacetamide												
2.5	0.40 ± 0.02	1.75 ± 0.07	0.90	1.26 ± 0.39	1.87 ± 0.10	0.13 ± 0.01	7.97 ± 0.58	0.93	5			
5	0.52 ± 0.01	1.33 ± 0.04	0.94	1.11 ± 0.05	4.00 ± 0.34	0.12 ± 0.10	5.00 ± 1.15	0.96	4			
10	0.82 ± 0.02	0.84 ± 0.02	0.98	-	0.16 ± 0.02	-	4.23 ± 0.50	0.88	5			
Methanol												
2.5	0.43 ± 0.01	1.60 ± 0.02	0.94	1.54 ± 0.22	5.00 ± 0.33	0.14 ± 0.03	8.53 ± 1.54	0.94	5			
5	0.47 ± 0.02	1.47 ± 0.08	0.93	1.41 ± 0.13	2.00 ± 0.37	0.18 ± 0.06	5.77 ± 0.35	0.91	4			
10	0.66 ± 0.02	1.05 ± 0.03	0.98	1.43 ± 0.09	3.23 ± 0.34	0.17 ± 0.01	6.57 ± 0.23	0.99	6			
Ethanol												
2.5	0.37 ± 0.02	1.87 ± 0.10	0.88	1.67 ± 0.09	1.68 ± 0.38	0.20 ± 0.05	6.77 ± 0.95	0.96	4			
5	0.53 ± 0.01	1.31 ± 0.04	0.87	1.48 ± 0.18	2.50 ± 0.16	0.23 ± 0.04	4.67 ± 0.37	0.97	4			
10	1.16 ± 0.01	0.60 ± 0.03	0.96	-	0.13 ± 0.01	-	5.00 ± 0.57	0.94	8			
Acetone												
2.5	0.45 ± 0.01	1.55 ± 0.03	0.94	1.42 ± 0.19	2.90 ± 0.74	0.19 ± 0.05	5.83 ± 1.53	0.95	4			
5	0.47 ± 0.02	1.47 ± 0.06	0.93	1.22 ± 0.12	3.20 ± 0.44	0.17 ± 0.06	5.37 ± 0.77	0.95	4			
10	0.86 ± 0.02	0.81 ± 0.02	0.96	1.27 ± 0.02	4.50 ± 0.42	0.17 ± 0.04	6.03 ± 1.13	0.95	7			
Tetrahydrofuran												
2.5	1.02 ± 0.02	0.68 ± 0.01	0.99	1.47 ± 0.34	3.50 ± 0.36	0.20 ± 0.02	5.00 ± 0.70	0.97	7			
5	1.57 ± 0.02	0.44 ± 0.01	0.99	1.13 ± 0.06	11.80 ± 0.12	0.15 ± 0.01	5.53 ± 0.22	0.95	13			
10	5.33 ± 0.02	0.13 ± 0.01	0.99	-	0.25 ± 0.01	-	2.77 ± 0.12	0.93	21			
1,2-Dimethoxyethane												
2.5	0.82 ± 0.02	0.85 ± 0.02	0.99	1.17 ± 0.08	3.70 ± 0.79	0.23 ± 0.08	4.03 ± 0.79	0.96	5			
5	0.89 ± 0.02	0.78 ± 0.02	0.99	-	0.17 ± 0.01	-	4.20 ± 0.15	0.93	5			
10	1.21 ± 0.02	0.57 ± 0.01	0.99	-	0.24 ± 0.02	-	2.87 ± 0.18	0.97	5			
1,4-Dioxane												
2.5	0.31 ± 0.02	2.20 ± 0.06	0.85	1.38 ± 0.09	2.90 ± 0.40	0.19 ± 0.02	5.27 ± 0.35	0.98	2			
5	0.48 ± 0.02	1.43 ± 0.07	0.94	1.16 ± 0.07	4.00 ± 0.12	0.20 ± 0.02	4.30 ± 0.10	0.98	3			
10	1.00 ± 0.02	0.69 ± 0.05	0.99	-	0.24 ± 0.01	-	2.97 ± 0.18	0.86	4			

Mean value ± SE, $n = 3$.

Table 4.11 Inactivation parameters of β -D-glucosidase expressed by soluble and immobilized naringinase within cosolvent systems.

		β -D-Glucosidase										
Cosolvent	[% (V/V)]	(Expressed by soluble naringinase)					(Expressed by sol-gel immobilized naringinase)					
		α_1	k_1 (h ⁻¹)	k_2 (h ⁻¹)	$t_{1/2, \text{sol}}$ (h)	R^2	α_1	k_1 (h ⁻¹)	k_2 (h ⁻¹)	$t_{1/2, \text{imm}}$ (h)	R^2	
		$t_{1/2, \text{imm.}}, t_{1/2, \text{sol}}^{-1}$										
Dimethyl sulfoxide												
0		0.76 ± 0.03	2.84 ± 0.84	0.074 ± 0.01	6.18 ± 0.55	0.99	1.29 ± 0.01	2.18 ± 0.79	0.21 ± 0.00	33.6 ± 4.0	0.99	5
2.5		-	0.19 ± 0.01	-	3.72 ± 0.12	0.89	1.15 ± 0.06	26.3 ± 8.2	0.037 ± 0.02	20.7 ± 3.7	0.91	6
5		-	0.20 ± 0.01	-	3.10 ± 0.14	0.95	1.15 ± 0.03	3.16 ± 0.10	0.053 ± 0.01	13.8 ± 1.0	0.91	4
10		-	0.32 ± 0.00	-	2.16 ± 0.03	0.95	1.16 ± 0.10	0.65 ± 0.08	0.071 ± 0.02	12.9 ± 0.5	0.88	6
N,N-Dimethylacetamide												
2.5		-	0.25 ± 0.01	-	2.72 ± 0.08	0.89	1.34 ± 0.24	24.9 ± 7.5	0.039 ± 0.01	25.4 ± 2.6	0.88	9
5		-	0.42 ± 0.01	-	1.84 ± 0.05	0.93	1.30 ± 0.05	2.70 ± 0.78	0.056 ± 0.01	15.3 ± 1.4	0.97	8
10		-	1.40 ± 0.09	-	0.49 ± 0.03	0.96	1.43 ± 0.43	0.93 ± 0.08	0.104 ± 0.08	11.7 ± 1.6	0.99	24
Methanol												
2.5		-	0.27 ± 0.01	-	2.54 ± 0.06	0.90	1.43 ± 0.17	30.8 ± 9.5	0.059 ± 0.01	17.4 ± 1.5	0.92	7
5		-	0.30 ± 0.02	-	2.33 ± 0.16	0.92	1.38 ± 0.02	3.37 ± 0.18	0.056 ± 0.00	18.0 ± 2.1	0.84	8
10		-	0.44 ± 0.03	-	1.56 ± 0.09	0.85	1.11 ± 0.10	1.77 ± 0.53	0.047 ± 0.01	17.5 ± 2.2	0.99	11
Ethanol												
2.5		-	0.28 ± 0.01	-	2.47 ± 0.06	0.89	1.40 ± 0.13	23.2 ± 2.3	0.063 ± 0.01	17.3 ± 2.1	0.87	7
5		-	0.31 ± 0.01	-	2.25 ± 0.11	0.86	1.37 ± 0.03	30.0 ± 9.7	0.050 ± 0.01	18.3 ± 1.5	0.87	8
10		-	0.94 ± 0.01	-	0.74 ± 0.02	0.94	1.27 ± 0.07	3.43 ± 0.67	0.051 ± 0.00	18.0 ± 1.0	0.97	24
Acetone												
2.5		-	0.32 ± 0.02	-	2.14 ± 0.07	0.92	1.27 ± 0.06	26.5 ± 8.5	0.027 ± 0.00	31.7 ± 2.2	0.93	15
5		-	0.38 ± 0.01	-	1.80 ± 0.06	0.93	1.35 ± 0.10	0.87 ± 0.05	0.058 ± 0.02	20.9 ± 4.5	0.92	12
10		-	0.95 ± 0.03	-	0.73 ± 0.03	0.98	1.61 ± 0.08	0.18 ± 0.43	0.148 ± 0.01	13.4 ± 2.4	0.80	18
Tetrahydrofuran												
2.5		-	0.30 ± 0.01	-	2.31 ± 0.10	0.95	1.34 ± 0.01	20.8 ± 0.8	0.046 ± 0.01	24.7 ± 5.0	0.96	11
5		-	0.41 ± 0.02	-	1.69 ± 0.10	0.83	1.45 ± 0.02	2.07 ± 0.74	0.069 ± 0.00	16.1 ± 1.2	0.97	10
10		-	2.12 ± 0.04	-	0.33 ± 0.01	0.97	1.29 ± 0.02	3.43 ± 0.17	0.050 ± 0.00	19.2 ± 1.0	0.90	59
1,2-Dimethoxyethane												
2.5		-	0.25 ± 0.00	-	2.77 ± 0.04	0.92	1.56 ± 0.02	2.58 ± 0.97	0.063 ± 0.00	17.8 ± 0.9	0.98	6
5		-	0.33 ± 0.00	-	2.06 ± 0.02	0.98	1.46 ± 0.10	4.51 ± 0.77	0.066 ± 0.01	16.5 ± 2.3	0.97	8
10		-	0.53 ± 0.04	-	1.30 ± 0.08	0.92	1.36 ± 0.04	5.16 ± 0.96	0.052 ± 0.01	17.7 ± 2.9	0.96	14
1,4-Dioxane												
2.5		-	0.21 ± 0.02	-	3.36 ± 0.33	0.92	1.37 ± 0.03	3.46 ± 0.74	0.047 ± 0.00	21.3 ± 2.2	0.99	6
5		-	0.28 ± 0.00	-	2.50 ± 0.03	0.85	1.20 ± 0.02	30.1 ± 0.8	0.043 ± 0.00	20.2 ± 0.5	0.91	8
10		-	0.47 ± 0.01	-	1.46 ± 0.04	0.94	1.19 ± 0.02	20.2 ± 0.1	0.084 ± 0.01	19.2 ± 3.7	0.89	13

Mean value ± SE, $n = 3$.

4.3.2.4 Kinetic study of naringin bioconversion

A kinetic study of naringin hydrolysis was carried out in free cosolvent and 10 % aqueous cosolvent systems of 1,2-dimethoxyethane; 1,4- dioxane and tetrahydrofuran.

A maximum naringin concentration of 2.5 mM was dissolved in the free cosolvent aqueous system, while increased naringin concentrations were used in the 10 % aqueous cosolvent systems, with a maximum concentration, of 5 mM in 1,2-dimethoxyethane and 15 mM in 1,4- dioxane and tetrahydrofuran, respectively, (Figure 4.12). The less toxic cosolvents were respectively, 1,2-dimethoxyethane, 1,4-dioxane, and tetrahydrofuran. Kinetic constants were evaluated on naringin hydrolysis by naringinase within these aqueous cosolvent systems. 1,4-dioxane and 1,2-dimethoxyethane showed a higher naringinase specific activity, being considered the most favourable (Figure 4.12). Naringin shows a higher solubility in 1,4-dioxane (Table 4.8), but a higher k_{cat} and a lower K_M was observed with 1,2-dimethoxyethane (Table 4.12).

Different concentrations of 1,2-imethoxyethane (1, 2 and 3 %) were tested using different naringin concentrations, allowing kinetic constant evaluation (Figure 4.13). According to the results reported on Figure 4.13 and Table 4.13, the presence of 1,2-dimethoxyethane in aqueous systems led to a slight increase in k_{cat} and higher K_M . The k_{cat} was much less affected with the presence of the cosolvent, than the apparent K_M , also a sharp decrease of the catalytic efficiency ($k_{cat}.K_M^{-1}$) was observed.

An increase in the Michaelis-Menten constant, K_M for the hydrolysis of naringin in the aqueous cosolvent system of 1,2-dimethoxyethane in water reflects changes in the affinity of the enzyme for the substrate, which is common in reactions involving hydrophobic interactions during the enzyme-substrate complex formation. Similar results were obtained in other works, showing increased Michaelis-Menten constant for the hydrolytic activity of α -chymotrypsin (Kise and Tomiuchi, 1991) in cosolvent systems.

Table 4.12 Kinetic parameters of soluble naringinase, in 10 % (v/v) aqueous cosolvent systems.

Cosolvent	k_{cat} ($\mu\text{mol min}^{-1} \text{mg}^{-1}$)	K_M (mM)	$k_{cat} K_M^{-1}$ ($\text{L min}^{-1} \text{g}^{-1}$)	R^2
Without	2.05 ± 0.14	1.92 ± 0.27	1.07	0.99
1,2-Dimethoxyethane	2.52 ± 0.09	4.26 ± 0.30	0.59	0.99
1,4-Dioxane	1.91 ± 0.17	5.15 ± 0.22	0.37	0.99
Tetrahydrofuran	1.46 ± 0.18	8.00 ± 2.72	0.18	0.97

Mean value \pm SE, $n = 3$.

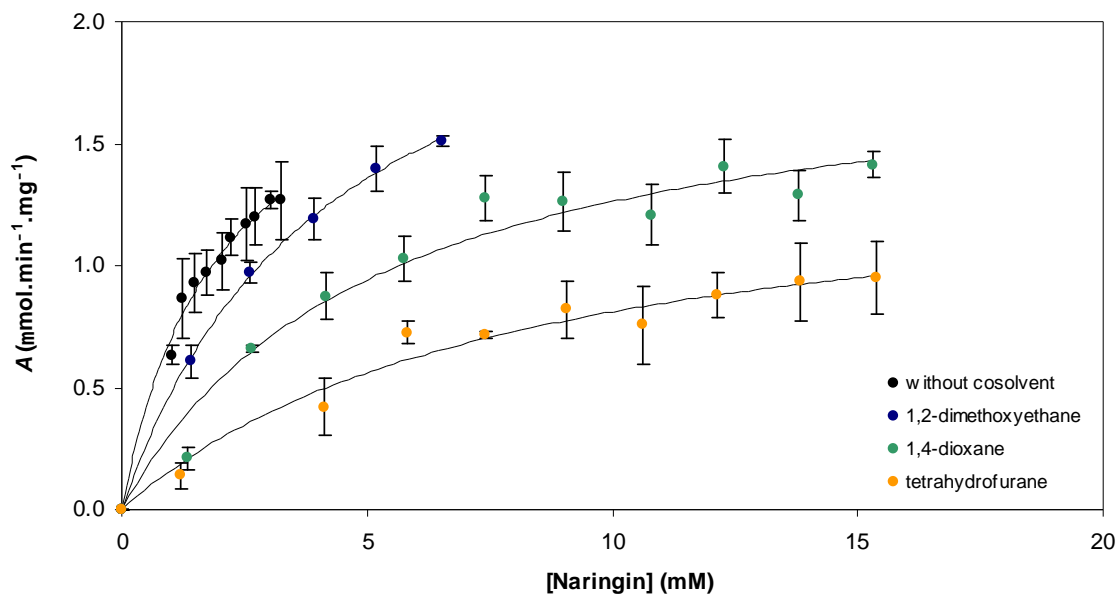


Figure 4.12 Michaelis-Menten kinetics of soluble naringinase, in several aqueous cosolvent systems (10 %).

Table 4.13 Kinetic parameters of soluble naringinase, in aqueous cosolvent system composed of 1,2-dimethoxyethane.

1,2-Dimethoxyethane (%)	k_{cat} ($\mu\text{mol}\cdot\text{min}^{-1}\text{mg}^{-1}$)	K_M (mM)	$k_{cat}\cdot K_M^{-1}$ ($\text{L}\cdot\text{min}^{-1}\text{g}^{-1}$)	R^2
0	2.40 ± 0.18	2.21 ± 0.33	1.08	0.99
1	2.45 ± 0.12	3.03 ± 0.42	0.81	0.98
2	2.54 ± 0.10	3.58 ± 0.53	0.71	0.98
3	2.60 ± 0.08	4.41 ± 0.59	0.59	0.98

Mean values \pm SE, $n = 3$.

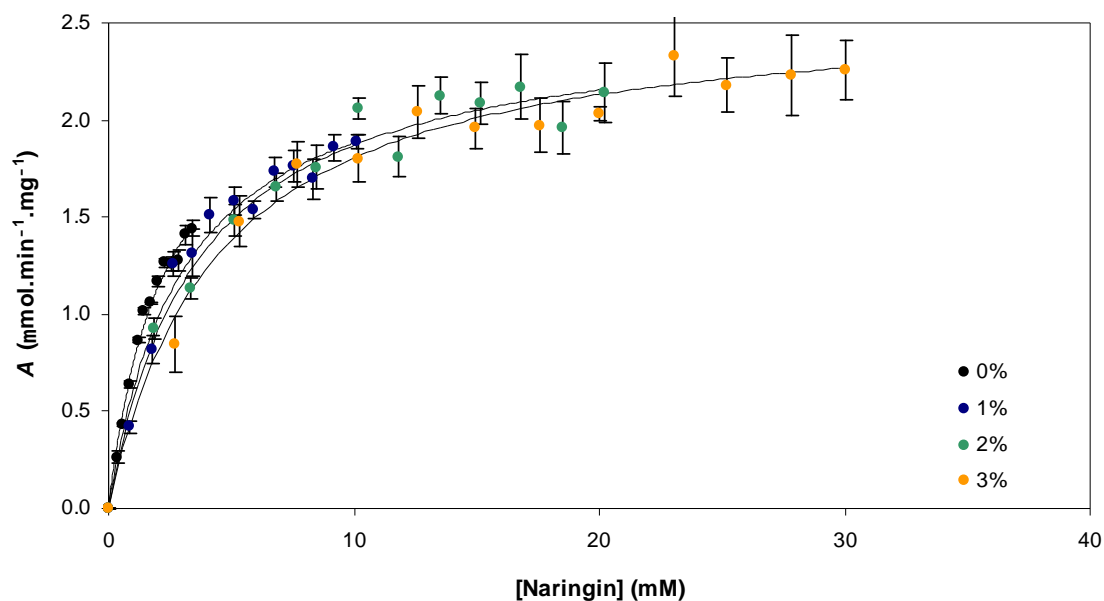


Figure 4.13 Michaelis-Menten kinetics of naringinase, in aqueous cosolvent system composed of different concentrations of 1,2-dimethoxyethane (1, 2 and 3 %).

4.3.3 Sol-gel immobilization of naringinase using ILs as additives

In preliminary studies, the ILs: [EMIM][DMP], [C₂OHMIM][BF₄], [BMIM][MeOEtOEtOSO₃] and [E₂-MPy][ESO₄] were tested in the production of the sol-gel matrices as additives with TMOS and in combination with glycerol. In these experiments, ILs were added during the sol formation leading to a homogenous silica colloid. They were tested in 3% (*w/w*) relative proportion to the gel mass. This value (3%) was selected after preliminary assays using different ILs proportions (*w/w*) relative to the gel mass before aging (data not shown). The hydrolytic reactions of the substrates 4-NRP and 4-NGP, with respectively α -L-rhamnosidase and β -D-glucosidase, were used as reaction models to study the effects of the different ILs on sol-gel matrices.

Figure 4.14 presents the results obtained for α -L-rhamnosidase and β -D-glucosidase activities immobilized within sol-gel matrices of TMOS/ILs and TMOS/Glycerol/ILs, during 19 consecutive reutilizations. In both cases the enzyme activity was higher for immobilized enzyme within sol-gel matrices of TMOS/Glycerol/ILs, than for matrices made of TMOS/ILs. In fact, the presence of glycerol, showed to be important in all matrices produced with ILs, resulting in higher α -L-rhamnosidase (Figure 4.14a) and β -D-glucosidase (Figure 4.14b) efficiencies, respectively, of about ~60% and ~75%. Moreover, the use of glycerol with [E₂-MPy][ESO₄], as additives, led to an increase on the efficiency of α -L-rhamnosidase from 11 to 62% and a β -D-glucosidase efficiency increase from 21% to 78%. Also, the efficiency of β -D-glucosidase of naringinase encapsulated on TMOS/Glycerol/ILs was higher compared with those obtained (72%) with sol-gel matrices of TMOS/Glycerol (matrix B).

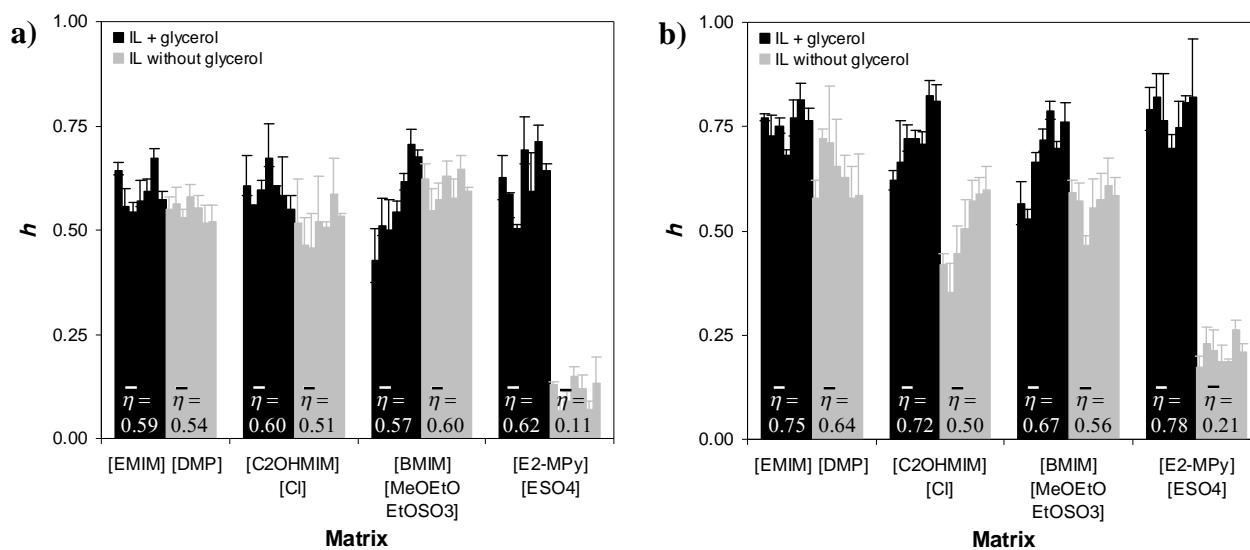


Figure 4.14 Influence of ILs on the efficiency of α -L-rhamnosidase (a) and β -D-glucosidase (b) immobilized in TMOS sol-gel matrices with and without glycerol, after 19 consecutive runs (bars: 1st, 4th, 7th, 10th, 13th, 16th and 19th runs) (mean value \pm SE, $n = 8$).

The addition of ILs on sol-gel matrices can be performed in the sol preparation incorporated in the silica sol (Liu *et al.*, 2005a, b; Lee *et al.*, 2007b) or during the gel formation, dissolved in the enzymatic solution (Zarcuła *et al.*, 2009). After 19 consecutive reutilizations, no significant differences (Figure 4.15) were observed on the efficiency of α -L-rhamnosidase (~65%) and β -D-glucosidase (~80%) immobilized within sol-gel matrices of TMOS/Glycerol with ILs incorporated in the silica sol (Figure 4.15a) or in the enzymatic solution (Figure 4.15b). The exception was the incorporation of the IL, [E₂-MPy][ESO₄], on silica sol that allowed higher efficiencies of α -L-rhamnosidase (17% to 62%) and β -D-glucosidase (50% to 78%) of naringinase. Lee *et al.* (2007b) found a higher activity for immobilized lipase when ILs and TEOS were hydrolyzed before lipase addition. In further studies, the ILs were added to the silica sol, unless stated otherwise.

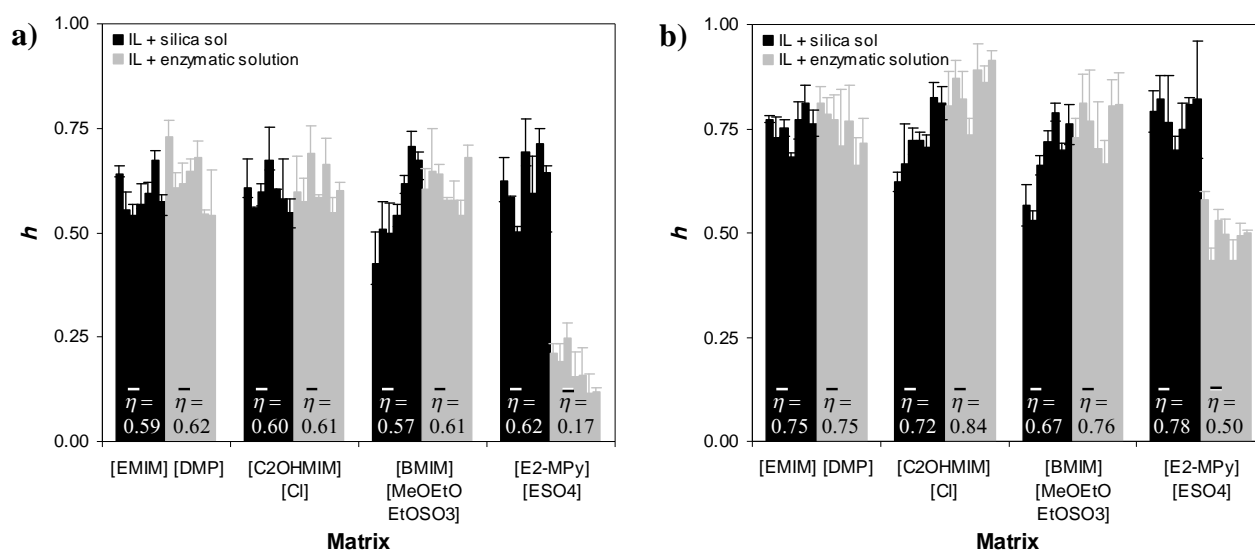


Figure 4.15 Influence of the incorporation of ILs in silica sol (TMOS/Glycerol) and in the enzymatic solution, on the efficiency of α -L-rhamnosidase (a) and β -D-glucosidase (b), after 19 consecutive reutilizations (bars: 1st, 4th, 7th, 10th, 13th, 16th and 19th runs) (mean value \pm SE, $n = 8$).

4.3.3.1 Influence of ILs structure on sol-gel naringinase immobilization efficiency

As indicated in 4.2.5.2 (method 1), the silica sol-gel materials were obtained through a sol-gel method using TMOS/Glycerol and the following ILs: [C₂OHMIM][Cl], [EMIM][DMP], [BMIM][MeOEtOEtOSO₃], [C₂OHMIM][BF₄], [EMIM][PF₆], [BMIM][PF₆], [OMIM][Tf₂N], [E₂-MPy][ESO₄] and [E₃-MPy][ESO₄]. When method 1 was used for the ILs [C₂OHMIM][PF₆], [OMIM][PF₆] and [BMIM][Tf₂N], a colloid system wasn't formed even after one hour of sonication. So, a higher concentration of catalyst was needed to obtain one layer of silica sol, leading to the development of

method 2, as described in 4.2.5.2. The ILs [BMIM][TFA], [BIM][BF₄] and [BMIM][BF₄] added to the silica sol formed an unstable colloid gel in a very fast way, turning it impossible to make the gel. On the basis of this of this colloid instability is the Derjaguin-Landau-Verwey-Overbeek (DLVO) theory (Ueno *et al.*, 2008); therefore a third method (method 3) was established for these ILs, by mixing them with the solution of enzyme, as described in 4.2.5.2. Besides the previous mentioned ILs, 1-butyl-3-methylimidazolium tetrafluoroborate was also tested as sol-gel additive but it led to a very fast gel formation when added to the silica sol and as it isn't miscible with water it couldn't have been studied even using method 3.

Immobilized α -L-rhamnosidase (Figure 4.16) and β -D-glucosidase (Figure 4.17) were greatly influenced by ILs (3% *w/w*) used as templates of sol-gel (TMOS/Glycerol). Stability was measured through the average retention of enzyme activity over fifty reutilizations (Table 4.14). The most striking feature concerning Figure 4.16 and 4.17 is the positive impact of ILs present on TMOS/Glycerol matrices over the enzyme activity and stability. The efficiency of α -L-rhamnosidase within TMOS/Glycerol/ILs matrices (Figure 4.16) is dependent on the structure of the IL cation as follows: [OMIM] > [BMIM] > [EMIM] > [C₂OHMIM] > [BIM] and [OMIM] \approx [E₂-MPy] >> [E₃-MPy]. Considering these series, the hydrophobic nature of the ILs cation appears to be fundamental for α -L-rhamnosidase activity and stability. Regarding the imidazolium family, the efficiency of α -L-rhamnosidase is influenced by the hydrophobic nature of the cation. Indeed, an increase in the cation hydrophobicity lead to higher α -L-rhamnosidase efficiencies: [BIM]BF₄ << [C₂OHMIM] BF₄ << [BMIM]BF₄. Also, the structure of the cation is essential for enzyme activity and stability. Small differences in the IL cation structure led to important differences in the enzyme activity and stability, for instance, when using [E₃-MPy] and [E₂-MPy] an impressive difference in the α -L-rhamnosidase activity and stability of almost 150% was observed (Figure 4.16).

Comparing the anions used in this study, similarly to what happened with the hydrophobic nature of the cation, an increase in the anion hydrophobicity led to an increase in α -L-rhamnosidase efficiency. In the BMIM series the more hydrophobic anions (PF₆⁻, BF₄⁻ and Tf₂N⁻) led to higher activities than TFA (Figure 4.16).

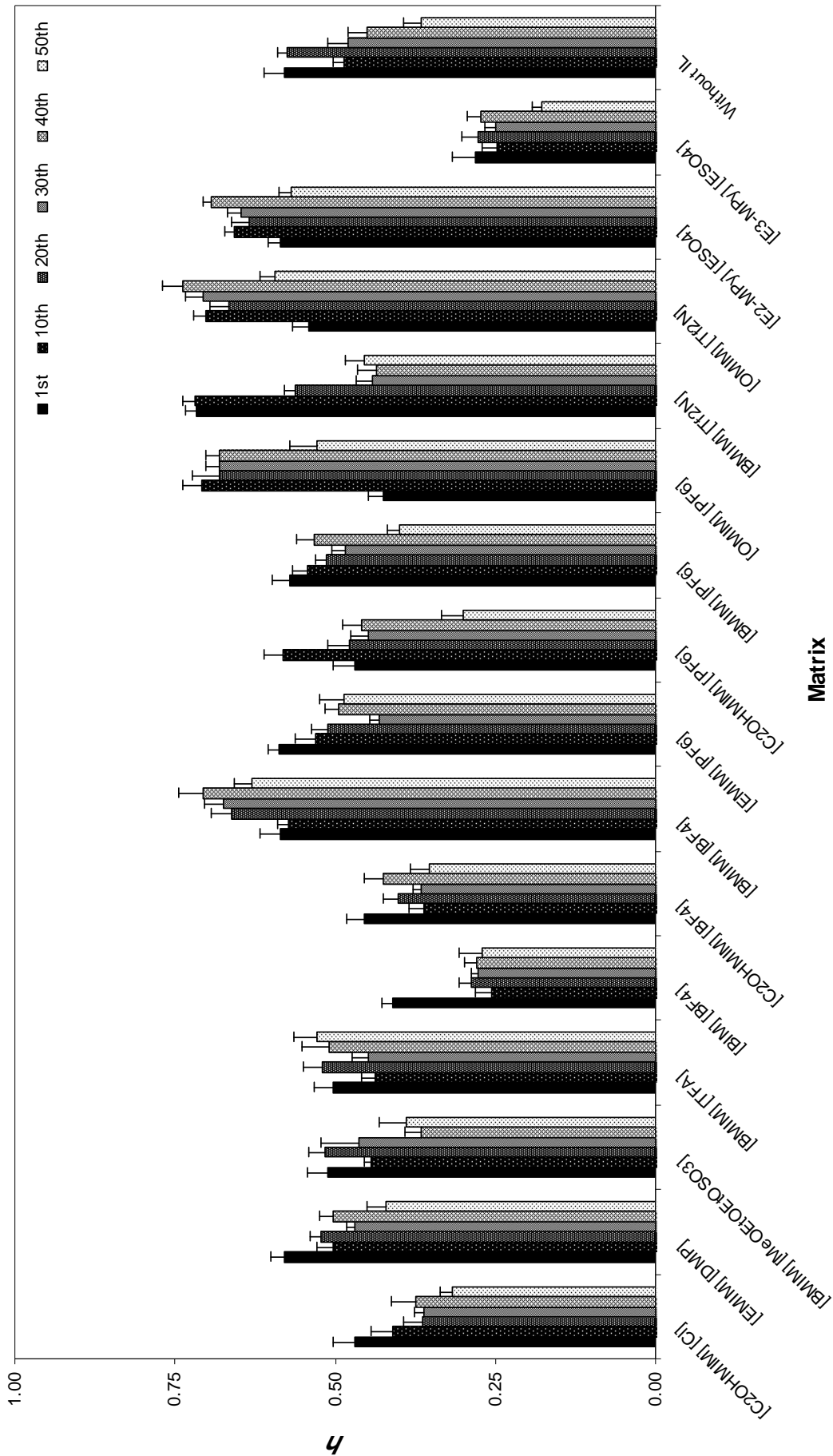


Figure 4.16 Influence of ILs on the immobilization reuse efficiency of α -L-rhamnosidase encapsulated within sol-gel matrices repeatedly used over 50 runs (mean value \pm SE, $n = 10$).

Table 4.14 Influence of ILs on the immobilization reuse efficiency of α -L-rhamnosidase and β -D-glucosidase encapsulated within sol-gel matrices.

Additives	α -L-rhamnosidase						β -D-glucosidase					
	Specific activity ($\mu\text{mol min}^{-1} \text{mg}^{-1}$)	Efficiency (1 st run)	Relative activity to control	Reuse efficiency average (50 runs)	Residual activity after 50 th reuse		Specific activity ($\mu\text{mol min}^{-1} \text{mg}^{-1}$)	Efficiency (1 st run)	Relative activity to control	Reuse efficiency average (50 runs)	Residual activity after 50 th reuse	
Free enzyme	0.108 \pm 0.001	-	-	-	-	-	0.088 \pm 0.002	-	-	-	-	
Control (without IL)	0.062 \pm 0.004	0.58 \pm 0.03	1.00	0.49 \pm 0.04	0.84	0.065 \pm 0.002	0.74 \pm 0.03	1.00	0.73 \pm 0.01	0.99		
[C2OHMIM] [Cl]	0.051 \pm 0.004	0.47 \pm 0.03	0.82	0.38 \pm 0.03	0.81	0.060 \pm 0.002	0.68 \pm 0.02	0.92	0.69 \pm 0.01	1.01		
[EMIM][DMP][BMIM]	0.062 \pm 0.002	0.58 \pm 0.02	1.00	0.50 \pm 0.03	0.86	0.067 \pm 0.002	0.77 \pm 0.02	1.03	0.76 \pm 0.01	0.99		
[MeOEtOEtOSO ₃]	0.055 \pm 0.003	0.51 \pm 0.03	0.89	0.45 \pm 0.03	0.88	0.068 \pm 0.003	0.77 \pm 0.03	1.05	0.73 \pm 0.02	0.95		
[BMIM] [TFA]	0.054 \pm 0.003	0.50 \pm 0.03	0.87	0.49 \pm 0.02	0.98	0.060 \pm 0.001	0.69 \pm 0.01	0.92	0.71 \pm 0.02	1.03		
[BIM] [BF ₄]	0.044 \pm 0.002	0.41 \pm 0.02	0.71	0.30 \pm 0.03	0.73	0.063 \pm 0.002	0.72 \pm 0.02	0.97	0.66 \pm 0.01	0.92		
[C ₂ OHMIM] [BF ₄]	0.049 \pm 0.003	0.45 \pm 0.03	0.79	0.39 \pm 0.02	0.87	0.067 \pm 0.001	0.77 \pm 0.02	1.03	0.78 \pm 0.02	1.01		
[BMIM] [BF ₄]	0.063 \pm 0.003	0.59 \pm 0.03	1.02	0.64 \pm 0.03	1.08	0.068 \pm 0.002	0.77 \pm 0.03	1.05	0.77 \pm 0.02	1.00		
[OMIM] [BF ₄]	0.063 \pm 0.002	0.59 \pm 0.02	1.02	0.52 \pm 0.02	0.88	0.065 \pm 0.001	0.74 \pm 0.01	1.00	0.76 \pm 0.02	1.03		
[EMIM] [PF ₆]	0.063 \pm 0.002	0.59 \pm 0.02	1.02	0.51 \pm 0.03	0.86	0.069 \pm 0.002	0.78 \pm 0.03	1.06	0.80 \pm 0.02	1.03		
[C ₂ OHMIM] [PF ₆]	0.050 \pm 0.004	0.47 \pm 0.03	0.81	0.46 \pm 0.05	0.98	0.066 \pm 0.003	0.75 \pm 0.04	1.02	0.82 \pm 0.03	1.09		
[BMIM] [PF ₆]	0.061 \pm 0.003	0.57 \pm 0.03	0.98	0.51 \pm 0.03	0.89	0.068 \pm 0.002	0.77 \pm 0.02	1.05	0.77 \pm 0.01	1.00		
[OMIM] [PF ₆]	0.046 \pm 0.002	0.43 \pm 0.02	0.74	0.62 \pm 0.06	1.44	0.059 \pm 0.003	0.67 \pm 0.04	0.91	0.80 \pm 0.03	1.19		
[BMIM] [Tf ₂ N]	0.077 \pm 0.002	0.72 \pm 0.02	1.24	0.55 \pm 0.07	0.76	0.075 \pm 0.002	0.85 \pm 0.02	1.15	0.81 \pm 0.02	0.95		
[OMIM] [Tf ₂ N]	0.058 \pm 0.003	0.54 \pm 0.02	0.94	0.66 \pm 0.04	1.22	0.055 \pm 0.003	0.62 \pm 0.03	0.85	0.75 \pm 0.03	1.21		
[E ₂ -MPy] [ESO ₄]	0.063 \pm 0.002	0.59 \pm 0.02	1.02	0.63 \pm 0.02	1.07	0.062 \pm 0.002	0.70 \pm 0.02	0.95	0.70 \pm 0.01	1.00		
[E ₃ -MPy] [ESO ₄]	0.030 \pm 0.004	0.28 \pm 0.03	0.48	0.25 \pm 0.02	0.89	0.054 \pm 0.002	0.61 \pm 0.02	0.83	0.60 \pm 0.01	0.98		

Mean value \pm SE, $n = 10$.

The positive impact of [BMIM][BF₄], [E₂-MPy][ESO₄], [OMIM][PF₆] and [OMIM][Tf₂N] on TMOS/Glycerol matrices, was also observed on the high α -L-rhamnosidase reuse efficiency average (Table 4.14). The TMOS/Glycerol matrices produced without IL, after fifty runs, led to a 40% α -L-rhamnosidase inactivation 40% (1st run 0.58 and 50th 0.37), while matrices with incorporated ILs, as [E₂-MPy][ESO₄], [BMIM][BF₄] and [OMIM][Tf₂N] allowed an increase in the average reuse efficiency, respectively, of 29%, 31% and 35% (Figure 4.16 and Table 4.14), comparing with sol-gel matrices without ILs.

In the case of β -D-glucosidase activity almost all TMOS/Glycerol/ILs matrices led to average efficiencies around 70-75%, with the exception of [E₃-MPy][SO₄] (Figure 4.17 and Table 4.14). [C₂OHMIM][PF₆] allowed the best average reuse efficiency (0.82) which was 12% higher than the matrix without IL.

4.3.3.2 Influence of ILs on the sol-gel matrices structure and properties

The sol-gel matrices that showed the best average reuse efficiency for each enzymatic activity were chosen for further studies, which includes the matrices produced with TMOS/Glycerol/[OMIM][Tf₂N] in the case of α -L-rhamnosidase activity and TMOS/Glycerol/[C₂OHMIM][PF₆] in the case of β -D-glucosidase. The macroscopic structure of these hydrogel matrices was translucent without cracking, except for [OMIM][Tf₂N] sol-gel matrices that showed some opacity (Figure 4.18). Indeed after several reutilizations the lens became also translucent; showing an increase on α -L-rhamnosidase (Figure 4.16) and β -D-glucosidase (Figure 4.17) activities. Figure 4.18, also highlights the higher mechanical resistance against cracking after fifty runs of the matrix produced with [OMIM][Tf₂N] (III₅₀) when comparing with the other two matrices: I₅₀ (TMOS/Glycerol) and II₅₀ (TMOS/Glycerol/[C₂OHMIM][PF₆]), which show a markedly cracked structure after fifty reutilizations. The matrix integrity is a crucial criterion in a bioprocess implementation, namely at large scale, in order to avoid enzyme loss between batches.

Figure 4.19 shows SEM micrographs of matrices produced with TMOS/Glycerol, TMOS/Glycerol/[C₂OHMIM][PF₆] and TMOS/Glycerol/[OMIM][Tf₂N]. The porosity of TMOS/Glycerol matrices, in the first use and after 50 consecutive reutilizations, respectively, I and I₅₀, showed a finer structure with porosity (average dimension of the pores) of 20 – 30 nm (Figure 4.19). The SEM micrographs of

TMOS/Glycerol/[C₂OHMIM][PF₆] matrices, before and after 50 reutilizations (II₁ and II₅₀), showed matrices of the same type, porous, in which the structure after successive uses II₅₀ is finer than II₁. The matrices of TMOS/Glycerol/[OMIM][Tf₂N] (III₁ and III₅₀) showed a sandwich like structure where two films (one in each side) and the inside with a porous structure can be observed (Figure 4.20). The interior of matrix TMOS/Glycerol/[OMIM][Tf₂N] (in the first use) (I₁) is a compact material with a dispersion of closed bubbles, of IL ([OMIM][Tf₂N]) with non-uniform size. The bubbles show a spherical inner aspect. Apparently there is a surface film. The same matrix, but after successive reutilizations, III₅₀, has a similar structure, with some large bubbles, but with regions of bubbles of smaller and more uniform size. The wall thickness of the bubbles in matrix III₅₀ varies between 0.5 to 1 μm. From the first use (III₁) to the fifth (III₅₀) there was a refinement of the structure, becoming more uniform. This behaviour is characteristic of the dispersion of a hydrophobic compound (e.g. IL, [OMIM][Tf₂N]) in a hydrophilic matrix (e.g. TMOS/Glycerol). In conclusion, clearly the matrices III₁ and III₅₀ presented a microstructure with closed bubbles but with different sizes. This modification of the matrix may play an important role on enzyme efficiency, as well as on the enzyme/matrix interactions.

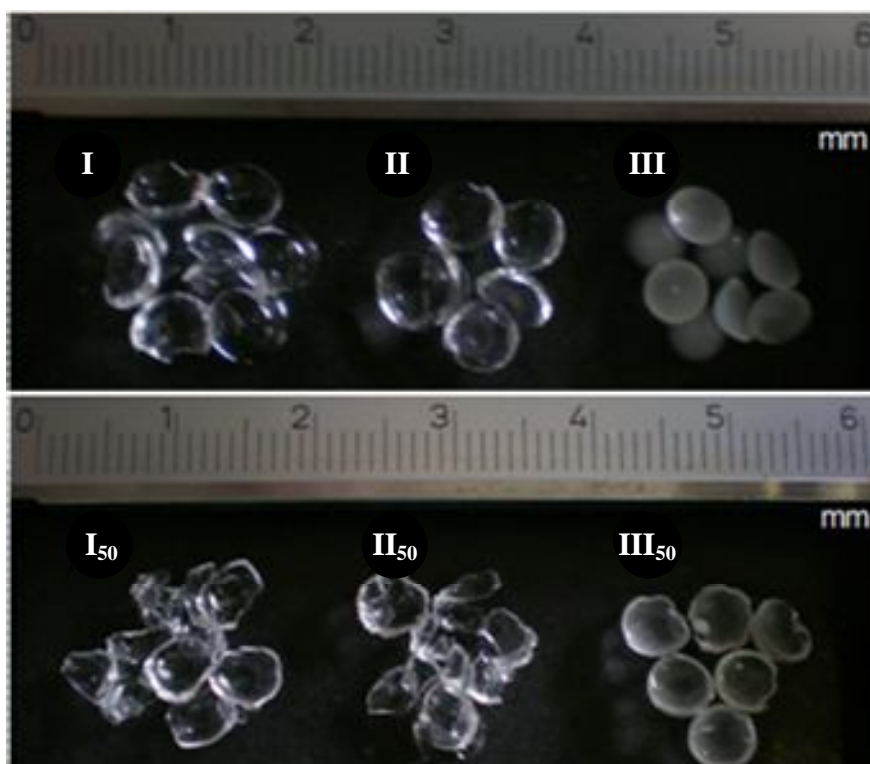


Figure 4.18 Macroscopic structure of matrices before use: **I** (TMOS/Glycerol), **II** (TMOS/Glycerol/[C₂OHMIM][PF₆]) and **III** (TMOS/Glycerol/[OMIM][Tf₂N]); and matrices reused over 50 runs: **I₅₀** (TMOS/Glycerol), **II₅₀** (TMOS/Glycerol/[C₂OHMIM][PF₆]) and **III₅₀** (TMOS/Glycerol/[OMIM][Tf₂N]).

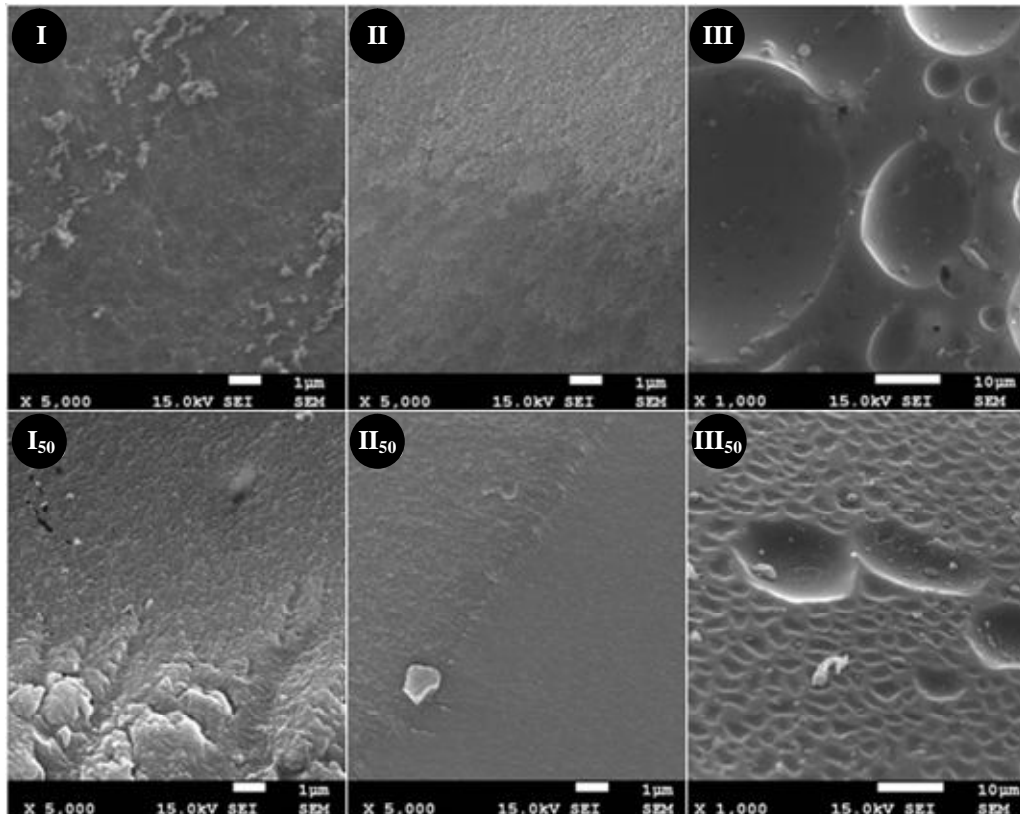


Figure 4.19 SEM microphotographs of matrices before use: **I** (TMOS/Glycerol), **II** (TMOS/Glycerol/[C₂OHMIM][PF₆]) and **III** (TMOS/Glycerol/[OMIM][Tf₂N]); and matrices reused over 50 runs: **I₅₀** (TMOS/Glycerol), **II₅₀** (TMOS/Glycerol/[C₂OHMIM][PF₆]) and **III₅₀** (TMOS/Glycerol/[OMIM][Tf₂N]).

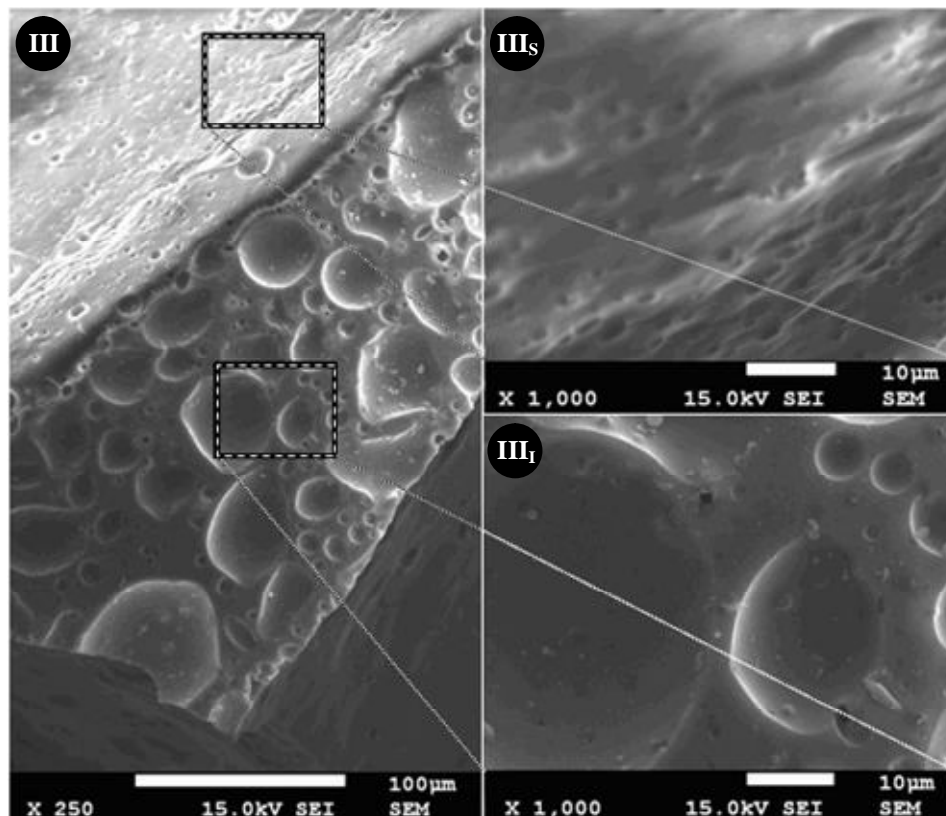


Figure 4.20 SEM structure detail of the sol-gel matrix **III** (TMOS/Glycerol/[OMIM][Tf₂N]). **III_s** corresponds to the surface of the lens while **III_i** is the inner part of the matrix.

SEM analysis showed that matrices (I, II and III) are shaped lens with a film structure which varies within the lens, depending on the nature of ILs. The microstructure of the lens varies from granular to porous, depending on the material type. Additionally, some physical properties of the matrices, like partition coefficients (Table 4.15), diameter, volume, density were evaluated (Table 4.16).

Table 4.15. Partition coefficients between matrix and 20 mM acetate buffer, pH 4, of the substrates and products used in this study.

Sol-gel matrices	$P_{m/s}$					
	Naringin	Prunin	Naringenin	4-NRP	4-NGP	4-Nitrophenol
TMOS/Glycerol	0.57 ± 0.04	0.53 ± 0.03	0.56 ± 0.03	0.74 ± 0.05	0.82 ± 0.04	0.87 ± 0.04
TMOS/Glycerol/ [C ₂ OHMIM][PF ₆]	0.47 ± 0.03	0.48 ± 0.03	0.53 ± 0.03	0.86 ± 0.04	0.92 ± 0.05	1.04 ± 0.02
TMOS/Glycerol/ [OMIM][Tf ₂ N]	0.42 ± 0.02	0.42 ± 0.05	0.49 ± 0.02	0.41 ± 0.04	0.47 ± 0.04	0.68 ± 0.05

Mean value ± SE, *n* = 6.

Table 4.16 Physical properties of TMOS/Glycerol/[OMIM][Tf₂N], TMOS/Glycerol/[C₂OHMIM][PF₆] and TMOS/Glycerol matrices.

Sol-gel matrix	D_m (mm)	V_m (μL)	w_m (mg)	d_m (g mL ⁻¹)	V_{is} (μL)
TMOS/Glycerol	5.34 ± 0.05	19.3 ± 0.7	19.6 ± 0.5	1.02 ± 0.05	13.0 ± 0.4
TMOS/Glycerol/[C ₂ OHMIM][PF ₆]	5.36 ± 0.05	20.8 ± 0.7	21.4 ± 0.8	1.03 ± 0.03	14.9 ± 0.5
TMOS/Glycerol/[OMIM][Tf ₂ N]	4.60 ± 0.02	17.2 ± 0.9	18.1 ± 0.2	1.06 ± 0.06	10.7 ± 0.2

Mean value ± SE, *n* = 6.

The substrate concentration achieved inside the matrix is important for enzyme activity once the enzyme movement is restricted within the semi-solid structure. The partition coefficient ($P_{m/s}$) of 4-NRP and 4-NGP using the TMOS/Glycerol, TMOS/Glycerol/[C₂OHMIM][PF₆] and TMOS/Glycerol/[OMIM][Tf₂N] matrices were determined according to Equation 4.2 (Table 4.15). A slight increase in the partition coefficients of TMOS/Glycerol/[C₂OHMIM][PF₆] matrices were obtained, comparing with TMOS/Glycerol matrices. As both matrices have hydrophilic characteristics, this difference may be due to the presence of a nitro group in 4-nitrophenol derived substrates, which is a strong electron-attracting group that may interact through electrostatic interactions (Liu *et al.*, 2005a, b) with the IL present within the matrix.

According to this a substrate concentration increase inside the matrix is expected (Table 4.15). Moreover, lower partition coefficients were accomplished with TMOS/Glycerol/[OMIM][Tf₂N] than with TMOS/Glycerol matrices; which is in agreement with the hydrophobic characteristics of [OMIM][Tf₂N] (Table 4.15).

The TMOS/Glycerol and TMOS/Glycerol/[C₂OHMIM][PF₆] matrices, the more hydrophylic matrices, showed similar properties (Table 4.16). A small decrease in TMOS/Glycerol/[OMIM][Tf₂N] matrix diameter caused a decrease in matrix volume (Figure 4.18, Table 4.15). Moreover, the three matrices showed similar densities.

In conclusion, the ILs as additives of TMOS/Glycerol sol-gel matrices had a higher impact on the activity and stability of α -L-rhamnosidase than on β -D-glucosidase expressed by naringinase. Regarding the higher efficiencies of the sol-gel matrices produced with [OMIM][Tf₂N] and [C₂OHMIM][PF₆], they were chosen for the hydrolysis of flavone glycosides including naringin and prunin.

4.3.3.3 Kinetic study of naringin and prunin bioconversion

Naringin was bioconverted into prunin, using α -L-rhamnosidase activity, expressed by naringinase immobilized, within sol-gel matrices of TMOS/Glycerol/[OMIM][Tf₂N] and TMOS/Glycerol (Figure 4.21a). Its kinetic parameters were determined. Moreover, kinetic parameters of prunin hydrolysis into naringenin by means of β -D-glucosidase, expressed by naringinase, immobilized within sol-gel matrices of TMOS/Glycerol/[C₂OHMIM][PF₆] and TMOS/Glycerol were also evaluated (Figure 4.21b). The kinetic profile of both naringin and prunin hydrolysis using free and immobilized naringinase obeys to the Michaelis-Menten model. According to the results shown on Figure 4.21a and Table 4.17 a slight increase in K_M , similar k_{cat} and a sharp decrease of the catalytic efficiency ($k_{cat} \cdot K_M^{-1}$) was obtained for α -L-rhamnosidase encapsulated within TMOS/Glycerol/[OMIM][Tf₂N], when comparing with TMOS/Glycerol matrix. The increase of K_M reflects changes in the affinity of enzyme for naringin, which supports hydrophobic interactions involved in the enzyme-substrate complex formation, due to the more hydrophobic characteristics of this IL. In addition, the partition coefficient of naringin, prunin and naringenin decreased with the addition of [OMIM][Tf₂N] to TMOS/Glycerol matrices (Table 4.15), which, is also supported by the hydrophobic characteristic of [OMIM][Tf₂N].

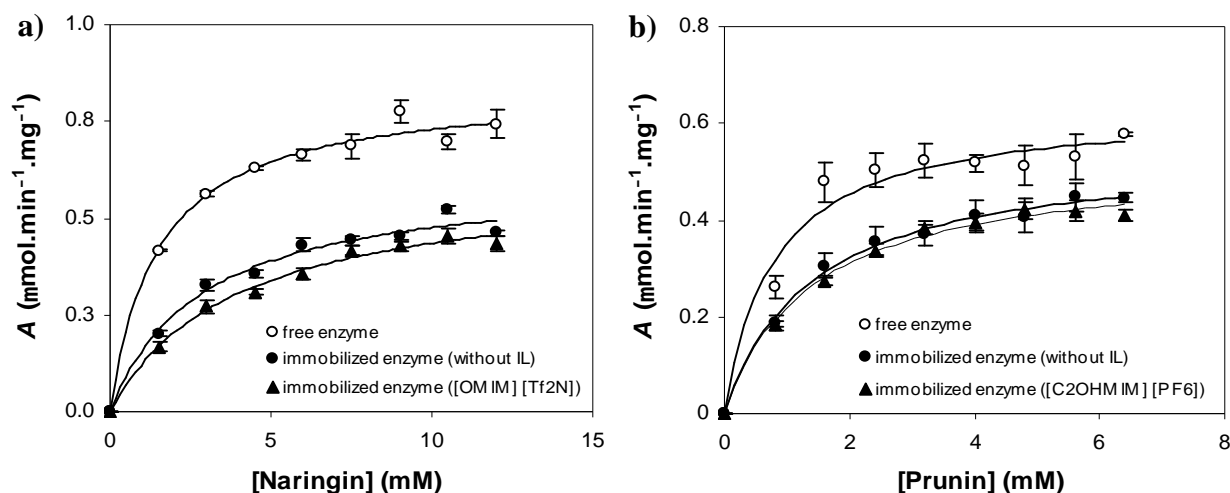


Figure 4.21 a) Michaelis-Menten kinetics of naringin hydrolysis into prunin by α -L-rhamnosidase b) Michaelis-Menten kinetics of prunin hydrolysis into naringenin by β -D-glucosidase (mean value \pm SE, $n = 3$).

Table 4.17 Kinetic parameters of the hydrolysis of naringin and prunin by α -L-rhamnosidase and β -D-glucosidase using free and immobilized naringinase within sol-gel matrices.

Substrate	Naringinase	k_{cat} ($\mu\text{mol min}^{-1} \text{mg}^{-1}$)	K_M (mM)	$k_{cat} \cdot K_M^{-1}$ ($\text{L min}^{-1} \text{g}^{-1}$)	y (%)	R^2
Naringin	Free	0.84 ± 0.03	1.51 ± 0.14	0.56	-	0.999
	TMOS/Glycerol	0.62 ± 0.02	3.06 ± 0.26	0.20	92	0.995
	TMOS/Glycerol/ [OMIM] [Tf ₂ N]	0.61 ± 0.05	3.97 ± 0.60	0.15	92	0.997
Prunin	Free	0.63 ± 0.02	0.81 ± 0.10	0.78	-	0.999
	TMOS/Glycerol	0.55 ± 0.03	1.42 ± 0.24	0.38	92	0.999
	TMOS/Glycerol/ [C ₂ OHNIN] [PF ₆]	0.53 ± 0.02	1.38 ± 0.09	0.38	100	0.997

Mean value \pm SE, $n = 3$.

Prunin hydrolysis, by β -D-glucosidase immobilized within TMOS/Glycerol/[C₂OHNIN][PF₆] and TMOS/Glycerol led to similar K_M , k_{cat} and catalytic efficiency ($k_{cat} \cdot K_M^{-1}$). The prunin partition coefficient of TMOS/Glycerol/[C₂OHNIN][PF₆] and TMOS/Glycerol matrices (Table 4.15) almost did not change (0.48 ± 0.03 and 0.53 ± 0.03). Indeed the TMOS/Glycerol/[C₂OHNIN][PF₆] matrix shows hydrophilic characteristics as TMOS/Glycerol matrix.

When the kinetic parameters of encapsulated naringinase are compared to those obtained with soluble enzyme, mass transfer effects seem to occur in all cases of immobilized enzyme, resulting in lower k_{cat} and $k_{\text{cat}} \cdot K_{\text{M}}^{-1}$.

The high immobilization yield (> 90%) for all three sol-gel matrices (TMOS + Glycerol without IL, with [OMIM][Tf₂N] and with [C₂OHMIM][PF₆]) indicates a small loss of enzyme during the immobilization procedure.

4.3.3.4 Pressure influence on the stability of immobilized naringinase

Preliminary assays were made, concerning the influence of pressure on the stability of immobilized naringinase. A pressure magnitude of 150 MPa was used to accomplish these assays. The matrices studied were made of TMOS/Glycerol, TMOS/Glycerol/[OMIM][Tf₂N] and TMOS/Glycerol/[C₂OHMIM][PF₆]. In the case of the matrix made of TMOS/Glycerol both the stabilities of α -L-rhamnosidase and β -D-glucosidase activities were investigated (Figure 4.22). Both activities show a similar behaviour. The matrices submitted to 150 MPa, as well as the matrices kept at atmospheric pressure show a constant residual activity along the six hour study. In the case of the pressurized matrices the residual activity was slightly lower than non-pressurized matrices. This fact is however not much relevant attending to the above mentioned fact of residual activity constancy during the assay. In addition the matrices showed to be mechanical resistant against such a high pressure magnitude of 150 MPa.

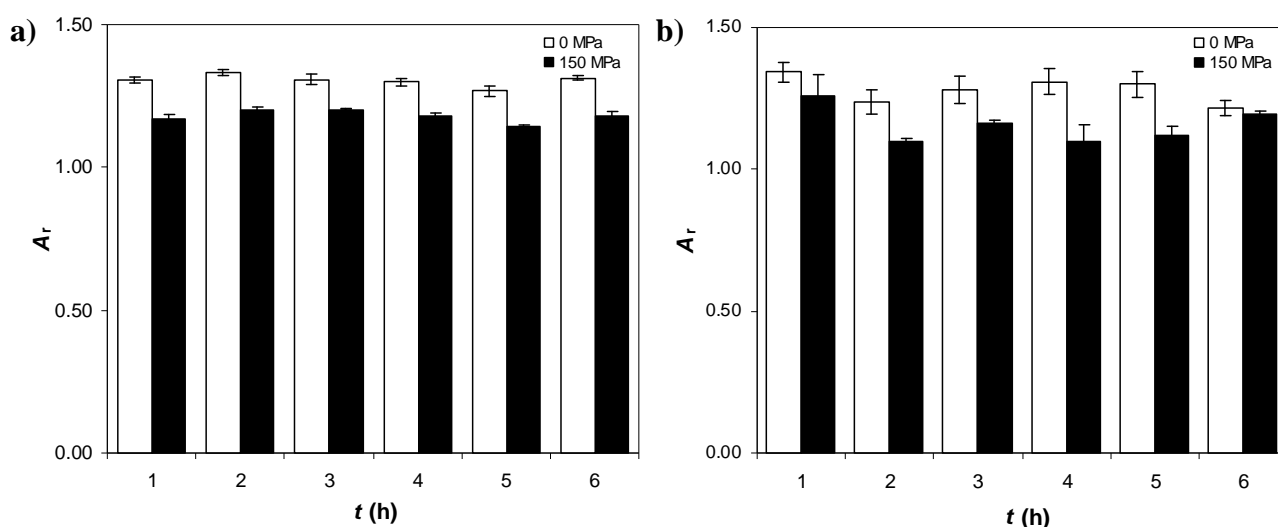


Figure 4.22 Residual activity of α -L-rhamnosidase (a) and β -D-glucosidase (b), from immobilized naringinase entrapped within a TMOS/Glycerol matrix, under 0 or 150 MPa, at 50.0 °C.

Considering the good results of α -L-rhamnosidase activity inside a matrix made of TMOS/Glycerol/[OMIM][Tf₂N], the influence of pressure on its residual activity was also investigated. Interestingly, regarding Figure 4.23 it seems that in this case pressurized matrices not only show a constant residual activity along the 4 hours assay, but also have a higher residual activity than non-pressurized matrices. In addition in the case of matrices kept at atmospheric pressure seems to occur a decrease of the residual activity. An eventual protecting effect of pressure against inactivation may have occurred.

In the case of matrices made of TMOS/Glycerol/[C₂OHMIM][PF₆], it happened that they were crashed by pressure at a magnitude of 150 MPa.

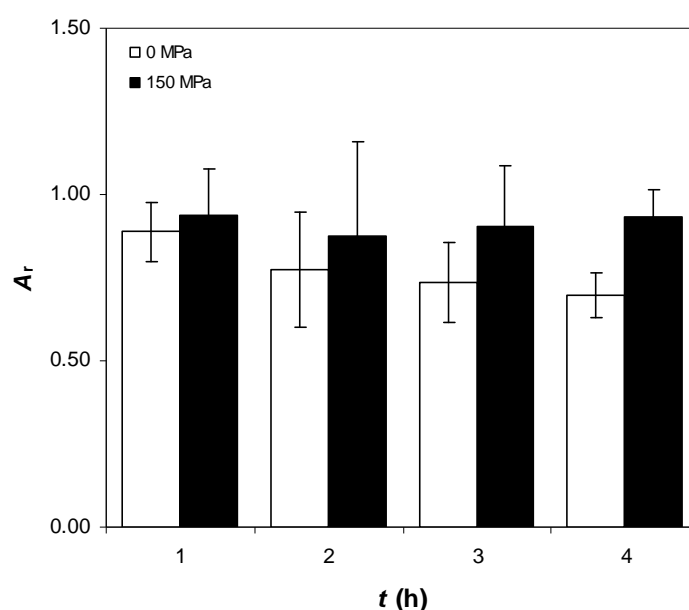


Figure 4.23 Residual activity of α -L-rhamnosidase, from immobilized naringinase entrapped within a TMOS/Glycerol/[OMIM][Tf₂N] matrix, under 0 or 150 MPa, at 50.0 °C.

4.4. Conclusions

Glycerol and DGS respectively present on matrices B (TMOS/glycerol) and D (TMOS/DGS), were able to improve immobilization using TMOS. Aging time was an important parameter for improving sol-gel encapsulated naringinase activity. The best results were obtained with TMOS and TMOS/DGS after 4 h and TMOS/glycerol and DGS at 14 h aging time. Also the immobilization conditions of matrices B and D made them the best matrices, with very high immobilization yields (89% and 92%, respectively) and efficiency (72% and 76%, respectively). At an optimum pH of 4.3, a maximum naringinase specific activity of $0.86 \mu\text{mol min}^{-1} \text{mg}^{-1}$ was obtained with the enzyme immobilized within matrices A (TMOS) and D (TMOS/DGS).

Matrix B remained without any activity loss and 100% residual activity after 50 successive reutilizations. Both matrix B and D showed outstanding naringinase operational stability due to a long-term activity and resistance to leaching, which are two major requirements for bio-immobilization, contributing to the importance and innovation of this work.

Naringinase improved stability was achieved against several organic cosolvents studied. Aqueous cosolvent systems were developed, possessing a high enzyme retention activity. In all cosolvent systems tested a decrease in the inactivation parameters k_1 and k_2 occurred along with a correspondent increase of the half-life time in the case of sol-gel immobilized naringinase, reflecting an improved stabilization. Beyond the possible restriction effect against protein unfolding caused by the immobilization method itself, the presence of glycerol within de sol-gel glasses, known to be a stabilizer of the protein structure, is certainly behind the stabilization effect of this sol-gel glasses (TMOS/glycerol).

For all the aqueous cosolvents systems studied a half-life time increase, greater than 3 fold, was observed for the immobilized naringinase, comparing with the soluble enzyme. The sol-gel protective effect was very pronounced at the highest cosolvent concentrations tested (10 %), as shown by the half-life times increase of the immobilized β -D-glucosidase activity, respectively, 13, 14, 24 and 59-fold for 1,4 dioxane; 1,2 dimethoxyethane; *N,N*-dimethylacetamide and tetrahydrofuran. Furthermore, the cosolvent system consisting of 1,2 dimethoxyethane showed to be a very interesting system for the hydrolysis of flavone rutinosides, such as naringin.

This study also showed that an IL content of 3% w/w can influence the enzymatic reuse efficiency; being mainly incorporated in the silica sol. The addition of the ILs: [OMIM][Tf₂N] and [C₂OHMIM][PF₆] to the sol-gel matrices increased not only the efficiency of respectively 4-NRP and 4-NGP hydrolysis, but reduced the enzyme inactivation that occurred in TMOS/Glycerol matrices. In addition, the presence of the IL [OMIM][Tf₂N] within the sol-gel matrices led to a higher mechanical resistance against cracking, which is important for industrial purposes. The macroscopic evaluation and SEM analysis showed that [OMIM][Tf₂N] greatly influence the characteristics of the matrices, more robust and with regions of bubbles of smaller and more uniform size after several reutilizations, characteristic of a hydrophobic compound dispersion in a hydrophilic matrix. Moreover, ILs were also important to modulate the substrate and products partition between solvent and matrix acting as partition controlling agents.

ILs as well as glycerol, used as template agents to produce nanostructured sol-gel matrices, improved the immobilization efficiency and stability of α -L-rhamnosidase and β -D-glucosidase expressed by naringinase. ILs influenced the structural characteristics of the sol-gel matrix suggesting that they play an important role in enzyme performance and on the high efficiency and stability achieved; which highlights the potential of this strategy for the finer tuning of the encapsulated enzymes properties within sol-gel/ILs matrices.

In addition, considering the study of immobilized naringinase under pressure is important to point out the mechanical resistance and good stability profile of naringinase immobilized within TMOS/Glycerol and TMOS/Glycerol/[OMIM][Tf₂N] matrices, under high-pressure conditions.

**STUDY OF THE FLAVANONES: NARINGIN, PRUNIN AND
NARINGENIN IN CELL CULTURE AND ANIMAL MODELS**

Chapter 5

5.1 Introduction

Inflammation is present in AD pathology and some anti-inflammatory approaches have been proposed to treat AD (*cf.* 1.2.2.3). Also, as described on 1.3.2, anti-inflammatory activity is a common pharmacological activity shared by flavonoids. Both naringin (*cf.* 1.3.2.1) and naringenin (*cf.* 1.3.2.3) are reported to possess anti-inflammatory activity. In line with this, is important to evaluate their activity in CNS cells.

The anti-inflammatory activity of a certain compound can be evaluated through the reduction of TNF- α secretion after stimulation with lipopolysaccharide (LPS). TNF- α is among the best characterized early response cytokines (Saliba and Henrot, 2001), produced by cells of the central nervous system responsible for proinflammatory action (Quan *et al.*, 1999). LPS induces the release of TNF- α in nerve cells such as astrocytes (Fernandes *et al.*, 2004) and indomethacin was pointed to abrogate this effect (Repovic and Benveniste, 2002). The aim of this study, concerning this cell culture model, is to determine the efficacy of the anti-inflammatory properties of both naringin and naringenin in LPS-stimulated astrocytes and to establish the efficiency of each compound relatively to that of indomethacin.

From another point of view, it's important to study whether the flavanones: naringin, prunin and naringenin or some of their metabolites can cross the BBB and reach the brain. The analysis of their distribution in plasma and brain may elucidate the potential role of these compounds to reach and act on a brain disease, such as AD.

The route of administration of a certain compound may decisively influence the therapy success. Concerning these compounds regardless of the oral administration of naringin, prunin or naringenin the observed circulating metabolites are glucuronoconjugates, sulfates and glucuronosulfoconjugated of naringenin (Felgines *et al.*, 2000; Wang *et al.*, 2006b); naringenin glycosides, naringin and prunin, are not detected in plasma nor in urine (Felgines *et al.*, 2000). In the case of naringin is suggested that it is hydrolyzed to its corresponding aglycone by glycosidases produced by intestinal bacteria (Felgines *et al.*, 2000). Also, Hsiu *et al.* (2002) found that after oral administration of naringin an extensive glucuronidation and sulfation must occur during the first pass in the gut wall. In the case of prunin, both human cytosolic β -glucosidase (hCBG) and lactase-phlorizin hydrolase (LPH) may be responsible for its hydrolysis. hCBG is located intracellularly (Nemeth *et al.*, 2003) and is a xenobiotic metabolizing enzyme that shows high

specificity for 4- and 7-glucosides of isoflavones, flavonols, flavones and flavanones and is present in the liver, kidney, intestine and spleen of humans (Glew *et al.*, 1993). LPH is anchored in the mucosal membrane in the brush-border of the small intestine (Zecca *et al.*, 1998; Hollox *et al.*, 2001). LPH is also a human β -glucosidase that hydrolyses a broad range of flavonoid glucosides, including flavonols, flavones, flavanones, and isoflavones (Nemeth *et al.*, 2003).

Following this, intraperitoneal administration was used in the animal model, in order to avoid the reported first pass metabolism that may occur in the gut wall. After intraperitoneal administration, each flavanone: naringin, prunin and naringenin, is quickly absorbed into the bloodstream. Within the bloodstream, it is then possible to study the influence of the structural differences of these flavanones on their distribution into the brain. The aim of this study, concerning the animal model, is to show the advantage of using aglycones and glucosides to cross the BBB, instead of rutinosides, in order to treat AD. On the basis of this idea is a possible passive diffusion of hydrophobic aglycones across the BBB and also an eventual transport of glucosides, through receptors recognition, as described on 1.3.4. In preliminary studies the flavanones naringin, prunin and naringenin were studied. The administration of these compounds to the animal model, and their determination as well as possible metabolites in plasma and brain may be helpful to determine whether these hypothesis are correct.

5.3 Material and methods

5.2.1 Chemicals

Naringin, naringenin and daidzein were purchased from Sigma-Aldrich. Prunin was biosynthesized according to the method described on Chapter 2. Dulbecco's modified Eagle's medium (DMEM) and fetal calf serum (FCS) were purchased from Biochrom AG (Berlin, Germany). Antibiotic antimycotic solution and rabbit antibody anti-gial fibrillary acidic protein (GFAP) were acquired from Sigma (St. Louis, MO, USA). The monoclonal antibody against the CR3 complement receptor of microglia (OX-42) was obtained from Serotec (Raleigh, NC, USA). Recombinant TNF- α was purchased from R&D Systems (Minneapolis, MN, USA). *Escherichia coli* O111:B4 (LPS) was purchased from Calbiochem (La Jolla, CA, USA), dissolved at 1 mg mL⁻¹ in phosphate buffered saline (PBS) at pH 7.4 and kept at 4 °C.

All other chemicals were analytical grade and obtained from various sources.

5.2.2 Cell cultures

Astrocytes were isolated from 2-day-old rats according to Blondeau *et al.* (1993) and Silva *et al.* (1999). The brains of decapitated rats were collected in DMEM containing 11 mM sodium bicarbonate, 71 mM glucose and 1% antibiotic antimycotic solution. Following this, meninges, blood vessels and white matter were removed. The neocortices were homogenized by mechanical fragmentation and the cells collected by centrifugation at 700 g for 10 min. Finally, cells were resuspended in culture medium supplemented with 10% FCS, plated (2.0×10^5 cells cm⁻²) on 12-well tissue culture plates (Corning Costar, Cambridge, MA, USA) and cultured for 10 days. Microglial contamination was assessed by immunocytochemical staining using primary antibodies raised against OX-42 (mouse) (Liu *et al.*, 2002) and GFAP (rabbit), followed by a species-specific fluorescent-labeled secondary antibody, and was inferior to 2.5%. Thus, the high purity level of astrocyte cultures excludes interference of contaminant microglial cells that would account for the released cytokines (Hanisch, 2002; Nakamura *et al.*, 2003; Fernandes *et al.*, 2004).

Primary cultures of rat cortical astrocytes were incubated for 4, 8 and 24 h with 100 ng mL⁻¹ LPS, 100 μ g mL⁻¹ indomethacin, 3.2 μ g mL⁻¹ naringin or 10 μ g mL⁻¹ naringenin, at 37°C. In sister cultures cells were incubated with LPS + naringin, LPS +

indomethacin or LPS + naringenin. In addition both naringin and naringenin were studied in a 1/10 dilution. Cytokine release was assessed by ELISA.

5.2.3 Animals

Male mice ($n = 32$, 8 – 12 weeks, weighing 25 – 35 g) were purchased from Harlan Ibérica, Barcelona, Spain. All animals received a standard diet and water ad libitum. Experiments were conducted according to the Home Office Guidance in the Operation of Animals (Scientific Procedures) Act 1986, published by Her Majesty's Stationary Office, London, UK and the Institutional Animal Research Committee Guide for the Care and Use of Laboratory Animals published by the US National Institutes of Health (NIH Publication No. 85-23, revised 1996), as well as to the EC regulations (O.J. of E.C. L 358/1 18/12/1986).

Before experiments animals fasted for 24h. A solution of saline/DMSO (9:1, v/v) was used for the preparation of all solutions. Naringin, prunin and naringenin were intraperitoneally (i.p.) injected at a dose of $40 \mu\text{mol kg}^{-1}$ mM.

5.2.4 Distribution studies

Eight mice were used to study each of the three substances (naringin, prunin and naringenin). Experiments were done in duplicate. Mice were sacrificed at 0.25, 0.5, 1 and 4 hours after dosing and were previously anesthetized with sodium pentobarbital (6 mg kg^{-1} i.p.) for collection of blood by cardiac puncture and brain tissue was perfused by intraventricular injection of 5 mL of chilled saline solution to remove residual blood.

5.2.5 Blood sample preparation

Serum was isolated from the blood samples by centrifugation at $657 g$ for 10 min, at 4°C (Li *et al.*, 2007). Serum was stored at -20°C prior to extraction. $10 \mu\text{L}$ of the internal standard solution, daidzein, ($10 \mu\text{g mL}^{-1}$) were added to $100 \mu\text{L}$ of serum sample and also $10 \mu\text{L}$ of an acetic acid/water (1:2) (v/v) solution (Li *et al.*, 2004). $400 \mu\text{L}$ of acetone were added to serum sample, and samples were shaken using vortex (15''). The homogenate was centrifuged at $1500 g$ for 5 min at 4°C (Mullen *et al.*, 2009). The supernatants were evaporated under a flow of nitrogen gas 30°C till approximately $50 \mu\text{L}$. The aqueous phase was extracted with $400 \mu\text{L}$ of ethyl acetate.

Extraction was performed by mixing the tubes for 1.5 min, followed by centrifugation for 2 min at 16000 g. The organic layer was transferred into a clean tube and dried under a flow of nitrogen gas 30°C. Samples were stored at -20°C prior analysis.

5.2.6 Brain sample preparation

Brain was promptly removed and washed with saline (PBS) and blotted dry. Meninges were removed. Brain was weighted (Mullen *et al.*, 2009). Brain samples were stored at -20°C prior to extraction. The brain was diluted with 2 volumes (*V/w*) of phosphate buffer solution containing 0.1% EDTA and the internal standard, daidzein, ($1 \mu\text{g mL}^{-1}$) (pH 7.4) (Mullen *et al.*, 2009), and was homogenized using firstly a pestle and then a pipette and finally a sonicator. 600 μL of acetone were added to the homogenate, and extraction occurred through shaking using vortex. The homogenate was centrifuged at 1500 g for 5 min at 4°C (Mullen *et al.*, 2009). The supernatants were evaporated under a flow of nitrogen gas 30°C till approximately 150 μL . The aqueous extract was acidified with 15 μL of acetic acid/water (1:2) (v/v) (Li *et al.*, 2004). The aqueous phase was extracted with 600 μL of ethyl acetate. Extraction was performed by mixing the tubes for 1.5 min, followed by centrifugation for 2 min at 16000 g. The organic layer was transferred into a clean tube and dried under a flow of nitrogen gas 30°C. Samples were stored at -20°C prior analysis.

5.2.7 HPLC-MS analysis

The sample residues were reconstituted in 80 μL of acetonitrile plus 20 μL of formic acid solution (0.25%). The samples were centrifuged at 12000 rpm during 5 minutes (Biofuge).

The HPLC-DAD-ESI-MS/MS experiments used to identify the compounds (naringin, prunin, naringenin and their metabolites) were performed with a liquid chromatograph (Alliance, Waters 2695 Separation Module) system with a photodiode array detector (DAD, Waters 2996) set at 280 nm (for monitoring) in tandem with a mass spectrometer (Micromass Quattro Micro API) with a Triple Quadrupole (TQ) and an electrospray ion source (ESI) operating in negative mode. Chromatographic conditions were as follow: column C18 (Synergi, Phenomenex) 100 mm \times 2.0 mm, 2.5 μm ; eluent (A) water-formic acid (99.5:0.5, v/v), (B) acetonitrile (LC-MS grade, Merck). The linear gradient was at initial time 95 % eluent A, at 30 min 60 % eluent A, at 45 min 10 % eluent A.

The flow rate was 0.25 mL min^{-1} and the column temperature $35 \text{ }^\circ\text{C}$. Mass range was measured from 100-1000 amu. The ESI source conditions were adjusted as follows: source capillary operating at 2.5 kV and the extraction cone at 30 V: the source temperature was $150 \text{ }^\circ\text{C}$ and the desolvation temperature was $350 \text{ }^\circ\text{C}$.

The sample analysis in order to detect naringin, prunin and naringenin as well as its metabolites it was used the SIR method in negative mode for the molecular ions $[\text{M}-\text{H}^+]^-$ of each compound in analysis. The metabolites studied corresponded to glucorunoconjugates, sulfates and glucuronosulfoconjugated of the administered compounds.

5.3 Results and discussion

5.3.1 *In vitro* anti-inflammatory effect of naringin and naringenin

LPS induced a 10-fold maximum increase in the release of TNF- α at 24 h ($p < 0.05$). Naringin, as well as naringenin did not induce any increase in the cytokine secretion by astrocytes at 4, 8 and 24 h incubation, except in the case of naringin ($2.3 \mu\text{g L}^{-1}$) and naringenin (1 mg mL^{-1}). When astrocytes were co-incubated for 24 h, but not at 4 or 8 h, with LPS and naringin ($0.23 \mu\text{g mL}^{-1}$) a 2.5-fold decrease ($p < 0.10$) was noticed, while a 3.7-fold decrease ($p < 0.05$) was obtained for naringenin ($10 \mu\text{g mL}^{-1}$).

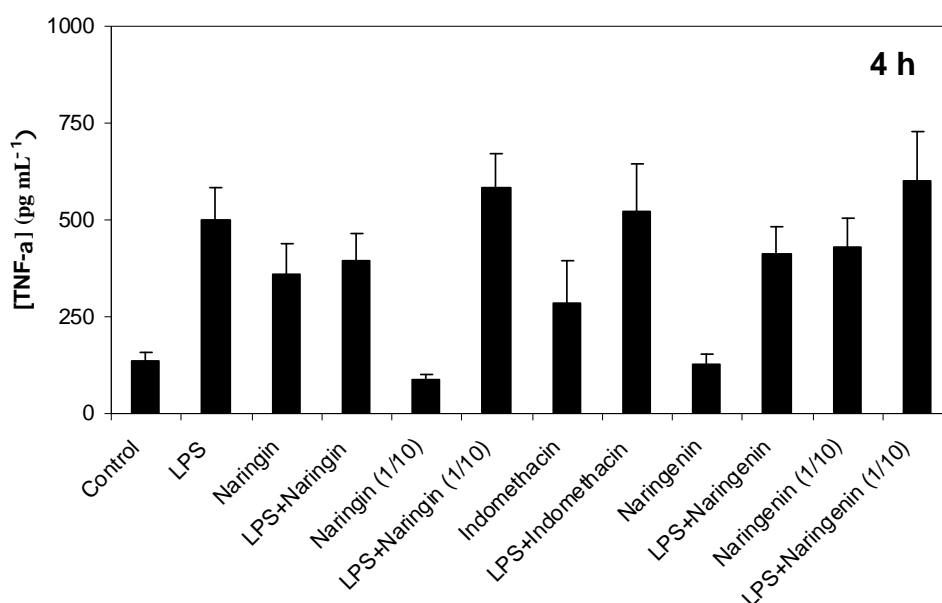


Figure 5.1 Determination of TNF- α concentration, after an incubation time period of 4h with: LPS, naringin, indomethacin and naringenin; as well as co-incubation of LPS with naringin, indomethacin and naringenin.

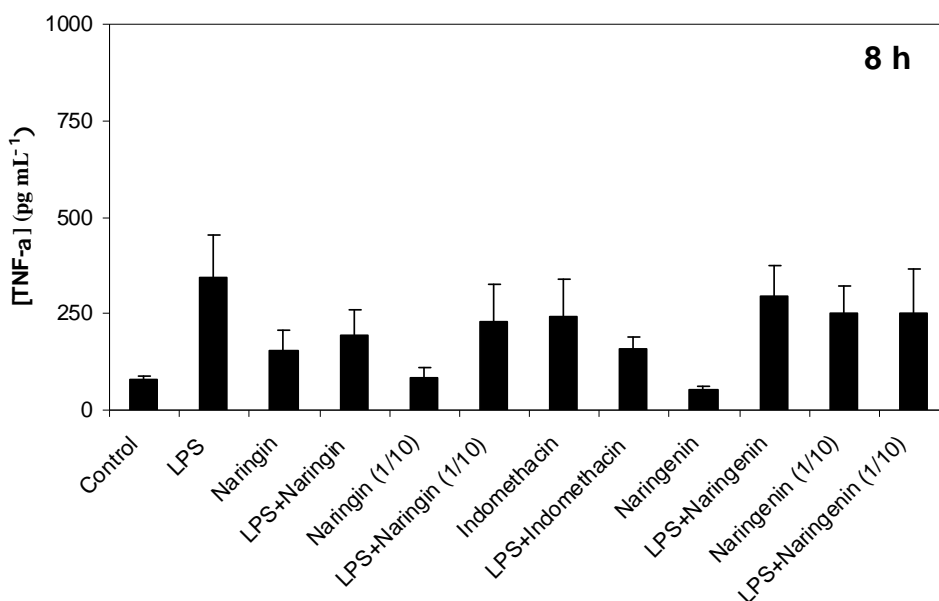


Figure 5.2 Determination of TNF- α concentration, after an incubation time period of 8h with: LPS, naringin, indomethacin and naringenin; as well as co-incubation of LPS with naringin, indomethacin and naringenin.

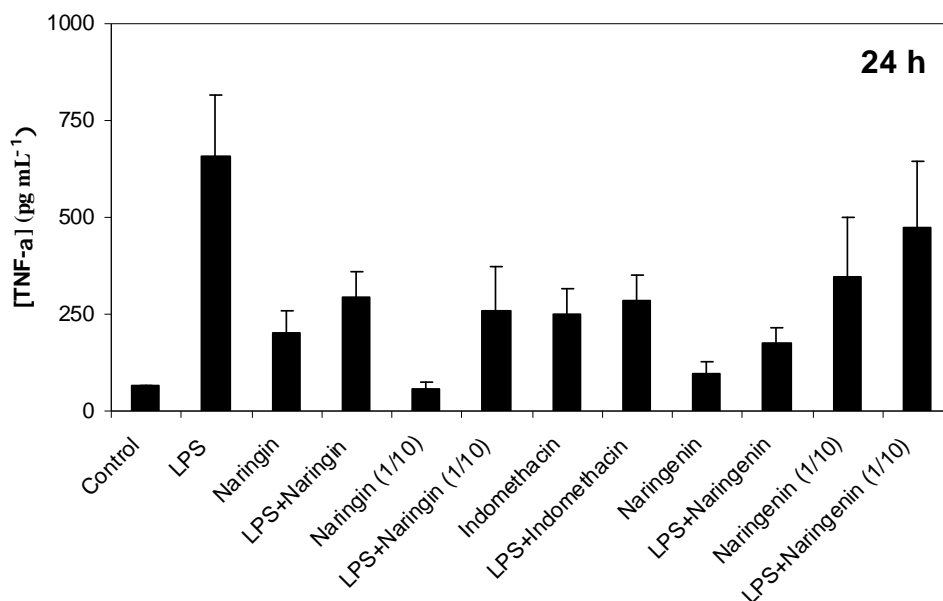


Figure 5.3 Determination of TNF- α concentration, after an incubation time period of 24h with: LPS, naringin, indomethacin and naringenin; as well as co-incubation of LPS with naringin, indomethacin and naringenin.

These anti-inflammatory effects were similar to those obtained in an *in vivo* model (Ribeiro *et al.*, 2008b) and reinforce a higher protection after 24 h of interaction. Interestingly, the levels of secreted TNF- α achieved in both conditions are not different from control values, what also agrees with the previous mentioned study. In addition, it is worthwhile to mention that the protection achieved by naringin ($0.23 \mu\text{g mL}^{-1}$) was at the same level as that produced by indomethacin at $100 \mu\text{g mL}^{-1}$, and that obtained by naringenin ($10 \mu\text{g mL}^{-1}$) was even better (40% increase).

5.3.2 Preliminary studies concerning the distribution of the flavanones: naringin, prunin and naringenin in plasma and brain of mice after intraperitoneal administration.

Naringin, prunin and naringenin were detected in plasma thirty minutes after intraperitoneal administration, but only prunin and naringenin were found in brain after this period (Annex 2). These preliminary results clearly demonstrate the capacity of both prunin and naringenin to cross the BBB, in opposition to naringin that wasn't found in brain. Comparing both prunin and naringin, it can be concluded that the glucose moiety of prunin plays an important role during the crossing of BBB, in opposition to the terminal rhamnase sugar moiety of naringin. One hypothetical scenario for the transport of prunin across the BBB is its active transportation by means of SLGT 1. Concerning naringenin, a possible way to cross the BBB is through passive

diffusion.

All the possible metabolites were analysed including: glucuronoconjugates, sulfates and glucuronosulfoconjugated and also the metabolites that result from the hydrolysis of the sugar moiety. The glucuronide of naringenin was found in all samples including both plasma and brain, which supports a metabolization of the flavanones into the aglycone naringenin which suffers glucuronidation afterwards. In the case of prunin administration, the glucuronide of naringenin, which was found in brain, supports hypothetical sequential steps of deglycosylation followed by glucuronidation of prunin. Glucocerebrosidase is a human β -glucosidase present in the brain that eventually may be responsible for the hydrolysis of the glucose moiety of prunin. Gee *et al.* (2000) reported a process for the intestinal epithelium passage of quercetin-3-glucoside that can be similar to what happens to prunin, where it is rapidly deglycosylated and then glucuronidated (Gee *et al.*, 2000).

5.4 Conclusions

In conclusion, although naringin and naringenin revealed to be effective anti-inflammatory agents on astrocyte reactivity to LPS, naringenin demonstrated a higher efficacy that even surpassed that of indomethacin, after an incubation period of 24 hours.

Preliminary studies focusing on the distribution of the studied flavanones in plasma and brain of mice support the hypothesis of using the glucoside prunin as well as the aglycone naringenin in a way to cross the BBB. In addition, the eventual transformation of prunin into naringenin inside the brain makes it a prodrug of naringenin.

These findings, together with those reported for the activity of naringenin against AD (*cf.* 1.3.2), place prunin and naringenin as potential useful drugs against AD.

GENERAL DISCUSSION

Chapter 6

This thesis reports several major biotechnological achievements in order to produce potential active drugs against AD. These achievements are mainly guided by a bioprocess optimization, consisting on the enzymatic deglycosylation of natural flavone glycosides, including naringin and rutin. An exception to this kind of achievements is found on Chapter 5, whose main purpose consists on filling the gap between research and therapeutics.

Focusing on bioprocess optimization, the achievements can be divided into three conducting wires that include: the design of a biocatalytic process to produce the flavone glucosides (prunin and isoquercetin) and aglycones (naringenin and quercetin); the enzymatic biocatalysis using naringinase under pressure; and the immobilization of naringinase within silica glasses through sol-gel method.

- a) The flavone glucosides (prunin and isoquercetin) and aglycones (naringenin and quercetin) were produced, starting from the natural occurring rutinoides (naringin and rutin) (Chapter 2). The products were obtained in high purity and good yield attending to the high cost of these products, mainly the flavone glucosides: prunin and isoquercetin. Focusing on the production of the glucosides, a cheap production method was developed, based on a selective inactivation of β -D-glucosidase from naringinase by means of optimal deactivation conditions of temperature and pH, determined by means of RSM (81.5 °C and pH 3.9). This achievement comprised simultaneously a high remaining α -L-rhamnosidase activity. Some expensive methods have been described to accomplish this task, including chromatographic purification procedures of either α -L-rhamnosidase from naringinase or the final products mixture (glucoside + aglycone); some even have used specific inhibitors of β -D-glucosidase in order to stop the reaction just after the rhamnose release. More than this economical advantage, this method can be generalized for obtaining others also expensive flavone glucosides starting from their rutinoides.
- b) On the enzymatic biocatalysis using naringinase under pressure (Chapter 3), two different approaches were studied in order to increase the overall bioprocess efficiency.

A first one, consisted on increasing the stability of enzymes against heat using pressure, based on the elliptic phase protein denaturing diagram (Figure 1.12). On

Chapter 3 it is shown how pressure can be used as a tool to protect naringinase, from inactivation caused by heat. At high temperature conditions, pressure decreased the inactivation proneness of both α -L-rhamnosidase (32-fold at 250 MPa and 85.0 °C) and β -D-glucosidase (30-fold at 200 MPa and 75.0 °C) activities, when compared with atmospheric pressure. This protecting effect was dependent on the pressure magnitude and is supported by the antagonistic behavior between pressure and temperature, concerning the stability of proteins. This pressure protecting effect is very useful to rise the temperature condition of the biocatalytic reaction, which not only leads to an increased reaction rate, but also helps on the dissolution of the flavone substrates (naringin and rutin), whose solubility increases with temperature.

A second potential application of pressure aimed to increase the reaction rate constants of both α -L-rhamnosidase and β -D-glucosidase from naringinase. From this study it was found that while α -L-rhamnosidase activity increased with pressure ($\Delta^\ddagger V = -7.7 \pm 1.5 \text{ mL mol}^{-1}$), β -D-glucosidase activity decreased ($\Delta^\ddagger V = 6.5 \pm 1.9 \text{ mL mol}^{-1}$). According to these results pressure seemed to be only adequate to increase the deglycosylation rate of rutinoides into glucosides. A study concerning the naringin hydrolysis into the aglycone naringenin showed that this affirmation is not necessarily true. In the case of the production of aglycones from rutinoides, both α -L-rhamnosidase and β -D-glucosidase activities are needed and the final activity under pressure is dependent on both activities. Indeed the naringin hydrolysis into naringenin was favored by pressure ($\Delta^\ddagger V = -20.0 \pm 5.2 \text{ mL mol}^{-1}$), eventually driven by a first hydrolytic step involving α -L-rhamnosidase, which is favored by pressure. In addition, the naringin hydrolysis into naringenin under several temperature conditions, at atmospheric pressure and 150 MPa supports the pressure stabilization of naringinase native state, at high temperature conditions. At 70.0 °C and 80.0 °C the $k_{\text{cat}} \cdot K_M$ is respectively 3 and 4-fold higher at 150 MPa than at atmospheric pressure. Finally, concerning the equilibrium constants, despite the decrease in the hydrolysis equilibrium constants of both α -L-rhamnosidase and β -D-glucosidase caused by pressure the hydrolysis degree is still high (> 75%) in both cases at the highest pressure studied (200 MPa).

Following this, pressure showed to be a powerful tool in order to increase the overall process efficiency.

- c) Naringinase immobilization within silica glasses through sol-gel method was successfully achieved (Chapter 4). The combination of the sol-gel precursors DGS and TMOS, as well as the combination of glycerol and TMOS led to the production of two interesting sol-gel matrices where naringinase was entrapped. Both these matrices showed outstanding operational stability coupled with high immobilization yields and efficiency. The best matrix, produced from TMOS and glycerol was used in further studies (89% yield, 72% efficiency and 100% residual activity after 50 successive reutilizations), involving the stability of immobilized naringinase against organic cosolvent systems as well as in a final study involving the use of ILs in order to increase the immobilized naringinase efficiency.

The study of the stability of immobilized naringinase within organic cosolvent systems showed that the immobilization within sol-gel matrices protects naringinase from inactivation. The cosolvents used in these stabilization studies were firstly tested for the dissolution of naringin, and only the best were chosen. The stability of immobilized naringinase against organic cosolvents was dependent on the organic cosolvent tested, but for all the aqueous cosolvent systems studied at least a 3 fold stability increase was observed for immobilized naringinase when compared with soluble naringinase. The interesting results of naringin hydrolysis within a cosolvent system consisting of 1,2 dimethoxyethane, corroborate the advantage of using of organic cosolvents to increase the solubility of natural flavone substrates during biocatalytic reaction.

ILs were used as templating additives of sol-gel matrices. From the huge amount of ILs studied, [OMIM][Tf₂N] and [C₂OHMIM][PF₆] led to an efficiency increase of α -L-rhamnosidase and β -D-glucosidase, and in the case of α -L-rhamnosidase an operational stability increase was also observed. In addition, sol-gel matrices produced with [OMIM][Tf₂N], showed a robust mechanical resistance against cracking. The good performance showed by these matrices was supported by an interesting microscopic structure, through SEM analysis. The production of prunin and naringenin was preformed using sol-gel matrices produced with ILs.

Also, the relevancy of the results of immobilized naringinase under pressure is high in order to build a process that combines both the advantages of the immobilization of biocatalysts and pressurized reactions.

Considering a potential application of the produced drugs on the therapeutics of AD, preliminary studies (Chapter 5) support the hypothesis of using the glucoside prunin as well as the aglycone naringenin in a way to cross the BBB. This fact may be a striking advantage to target AD, when comparing with the rutinoside naringin that doesn't seem to be able to cross the BBB. As for prunin, evidences were shown to be metabolized into naringenin, meaning that acts as a prodrug of naringenin. Naringenin has been pointed out as potential active drug against AD as reported on 1.3.2, acting as a chemopreventive agent against AD, by reducing the micromolecular A β -induced oxidative cell stress (Heo *et al.*, 2004) and a possible molecular mechanism has been proposed by Tedeschi *et al.* (2010). Also naringenin is reported to inhibit NF- κ B which is responsible for triggering pro-inflammatory molecules (Kanno *et al.*, 2006; Shi *et al.*, 2009) leading to a reduction of the redox imbalance and the consecutive chronic inflammation which is pointed out as one of the AD progression mechanisms.

GENERAL CONCLUSIONS AND FUTURE PERSPECTIVES

Chapter 7

This thesis work encloses achievements both focusing on bioprocess design and potential therapeutics against AD.

Considering bioprocess design, the achievements are divided in three:

- a) The aglycones: quercetin and naringenin and the glucosides: isoquercetin and prunin were produced starting from the natural occurring rutinoides: rutin and naringin, by means of naringinase and partially inactivated naringinase respectively;
- b) Pressure was found to increase naringinase stability against heat and also the α -L-rhamnosidase activity from naringinase. The naringin hydrolysis under pressure (150 MPa) was faster than at atmospheric pressure.
- c) Naringinase entrapped within silica glasses through sol-gel method coupled with glycerol and ionic liquids showed a very high performance and resistance against cosolvent inactivation. Some matrices with immobilized naringinase showed mechanical resistance and good stability profile of naringinase under pressure (150 MPa).

Regarding the potential application of the produced drugs on the therapeutics of AD, preliminary studies support the hypothesis of using the glucoside prunin as well as the aglycone naringenin in a way to cross the BBB, which is a striking advantage to target AD, when comparing with the rutinoides naringin that doesn't seem to be able to cross the BBB.

Due to experimental time restriction the flavonols rutin, isoquercetin and quercetin were placed in second level comparing to the flavanones naringin, prunin and naringenin. Only in Chapter 2, that describes the production of the glucosides and aglycones from the substrates rutinoides, it was possible to study together all these flavones.

The aglycone quercetin and the glucoside isoquercetin weren't studied on Chapter 5. But in an analogous way, future experiments may show evidence of an identical behaviour to naringenin (aglycone) and prunin (glucoside). Several findings also report quercetin as a potential active drug against AD. As stated on 1.3.2, quercetin inhibits A β aggregation and destabilizes pre-formed A β fibrils (Ono *et al.*, 2003) and shows protective effects of neuronal cells from oxidative stress-induced by A β peptide (Ansari *et al.*, 2009). Even more interesting is the possible inhibition of β -secretase by quercetin (Shimmyo *et al.*, 2008). Future studies should focus on using the studied flavones in

mice models of AD in order to achieve robust scientific evidence that may launch some of these compounds into clinical trials, against AD. At this time a biotechnological method shall be set up, considering the compound of interest and all the achievements reported on this thesis in order to maximize its production.

A study that may arise from this thesis work is the glycosylation of some good BACE1 inhibitors that hardly penetrate the BBB, though a reverse reaction, and expecting a recognition followed by transportation through SLGT1 receptors on the BBB.

References

- Albuquerque, L., Efeitos da Temperatura e da Pressão na Cinética de Reações de Solvólise em Etilenoglicol e Glicerol. Tese de doutoramento, Lisboa: FFUL, 1979.
- Ali, M.; Agha, F.; El-Sammad, N.; Hassan, S., Modulation of anticancer drug-induced P-glycoprotein expression by naringin. *Journal of Biosciences* **2009**, 64, (1-2), 109-116.
- Alzheimer, A.; Stelzmann, R.; Schnitzlein, H.; Murtagh, F., An English translation of Alzheimer's 1907 paper, "Uber eine eigenartige Erkrankung der Hirnrinde". *Clinical Anatomy* **1995**, 8, (6), 429.
- Amaro, M.I.; Rocha, J.; Vila-Real, H.; Eduardo-Figueira, M.; Mota-Filipe, H.; Sepodes, B.; Ribeiro, M.H., Anti-inflammatory activity of naringin and the biosynthesised naringenin by naringinase immobilized in microstructured materials in a model of DSS-induced colitis in mice. *Food Research International* **2009**, 42, (8), 1010-1017.
- Andrade, J.; Burgess, J., Effect of the citrus flavanone naringenin on oxidative stress in rats. *Journal of Agricultural and Food Chemistry* **2007**, 55, (6), 2142-2148.
- Ansari, M.; Abdul, H.; Joshi, G.; Opii, W.; Butterfield, D., Protective effect of quercetin in primary neurons against A [beta](1-42): relevance to Alzheimer's disease. *The Journal of Nutritional Biochemistry* **2009**, 20, (4), 269-275.
- Arendash, G.; Schleif, W.; Rezai-Zadeh, K.; Jackson, E.; Zacharia, L.; Cracchiolo, J.; Shippy, D.; Tan, J., Caffeine protects Alzheimer's mice against cognitive impairment and reduces brain [beta]-amyloid production. *Neuroscience* **2006**, 142, (4), 941-952.
- Arrhenius, S., On the dissociation of substances dissolved in water. *Z. Phys. Chem* **1887**, 1, (631), 136.
- Avnir, D., Organic chemistry within ceramic matrixes: doped sol-gel materials. *Accounts of Chemical Research* **1995**, 28, (8), 328-334.
- Bader-Lange, M.; Cenini, G.; Piroddi, M.; Mohmmad Abdul, H.; Sultana, R.; Galli, F.; Memo, M.; Butterfield, D., Loss of phospholipid asymmetry and elevated brain apoptotic protein levels in subjects with amnesic mild cognitive impairment and Alzheimer disease. *Neurobiology of disease* **2008**, 29, (3), 456-464.
- Baker, G.; Jordan, J.; Bright, F., Effects of poly (ethylene glycol) doping on the behavior of pyrene, rhodamine 6G, and acrylodan-labeled bovine serum albumin sequestered within tetramethylorthosilane-derived sol-gel-processed composites. *Journal of Sol-Gel Science and Technology* **1998**, 11, (1), 43-54.
- Baliga, B.; Whalley, E., Effect of pressure on the rate of solvolysis of t-butyl chloride in ethanol-water mixtures. *Canadian Journal of Chemistry* **1970**, 48, (4), 528-536.
- Balny, C., Pressure effects on weak interactions in biological systems. *Journal of Physics: Condensed Matter* **2004**, 16, S1245-S1253.
- Baquer, N.; Taha, A.; Kumar, P.; McLean, P.; Cowsik, S.; Kale, R.; Singh, R.; Sharma, D., A metabolic and functional overview of brain aging linked to neurological disorders. *Biogerontology* **2009**, 10, (4), 377-413.
- Beal, M., Mitochondrial dysfunction and oxidative damage in Alzheimer's and Parkinson's diseases and coenzyme Q 10 as a potential treatment. *Journal of Bioenergetics and Biomembranes* **2004**, 36, (4), 381-386.
- Beck, J.; Vartuli, J., Recent advances in the synthesis, characterization and applications of mesoporous molecular sieves. *Current Opinion in Solid State and Materials Science* **1996**, 1, (1), 76-87.

REFERENCES

- Berger, M., Can oxidative damage be treated nutritionally? *Clinical Nutrition* **2005**, *24*, (2), 172-183.
- Bernardino, S.; Fernandes, P.; Fonseca, L., A new biocatalyst: Penicillin G acylase immobilized in sol-gel micro-particles with magnetic properties. *Biotechnology Journal* **2009**, *4*, (5), 695-702.
- Blagosklonny, M., Validation of anti-aging drugs by treating age-related diseases. *Aging* **2009**, *1*, (3), 281-288.
- Bodamyali, T.; Stevens, C.; Blake, D.; Winyard, P., Reactive oxygen/nitrogen species and acute inflammation: a physiological process. *Free Radicals and Inflammation* **2000**, 11-16.
- Blondeau, J.; Beslin, A.; Chantoux, F.; Francon, J., Triiodothyronine Is a High Affinity Inhibitor of Amino Acid Transport System L1 in Cultured Astrocytes. *Journal of Neurochemistry* **1993**, *60*, (4), 1407-1413.
- Böhrer, H.; Qiu, F.; Zimmermann, T.; Zhang, Y.; Jllmer, T.; Männel, D.; Böttiger, B.; Stern, D.; Waldherr, R.; Saeger, H., Role of NFkappaB in the mortality of sepsis. *Journal of Clinical Investigation* **1997**, *100*, (5), 972-985.
- Boots, H.; De Bokx, P., Theory of enthalpy-entropy compensation. *The Journal of Physical Chemistry* **1989**, *93*, (25), 8240-8243.
- Bradford, M., A rapid and sensitive method for the quantitation of microgram quantities of protein utilizing the principle of protein-dye binding. *Analytical Biochemistry* **1976**, *72*, (1-2), 248-254.
- Brand, K.; Page, S.; Rogler, G.; Bartsch, A.; Brandl, R.; Knuechel, R.; Page, M.; Kaltschmidt, C.; Baeuerle, P.; Neumeier, D., Activated transcription factor nuclear factor-kappa B is present in the atherosclerotic lesion. *Journal of Clinical Investigation* **1996**, *97*, (7), 1715-1722.
- Braun, S.; Rappoport, S.; Zusman, R.; Avnir, D.; Ottolenghi, M., Biochemically active sol-gel glasses: the trapping of enzymes. *Materials Letters* **1990**, *10*, (1-2), 1-5.
- Brena, B.; Irazoqui, G.; Giacomini, C.; Batista-Viera, F., Effect of increasing co-solvent concentration on the stability of soluble and immobilized [beta]-galactosidase. *Journal of Molecular Catalysis B: Enzymatic* **2003**, *21*, (1-2), 25-29.
- Brennan, J.; Benjamin, D.; DiBattista, E.; Gulcev, M., Using Sugar and Amino Acid Additives to Stabilize Enzymes within Sol- Gel Derived Silica. *Chemistry of Materials* **2003**, *15*, (3), 737-745.
- Brook, M.; Chen, Y.; Guo, K.; Zhang, Z.; Brennan, J., Sugar-modified silanes: precursors for silica monoliths. *Journal of Materials Chemistry* **2004a**, *14*, (9), 1469-1479.
- Brook, M.; Chen, Y.; Guo, K.; Zhang, Z.; Jin, W.; Deisingh, A.; Cruz-Aguado, J.; Brennan, J., Proteins entrapped in silica monoliths prepared from glyceroxysilanes. *Journal of Sol-Gel Science and Technology* **2004b**, *31*, (1), 343-348.
- Bu, G., Apolipoprotein E and its receptors in Alzheimer's disease: pathways, pathogenesis and therapy. *Nature Reviews Neuroscience* **2009**, *10*, (5), 333-344.
- Buckow, R. Pressure and temperature effects on the enzymatic conversion of biopolymers. Universitätsbibliothek, 2006.

- Buckow, R.; Weiss, U.; Heinz, V.; Knorr, D., Stability and catalytic activity of α -amylase from barley malt at different pressure-temperature conditions. *Biotechnology and bioengineering* **2007**, *97*, (1), 1-11.
- Bulic, B.; Pickhardt, M.; Schmidt, B.; Mandelkow, E.; Waldmann, H.; Mandelkow, E., Development of tau aggregation inhibitors for Alzheimer's disease. *Angewandte Chemie International Edition* **2009**, *48*, (10), 1740-1752.
- Bulzomi, P.; Bolli, A.; Galluzzo, P.; Leone, S.; Acconcia, F.; Marino, M., Naringenin and 17 β -estradiol coadministration prevents hormone-induced human cancer cell growth. *IUBMB life* **2010**, *62*, (1), 51-60.
- Burris, C.; Laidler, K., The influence of hydrostatic pressure on the rates of ionic reactions. *Transactions of the Faraday Society* **1955**, *51*, 1497-1505.
- Busby, W.; Ackermann, J.; Crespi, C., Effect of methanol, ethanol, dimethyl sulfoxide, and acetonitrile on in vitro activities of cDNA-expressed human cytochromes P-450. *Drug Metabolism and Disposition* **1999**, *27*, (2), 246-249.
- Bustacchini, S.; Corsonello, A.; Onder, G.; Guffanti, E.; Marchegiani, F.; Abbatecola, A.; Lattanzio, F., Pharmacoeconomics and Aging. *Drugs Aging* **2009**, *26*, (Supplement 1), 75-87.
- Cabral, J.; Aires-Barros, M.; Gama, M., *Engenharia enzimática*. Lidel: 2003.
- Caccamese, S.; Manna, L.; Scivoli, G., Chiral HPLC separation and CD spectra of the C-2 diastereomers of naringin in grapefruit during maturation. *Chirality* **2003**, *15*, (8), 661-667.
- Calado, A., Reações de Menschutkin am Alcoóis: Termodinâmica e Cinética. Tese de doutoramento, Lisboa: FCUL, 1986.
- Cariño-Cortés, R.; Álvarez-González, I.; Martino-Roaro, L.; Madrigal-Bujaidar, E., Effect of Naringin on the DNA Damage Induced by Daunorubicin in Mouse Hepatocytes and Cardiocytes. *Biological & Pharmaceutical Bulletin* **2010**, *33*, (4), 697-701.
- Carluccio, M.; Siculella, L.; Ancora, M.; Massaro, M.; Scoditti, E.; Storelli, C.; Visioli, F.; Distanto, A.; De Caterina, R., Olive oil and red wine antioxidant polyphenols inhibit endothelial activation: antiatherogenic properties of Mediterranean diet phytochemicals. *Arteriosclerosis, Thrombosis, and Vascular Biology* **2003**, *23*, (4), 622-629.
- Cavia-Saiz, M.; Busto, M.; Pilar-Izquierdo, M.; Ortega, N.; Perez-Mateos, M.; Muñoz, P., Antioxidant properties, radical scavenging activity and biomolecule protection capacity of flavonoid naringenin and its glycoside naringin: a comparative study. *Journal of the Science of Food and Agriculture* **2010**, *90*, (7), 1238-1244.
- Chan, A.; Shea, T., Supplementation with apple juice attenuates presenilin-1 overexpression during dietary and genetically-induced oxidative stress. *Journal of Alzheimer's Disease* **2006**, *10*, (4), 353-358.
- Chang, P.; Muir, A., Extraction, purification and conversion of flavonoids from plant biomass. In Google Patents: 2003.
- Cho, C.; Kim, H.; Chung, S.; Jung, K.; Shim, K.; Yu, B.; Yodoi, J.; Chung, H., Modulation of glutathione and thioredoxin systems by calorie restriction during the aging process. *Experimental Gerontology* **2003**, *38*, (5), 539-548.

REFERENCES

- Choi, J.; Yokozawa, T.; Oura, H., Antihyperlipidemic effect of flavonoids from *Prunus davidiana*. *Journal of Natural Products* **1991a**, 54, (1), 218-224.
- Choi, J.; Yokozawa, T.; Oura, H., Improvement of hyperglycemia and hyperlipemia in streptozotocin-diabetic rats by a methanolic extract of *Prunus davidiana* stems and its main component, prunin. *Planta Medica* **1991b**, 57, (3), 208-211.
- Chung, H.; Sung, B.; Jung, K.; Zou, Y.; Yu, B., The molecular inflammatory process in aging. *Antioxidants & Redox Signaling* **2006**, 8, (3-4), 572-581.
- Chung, H.; Cesari, M.; Anton, S.; Marzetti, E.; Giovannini, S.; Seo, A.; Carter, C.; Yu, B.; Leeuwenburgh, C., Molecular inflammation: underpinnings of aging and age-related diseases. *Ageing research reviews* **2009**, 8, (1), 18-30.
- Citron, M., Alzheimer's disease: strategies for disease modification. *Nature Reviews Drug Discovery*, **2010**, 9, (5), 387-398.
- Clark, D., Rapid calculation of polar molecular surface area and its application to the prediction of transport phenomena. 1. Prediction of intestinal absorption. *Journal of Pharmaceutical Sciences* **1999**, 88, (8), 807-814.
- Cooper, A., Thermodynamics of protein folding and stability. *Protein: A comprehensive treatise* **1999**, 2, 217-270.
- Coradin, T.; Boissiere, M.; Livage, J., Sol-gel chemistry in medicinal science. *Current Medicinal Chemistry* **2006**, 13, (1), 99-108.
- Crozier, A.; Jaganath, I.; Clifford, M., Dietary phenolics: chemistry, bioavailability and effects on health. *Natural Product Reports* **2009**, 26, (8), 1001-1043.
- Cruts, M.; vanBroeckhoven, C., Molecular genetics of Alzheimer's disease. *Annals of Medicine* **1998**, 30, (6), 560-565.
- D'Archivio, M.; Filesi, C.; Vari, R.; Scazzocchio, B.; Masella, R., Bioavailability of the Polyphenols: Status and Controversies *International Journal of Molecular Sciences* **2010**, (11), 1321-1342.
- Deane, R.; Wu, Z.; Zlokovic, B., RAGE (Yin) Versus LRP (Yang) Balance Regulates Alzheimer Amyloid {beta}-Peptide Clearance Through Transport Across the Blood-Brain Barrier. *Stroke* **2004**, 35, (1), 2628.
- Devore, E.; Grodstein, F.; van Rooij, F.; Hofman, A.; Stampfer, M.; Witteman, J.; Breteler, M., Dietary antioxidants and long-term risk of dementia. *Archives of Neurology* **2010**, 67, (7), 819-825.
- Dickey, F., Specific adsorption. *Journal of Physical Chemistry* **1955**, 58, 695-707.
- Dovey, H.; John, V.; Anderson, J.; Chen, L.; de Saint Andrieu, P.; Fang, L.; Freedman, S.; Folmer, B.; Goldbach, E.; Holsztynska, E., Functional gamma secretase inhibitors reduce beta amyloid peptide levels in brain. *Journal of Neurochemistry* **2001**, 76, (1), 173-181.
- Dupont, J.; de Souza, R.; Suarez, P., Ionic liquid (molten salt) phase organometallic catalysis. *Chemical Reviews* **2002**, 102, (10), 3667-3692.
- Durham, T.; Shepherd, T., Progress toward the discovery and development of efficacious BACE inhibitors. *Current Opinion in Drug Discovery and Development* **2006**, 9, (6), 776-791.

- Eckman, E.; Eckman, C., A -degrading enzymes: modulators of Alzheimer's disease pathogenesis and targets for therapeutic intervention. *Biochemical Society Transactions* **2005**, 33, 1101-1105.
- Eisenmenger, M.; Reyes-De-Corcuera, J., High hydrostatic pressure increased stability and activity of immobilized lipase in hexane. *Enzyme and Microbial Technology* **2009**, 45, (2), 118-125.
- Ellenrieder, G.; Daz, M., Thermostabilization of naringinase from *Penicillium decumbens* by proteins in solution and immobilization on insoluble proteins. *Biocatalysis and Biotransformation* **1996**, 14, (2), 113-123.
- Ellenrieder, G.; Blanco, S.; Daz, M., Hydrolysis of supersaturated naringin solutions by free and immobilized naringinase. *Biotechnology Techniques* **1998**, 12, (1), 63-65.
- Emura, K.; Yokomizo, A.; Toyoshi, T.; Moriwaki, M., Effect of enzymatically modified isoquercitrin in spontaneously hypertensive rats. *Journal of Nutritional Science and Vitaminology* **2007**, 53, (1), 68-74.
- Evans, A., G., and Polanyi, M. Some applications of the transition state method to the calculation of reaction velocities, especially in solution. *Transactions of the Faraday Society* **1935**, 31, 875.
- Evans, M.; Polanyi, M., On the introduction of thermodynamic variables into reaction kinetics. *Transactions of the Faraday Society* **1937**, 33, 448-452.
- Eyring, H., The Activated Complex and the Absolute Rate of Chemical Reactions. *Chemical Reviews* **1935**, 17, (1), 65-77.
- Fagan, A.; Watson, M.; Parsadanian, M.; Bales, K.; Paul, S.; Holtzman, D., Human and murine ApoE markedly alters A metabolism before and after plaque formation in a mouse model of Alzheimer's disease. *Neurobiology of Disease* **2002**, 9, (3), 305-318.
- Fang, S.; Hsu, C.; Lin, H.; Yen, G., Anticancer Effects of Flavonoid Derivatives Isolated from *Millettia reticulata* Benth in SK-Hep-1 Human Hepatocellular Carcinoma Cells. *Journal of Agricultural and Food Chemistry* **2010**, 58, (2), 814-820.
- Felgines, C.; Texier, O.; Morand, C.; Manach, C.; Scalbert, A.; Regerat, F.; Remesy, C., Bioavailability of the flavanone naringenin and its glycosides in rats. *American Journal of Physiology- Gastrointestinal and Liver Physiology* **2000**, 279, (6), 1148-1154.
- Feng, Z.; Qin, C.; Chang, Y.; Zhang, J., Early melatonin supplementation alleviates oxidative stress in a transgenic mouse model of Alzheimer's disease. *Free Radical Biology and Medicine* **2006**, 40, (1), 101-109.
- Feres, C.; Madalosso, R.; Rocha, O.; Leite, J.; Guimarães, T.; Toledo, V.; Tagliati, C., Acute and chronic toxicological studies of *Dimorphandra mollis* in experimental animals. *Journal of Ethnopharmacology* **2006**, 108, (3), 450-456.
- Fernandes, A.; Silva, R.; Falcão, A.; Brito, M.; Brites, D., Cytokine production, glutamate release and cell death in rat cultured astrocytes treated with unconjugated bilirubin and LPS. *Journal of Neuroimmunology* **2004**, 153, (1-2), 64-75.
- Fernandez, J.; Reyes, R.; Ponce, H.; Oropeza, M.; VanCalsteren, M.; Jankowski, C.; Campos, M., Isoquercitrin from *Argemone platyceras* inhibits carbachol and leukotriene D4-induced contraction in guinea-pig airways. *European Journal of Pharmacology* **2005**, 522, (1-3), 108-115.

REFERENCES

- Fernández, S.; Wasowski, C.; Loscalzo, L.; Granger, R.; Johnston, G.; Paladini, A.; Marder, M., Central nervous system depressant action of flavonoid glycosides. *European Journal of Pharmacology* **2006**, 539, (3), 168-176.
- Ferreira, L.; Afonso, C.; Vila-Real, H.; Alfaia, A.; Ribeiro, M., Evaluation of the effect of high pressure on naringin hydrolysis in grapefruit juice with naringinase immobilised in calcium alginate beads. *Food Technology and Biotechnology* **2008**, 46, 146-150.
- Ferry, D.; Smith, A.; Malkhandi, J.; Fyfe, D.; deTakats, P.; Anderson, D.; Baker, J.; Kerr, D., Phase I clinical trial of the flavonoid quercetin: pharmacokinetics and evidence for in vivo tyrosine kinase inhibition. *Clinical Cancer Research* **1996**, 2, (4), 659-668.
- Villela Filho, M.; Stillger, T.; Müller, M.; Liese, A.; Wandrey, C., Is log P a convenient criterion to guide the choice of solvents for biphasic enzymatic reactions? *Angewandte Chemie* **2003**, 115, (26), 3101-3104.
- Fisher, G.; Datta, S.; Talwar, H.; Wang, Z.; Varani, J.; Kang, S.; Voorhees, J., Molecular basis of sun-induced premature skin ageing and retinoid antagonism. *Nature* **1996**, 379, (6563), 335-339.
- Fischer, H.; Gottschlich, R.; Seelig, A., Blood-brain barrier permeation: molecular parameters governing passive diffusion. *Journal of Membrane Biology* **1998**, 165, (3), 201-211.
- Fischer, P.; Lane, D., Inhibitors of cyclin-dependent kinases as anti-cancer therapeutics. *Current Medicinal Chemistry* **2000**, 7, (12), 1213-1245.
- Fleisher, A.; Raman, R.; Siemers, E.; Becerra, L.; Clark, C.; Dean, R.; Farlow, M.; Galvin, J.; Peskind, E.; Quinn, J., Phase 2 Safety Trial Targeting Amyloid {beta} Production With a {gamma}-Secretase Inhibitor in Alzheimer Disease. *Archives of Neurology* **2008**, 65, (8), 1031-1038.
- Fotuhi, M.; Hachinski, V.; Whitehouse, P., Changing perspectives regarding late-life dementia. *Nature Reviews Neurology* **2009**, 5, (12), 649-658.
- Fukui, S.; Tanaka, A.; Iida, T., Immobilization of biocatalysts for bioprocesses in organic solvent media. *Studies in Organic Chemistry* **1987**, 29, 21-41.
- Fusco, D.; Colloca, G.; Monaco, M.; Cesari, M., Effects of antioxidant supplementation on the aging process. *Clinical Interventions in Aging* **2007**, 2, (3), 377-387.
- Galbusera, C.; Facheris, M.; Magni, F.; Galimberti, G.; Sala, G.; Tremolada, L.; Isella, V.; Guerini, F.; Appollonio, I.; Galli-Kienle, M., Increased susceptibility to plasma lipid peroxidation in Alzheimer disease patients. *Current Alzheimer Research* **2004**, 1, (2), 103-109.
- Gallego, M. V.; Pinaga, F.; Ramon, D.; Valles, S., Purification and characterization of an alpha-L-rhamnosidase from *Aspergillus terreus* of interest in winemaking. *Journal of Food Science* **2001**, 66, (2), 204-209.
- Gaur, V.; Aggarwal, A.; Kumar, A., Protective effect of naringin against ischemic reperfusion cerebral injury: Possible neurobehavioral, biochemical and cellular alterations in rat brain. *European Journal of Pharmacology* **2009**, 616, (1-3), 147-154.
- Gauthier, A.; Gulick, P.; Ibrahim, R., Characterization of two cDNA clones which encode O-methyltransferases for the methylation of both flavonoid and

- phenylpropanoid compounds. *Archives of Biochemistry and Biophysics* **1998**, 351, (2), 243-249.
- Gee, J.; DuPont, M.; Day, A.; Plumb, G.; Williamson, G.; Johnson, I., Intestinal transport of quercetin glycosides in rats involves both deglycosylation and interaction with the hexose transport pathway. *Journal of Nutrition* **2000**, 130, (11), 2765-2771.
- Gill, I.; Ballesteros, A., Encapsulation of Biologicals within Silicate, Siloxane, and Hybrid Sol- Gel Polymers: An Efficient and Generic Approach. *Journal of the American Chemical Society* **1998**, 120, (34), 8587-8598.
- Gill, I.; Ballesteros, A., Bioencapsulation within synthetic polymers (Part 1): sol-gel encapsulated biologicals. *Trends in Biotechnology* **2000**, 18, (7), 282-296.
- Gill, I., Bio-doped Nanocomposite Polymers: Sol- Gel Bioencapsulates. *Chemistry of Materials* **2001**, 13, (10), 3404-3421.
- Giovanni, M., Response surface methodology and product optimization. *Food Technology* **1983**, 37, (11), 41-45.
- Glew, R.; Gopalan, V.; Forsyth, G.; VanderJagt, D., The mammalian cytosolic broad-specificity -glucosidase. -glucosidases: *Biochemistry and Molecular Biology*, American Chemical Society **1993**, 83-112.
- Gocan, S.; Cimpan, G., Review of the analysis of medicinal plants by TLC: Modern approaches. *Journal of Liquid Chromatography & Related Technologies* **2004**, 27, (7-9), 1377-1411.
- Goedert, M.; Klug, A.; Crowther, R., Tau protein, the paired helical filament and Alzheimer's disease. *Journal of Alzheimer's Disease* **2006**, 9, 195-207.
- Golinkin, H.; Laidlaw, W.; Hyne, J., ON THE PRESSURE DEPENDENCE OF REACTION RATES. *Canadian Journal of Chemistry* **1966**, 44, (18), 2193-2203.
- Gomez-Mejiba, S.; Zhai, Z.; Akram, H.; Pye, Q.; Hensley, K.; Kurien, B.; Scofield, R.; Ramirez, D., Inhalation of environmental stressors & chronic inflammation: autoimmunity and neurodegeneration. *Mutation Research/Genetic Toxicology and Environmental Mutagenesis* **2009**, 674, (1-2), 62-72.
- Greaves, T.; Drummond, C., Protic ionic liquids: properties and applications. *Chemical Reviews* **2008**, 108, (1), 206-237.
- Grodstein, F.; Chen, J.; Willett, W., High-dose antioxidant supplements and cognitive function in community-dwelling elderly women. *American Journal of Clinical Nutrition* **2003**, 77, (4), 975-984.
- Guo, W.; Kong, E.; Meydani, M., Dietary Polyphenols, Inflammation, and Cancer. *Nutrition and Cancer* **2009**, 61, (6), 807-810.
- Han, X.; Ren, D.; Fan, P.; Shen, T.; Lou, H., Protective effects of naringenin-7-O-glucoside on doxorubicin-induced apoptosis in H9C2 cells. *European Journal of Pharmacology* **2008**, 581, (1-2), 47-53.
- Handel, M.; Mcmorrow, L.; Gravallesse, E., Nuclear factor-kB in rheumatoid synovium. Localization of p50 and p65. *Arthritis & Rheumatism* **1995**, 38, (12), 1762-1770.
- Handique, J.; Baruah, J., Polyphenolic compounds: an overview. *Reactive and Functional Polymers* **2002**, 52, (3), 163-188.
- Hanisch, U., Microglia as a source and target of cytokines. *Glia* **2002**, 40, (2), 140-155.

REFERENCES

- Harman, D., Aging: a theory based on free radical and radiation chemistry. *The Journal of Gerontology* **1956**, 11, (3), 298-300.
- Harman, D., The biologic clock: the mitochondria? *Journal of the American Geriatrics Society* **1972**, 20, (4), 145-147.
- Harman, D., The free radical theory of aging. *Antioxid Redox Signal* **2003**, 5, 557-561.
- Havsteen, B., The biochemistry and medical significance of the flavonoids. *Pharmacology & Therapeutics* **2002**, 96, (2-3), 67-202.
- Hawley, S., Reversible pressure-temperature denaturation of chymotrypsinogen. *Biochemistry* **1971**, 10, (13), 2436-2442.
- Hay, S.; Sutcliffe, M.; Scrutton, N., Promoting motions in enzyme catalysis probed by pressure studies of kinetic isotope effects. *Proceedings of the National Academy of Sciences* **2007**, 104, (2), 507-512.
- Hebert, L.; Scherr, P.; Bienias, J.; Bennett, D.; Evans, D., Alzheimer disease in the US population. *Archives of Neurology* **2003**, 60, (8), 1119-1122.
- Heller, J.; Heller, A., Loss of activity or gain in stability of oxidases upon their immobilization in hydrated silica: significance of the electrostatic interactions of surface arginine residues at the entrances of the reaction channels. *Journal of the American Chemical Society* **1998**, 120, (19), 4586-4590.
- Henley, J. P.; Sadana, A., Categorization of enzyme deactivations using a series-type mechanism. *Enzyme and Microbial Technology* **1985**, 7, (2), 50-60.
- Hensley, K.; Maitt, M.; Yu, Z.; Sang, H.; Markesbery, W.; Floyd, R., Electrochemical analysis of protein nitrotyrosine and dityrosine in the Alzheimer brain indicates region-specific accumulation. *Journal of Neuroscience* **1998**, 18, (20), 8126-8132.
- Heo, H.; Kim, D.; Shin, S.; Kim, M.; Kim, B.; Shin, D., Effect of antioxidant flavanone, naringenin, from Citrus junos on neuroprotection. *Journal of Agricultural Food Chemistry* **2004**, 52, (6), 1520-1525.
- Heremans, K.; Smeller, L., Protein structure and dynamics at high pressure1. *Biochimica et Biophysica Acta (BBA)-Protein Structure and Molecular Enzymology* **1998**, 1386, (2), 353-370.
- Hollman, P.; Bijman, M.; van Gameren, Y.; Cnossen, E.; de VRIES, J.; Katan, M., The sugar moiety is a major determinant of the absorption of dietary flavonoid glycosides in man. *Free Radical Research* **1999**, 31, (6), 569-573.
- Hollox, E.; Poulter, M.; Zvarik, M.; Ferak, V.; Krause, A.; Jenkins, T.; Saha, N.; Kozlov, A.; Swallow, D., Lactase haplotype diversity in the Old World. *The American Journal of Human Genetics* **2001**, 68, (1), 160-172.
- Holmes, C.; Boche, D.; Wilkinson, D.; Yadegarfar, G.; Hopkins, V.; Bayer, A.; Jones, R.; Bullock, R.; Love, S.; Neal, J., Long-term effects of A [beta] 42 immunisation in Alzheimer's disease: follow-up of a randomised, placebo-controlled phase I trial. *The Lancet* **2008**, 372, (9634), 216-223.
- Hsiu, S.; Huang, T.; Hou, Y.; Chin, D.; Chao, P., Comparison of metabolic pharmacokinetics of naringin and naringenin in rabbits. *Life Sciences* **2002**, 70, (13), 1481-1489.

- Hsu, C.; Cheng, A., Clinical studies with curcumin. *The Molecular Targets and Therapeutic Uses of Curcumin in Health and Disease* **2007**, 471-480.
- Hussain, T.; Gupta, S.; Adhami, V.; Mukhtar, H., Green tea constituent epigallocatechin-3-gallate selectively inhibits COX-2 without affecting COX-1 expression in human prostate carcinoma cells. *International Journal of Cancer* **2005**, 113, (4), 660-669.
- Hutton, M.; Lendon, C.; Rizzu, P.; Baker, M.; Froelich, S.; Houlden, H.; Pickering-Brown, S.; Chakraverty, S.; Isaacs, A.; Grover, A., Association of missense and 5 - splice-site mutations in tau with the inherited dementia FTDP-17. *Nature* **1998**, 393, (6686), 702-705.
- Iler, R., The chemistry of silica. In Wiley, New York: 1979.
- Itoh, K.; Masuda, M.; Naruto, S.; Murata, K.; Matsuda, H., Antiallergic activity of unripe Citrus hassaku fruits extract and its flavanone glycosides on chemical substance-induced dermatitis in mice. *Journal of Natural Medicines* **2009**, 63, (4), 443-450.
- Jagetia, G.; Venkatesha, V.; Reddy, T., Naringin, a citrus flavonone, protects against radiation-induced chromosome damage in mouse bone marrow. *Mutagenesis* **2003**, 18, (4), 337-343.
- Jarrett, J.; Berger, E.; Lansbury Jr, P., The carboxy terminus of the beta. amyloid protein is critical for the seeding of amyloid formation: Implications for the pathogenesis of Alzheimer's disease. *Biochemistry* **1993**, 32, (18), 4693-4697.
- Jeon, S.; Bok, S.; Jang, M.; Lee, M.; Nam, K.; Park, Y.; Rhee, S.; Choi, M., Antioxidative activity of naringin and lovastatin in high cholesterol-fed rabbits. *Life Sciences* **2001**, 69, (24), 2855-2866.
- Jeon, S.; Kim, H.; Kim, H.; Do, G.; Jeong, T.; Park, Y.; Choi, M., Hypocholesterolemic and antioxidative effects of naringenin and its two metabolites in high-cholesterol fed rats. *Translational Research* **2007**, 149, (1), 15-21.
- Jin, W.; Brennan, J., Properties and applications of proteins encapsulated within sol-gel derived materials. *Analytica Chimica Acta* **2002**, 461, (1), 1-36.
- Johnson, P.; Whateley, T., On the use of polymerizing silica gel systems for the immobilization of trypsin. *Journal of Colloid and Interface Science* **1971**, 37, (3), 557-563.
- Johnson, M.; Loo, G., Effects of epigallocatechin gallate and quercetin on oxidative damage to cellular DNA. *Mutation Research/DNA Repair* **2000**, 459, (3), 211-218.
- Jolivet, J.; Henry, M.; Livage, J., *Metal Oxide Chemistry and Synthesis: From Solution to Oxide*. John Wiley: 2000.
- Joseph, J.; Cole, G.; Head, E.; Ingram, D., Nutrition, brain aging, and neurodegeneration. *Journal of Neuroscience* **2009**, 29, (41), 12795-12801.
- Jung, U.; Kim, H.; Lee, J.; Lee, M.; Kim, H.; Park, E.; Kim, H.; Jeong, T.; Choi, M., Naringin supplementation lowers plasma lipids and enhances erythrocyte antioxidant enzyme activities in hypercholesterolemic subjects. *Clinical Nutrition (Edinburgh, Scotland)* **2003**, 22, (6), 561-568.
- Jung, U.; Lee, M.; Jeong, K.; Choi, M., The hypoglycemic effects of hesperidin and naringin are partly mediated by hepatic glucose-regulating enzymes in C57BL/KsJ-db/db mice. *Journal of Nutrition* **2004**, 134, (10), 2499-2503.

REFERENCES

- Jung, U.; Lee, M.; Park, Y.; Kang, M.; Choi, M., Effect of citrus flavonoids on lipid metabolism and glucose-regulating enzyme mRNA levels in type-2 diabetic mice. *The International Journal of Biochemistry & Cell Biology* **2006**, 38, (7), 1134-1145.
- Jurado, E.; Camacho, F.; Luzón, G.; Vicaria, J. M., Kinetic models of activity for [beta]-galactosidases: influence of pH, ionic concentration and temperature. *Enzyme and Microbial Technology* **2004**, 34, (1), 33-40.
- Kamat, C.; Gadal, S.; Mhatre, M.; Williamson, K.; Pye, Q.; Hensley, K., Antioxidants in central nervous system diseases: preclinical promise and translational challenges. *Journal of Alzheimer's Disease* **2008**, 15, (3), 473-493.
- Kanno, S.; Shouji, A.; Tomizawa, A.; Hiura, T.; Osanai, Y.; Ujibe, M.; Obara, Y.; Nakahata, N.; Ishikawa, M., Inhibitory effect of naringin on lipopolysaccharide (LPS)-induced endotoxin shock in mice and nitric oxide production in RAW 264.7 macrophages. *Life Sciences* **2006**, 78, (7), 673-681.
- Karin, M., Role for IKK2 in muscle: waste not, want not. *Journal of Clinical Investigation* **2006**, 116, (11), 2866-2868.
- Kaul, T.; Middleton Jr, E.; Ogra, P., Antiviral effect of flavonoids on human viruses. *Journal of Medical Virology* **1985**, 15, (1), 71-79.
- Keeling-Tucker, T.; Rakic, M.; Spong, C.; Brennan, J., Controlling the Material Properties and Biological Activity of Lipase within Sol- Gel Derived Bioglasses via Organosilane and Polymer Doping. *Chemistry of Materials* **2000**, 12, (12), 3695-3704.
- Keeling-Tucker, T.; Brennan, J., Fluorescent Probes as Reporters on the Local Structure and Dynamics in Sol- Gel-Derived Nanocomposite Materials. *Chemistry of Materials* **2001**, 13, (10), 3331-3350.
- Khansari, N.; Shakiba, Y.; Mahmoudi, M., Chronic inflammation and oxidative stress as a major cause of age-related diseases and cancer. *Recent Patents on Inflammation Allergy Drug Discovery* **2009**, 3, (1), 73-80.
- Kim, S.; Kim, H.; Lee, M.; Jeon, S.; Do, G.; Kwon, E.; Cho, Y.; Kim, D.; Jeong, K.; Park, Y., Naringin time-dependently lowers hepatic cholesterol biosynthesis and plasma cholesterol in rats fed high-fat and high-cholesterol diet. *Journal of Medicinal Food* **2006**, 9, (4), 582-586.
- Kise, H.; Tomiuchi, Y., Unusual solvent effect on protease activity and effective optical resolution of amino acids by hydrolytic reactions in organic solvents. *Biotechnology Letters* **1991**, 13, (5), 317-322.
- Kolosova, N.; Shcheglova, T.; Sergeeva, S.; Loskutova, L., Long-term antioxidant supplementation attenuates oxidative stress markers and cognitive deficits in senescent-accelerated OXYS rats. *Neurobiology of Aging* **2006**, 27, (9), 1289-1297.
- Kong, A.; Yu, R.; Chen, C.; Mandlekar, S.; Primiano, T., Signal transduction events elicited by natural products: role of MAPK and caspase pathways in homeostatic response and induction of apoptosis. *Archives of pharmacal research* **2000**, 23, (1), 1-16.
- Kreft, S.; Knapp, M.; Kreft, I., Extraction of rutin from buckwheat (*Fagopyrum esculentum* Moench) seeds and determination by capillary electrophoresis. *Journal of Agricultural and Food Chemistry* **1999**, 47, (11), 4649-4652.

- Kren, V.; Martinkova, L., Glycosides in Medicine: " The Role of Glycosidic Residue in Biological Activity". *Current Medicinal Chemistry* **2001**, 8, (11), 1303-1328.
- Kukar, T.; Ladd, T.; Bann, M.; Fraering, P.; Narlawar, R.; Maharvi, G.; Healy, B.; Chapman, R.; Welzel, A.; Price, R., Substrate-targeting -secretase modulators. *Nature* **2008**, 453, (7197), 925-929.
- Kwon, O.; Eck, P.; Chen, S.; Corpe, C.; Lee, J.; Kruhlak, M.; Levine, M., Inhibition of the intestinal glucose transporter GLUT2 by flavonoids. *The FASEB Journal* **2007**, 21, (2), 366-377.
- La, V.; Tanabe, S.; Grenier, D., Naringenin inhibits human osteoclastogenesis and osteoclastic bone resorption. *Journal of Periodontal Research* **2009**, 44, (2), 193-198.
- Laane, C.; Boeren, S.; Hilhorst, R.; Veeger, C., Optimization of biocatalysis in organic media. *Studies in Organic Chemistry* **1987**, 29, 65-84.
- Lambert, J.; Heath, S.; Even, G.; Campion, D.; Slegers, K.; Hiltunen, M.; Combarros, O.; Zelenika, D.; Bullido, M.; Tavernier, B., Genome-wide association study identifies variants at CLU and CR1 associated with Alzheimer's disease. *Nature Genetics* **2009**, 41, 1094-1099.
- Lannfelt, L.; Blennow, K.; Zetterberg, H.; Batsman, S.; Ames, D.; Harrison, J.; Masters, C.; Targum, S.; Bush, A.; Murdoch, R., Safety, efficacy, and biomarker findings of PBT2 in targeting A [beta] as a modifying therapy for Alzheimer's disease: a phase IIa, double-blind, randomised, placebo-controlled trial. *The Lancet Neurology* **2008**, 7, (9), 779-786.
- Laurin, D.; Masaki, K.; Foley, D.; White, L.; Launer, L., Midlife dietary intake of antioxidants and risk of late-life incident dementia: the Honolulu-Asia Aging Study. *American Journal of Epidemiology* **2004**, 159, (10), 959-967.
- Lee, S.; Doan, T.; Ha, S.; Chang, W.; Koo, Y., Influence of ionic liquids as additives on sol-gel immobilized lipase. *Journal of Molecular Catalysis B: Enzymatic* **2007a**, 47, (3-4), 129-134.
- Lee, S.; Doan, T.; Ha, S.; Koo, Y., Using ionic liquids to stabilize lipase within sol-gel derived silica. *Journal of Molecular Catalysis B: Enzymatic* **2007b**, 45, (1-2), 57-61.
- Lee, E.; Moon, G.; Choi, W.; Kim, W.; Moon, S., Naringin-induced p21WAF1-mediated G1-phase cell cycle arrest via activation of the Ras/Raf/ERK signaling pathway in vascular smooth muscle cells. *Food and Chemical Toxicology* **2008**, 46, (12), 3800-3807.
- Lee, E.; Kim, D.; Kim, W.; Moon, S., Naringin inhibits matrix metalloproteinase-9 expression and AKT phosphorylation in tumor necrosis factor- α -induced vascular smooth muscle cells. *Molecular Nutrition & Food Research* **2009**, 53, (12), 1582-1591.
- Lehninger, A.; Nelson, D.; Cox, M., *Lehninger principles of biochemistry*. Wh Freeman: 2005.
- Lentini, A.; Forni, C.; Provenzano, B.; Beninati, S., Enhancement of transglutaminase activity and polyamine depletion in B16-F10 melanoma cells by flavonoids naringenin and hesperitin correlate to reduction of the in vivo metastatic potential. *Amino acids* **2007**, 32, (1), 95-100.

REFERENCES

- Letenneur, L.; Proust-Lima, C.; Le Gouge, A.; Dartigues, J.; Barberger-Gateau, P., Flavonoid intake and cognitive decline over a 10-year period. *American Journal of Epidemiology* **2007**, 165, (12), 1364-1371.
- Leifert, W.; Abeywardena, M., Grape seed and red wine polyphenol extracts inhibit cellular cholesterol uptake, cell proliferation, and 5-lipoxygenase activity. *Nutrition Research* **2008**, 28, (12), 842-850.
- Leuchtenberger, S.; Beher, D.; Weggen, S., Selective Modulation of A β Production in Alzheimers Disease: Non-Steroidal Anti-Inflammatory Drugs and Beyond. *Current Pharmaceutical Design* **2006**, 12, (33), 4337-4355.
- Li, X.; Yu, C.; Sun, W.; Liu, G.; Jia, J.; Wang, Y., Simultaneous determination of magnesium lithospermate B, rosmarinic acid, and lithospermic acid in beagle dog serum by liquid chromatography/tandem mass spectrometry. *Rapid Communications in Mass Spectrometry* **2004**, 18, (23), 2878-2882.
- Li, X.; Yu, C.; Lu, Y.; Gu, Y.; Lu, J.; Xu, W.; Xuan, L.; Wang, Y., Pharmacokinetics, tissue distribution, metabolism, and excretion of depside salts from *Salvia miltiorrhiza* in rats. *Drug Metabolism and Disposition* **2007**, 35, (2), 234-239.
- Lim, G.; Yang, F.; Chu, T.; Chen, P.; Beech, W.; Teter, B.; Tran, T.; Ubeda, O.; Ashe, K.; Frautschy, S., Ibuprofen suppresses plaque pathology and inflammation in a mouse model for Alzheimer's disease. *Journal of Neuroscience* **2000**, 20, (15), 5709-5714.
- Lineweaver, H.; Burk, D., The determination of enzyme dissociation constants. *Journal of the American Chemical Society* **1934**, 56, (3), 658-666.
- Liu, Y.; Qin, L.; Wilson, B.; An, L.; Hong, J.; Liu, B., Inhibition by naloxone stereoisomers of β -amyloid peptide (1-42)-induced superoxide production in microglia and degeneration of cortical and mesencephalic neurons. *Journal of Pharmacology and Experimental Therapeutics* **2002**, 302, (3), 1212.
- Liu, Y.; Shi, L.; Wang, M.; Li, Z.; Liu, H.; Li, J., A novel room temperature ionic liquid sol-gel matrix for amperometric biosensor application. *Green Chemistry* **2005a**, 7, (9), 655-658.
- Liu, Y.; Wang, M.; Li, J.; Li, Z.; He, P.; Liu, H., Highly active horseradish peroxidase immobilized in 1-butyl-3-methylimidazolium tetrafluoroborate room-temperature ionic liquid based sol-gel host materials. *Chemical Communications* **2005b**, (13), 1778-1780.
- Livage, J., Sol-gel processes. *Current Opinion in Solid State and Materials Science* **1997**, 2, (2), 132-138.
- Livage, J.; Coradin, T.; Roux, C., Encapsulation of biomolecules in silica gels. *Journal of Physics: Condensed Matter* **2001**, 13, R673-R691.
- Lonhienne, T.; Gerday, C.; Feller, G., Psychrophilic enzymes: revisiting the thermodynamic parameters of activation may explain local flexibility. *Biochimica et Biophysica Acta (BBA)-Protein Structure and Molecular Enzymology* **2000**, 1543, (1), 1-10.
- Luchsinger, J.; Tang, M.; Shea, S.; Mayeux, R., Antioxidant vitamin intake and risk of Alzheimer disease. *Archives of Neurology* **2003**, 60, (2), 203 - 208.
- Lullien-Pellerin, V.; Balny, C., High-pressure as a tool to study some proteins' properties: conformational modification, activity and oligomeric dissociation. *Innovative Food Science & Emerging Technologies* **2002**, 3, (3), 209-221.

- Lüth, H.; Münch, G.; Arendt, T., Aberrant expression of NOS isoforms in Alzheimer's disease is structurally related to nitrotyrosine formation. *Brain Research* **2002**, 953, (1-2), 135-143.
- Lykkesfeldt, J.; Hagen, T.; Vinarsky, V.; Ames, B., Age-associated decline in ascorbic acid concentration, recycling, and biosynthesis in rat hepatocytes—reversal with (R)-{alpha}-lipoic acid supplementation. *The FASEB Journal* **1998**, 12, (12), 1183-1189.
- Mamma, D.; Kalogeris, E.; Hatzinikolaou, D.; Lekanidou, A.; Kekos, D.; Macris, B.; Christakopoulos, P., Biochemical characterization of the multi-enzyme system produced by *Penicillium decumbens* grown on rutin. *Food biotechnology* **2005**, 18, (1), 1-18.
- Manzanares, P.; Orejas, M.; Ibanez, E.; Valles, S.; Ramon, D., Purification and characterization of an alpha-L-rhamnosidase from *Aspergillus nidulans*. *Letters in Applied Microbiology* **2000**, 31, (3), 198-202.
- Manzanares, P.; van den Broeck, H. C.; de Graaff, L. H.; Visser, J., Purification and characterization of two different alpha-L-rhamnosidases, RhaA and RhaB, from *Aspergillus aculeatus*. *Applied and Environmental Microbiology* **2001**, 67, (5), 2230-2234.
- Marinov, B.; Evtodienko, J., Estimation of redox properties of chemical compounds by their reactions with free radicals. *Analytical biochemistry* **1994**, 220, (1), 154-159.
- Mark, R.; Hensley, K.; Butterfield, D.; Mattson, M., Amyloid beta-peptide impairs ion-motive ATPase activities: evidence for a role in loss of neuronal Ca²⁺ homeostasis and cell death. *Journal of Neuroscience* **1995**, 15, (9), 6239-6249.
- Marques, J.; Vila-Real, H. J.; Alfaia, A. J.; Ribeiro, M. H. L., Modelling of the high pressure-temperature effects on naringin hydrolysis based on response surface methodology. *Food Chemistry* **2007**, 105, (2), 504-510.
- Martins, M.; Frizzo, C.; Moreira, D.; Zanatta, N.; Bonacorso, H., Ionic liquids in heterocyclic synthesis. *Chemical Reviews* **2008**, 108, (6), 2015-2050.
- Masaki, K.; Losonczy, K.; Izmirlian, G.; Foley, D.; Ross, G.; Petrovitch, H.; Havlik, R.; White, L., Association of vitamin E and C supplement use with cognitive function and dementia in elderly men. *Neurology* **2000**, 54, (6), 1265-1272.
- Masella, R.; Di Benedetto, R.; Vari, R.; Filesi, C.; Giovannini, C., Novel mechanisms of natural antioxidant compounds in biological systems: involvement of glutathione and glutathione-related enzymes. *The Journal of Nutritional Biochemistry* **2005**, 16, (10), 577-586.
- Matern, U.; Potts, J.; Hahlbrock, K., Two flavonoid-specific malonyltransferases from cell suspension cultures of *Petroselinum hortense*: partial purification and some properties of malonyl-coenzyme A: flavone/flavonol-7-O-glycoside malonyltransferase and malonyl-coenzyme A: flavonol-3-O-glucoside malonyltransferase. *Archives of Biochemistry and Biophysics* **1981**, 208, (1), 233-241.
- Mateo, C.; Palomo, J.; Fernandez-Lorente, G.; Guisan, J.; Fernandez-Lafuente, R., Improvement of enzyme activity, stability and selectivity via immobilization techniques. *Enzyme and Microbial Technology* **2007**, 40, (6), 1451-1463.
- Matsunami, K.; Takamori, I.; Shinzato, T.; Aramoto, M.; Kondo, K.; Otsuka, H.; Takeda, Y., Radical-Scavenging Activities of New Megastigmane Glucosides from *Macaranga tanarius* (L.) Muell.-Arg. *Chemical & pharmaceutical bulletin* **2006**, 54, (10), 1403-1407.

REFERENCES

- McGeer, P.; McGeer, E., The inflammatory response system of brain: implications for therapy of Alzheimer and other neurodegenerative diseases. *Brain Research Reviews* **1995**, 21, (2), 195-218.
- McGeer, P.; Schulzer, M.; McGeer, E., Arthritis and anti-inflammatory agents as possible protective factors for Alzheimer's disease: a review of 17 epidemiologic studies. *Neurology* **1996**, 47, (2), 425-432.
- McGeer, P.; McGeer, E., NSAIDs and Alzheimer disease: epidemiological, animal model and clinical studies. *Neurobiology of Aging* **2007**, 28, (5), 639-647.
- McLaurin, J.; Kierstead, M.; Brown, M.; Hawkes, C.; Lambermon, M.; Phinney, A.; Darabie, A.; Cousins, J.; French, J.; Lan, M., Cyclohexanehexol inhibitors of A aggregation prevent and reverse Alzheimer phenotype in a mouse model. *Nature medicine* **2006**, 12, (7), 801-808.
- Meda, L.; Cassatella, M.; Szendrei, G.; Otvos, L.; Baron, P.; Villalba, M.; Ferrari, D.; Rossi, F., Activation of microglial cells by β -amyloid protein and interferon. *Nature* **1995**, 374, (6523), 647-650.
- Metzler, D., *Biochemistry: the chemical reactions of living cells*. Academic: 2001.
- Michaelis, L.; Menten, M., The kinetics of invertase activity. *Biochemische Zeitschrift* **1913**, 49, (333), 166-180.
- Milano, J.; McKay, J.; Dagenais, C.; Foster-Brown, L.; Pognan, F.; Gadiant, R.; Jacobs, R.; Zacco, A.; Greenberg, B.; Ciaccio, P., Modulation of notch processing by γ -secretase inhibitors causes intestinal goblet cell metaplasia and induction of genes known to specify gut secretory lineage differentiation. *Toxicological Sciences* **2004**, 82, 341-358.
- Miller, G., Use of DNS reagent for determination of reducing sugars. *Analytical Chemistry* **1959**, 31, (3), 426-428.
- Miller, E.; Peacock, J.; Bourland, T.; Taylor, S.; Wright, J.; Patil, B., Inhibition of oral carcinogenesis by citrus flavonoids. *Nutrition and Cancer* **2008**, 60, (1), 69-74.
- Montgomery, D.C., Myers, R. H., *Response Surface Methodology: Process and Product Optimization Using Designed Experiments*. Wiley-Interscience: 2002.
- Morikawa, K.; Nonaka, M.; Mochizuki, H.; Handa, K.; Hanada, H.; Hirota, K., Naringenin and hesperetin induce growth arrest, apoptosis, and cytoplasmic fat deposit in human preadipocytes. *Journal of Agricultural and Food Chemistry* **2008**, 56, (22), 11030-11037.
- Mozhaev, V.; Heremans, K.; Frank, J.; Masson, P.; Balny, C., High pressure effects on protein structure and function. *Proteins: Structure, Function, and Bioinformatics* **1996**, 24, (1), 81-91.
- Mullen, W.; Larcombe, S.; Arnold, K.; Welchman, H.; Crozier, A., Use of Accurate Mass Full Scan Mass Spectrometry for the Analysis of Anthocyanins in Berries and Berry-Fed Tissues†. *Journal of Agricultural and Food Chemistry* **2009**, 58, (7), 3910-3915.
- Musa, M.; Ziegelmann-Fjeld, K.; Vieille, C.; Zeikus, J.; Phillips, R., Xerogel-encapsulated W110A secondary alcohol dehydrogenase from *Thermoanaerobacter ethanolicus* performs asymmetric reduction of hydrophobic ketones in organic solvents. *Angewandte Chemie International Edition* **2007**, 46, (17), 3091-3094.

- Mutter, M.; Beldman, G.; Schols, H. A.; Voragen, A. G., Rhamnogalacturonan alpha-L-rhamnopyranohydrolase. A novel enzyme specific for the terminal nonreducing rhamnosyl unit in rhamnogalacturonan regions of pectin. *Plant Physiology* **1994**, 106, (1), 241-250.
- Naasani, I.; Oh-hashi, F.; Oh-hara, T.; Feng, W.; Johnston, J.; Chan, K.; Tsuruo, T., Blocking telomerase by dietary polyphenols is a major mechanism for limiting the growth of human cancer cells in vitro and in vivo. *Cancer Research* **2003**, 63, (4), 824-830.
- Nahmias, Y.; Goldwasser, J.; Casali, M.; van Poll, D.; Wakita, T.; Chung, R.; Yarmush, M., Apolipoprotein B-dependent hepatitis C virus secretion is inhibited by the grapefruit flavonoid naringenin. *Hepatology* **2008**, 47, (5), 1437-1445.
- Nakamura, Y.; Ohmaki, M.; Murakami, K.; Yoneda, Y., Involvement of protein kinase C in glutamate release from cultured microglia. *Brain research* **2003**, 962, (1-2), 122-128.
- Nemeth, K.; Plumb, G.; Berrin, J.; Juge, N.; Jacob, R.; Naim, H.; Williamson, G.; Swallow, D.; Kroon, P., Deglycosylation by small intestinal epithelial cell -glucosidases is a critical step in the absorption and metabolism of dietary flavonoid glycosides in humans. *European Journal of Nutrition* **2003**, 42, (1), 29-42.
- Noratto, G.; Porter, W.; Byrne, D.; Cisneros-Zevallos, L., Identifying peach and plum polyphenols with chemopreventive potential against estrogen-independent breast cancer cells. *Journal of Agricultural and Food Chemistry* **2009**, 57, (12), 5219-5126.
- Norouzian, D.; Hosseinzadeh, A.; Inanlou, D.; Moazami, N., Production and partial purification of naringinase by *Penicillium decumbens* PTCC 5248. *World Journal of Microbiology and Biotechnology* **2000**, 16, (5), 471-473.
- Nowak, T.; Handford, A., *Pathophysiology: concepts and applications for health care professionals*. McGraw-Hill Higher Education, Boston: 2004.
- Nunomura, A.; Castellani, R.; Zhu, X.; Moreira, P.; Perry, G.; Smith, M., Involvement of oxidative stress in Alzheimer disease. *Journal of Neuropathology & Experimental Neurology* **2006**, 65, (7), 631-641.
- Ofer, M.; Wolfram, S.; Koggel, A.; Spahn-Langguth, H.; Langguth, P., Modulation of drug transport by selected flavonoids: Involvement of P-gp and OCT? *European Journal of Pharmaceutical Sciences* **2005**, 25, (2-3), 263-271.
- Ono, M.; Tosa, T.; Chibata, I., Preparation and properties of naringinase immobilized by ionic binding to DEAE-Sephadex. *Journal of Fermentation Technology* **1977**, 55, 493-500.
- Ono, K.; Yoshiike, Y.; Takashima, A.; Hasegawa, K.; Naiki, H.; Yamada, M., Potent anti-amyloidogenic and fibril-destabilizing effects of polyphenols in vitro: implications for the prevention and therapeutics of Alzheimer's disease. *Journal of neurochemistry* **2003**, 87, (1), 172-181.
- Pang, W.; Wang, X.; Mok, S.; Lai, W.; Chow, H.; Leung, P.; Yao, X.; Wong, M., Naringin improves bone properties in ovariectomized mice and exerts oestrogen-like activities in rat osteoblast-like (UMR-106) cells. *British journal of pharmacology* **2010**, 159, (8), 1693-1703.
- Pardridge, W. M., Drug Delivery to the Brain. *Journal of Cerebral Blood Flow & Metabolism* **1997**, 17, (7), 713-731.

REFERENCES

- Park, S.; Kazlauskas, R., Biocatalysis in ionic liquids-advantages beyond green technology. *Current Opinion in Biotechnology* **2003**, 14, (4), 432-437.
- Paulo, A.; Martins, S.; Branco, P.; Dias, T.; Borges, C.; Rodrigues, A.; do Céu Costa, M.; Teixeira, A.; Mota-Filipe, H., The opposing effects of the flavonoids isoquercitrin and Sissotrin, isolated from *Pterospartum tridentatum*, on oral glucose tolerance in rats. *Phytotherapy Research* **2008**, 22, (4), 539-543.
- Pedro, H.; Alfaia, A.; Marques, J.; Vila-Real, H.; Calado, A.; Ribeiro, M., Design of an immobilized enzyme system for naringin hydrolysis at high-pressure. *Enzyme and Microbial Technology* **2007**, 40, (3), 442-446.
- Peila, R.; Launer, L., Inflammation and dementia: epidemiologic evidence. *Acta Neurologica Scandinavica* **2006**, 114, (s185), 102-106.
- Pekin, G.; Vardar-Sukan, F.; Kosaric, N., Production of sophorolipids from *Candida bombicola* ATCC 22214 using Turkish corn oil and honey. *Engineering in Life Sciences* **2005**, 5, (4), 357-362.
- Pelzer, H.; Wigner, E., The speed constants of the exchange reactions. *Z Phys Chem B* **1932**, 15, 445.
- Peyser, C.; Folstein, M.; Chase, G.; Starkstein, S.; Brandt, J.; Cockrell, J.; Bylsma, F.; Coyle, J.; McHugh, P.; Folstein, S., Trial of d-alpha-tocopherol in Huntington's disease. *American Journal of Psychiatry* **1995**, 152, (12), 1771-1775.
- Pierre, A., The sol-gel encapsulation of enzymes. *Biocatalysis and Biotransformation* **2004**, 22, (3), 145-170.
- Pinheiro, L., Efeito da pressão, temperatura e solvente na quaternização da trietilfosfina. Tese de doutoramento, Lisboa: FFUL, 1999.
- Pollard, D.; Woodley, J., Biocatalysis for pharmaceutical intermediates: the future is now. *TRENDS in Biotechnology* **2007**, 25, (2), 66-73.
- Pulley, G., Solubility of naringin in water. *Industrial & Engineering Chemistry Analytical Edition* **1936**, 8, (5), 360-360.
- Punithavathi, V.; Anuthama, R.; Prince, P., Combined treatment with naringin and vitamin C ameliorates streptozotocin-induced diabetes in male Wistar rats. *Journal of Applied Toxicology* **2008**, 28, (6), 806-813.
- Puri, M.; Banerjee, U., Production, purification, and characterization of the debittering enzyme naringinase. *Biotechnology advances* **2000**, 18, (3), 207-217.
- Puri, M.; Marwaha, S.; Kothari, R., Studies on the applicability of alginate-entrapped naringinase for the debittering of kinnow juice. *Enzyme and Microbial Technology* **1996**, 18, (4), 281-285.
- Puri, M.; Seth, M.; Marwaha, S.; Kothari, R., Debittering of Kinnow mandarin juice by covalently bound Naringinase on hen egg white. *Food biotechnology* **2001**, 15, (1), 13-23.
- Puri, M.; Kaur, H.; Kennedy, J., Covalent immobilization of naringinase for the transformation of a flavonoid. *Journal of Chemical Technology & Biotechnology* **2005**, 80, (10), 1160-1165.

- Pratico, D.; Uryu, K.; Leight, S.; Trojanowski, J.; Lee, V., Increased lipid peroxidation precedes amyloid plaque formation in an animal model of Alzheimer amyloidosis. *Journal of Neuroscience* **2001**, 21, (12), 4183-4187.
- Quan, N.; Stern, E.; Whiteside, M.; Herkenham, M., Induction of pro-inflammatory cytokine mRNAs in the brain after peripheral injection of subseptic doses of lipopolysaccharide in the rat. *Journal of Neuroimmunology* **1999**, 93, (1-2), 72.
- Quinn, J.; Bussiere, J.; Hammond, R.; Montine, T.; Henson, E.; Jones, R.; Stackman Jr, R., Chronic dietary [alpha]-lipoic acid reduces deficits in hippocampal memory of aged Tg2576 mice. *Neurobiology of Aging* **2007**, 28, (2), 213-225.
- Radivoje, P.; Nenad, M.; Slobodan, J.; Olivera, P.; Tanja, C.V.; Zoran, V.; Ratko, J., Biocatal. and Biotrans. **2006**, 24, 195-200.
- Rajadurai, M.; Stanely Mainzen Prince, P., Preventive effect of naringin on cardiac markers, electrocardiographic patterns and lysosomal hydrolases in normal and isoproterenol-induced myocardial infarction in Wistar rats. *Toxicology* **2007**, 230, (2-3), 178-188.
- Rao, C., Regulation of COX and LOX by curcumin. *The Molecular Targets and Therapeutic Uses of Curcumin in Health and Disease* **2007**, 213-226.
- Reddy, P., Mitochondrial medicine for aging and neurodegenerative diseases. *Neuromolecular Medicine* **2008**, 10, (4), 291-315.
- Reetz, M.; Tielmann, P.; Wiesenhöfer, W.; Könen, W.; Zonta, A., Second generation sol-gel encapsulated lipases: Robust heterogeneous biocatalysts. *Advanced Synthesis & Catalysis* **2003**, 345, (6-7), 717-728.
- Repovic, P.; Benveniste, E., Prostaglandin E2 is a novel inducer of oncostatin-M expression in macrophages and microglia. *Journal of Neuroscience* **2002**, 22, (13), 5334.
- Rezai-Zadeh, K.; Shytle, D.; Sun, N.; Mori, T.; Hou, H.; Jeanniton, D.; Ehrhart, J.; Townsend, K.; Zeng, J.; Morgan, D., Green tea epigallocatechin-3-gallate (EGCG) modulates amyloid precursor protein cleavage and reduces cerebral amyloidosis in Alzheimer transgenic mice. *Journal of Neuroscience* **2005**, 25, (38), 8807-8814.
- Ribeiro, M. H. L., Produção de L-Triptofano a partir de L-serina e Indol com Células de E. coli em Sistema Aquoso/Orgânico; Separação e Isolamento do Produto. Tese de doutoramento, Lisboa; FFUL, 1994.
- Ribeiro, M.; Silveira, D.; Ebert, C.; Ferreira-Dias, S., Response surface modelling of the consumption of bitter compounds from orange juice by *Acinetobacter calcoaceticus*. *Journal of Molecular Catalysis B: Enzymatic* **2003**, 21, (1-2), 81-88.
- Ribeiro, M.; Manha, S.; Brito, L., The effects of salt and pH stress on the growth rates of persistent strains of *Listeria monocytogenes* collected from specific ecological niches. *Food Research International* **2006**, 39, (7), 816-822.
- Ribeiro, I.; Ribeiro, M., Kinetic modelling of naringin hydrolysis using a bitter sweet alfa-rhamnopyranosidase immobilized in k-carrageenan. *Journal of Molecular Catalysis B: Enzymatic* **2008a**, 51, (1-2), 10-18.
- Ribeiro, I.; Rocha, J.; Sepodes, B.; Mota-Filipe, H.; Ribeiro, M., Effect of naringin enzymatic hydrolysis towards naringenin on the anti-inflammatory activity of both compounds. *Journal of Molecular Catalysis B: Enzymatic* **2008b**, 52, 13-18.

REFERENCES

- Ribeiro, M.; Afonso, C.; Vila-Real, H.; Alfaia, A.; Ferreira, L., Contribution of response surface methodology to the modeling of naringin hydrolysis by naringinase Ca-alginate beads under high pressure. *LWT-Food Science and Technology* **2010**, 43, 482-487.
- Ritchie, C. D. *Physical organic chemistry*. Marcel Dekker, Inc, New York: 1990.
- Ritchie, R.; Prvan, T., Current statistical methods for estimating the Km and Vmax of Michaelis-Menten kinetics. *Biochemical Education* **1996**, 24, (4), 196-206.
- Roccatano, D.; Wong, T.; Schwaneberg, U.; Zacharias, M., Toward understanding the inactivation mechanism of monooxygenase P450 BM-3 by organic cosolvents: A molecular dynamics simulation study. *Biopolymers* **2006**, 83, (5), 467-476.
- Rogério, A.; Kanashiro, A.; Fontanari, C.; da Silva, E.; Lucisano-Valim, Y.; Soares, E.; Faccioli, L., Anti-inflammatory activity of quercetin and isoquercitrin in experimental murine allergic asthma. *Inflammation research* **2007**, 56, (10), 402-408.
- Roux, C.; Livage, J.; Farhati, K.; Monjour, L., Antibody-antigen reactions in porous sol-gel matrices. *Journal of Sol-Gel Science and Technology* **1997**, 8, (1), 663-666.
- Sadik, C.; Sies, H.; Schewe, T., Inhibition of 15-lipoxygenases by flavonoids: structure-activity relations and mode of action. *Biochemical pharmacology* **2003**, 65, (5), 773-781.
- Saliba, E.; Henrot, A., Inflammatory mediators and neonatal brain damage. *Biology of the Neonate* **2001**, 79, (3-4), 224-227.
- Salloway, S.; Sperling, R.; Gilman, S.; Fox, N.; Blennow, K.; Raskind, M.; Sabbagh, M.; Honig, L.; Doody, R.; van Dyck, C., A phase 2 multiple ascending dose trial of bapineuzumab in mild to moderate Alzheimer disease. *Neurology* **2009**, 73, (24), 2061-2070.
- Scarpini, E.; Scheltens, P.; Feldman, H., Treatment of Alzheimer's disease: current status and new perspectives. *Lancet neurology* **2003**, 2, (9), 539-547.
- Scharnagl, C.; Reif, M.; Friedrich, J., Stability of proteins: Temperature, pressure and the role of the solvent. *Biochimica et Biophysica Acta (BBA)-Proteins & Proteomics* **2005**, 1749, (2), 187-213.
- Schindler, R.; Mentlein, R., Flavonoids and vitamin E reduce the release of the angiogenic peptide vascular endothelial growth factor from human tumor cells. *Journal of nutrition* **2006**, 136, (6), 1477-1482.
- Schneider, A.; Mandelkow, E., Tau-based treatment strategies in neurodegenerative diseases. *Neurotherapeutics* **2008**, 5, (3), 443-457.
- Schuessel, K.; Schäfer, S.; Bayer, T.; Czech, C.; Pradier, L.; Müller-Spahn, F.; Müller, W.; Eckert, A., Impaired Cu/Zn-SOD activity contributes to increased oxidative damage in APP transgenic mice. *Neurobiology of disease* **2005**, 18, (1), 89-99.
- Segurado, M., Reações de Menshutkin na série da piridina; Análise do Parâmetro ρ da Equação de Hammett. Tese de doutoramento, Lisboa: FFUL, 1989.
- Şekeroğlu, G.; Fadiloğlu, S.; Göğüş, F., Immobilization and characterization of naringinase for the hydrolysis of naringin. *European Food Research and Technology* **2006**, 224, (1), 55-60.
- Sheldon, R.; Lau, R.; Sorgedraeger, M.; Rantwijk, F.; Seddon, K., Biocatalysis in ionic liquids. *Green Chemistry* **2002**, 4, (2), 147-151.

- Shi, Y.; Dai, J.; Liu, H.; Li, R.; Sun, P.; Du, Q.; Pang, L.; Chen, Z.; Yin, K., Naringenin inhibits allergen-induced airway inflammation and airway responsiveness and inhibits NF- κ B activity in a murine model of asthma. *Canadian Journal of Physiology and Pharmacology* **2009**, 87, (9), 729-735.
- Shimmyo, Y.; Kihara, T.; Akaike, A.; Niidome, T.; Sugimoto, H., Flavonols and flavones as BACE-1 inhibitors: structure-activity relationship in cell-free, cell-based and in silico studies reveal novel pharmacophore features. *Biochimica et Biophysica Acta (BBA)-General Subjects* **2008**, 1780, (5), 819-825.
- Shineman, D.; Salthouse, T.; Launer, L.; Hof, P.; Bartzokis, G.; Kleiman, R.; Luine, V.; Buccafusco, J.; Small, G.; Aisen, P., Therapeutics for cognitive aging. *Annals of the New York Academy of Sciences* **2010**, 1191, E1-E15.
- Siemers, E.; Friedrich, S.; Dean, R., Safety, tolerability and biomarker effects of an Abeta monoclonal antibody administered to patients with Alzheimer's disease. *Alzheimers Dement* **2008**, 4 (1), T774.
- Silva, R., Rat cultured neuronal and glial cells respond differently to toxicity of unconjugated bilirubin. *Pediatric research* **2002**, 51, (4), 535.
- Sinclair, A.; Bayer, A.; Johnston, J.; Warner, C.; Maxwell, S., Altered plasma antioxidant status in subjects with Alzheimer's disease and vascular dementia. *International journal of geriatric psychiatry* **1998**, 13, (12), 840-845.
- Smeller, L., Pressure-temperature phase diagrams of biomolecules. *Biochimica et Biophysica Acta (BBA)-Protein Structure and Molecular Enzymology* **2002**, 1595, (1-2), 11-29.
- Sonkusare, S.; Kaul, C.; Ramarao, P., Dementia of Alzheimer's disease and other neurodegenerative disorders--memantine, a new hope. *Pharmacological Research* **2005**, 51, (1), 1-17.
- Soria, F.; Ellenrieder, G., Thermal inactivation and product inhibition of *Aspergillus terreus* CECT 2663 alpha-L-rhamnosidase and their role on hydrolysis of naringin solutions. *Biosci Biotechnol Biochem* **2002**, 66, (7), 1442-1449.
- Soundararajan, R.; Wishart, A.; Rupasinghe, H.; Arcellana-Panlilio, M.; Nelson, C.; Mayne, M.; Robertson, G., Quercetin 3-glucoside protects neuroblastoma (SH-SY5Y) cells in vitro against oxidative damage by inducing sterol regulatory element-binding protein-2-mediated cholesterol biosynthesis. *Journal of Biological Chemistry* **2008**, 283, (4), 2231-2245.
- Sultana, R.; Perluigi, M.; Butterfield, D., Protein oxidation and lipid peroxidation in brain of subjects with Alzheimer's disease: insights into mechanism of neurodegeneration from redox proteomics. *Antioxidants & Redox Signaling* **2006**, 8, (11-12), 2021-2037.
- Summerfield, S.; Stevens, A.; Cutler, L.; del Carmen Osuna, M.; Hammond, B.; Tang, S.; Hersey, A.; Spalding, D.; Jeffrey, P., Improving the in vitro prediction of in vivo central nervous system penetration: integrating permeability, P-glycoprotein efflux, and free fractions in blood and brain. *Journal of Pharmacology and Experimental Therapeutics* **2006**, 316, (3), 1282.
- Summerfield, S.; Read, K.; Begley, D.; Obradovic, T.; Hidalgo, I.; Coggon, S.; Lewis, A.; Porter, R.; Jeffrey, P., Central nervous system drug disposition: the relationship

REFERENCES

- between in situ brain permeability and brain free fraction. *Journal of Pharmacology and Experimental Therapeutics* **2007**, 322, (1), 205-213.
- Sun, T.; Powers, J.; Tang, J., Enzyme-Catalyzed Change of Antioxidants Content and Antioxidant Activity of Asparagus Juice. *Journal of Agricultural and Food Chemistry* **2007**, 55, (1), 56-60.
- Sung, S.; Yao, Y.; Uryu, K.; Yang, H.; Lee, V.; Trojanowski, J.; Pratico, D., Early vitamin E supplementation in young but not aged mice reduces A levels and amyloid deposition in a transgenic model of Alzheimer's disease. *The FASEB Journal* **2003**, 309611.
- Tamai, I.; Tsuji, A., Transporter mediated permeation of drugs across the blood-brain barrier. *Journal of pharmaceutical sciences* **2000**, 89, (11), 1371-1388.
- Tanaka, Y.; Tao, W.; Blanchard, J.; Hehre, E., Transition state structures for the hydrolysis of alpha-D-glucopyranosyl fluoride by retaining and inverting reactions of glycosylases. *Journal of Biological Chemistry* **1994**, 269, (51), 32306-32312.
- Tedeschi, A.; D'Errico, G.; Lauro, M. R.; Sansone, F.; Di Marino, S.; D'Ursi, A. M.; Aquino, R. P., Effect of flavonoids on the A[beta](25-35)-phospholipid bilayers interaction. *European Journal of Medicinal Chemistry* **2010**, 45, (9), 3998-4003.
- Thal, D.; Holzer, M.; Rüb, U.; Waldmann, G.; Günzel, S.; Zedlick, D.; Schober, R., Alzheimer-Related [tau]-Pathology in the Perforant Path Target Zone and in the Hippocampal Stratum Oriens and Radiatum Correlates with Onset and Degree of Dementia. *Experimental neurology* **2000**, 163, (1), 98-110.
- Tischer, W.; Kasche, V., Immobilized enzymes: crystals or carriers? *Trends in biotechnology* **1999**, 17, (8), 326-335.
- Townsend, K.; Pratico, D., Novel therapeutic opportunities for Alzheimer's disease: focus on nonsteroidal anti-inflammatory drugs. *The FASEB Journal* **2005**, 19, (12), 1592-1601.
- Truhlar, D.; Garrett, B.; Klippenstein, S., Current status of transition-state theory. *Journal of Physical Chemistry* **1996**, 100, (31), 12771-12800.
- Tückmantel, W.; Kozikowski, A.; Romanczyk Jr, L., Studies in Polyphenol Chemistry and Bioactivity. 1. Preparation of Building Blocks from (+)-Catechin. Procyanidin Formation. Synthesis of the Cancer Cell Growth Inhibitor, 3-O-Galloyl-(2R, 3R)-epicatechin-4, 8-[3-O-galloyl-(2R, 3R)-epicatechin]. *Journal of the American Chemical Society* **1999**, 121, (51), 12073-12081.
- Tsakanikas, D.; Shah, K.; Flores, C.; Assuras, S.; Relkin, N., Effects of uninterrupted intravenous immunoglobulin treatment of Alzheimer's disease for nine months. *Alzheimer's & Dementia* **2008**, 4, (4 suppl 2), T776.
- Tsen, H.; Tsai, S.; Yu, G., Fiber entrapment of naringinase from *Penicillium* sp. and application to fruit juice debittering. *Journal of Fermentation and Bioengineering* **1989**, 67, (3), 186-189.
- Tsen, H.; Yu, G., Limonin and naringin removal from grapefruit juice with naringinase entrapped in cellulose triacetate fibers. *Journal of food science* **1991**, 56, (1), 31-34.
- Ueno, K.; Inaba, A.; Kondoh, M.; Watanabe, M., Colloidal stability of bare and polymer-grafted silica nanoparticles in ionic liquids. *Langmuir* **2008**, 24, (10), 5253-5259.

- Utesch, D.; Feige, K.; Dasenbrock, J.; Broschard, T.; Harwood, M.; Danielewska-Nikiel, B.; Lines, T., Evaluation of the potential in vivo genotoxicity of quercetin. *Mutation Research/Genetic Toxicology and Environmental Mutagenesis* **2008**, 654, (1), 38-44.
- Vafeiadou, K.; Vauzour, D.; Lee, H.; Rodriguez-Mateos, A.; Williams, R.; Spencer, J., The citrus flavanone naringenin inhibits inflammatory signalling in glial cells and protects against neuroinflammatory injury. *Archives of Biochemistry and Biophysics* **2009**, 484, (1), 100-109.
- Van Eldik, R.; Asano, T.; Le Noble, W., Activation and reaction volumes in solution. 2. *Chemical Reviews* **1989**, 89, (3), 549-688.
- Vázquez, J.; González, M.; Murado, M., Preliminary tests on nisin and pediocin production using waste protein sources:: Factorial and kinetic studies. *Bioresource technology* **2006**, 97, (4), 605-613.
- Veinbergs, I.; Mallory, M.; Sagara, Y.; Masliah, E., Vitamin E supplementation prevents spatial learning deficits and dendritic alterations in aged apolipoproteinE-deficient mice. *European Journal of Neuroscience* **2000**, 12, (12), 4541-4546.
- Vermue, M.; Tramper, J., Biocatalysis in non-conventional media: medium engineering aspects. *Pure and applied chemistry* **1995**, 67, 345-345.
- Venton, D.; Cheesman, K.; Chatterton Jr, R.; Anderson, T., Entrapment of a highly specific antiprogestrone antiserum using polysiloxane copolymers. *Biochimica et Biophysica Acta (BBA)-General Subjects* **1984**, 797, (3), 343-347.
- Viana, C.; Reis, J., Pressure dependence of rate and equilibrium constants in solution. A guide to analytical equations. *Pure and applied chemistry* **1996**, 68, 1541-1551.
- Vila-Real, H.; Alfaia, A.; Calado, A.; Ribeiro, M., High pressure-temperature effects on enzymatic activity: Naringin bioconversion. *Food Chemistry* **2007**, 102, (3), 565-570.
- Vuataz, L. In J. R. Piggott (Ed.), *Statistical procedures in food research* London: Elsevier. **1986**, 100-123.
- Walgren, R.; Lin, J.; Kinne, R.; Walle, T., Cellular uptake of dietary flavonoid quercetin 4'- β -glucoside by sodium-dependent glucose transporter SGLT1. *Journal of Pharmacology and Experimental Therapeutics* **2000**, 294, (3), 837-843.
- Walle, T.; Walle, U., The β -D-glucoside and sodium-dependent glucose transporter 1 (SGLT1)-inhibitor phloridzin is transported by both SGLT1 and multidrug resistance-associated proteins 1/2. *Drug Metabolism and Disposition* **2003**, 31, (11), 1288-1291.
- Walling, C.; Tanner, D., Organic Reactions under High Pressure. VIII. The Pressure-Dependence of V^* and the Compressibility of Transition States. *Journal of the American Chemical Society* **1963**, 85, (5), 612-615.
- Walsh, D.; Selkoe, D., A oligomers—a decade of discovery. *Journal of neurochemistry* **2007**, 101, (5), 1172-1184.
- Wambolt, C.; Saavedra, S., Iodide fluorescence quenching of sol-gel immobilized BSA. *Journal of Sol-Gel Science and Technology* **1996**, 7, (1), 53-57.
- Wang, M.; Tadmor, Y.; Wu, Q.; Chin, C.; Garrison, S.; Simon, J., Quantification of protodioscin and rutin in asparagus shoots by LC/MS and HPLC methods. *Journal of Agricultural and Food Chemistry* **2003**, 51, (21), 6132-6136

REFERENCES

- Wang, J.; Ho, L.; Zhao, Z.; Seror, I.; Humala, N.; Dickstein, D.; Thiyagarajan, M.; Percival, S.; Talcott, S.; Pasinetti, G., Moderate consumption of Cabernet Sauvignon attenuates A β neuropathology in a mouse model of Alzheimer's disease. *The FASEB Journal* **2006a**, 20, (13), 2313-2320.
- Wang, M.; Chao, P.; Hou, Y.; Hsiu, S.; Wen, K.; Tsai, S., Pharmacokinetics and Conjugation Metabolism of Naringin and Naringenin in Rats after Single Dose and Multiple Dose Administrations. *Journal of Food and Drug Analysis* **2006b**, 14, (3), 247-253.
- Wasserscheid, P.; Keim, W., Ionic Liquids-New. *Solutions" for Transition Metal Catalysis". Angewandte Chemie International Edition* **2000**, 39, 3772-3789.
- Way, T.; Kao, M.; Lin, J., Degradation of HER2/neu by apigenin induces apoptosis through cytochrome c release and caspase-3 activation in HER2/neu-overexpressing breast cancer cells. *FEBS letters* **2005**, 579, (1), 145-152.
- Weemaes, C.; Ludikhuyze, L.; Van den Broeck, I.; Hendrickx, M., Kinetics of combined pressure-temperature inactivation of avocado polyphenoloxidase. *Biotechnology and bioengineering* **1998**, 60, (3), 292-300.
- Weggen, S.; Eriksen, J.; Das, P.; Sagi, S.; Wang, R.; Pietrzik, C.; Findlay, K.; Smith, T.; Murphy, M.; Bulter, T., A subset of NSAIDs lower amyloidogenic A β 42 independently of cyclooxygenase activity. *Nature* **2001**, 414, (6860), 212-216.
- Wei, Y.; Xu, J.; Feng, Q.; Dong, H.; Lin, M., Encapsulation of enzymes in mesoporous host materials via the nonsurfactant-templated sol-gel process. *Materials letters* **2000**, 44, (1), 6-11.
- Welton, T., Room-temperature ionic liquids. Solvents for synthesis and catalysis. *Chemical Reviews* **1999**, 99, (8), 2071-2084.
- Wiedersich, J.; Köhler, S.; Skerra, A.; Friedrich, J., Temperature and pressure dependence of protein stability: The engineered fluorescein-binding lipocalin FluA shows an elliptic phase diagram. *Proceedings of the National Academy of Sciences* **2008**, 105, (15), 5756-5761.
- Wischik, C.; Bentham, P.; Wischik, D.; Seng, K., Tau aggregation inhibitor (TAI) therapy with remberTM arrests disease progression in mild and moderate Alzheimer's disease over 50 weeks. *Alzheimer's and Dementia* **2008**, 4, (1), T167.
- Wolffram, S.; Block, M.; Ader, P., Quercetin-3-glucoside is transported by the glucose carrier SGLT1 across the brush border membrane of rat small intestine. *Journal of Nutrition* **2002**, 132, (4), 630-635.
- Wold, S.; Ahlberg, P., Evaluation of Activation Parameters for a First Order Reaction from One Kinetic Experiment-Theory, Numerical Methods and Computer Program. *Acta Chemica Scandinavica* **1970**, 24, 618-632
- Wong, R.; Rabie, A., Effect of naringin on bone cells. *Journal of Orthopaedic Research* **2006**, 24, (11), 2045-2050.
- Wood, N., Bound Sugars in Hepatic Glycoproteins from Male Rats During Dietary Citrus Bioflavonoid and/or Ascorbic Acid Supplementation. *Journal of Medicinal Food* **2005**, 8, (4), 512-517.

- Wu, X.; Choi, M., An optical glucose biosensor based on entrapped-glucose oxidase in silicate xerogel hybridised with hydroxyethyl carboxymethyl cellulose. *Analytica Chimica Acta* **2004**, 514, (2), 219-226.
- Wu, J.; Fong, Y.; Tsai, H.; Chen, Y.; Tsuzuki, M.; Tang, C., Naringin-induced bone morphogenetic protein-2 expression via PI3K, Akt, c-Fos/c-Jun and AP-1 pathway in osteoblasts. *European journal of pharmacology* **2008**, 588, (2-3), 333-341.
- Wynne Jones, W.; Eyring, H., The absolute rate of reactions in condensed phases. *The Journal of Chemical Physics* **1935**, 3, 492.
- Wyss-Coray, T.; Mucke, L., Inflammation in neurodegenerative disease-a double-edged sword. *Neuron* **2002**, 35, (3), 419-432.
- Yang, F.; Lim, G.; Begum, A.; Ubeda, O.; Simmons, M.; Ambegaokar, S.; Chen, P.; Kaye, R.; Glabe, C.; Frautschi, S., Curcumin inhibits formation of amyloid {beta} oligomers and fibrils, binds plaques, and reduces amyloid in vivo. *Journal of Biological Chemistry* **2005**, 280, (7), 5892-5901.
- Yalim, S.; Ozdemir, Y.; Ekiz, H., Naringin in Turkish Orange Juices and Its Reduction by Naringinase. *Journal of Food and Drug Analysis* **2004**, 12, (3), 273-276.
- Yoshihara, D.; Fujiwara, N.; Suzuki, K., Antioxidants: Benefits and risks for long-term health. *Maturitas* **2010**, 67 (2), 103-107.
- Yoshitake, T.; Kiyohara, Y.; Kato, I.; Ohmura, T.; Iwamoto, H.; Nakayama, K.; Ohmori, S.; Nomiyama, K.; Kawano, H.; Ueda, K., Incidence and risk factors of vascular dementia and Alzheimer's disease in a defined elderly Japanese population: the Hisayama Study. *Neurology* **1995**, 45, (6), 1161.
- Youdim, K.; Shukitt-Hale, B.; Joseph, J., Flavonoids and the brain: interactions at the blood-brain barrier and their physiological effects on the central nervous system. *Free Radical Biology and Medicine* **2004**, 37, (11), 1683-1693.
- Young, R.; Mitchell, R.; Brown, T.; Ganellin, C.; Griffiths, R.; Jones, M.; Rana, K.; Saunders, D.; Smith, I., Development of a new physicochemical model for brain penetration and its application to the design of centrally acting H2 receptor histamine antagonists. *Journal of medicinal chemistry* **1988**, 31, (3), 656-671.
- Yu, B.; Yang, R., Critical evaluation of the free radical theory of aging. *Annals of the New York Academy of Sciences* **1996**, 786, (1), 1-11.
- Yu, B.; Chung, H., The inflammatory process in aging. *Reviews in Clinical Gerontology* **2006**, 16, 179-187.
- Zandi, E.; Rothwarf, D.; Delhase, M.; Hayakawa, M.; Karin, M., The I [kappa] B kinase complex (IKK) contains two kinase subunits, IKK [alpha] and IKK [beta], necessary for I [kappa] B phosphorylation and NF-[kappa] B activation. *Cell* **1997**, 91, (2), 243-252.
- Zandi, P.; Anthony, J.; Khachaturian, A.; Stone, S.; Gustafson, D.; Tschanz, J.; Norton, M.; Welsh-Bohmer, K.; Breitner, J., Reduced risk of Alzheimer disease in users of antioxidant vitamin supplements: the Cache County Study. *Archives of neurology* **2004**, 61, (1), 82-88.
- Zarcula, C.; Croitoru, R.; Corîci, L.; Csunderlik, C.; Peter, F., Improvement of Lipase Catalytic Properties by Immobilization in Hybrid Matrices. *International Journal of Chemical and Biomolecular Engineering* **2009**, 2, (3), 138-143.

REFERENCES

Zecca, L.; Mesonero, J.; Stutz, A.; Poirée, J.; Giudicelli, J.; Cursio, R.; Gloor, S.; Semenza, G., Intestinal lactase-phlorizin hydrolase (LPH): the two catalytic sites; the role of the pancreas in pro-LPH maturation. *FEBS letters* **1998**, 435, (2-3), 225-228.

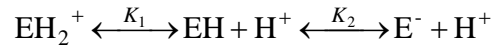
Zi, J.; Peng, B.; Yan, W., Solubilities of rutin in eight solvents at $T = 283.15, 298.15, 313.15, 323.15, \text{ and } 333.15 \text{ K}$. *Fluid Phase Equilibria* **2007**, 261, (1-2), 111-114.

Annex

ANNEX 1: Demonstrations

1. Demonstration of Equation 1.44

(Dependence of the enzyme specific activity with pH):



a) Development of Equation 1.41:

$$K_1 = \frac{[\text{EH}] \times [\text{H}^+]}{[\text{EH}_2^+]} \Leftrightarrow [\text{EH}_2^+] = \frac{[\text{EH}] \times [\text{H}^+]}{K_1}$$

b) Development of Equation 1.42:

$$K_2 = \frac{[\text{E}^-] \times [\text{H}^+]}{[\text{EH}]} \Leftrightarrow [\text{E}^-] = \frac{K_2 \times [\text{EH}]}{[\text{H}^+]}$$

c) Substitution of the species: EH_2^+ and E^- on the Equation 1.43 by the developed cases on a) and b):

$$\begin{aligned} [\text{E}_t] &= [\text{EH}_2^+] + [\text{EH}] + [\text{E}^-] \Leftrightarrow [\text{E}_t] = \frac{[\text{EH}] \times [\text{H}^+]}{K_1} + [\text{EH}] + \frac{K_2 \times [\text{EH}]}{[\text{H}^+]} \Leftrightarrow \\ &\Leftrightarrow \frac{[\text{E}_t]}{[\text{EH}]} = \frac{[\text{H}^+]}{K_1} + 1 + \frac{K_2}{[\text{H}^+]} \Leftrightarrow \frac{[\text{E}_t]}{[\text{EH}]} = 1 + \frac{10^{-\text{pH}}}{10^{-\text{p}K_1}} + \frac{10^{-\text{p}K_2}}{10^{-\text{pH}}} \Leftrightarrow \\ &\Leftrightarrow \frac{[\text{E}_t] \times k_{\text{cat}}}{[\text{EH}] \times k_{\text{cat}}} = 1 + 10^{\text{p}K_1 - \text{pH}} + 10^{\text{pH} - \text{p}K_2} \Leftrightarrow \frac{[\text{E}_t] \times k_{\text{cat}}}{[\text{E}_t] \times k_{\text{cat}}} = \frac{1}{1 + 10^{\text{p}K_1 - \text{pH}} + 10^{\text{pH} - \text{p}K_2}} \Leftrightarrow \\ &\Leftrightarrow v = \frac{v_{\text{max}}}{1 + 10^{\text{p}K_1 - \text{pH}} + 10^{\text{pH} - \text{p}K_2}} \Leftrightarrow v \times \frac{V_t}{w_E} = \frac{v_{\text{max}} \times \frac{V_t}{w_E}}{1 + 10^{\text{p}K_1 - \text{pH}} + 10^{\text{pH} - \text{p}K_2}} \Leftrightarrow \\ &\Leftrightarrow A = \frac{A_{\text{max}}}{1 + 10^{\text{p}K_1 - \text{pH}} + 10^{\text{pH} - \text{p}K_2}} \end{aligned}$$

2. Demonstration of Equation 1.45

(Determination of the optimum pH value):

a) First derivative of Equation 1.44:

$$A = \frac{A_{\max}}{1 + 10^{\text{p}K_1 - \text{pH}} + 10^{\text{pH} - \text{p}K_2}}$$

$$\frac{d}{d\text{pH}} A = \left(\frac{A_{\max}}{1 + 10^{\text{p}K_1 - \text{pH}} + 10^{\text{pH} - \text{p}K_2}} \right)' \Leftrightarrow$$

$$\Leftrightarrow \frac{d}{d\text{pH}} A = - \frac{A_{\max}}{\left(1 + 10^{\text{p}K_1 - \text{pH}} + 10^{\text{pH} - \text{p}K_2}\right)^2} \left(1 + 10^{\text{p}K_1 - \text{pH}} + 10^{\text{pH} - \text{p}K_2}\right)' \Leftrightarrow$$

$$\Leftrightarrow \frac{d}{d\text{pH}} A = -A_{\max} \frac{1}{\left(1 + 10^{\text{p}K_1 - \text{pH}} + 10^{\text{pH} - \text{p}K_2}\right)^2} \left[(\text{p}K_1 - \text{pH})' 10^{\text{p}K_1 - \text{pH}} + (\text{pH} - \text{p}K_2)' 10^{\text{pH} - \text{p}K_2} \right] \Leftrightarrow$$

$$\Leftrightarrow \frac{d}{d\text{pH}} A = - \frac{A_{\max} \left(-10^{\text{p}K_1 - \text{pH}} + 10^{\text{pH} - \text{p}K_2} \right)}{\left(1 + 10^{\text{p}K_1 - \text{pH}} + 10^{\text{pH} - \text{p}K_2}\right)^2}$$

b) Calculation of the zeros of the first derivative Equation 1.44:

$$\frac{d}{d\text{pH}} A = 0 \Leftrightarrow$$

$$\Leftrightarrow - \frac{A_{\max} \left(-10^{\text{p}K_1 - \text{pH}_{\text{opt}}} + 10^{\text{pH}_{\text{opt}} - \text{p}K_2} \right)}{\left(1 + 10^{\text{p}K_1 - \text{pH}_{\text{opt}}} + 10^{\text{pH}_{\text{opt}} - \text{p}K_2}\right)^2} = 0 \Leftrightarrow$$

$$\Leftrightarrow -10^{\text{p}K_1 - \text{pH}_{\text{opt}}} + 10^{\text{pH}_{\text{opt}} - \text{p}K_2} = 0 \Leftrightarrow$$

$$\Leftrightarrow 10^{\text{p}K_1 - \text{pH}_{\text{opt}}} = 10^{\text{pH}_{\text{opt}} - \text{p}K_2} \Leftrightarrow$$

$$\Leftrightarrow \text{p}K_1 - \text{pH}_{\text{opt}} = \text{pH}_{\text{opt}} - \text{p}K_2 \Leftrightarrow$$

$$\Leftrightarrow \boxed{\text{pH}_{\text{opt}} = \frac{\text{p}K_1 + \text{p}K_2}{2}}$$

ANNEX 2: LC-MS chromatograms

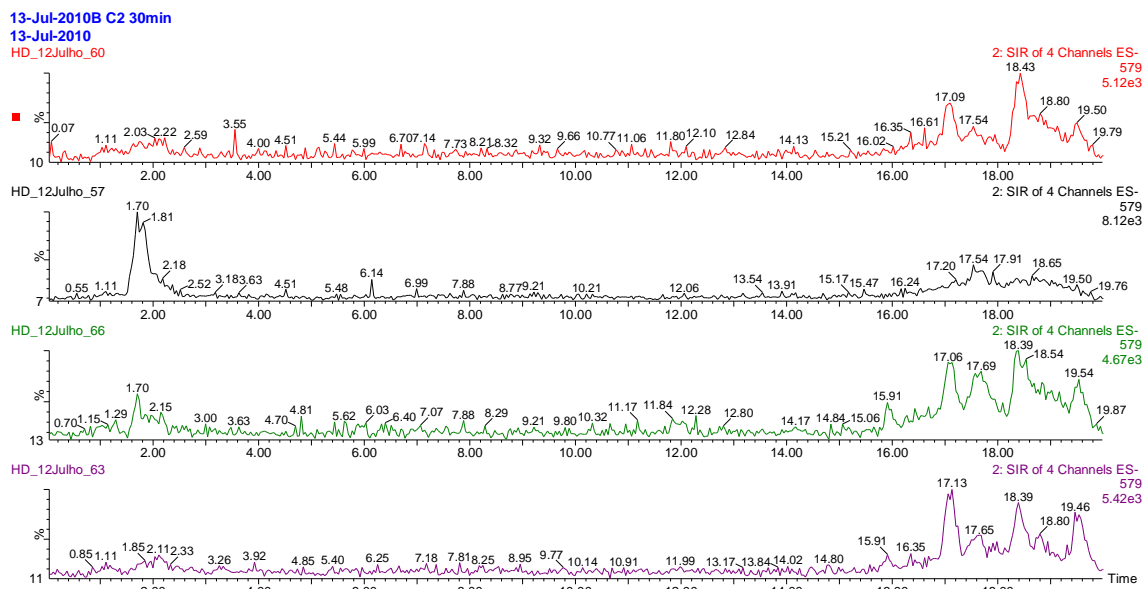


Figure I Chromatogram of the ion extracted for the controls (57 and 60) and extract brain samples (63 and 66) after naringin administration (w/z 579; retention time = 11.91 min).

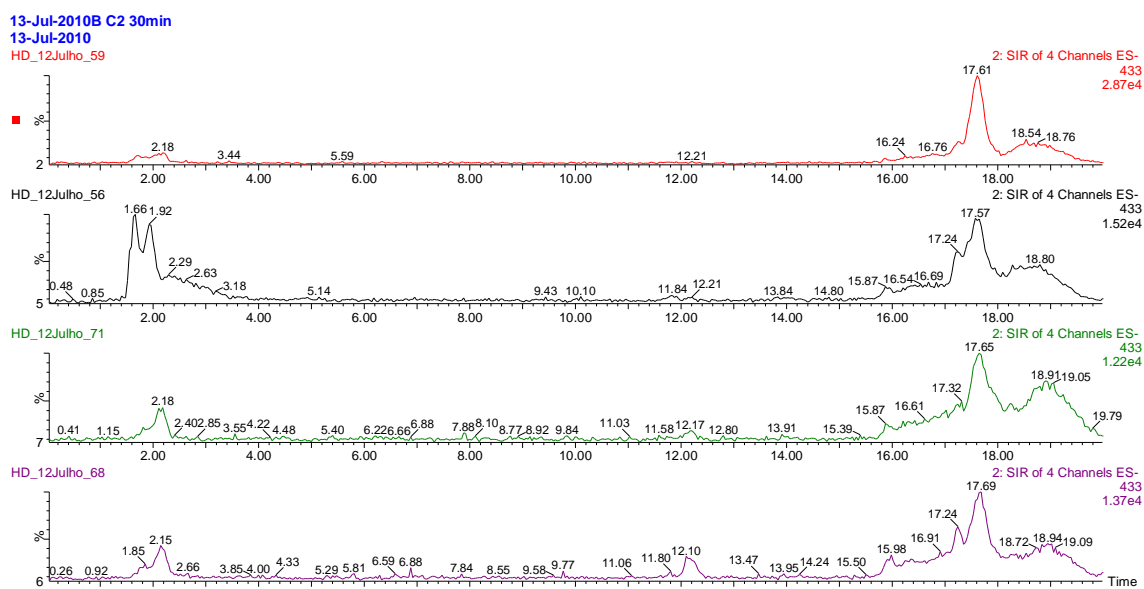


Figure II Chromatogram of the ion extracted for the controls (56 and 59) and extract brain samples (68 and 71) after prunin administration (w/z 433; retention time = 12.10 min).

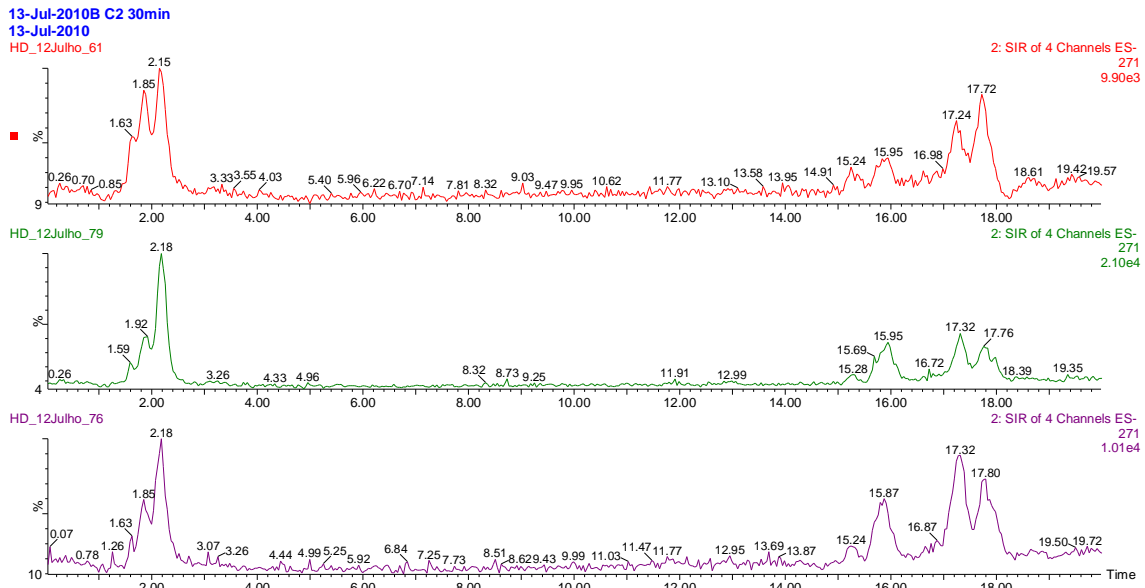


Figure III Chromatogram of the ion extracted for the control (61) and extract brain samples (76 and 79) after naringenin administration (w/z 271); retention time = 15.69 min.

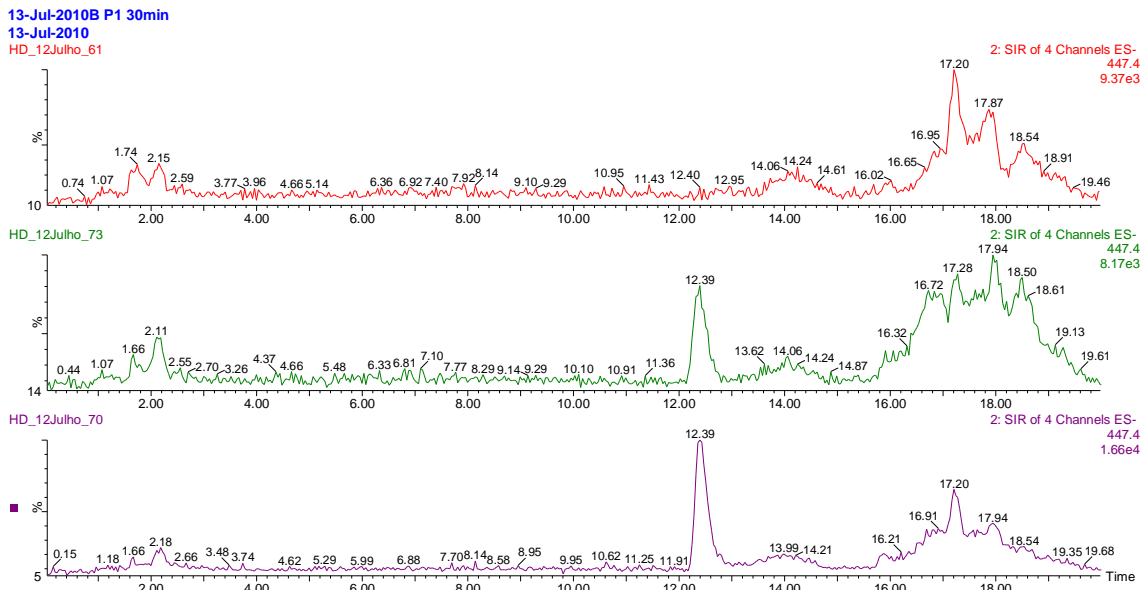


Figure IV Chromatogram of the ion extracted for the control (61) and extract brain samples (70 and 73) after prunin administration. Naringenin glucuronide (w/z 447).

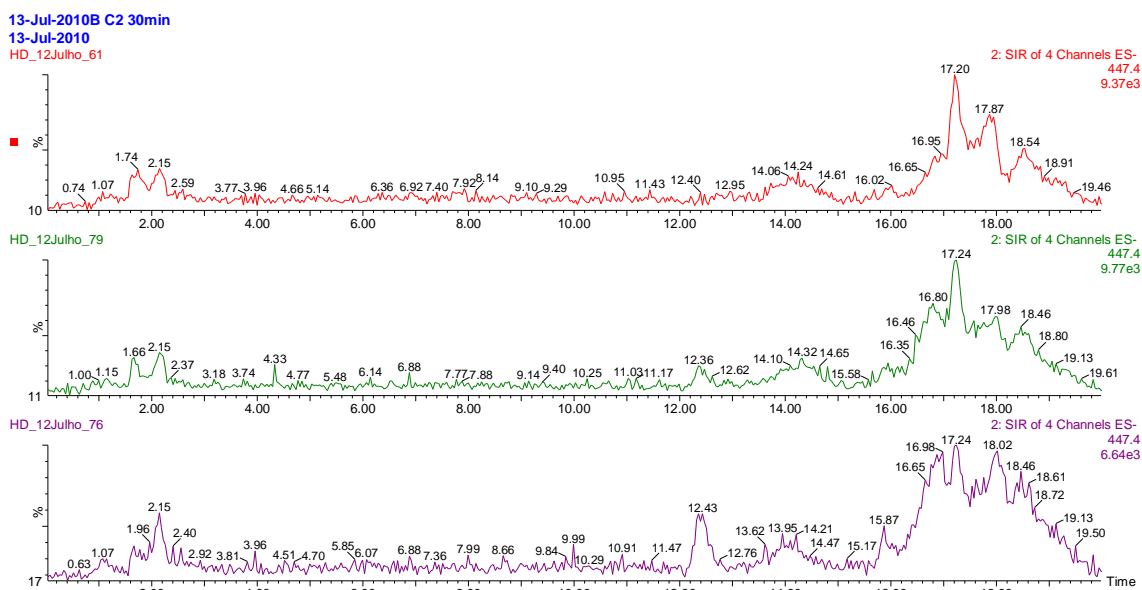


Figure V Chromatogram of the ion extracted for the control (61) and extract brain samples (76 and 79) after naringenin administration. Naringenin glucuronide (w/z 447).

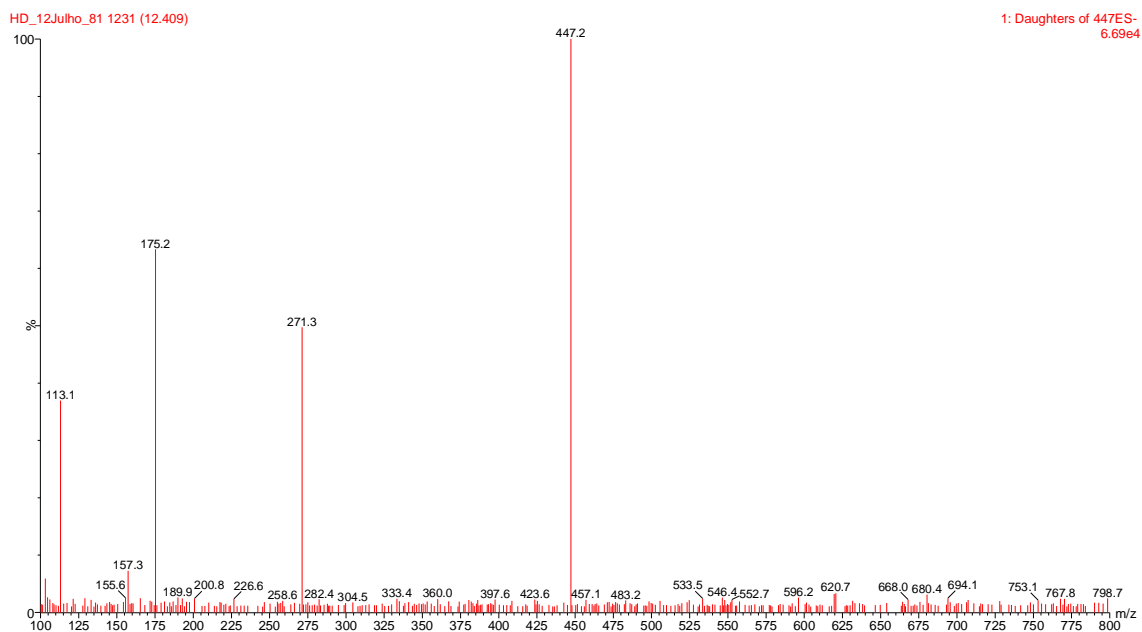


Figure VI Fragmentation spectrum of ion w/z 447 (retention time = 12.39) in extract blood samples after prunin administration. Naringenin (w/z 271).